Investigating the Effects of Proteasome Inhibition on Endothelial Cells

A thesis submitted to fulfil the requirement for the degree of PhD

Ahmed Hjazi

Imperial College London

Faculty of Medicine

Department of Immunology and Inflammation

Section for Haematology

December 2021

Declaration of Originality

I, Ahmed Hjazi, hereby state that this thesis is my own work unless indicated otherwise, and has been referenced accordingly.

Copyright Declaration

The copyright of this thesis rests with the author. Unless otherwise indicated, its contents are licensed under a Creative Commons Attribution Non-Commercial 4.0 International Public Licence.

Under the licence, you may copy or redistribute the material in any medium or format. You may also create and distribute modified versions of this work. This is on the condition that: you credit the author and do not use it, or any derivative works, for a commercial purpose.

When reusing or sharing this work, ensure you make the licence terms clear to others by naming the licence and linking to the licence text. Where work has been adapted, you should indicate that the work has been changed and describe those changes.

Acknowledgements

To almighty ALLAH, I am most grateful for providing me with the strength and courage to finish this task.

I am very grateful to my supervisor, Dr Tom McKinnon, for his guidance, unconditional support, and patience for all the concerns, complaints, and doubts that I experienced during my PhD; his continued support and passion have been a source of inspiration for inspiration my research. As well as being my supervisor, he has become a close friend throughout the journey of my PhD. There are no words to express my gratitude for his kindness, generosity, and approachable nature. I am also grateful that he has mostly tolerated my mess in the lab!

I would equally like to thank my second supervisor, Dr Theresa Page, for her help and assistance throughout my PhD journey and her valuable contributions and ideas that have expanded and developed my PhD. I am indebted to her for her comprehensive experience and genuine kindness, which I was lucky enough to experience while putting together my thesis

I would also like to thank my colleagues – Michael, Elena, and Derick for their support, assistance, and friendship during my time in the lab. Aruni, I want to thank you for being annoying(!), and being equally very helpful and giving me wise advice.

I would like to dedicate my PhD to my late father, **Mohammed Hjazi**. He was an inspirational role model in my life and taught me the importance and values of hard work and dedication. His death during my PhD journey was devastating; however, at the time, it gave me the motivation to strive for and achieve my goals. I hope you would be proud of my achievements. It could be that you are not present in the real-life, but your memories always shadow me and keep me warm.

My lovely mother, **Zainab Al-basha** – your love and support throughout my life since childhood has been invaluable. She has always been there for me, both in good and

bad times, and I cannot thank her enough for her unconditional love. As I promised you earlier to achieve; I am now almost one step behind this.

To my siblings – Amani, Bader, Border, Sultan, Abdulrahman, thank you for your unwavering love, support, and encouragement, without whom I would not have made it through the end of my PhD. Thank you for everything you mean to me.

To my wife Sarah Hjazi, and to my little angels Zainab and Bader, thank you for bringing such joy and happiness throughout my life. I know it was a hard time for you all, adjusting to life in the UK, but we have shared many happy memories, and hopefully, many more to come. Thank you for your constant support, infinite patience, and your belief that I was capable when I wasn't so sure; your love and care has been the secret ingredient for the success of this work.

Finally, I would like to thank my sponsor, Prince Sattam Bin Abdulaziz University and the Saudi Cultural Bureau for their unlimited support and generosity.

Abstract

Multiple myeloma is a genetically complex condition that affects plasma cells. Innovative treatment methods are rapidly emerging that improve clinical outcomes. Clinical success has been demonstrated with proteasome inhibitors that target the mechanism of cellular protein homeostasis. The Food and Drug Administration approved Carfilzomib (CFZ), a second-generation proteasome inhibitor, to treat multiple myeloma patients who have relapsed or are resistant to other treatment options. It inhibits the chymotrypsin-like activity of the 20S immunoproteasome from binding to the β5 subunits irreversibly. Proteasomes serve as important degradation mechanisms within the Endoplasmic reticulum (ER) that maintain cellular homeostasis. When the proteasome is compromised, chronic proteotoxic stress within the endoplasmic reticulum results, ultimately resulting in multiple myeloma cells' death. CFZ has a highly effective profile accompanied by low renal toxicity; despite this, clinical studies have linked the proteasome inhibitor to an increase in cardiovascular adverse events. Several studies have described cardiotoxicity caused by CFZ, with an endothelial component possible. However, CFZ has not yet been studied concerning endothelial dysfunction. This *in vitro* study aims to investigate the impact of CFZ on endothelium homeostasis in the potential adverse cardiovascular effects. This was accomplished by incubating human vein endothelial cells (HUVECs) with CFZ at a clinically relevant dose for one hour and sometimes with TNFα/IL-1β individually or combined following CFZ treatment. This was followed by detecting gene and protein expression of relevant markers of ER stress, inflammation, and thrombosis, and later, some functional studies were conducted at various time points after incubation. The data gathered from this study showed that CFZ increased ubiquitin expression up to 24 hours post-CFZ treatment in both sub-confluence and confluence HUVECs. However, while there was increased expression of BiP, the principal ER stress marker in sub-confluence cells indicating induction of ER stress, resting HUVECs were not affected by CFZ on the expression of BiP and other ER stress markers, suggesting the CFZ cannot cause ER stress in resting HUVECs.Interestingly, although CFZ had no consequence on the expression of procoagulant and pro-inflammatory endothelial cells markers, it enhanced the expression of some of the well-known endothelial-derived anticoagulants mediators,

thrombomodulin (TM), endothelial nitric oxide enzyme (eNOS), phosphorylated eNOS (P-eNOS), tissue plasminogen activator (t-PA), and Krüppel-like factor 4 (KLF4). Moreover, CFZ was able to diminish TNFα mediated TF, VWF, and ICAM-1 expression and promoted TM, eNOS, and KLF-4 upon TNFα treatment, suggesting a protective effect on the endothelium. Consistent with this, CFZ decreased clot formation and factor Xa (FXa) generation on the endothelium after TNFα treatment and, likewise, reduced platelet capture, leukocyte adhesion, and VWF string formation on HUVECs induced by TNFα. I also explored the role of eNOS in preserving ordinary ER statues and as an essential regulator of CFZ cytoprotective effect on HUVECs, while BiP did not exhibit the same role in these cells. In conclusion, the data obtained from this study revealed that CFZ is incapable of provoking ER stress in confluence resting ECs and attenuates the pro-thrombotic and pro-inflammatory effects of TNFα on the endothelium, thus displaying a potential cytoprotective profile on the endothelium.

List of Abbreviations

Abbreviation	Full Name
°C	Degree Celsius
µg/ml	Microgram per microliter
A2AP	α2-antiplasmin
AAs	Amino acids
ACh	Acetylcholine
ADP	Adenosine diphosphate
AF	Attachment factor
AMPKα	AMP-activated protein kinase
AP-1	Activator protein 1
AP-1	Activator protein 1
APC	Activated protein C
ASCVD	Atherosclerotic cardiovascular disease
ATF4	Activating transcription factor 4
ATF6	Activating transcription factor 6
ATP	Adenosine triphosphate
BCA	Bicinchoninic acid assay
BCL-2	B-cell lymphoma 2
BiP/GRP78	Immunoglobulin heavy-chain binding protein/78 kDa glucose-regulated protein
BM	Bone marrow
BP	Biological processes
c DNA	Complementary-Deoxyribonucleic acid
CAM-DR	Cell adhesion mediated drug resistance
CB	Carbonate-bicarbonate
CFZ	Carfilzomib
CHOP	C/EBP homologous protein
CNX	Calnexin
CO2	Carbon dioxide
CoA	Coenzyme A
COX	Cyclooxygenase
CR	Complete remission
CV	Cardiovascular
CVAEs	Cardiovascular adverse events
dH_2O	Distilled water
DiOC	Dihexyloxacarbocyanine Iodide
DMSO	Dimethyl sulfoxide
DUBs	Deubiquitinating enzymes
E1	Ubiquitin-activating enzyme
E2	Ubiquitin-conjugating enzyme
E3	Ubiquitin ligase
EBM-2	Endothelial cell basal medium-2
ECs	Endothelial cells
ED	Endothelial dysfunction
EDHF	Endothelium-derived hyperpolarizing factor
EGM-2	Endothelial cell growth medium

ELISA	Enzyme-Linked Immunosorbent Assay
eNOS	endothelial Nitric Oxide Synthase
EPCR	Endothelial protein C receptor
EPCs	Endothelial progenitor cells
ER	Endoplasmic reticulum
ERAD	Endoplasmic reticulum-associated degradation
ET-1	Endothelin-1
FACS	Fluorescence-activated cell sorting
FBS	Fetal bovine serum
FDA	Food and drug administration
FDPs	Fibrin degradation products
FIII	Factor III
FITC	Fluorescein isothiocyanate
FX	Factor X
FXa	Factor X activated
FXIII	Factor XIII
FXII	Factor XII
FXVII	Factor VII
g/L	Gram per liter
GADD34	Growth arrest and DNA-damage-inducible protein 34
GAPDH	Glyceraldehyde 3-phosphate dehydrogenase
GCN2	General control non-depressible 2
GEF	guanine exchange factors
GPCR	G protein coupled receptor
GPIbα	Glycoprotein Ibα
GraphPad	GraphPad Prism
HEK-293	Human embryonic kidney cells
HMWK	High molecular weight kininogen
HRP-conjugated	Horseradish peroxidase-conjugated
HSP	Heat shock protein
Hsp70	Heat-shock protein 70kDa
HUVECS	Human umbilical vein endothelial cells
ICAM-1	Intercellular adhesion molecule 1
IFNγ	Interferon gamma
IgG	Immunoglobulin G
IKKβ	Inhibitor of nuclear factor kappa-B kinase subunit beta
IL	Interleukin
IL-6	Interleukin-6
IMWG	International myeloma working group
iNOS	Inducible nitric oxide synthase
IRE1α	Inositol-requiring protein 1α
IκBα	Nuclear factor of kappa-light-polypeptide-gene-enhancer in B cells inhibitor alpha
JNK	Jun N-terminal Kinase
kDa	Kilodalton
KLF-2	Krüppel-like factor-2
KLF-4	Krüppel-like factor 4
LA	Lupus anticoagulant
LC3BII	Light chain 3B II
M	Molar

M protein	Monoclonal protein
MGUS	Monoclonal gammopathy of unknown significance
MIP-1β	Macrophage inflammatory protein-1β
MM	Multiple myeloma
MMCs	Multiple myeloma cells
mRNAs	Messenger RNAs
mTOR	Mammalian target of rapamycin
NaCl	Sodium chloride
NE	Not estimable
NFκB	Nuclear factor kappa-light-chain-enhancer of activated B cells
nM	Nano molar
NO	Nitric oxide
NOS	Nitric oxide synthase
OPM-2	Human multiple myeloma cell line
OS	Overall survival
P21	Cyclin-dependent kinase inhibitor 1
P26	Proteasome 26
P27	Cyclin-dependent kinase inhibitor 1B
PA	Plasminogen activator
PAI-1	Plasminogen activator inhibitor-1
PAI-2	Plasminogen activator inhibitor-2 and
PAR	Protease-activated receptors
PAR-1	Protease activated receptor 1
PBA	Phenybutyric Acid
PBMC	Peripheral blood mononuclear cells
PBS	Phosphate buffered saline
P-eIF2 α	Phosphorylated eukaryotic translation initiation factor 2, α subunit
PERK	PKR-like endoplasmic reticulum kinase
PFA	Paraformaldehyde
PGI2	Prostacyclin
PI3K	Phosphoinositide 3-kinase
PIP2	Phosphatidylinositol 4,5-bisphosphate
PIP3	Phosphatidylinositol (3,4,5)-trisphosphate
PIs	Proteasome Inhibitors
PK	plasma kallikrein
PL	Phospholipid
PLCγ	phospholipase Cγ
PP2A	Protein phosphatase 2A
PT	Prothrombin test
PTEN	Phosphatase and tensin homolog
PVDF	Polyvinylidene difluoride
RCL	Reactive centre loop
RNA	Ribonucleic acid
ROS	Reactive oxygen species
rpm	Revolutions per minute
RPMI	Roswell Park Memorial Institute
RRMM	Relapsed/refractory MM
RT-qPCR	Reverse transcription quantitative polymerase chain reaction
SD	Standard deviation

SDS	Sodium dodecyl sulphate
SDS- PAGE	Sodium dodecyl sulfate-polyacrylamide gel electrophoresis
SEM	Standard error of the mean
siRNA	Small interfering RNA
SPEP	Serum protein electrophoresis
TAFI	Thrombin-activatable fibrinolytic inhibitor
TAX_2	Thromboxane A2
TBST	Tris-Buffered Saline Tween
TF	Tissue factor
TFPI	Tissue factor pathway inhibitor
TM	Thrombomodulin
TMA	Thrombotic microangiopathy
TNFα	Tumour necrosis factor α
TP	Thromboxane-proteinoid
t-PA	Tissue-type plasminogen activator
Ub	Ubiquitin
u-PA	urokinase-type Plasminogen Activator
UPEP	Urine protein electrophoresis
UPR	Unfolded protein response
UPS	Ubiquitin-proteasome system
VCAM-1	Vascular cell adhesion molecule 1
VTEs	Venous thromboembolic events
VWF	Von Willebrand Factor
XBP1	X-box binding protein 1

List of Figures

Figure 1.1: Multiple myeloma. 20
Figure 1.2: The two main components of the 26S constitutive proteasome. 25
Figure 1.3: The anatomy of the 26S proteasome. 26
Figure 1.4: The ubiquitin-proteasome system (UPS). 28
Figure 1.5: The Unfolded Protein Response (UPR). 31
Figure 1.6: Consequences of prolonged ER stress. 33
Figure 1.7: Timeline of the proteasome inhibitor approval for clinical usage. 35
Figure 1.8: Different CFZ-cardiovascular associated events in patients with relapsed/refractory multiple myeloma 39
Figure 1.9: Nitric oxide production in the endothelium, and its influence on the vascular smooth muscle cell. 45
Figure 1.10: Graphic sketch of platelet adhesion to the injured vessel wall. 49
Figure 1.11. Graphic illustration demonstrating the heterogenic construction of a haemostatic plug. 51
Figure 1.12: The primary platelet plug. 54
Figure 1.13: Regulation of TF activity. 56
Figure 1.14: The coagulation cascade. 59
Figure 1.15: Negative regulation of the coagulation cascade. 60
Figure 1.16: Fibrinolysis. 64
Figure 1.17: Overview of fibrinolysis 68
Figure 1.18: The “solar system” of vascular inflammation mediated by VWF 71
Figure 1.19: VWF mediated primary hemostasis. 74
Figure 2.1: Schematic illustration of the turbidity assay 92
Figure 2.2: Schematic illustration of Factor X Human Chromogenic Activity Assay. 93
Figure 2.3: Schematic illustration of Activated Protein C (APC) generation Assay .. 94
Figure 3.1.1: CFZ induces a morphological change in HUVECs. 102
Figure 3.1.2: CFZ induced proteasome inhibition in HUVECs. 103
Figure 3.1.3: CFZ did not induce ER stress in HUVECs. 105
Figure 3.1.4: ER stress protein expression of CFZ treated HUVECs compared to controls 106
Figure 3.1.5: Tunicamycin treatment induces a morphological change in HUVECs. 108
Figure 3.1.6: Tunicamycin treatment induces ER stress in HUVECs. 109
Figure 3.1.7: ER stress protein expression of tunicamycin treated HUVECs compared to CFZ treated HUVECs and controls 110
Figure 3.1.8: Carfilzomib did not induce an accumulative effect on the endothelium. 112
Figure 3.1.9: Higher concentration of CFZ did not induce stress in the endothelium. 113
Figure 3.1.10: CFZ induced morphological change at early recovery time points in HUVECs. 115
Figure 3.1.11: CFZ induced ubiquitin expression at early recovery time points in HUVECs. 116
Figure 3.1.12: Emerged conflicting BiP protein expression in CFZ treated HUVECs 117
Figure 3.1.14: CFZ induces more morphological alterations in 80% confluence HUVECs 121

Figure 3.1.15: CFZ induced BiP upregulation in 80% confluence HUVECs, but not 100% confluence HUVECs 122
Figure 3.1.16: CFZ did not trigger apoptosis in 80% confluence HUVECs..... 124
Figure 3.1.17: CFZ did not trigger apoptosis in 100% confluence HUVECs..... 125
Figure 3.1.19: CFZ induced morphological change in HEK293 cells 127
Figure 3.1.20: CFZ did not induce ER stress in HUVECs or HEK293 cells but induced ER stress in OPM-2 cells 128
Figure 3.1.21: CFZ did not induce de novo proteasome synthesis in HUVECs 130
Figure 3.2.1: A schematic illustration of the experimental timelines 139
Figure 3.2.2: TNFα and IL-1β stimulation-induced morphological change in HUVECs 141
Figure 3.2.3: CFZ alone or combined with TNFα and IL-1β stimulation-induced morphological change in HUVECs 142
Figure 3.2.4: TNFα stimulation of HUVECs enhanced CFZ proteasome inhibition 143
Figure 3.2.5: TNFα and IL-1β stimulation did not enhance CFZ to cause ER stress in HUVECs. 145
Figure 3.2.6: Prolonged TNFα stimulation of HUVECs did not enhance CFZ proteasome inhibition. 147
Figure 3.2.7: Prolonged TNFα stimulation did not induce ER stress in HUVECs... 148
Figure 3.2.8: CFZ induces morphological alteration and F-actin rearrangement in the endothelium..... 150
Figure 3.2.9: CFZ did not induce endothelial cell ICAM-1 expression from HUVECs 152
Figure 3.2.10: CFZ induced the genes of some of the anti-thrombotic markers in HUVECS 155
Figure 3.2.11: CFZ induced the proteins of some of the anti-thrombotic markers in HUVECs 156
Figure 3.2.12: CFZ reduced TNFα mediated TF expression in HUVECS 157
Figure 3.2.13: CFZ reduced TNFα mediated VWF and Ang-2 expression in HUVECS. 158
Figure 3.3.1: CFZ attenuated TNFα-induced fibrin formation in HUVECs at 4h. 167
Figure 3.3.2: CFZ did not induce fibrin formation in HUVECs at 24h 169
Figure 3.3.3: CFZ reduces TNFα-induced Factor X formation in HUVECs 171
Figure 3.3.4: CFZ induces APC generation in HUVECs..... 173
Figure 3.3.6: CFZ did not induce VWF release from HUVECs at 4hr recovery 175
Figure 3.3.7: CFZ did not induce VWF release from HUVECs at 24hr recovery 176
Figure 3.3.8: CFZ reduced TNFα-mediated VWF release from HUVECs at 4hr stimulation 177
Figure 3.3.9: CFZ reduced TNFα-mediated VWF release from HUVECs at 24hr stimulation 178
Figure 3.3.10: CFZ reduced the platelet capture mediated by TNFα in HUVECs .. 180
Figure 3.3.11: CFZ did not induce the inflammation of HUVECs. 182
Figure 3.4.1: Optimisation of BiP knockdown in HUVECs..... 189
Figure 3.4.2: BiP knockdown did not enhance CFZ morphological change in HUVECs..... 190
Figure 3.4.3: BiP knockdown did not induce ER stress in HUVECs..... 192
Figure 3.4.4: BiP knockdown did not induce VWF release from HUVECs 193
Figure 3.4.5: Optimisation of eNOS knockdown in HUVECs..... 194
Figure 3.4.6: eNOS knockdown did not enhance CFZ morphological change in HUVECs..... 195

Figure 3.4.7: eNOS knockdown induced ER stress in HUVECs 196
Figure 3.4.8: eNOS knockdown induced soluble ICAM-1 expression by HUVECs 198
Figure 3.4.9: eNOS knockdown induced TF, reduced CFZ mediated t-PA and did not alter TM expression in HUVECs..... 199
Figure 3.4.10: eNOS knockdown induced fibrin formation in HUVECs at 48 hr 201
Figure 3.4.11: eNOS knockdown induced VWF release from CFZ treated HUVECs 203
Figure 4.1: Diagram of potential pathways involved in CFZ cytoprotective effect in HUVECs. 217
Figure 4.2: MM potential mechanisms to induce cardiovascular complications. 223

List of Tables

Table 2.1: Western Blotting Primary antibodies. 83
Table 2.2: Horseradish peroxidase (HRP)-conjugated secondary antibodies. 84
Table 2.3: cDNA synthesis reaction mix components. 85
Table 2.4: cDNA synthesis reaction mix protocol. 86
Table 2.5: Primer sequences for qRT-PCR. 87
Table 2.6: Flow assay solutions 96
Table 4.1: Summary of CFZ effect on some of the pro-thrombotic and pro-inflammatory markers 212

Table of Contents

Declaration of Originality 2
Copyright Declaration 3
Acknowledgements 4
Abstract 6
List of Abbreviations 8
List of Figures 12
List of Tables 15
1. Introduction 20
1.1 Multiple myeloma 20
1.2 Desynchronized cytokine production in multiple myeloma 22
1.3 Current treatments for multiple myeloma 23
1.4 The ubiquitin-proteasome system (UPS). 24
1.5 ER stress and the unfolded protein response (UPR) 28
1.6 Proteasome inhibitors (PIs) 34
1.6.1 Boronate and Salinosporamides 35
1.6.2 Epoxyketones 36
1.7 CFZ associated cardiovascular complications 39
1.8 The potential impact of CFZ on the endothelium 40
1.9 The endothelium & endothelial dysfunction 41
1.9.1 Physiological endothelium 41
1.9.1.1 Prostacyclin and Thromboxane A2 42
1.9.2 Endothelium Dysfunction (ED) 47
1.10 Coagulation and Haemostasis 47
1.10.1 Introduction to the coagulation system 47
1.10.2 Primary haemostasis 48
1.10.3 Secondary haemostasis 55
1.10.4 The coagulation inhibitors 60
1.11 Fibrinolysis and the control of blood coagulation 63
1.11.1 The fibrinolysis system 63
1.11.2 Clot structure and fibrin formation 65
1.11.3 Regulation of fibrinolysis 65
1.11.4 Clot-based fibrinolysis 66
1.11.5 Cell surface fibrinolysis 67
1.11.6 Fibrin degradation products 67

1.12 VWF and the endothelium ... 68
1.12.1 Introduction to VWF ... 68
1.12.2 The potential correlation between VWF and endothelium dysfunction ... 69
1.12.3 Synthesis, storage, and secretion of VWF ... 71
1.12.4 Platelet α-granules contain VWF ... 72
1.12.5 Interactions of VWF with coagulation proteins ... 72
1.12.6 VWF-mediated primary haemostasis ... 73
1.13 Hemostatic abnormalities in MM patients ... 75
2. Research hypothesis and aims ... 77
2. Materials and Methods ... 78
2.1 Cell culture and passage ... 78
2.2 Treatment of HUVECS with CFZ ... 79
2.2.2 Treatment of HUVECS with multiple doses of CFZ ... 79
2.2.3 Stimulation of HUVECS with inflammatory cytokines ... 80
2.2.4 CFZ treatment of Human embryonic kidney 293 (HEK 293) and multiple myeloma (OPM-2) cells ... 80
2.3. Western blotting ... 80
2.3.1 Cell harvesting and extraction of total protein ... 80
2.3.2 Measuring total protein concentration ... 81
2.3.3 SDS-page gel electrophoresis and Western Blotting ... 81
2.4. quantitative Real-Time Polymerase Chain Reaction (qRT-PCR) ... 84
2.4.1 Harvesting Cellular RNA lysate ... 84
2.4.2 Extracting total Cellular RNA and sscDNA synthesis ... 84
2.4.3 Real-time Quantitative PCR (RTq-PCR) ... 86
2.5 Enzyme-Linked Immunosorbent Assay (ELISA) ... 87
2.5.1 VWF ELISA ... 87
2.5.2 ICAM-1 and Ang2 ELISA ... 88
2.6 Immunofluorescence staining ... 88
2.6.1 Immunofluorescence staining for Actin and VWF ... 88
2.7 Flow cytometry ... 89
2.7.1 ICAM-1 flow cytometry ... 89
2.7.2 Annexin-V and Propidium Iodide (PI) apoptotic flowcytometry ... 90
2.8 Small interfering (si) RNA transfection ... 90
2.9 Functional studies on HUVECS ... 91
2.9.1Turbidity assay ... 91
2.9.2 Factor X activation assay ... 92

2.9.3 Activated Protein C (APC) generation Assay 93
2.9.4 Microfluidic perfusion assays 94
2.9.5 Leukocyte adhesion assay 98
2.10 Statistical analysis 98
3. Results 99
3.1 CFZ did not induce ER stress in HUVECs 99
3.1.1 Introduction 99
3.1.2 Results 101
3.1.2.1 Carfilzomib causes a distinct morphological change in HUVECS and induces protein ubiquitination. 101
3.1.2.2 carfilzomib did not induce ER stress in HUVECs 104
3.1.2.3 Tunicamycin induced ER stress in HUVECs 107
3.1.2.4 Repeated dosing of Carfilzomib did not induce ER stress in HUVECS111
3.1.2.5 Increasing concentrations of CFZ did not induce ER stress in the endothelium 113
3.1.2.6 Carfilzomib potentially induced ER stress in HUVECs at earlier recovery time points 114
3.1.2.7 CFZ mediated BiP expression was dependent on the confluence of HUVECs 118
3.1.2.8 CFZ did not induce apoptosis in either 80% or 100% confluence HUVECs 123
3.1.2.9 CFZ did not induce ER stress in human embryonic kidney 293 (HEK293) cells but did induce ER stress in multiple myeloma cells (OPM-2) 126
3.1.2.10 CFZ did not induce de novo proteasome synthesis in HUVECs 129
3.1.3 Discussion 131
3.2 CFZ induces cytoprotective and thrombo-protection effects in HUVECs 137
3.2.1 Introduction 137
3.2.2 Results 139
3.2.2.1 Combined treatment with CFZ and cytokines induced morphological change and ubiquitination expression but did not induce ER stress in the endothelium 139
3.2.2.2 Prolonged stimulation with TNFα did not induce ER stress in HUVECs 146
3.2.2.3 CFZ induces structural rearrangement of the endothelium 149
3.2.2.4 CFZ treatment did not induce endothelial ICAM-1 expression 151
3.2.2.5 CFZ induced an anti-thrombotic and cytoprotective effect on the endothelium 153
3.2.3 Discussion 159
3.3 CFZ enhances anti-thrombotic activity in HUVECs 165

3.3.1 Introduction 165
3.3.2 Results 166
3.3.2.1 CFZ reduces TNF-mediated fibrin clot formation in HUVECs 166
3.3.2.2 CFZ reduces TNFα-induced Factor Xa formation on HUVECs 170
3.3.2.3 CFZ enhanced the APC generation in HUVECs 172
3.3.2.4 CFZ reduced TNFα-mediation of VWF release from HUVECs..... 174
3.3.2.5 CFZ reduced TNFα-induced string formation on HUVECs 179
3.3.2.6 CFZ reduced TNFα-mediated leukocyte adhesion to HUVECs 181
3.3.3 Discussion..... 183
3.4 Nitric oxide is an important regulator of the endothelium and for CFZ cytoprotective effect in the endothelium 187
3.4.1 Introduction 187
3.4.2 Results 189
3.4.2.1 BiP knockdown did not induce ER stress or pro-thrombotic activation in HUVECs..... 189
3.4.2.2 eNOS knockdown induced ER stress in HUVECs 194
3.4.2.3 eNOS knockdown induced thrombotic and inflammatory responses in HUVECs..... 197
3.4.2.4 eNOS knockdown induced fibrin formation in HUVECs 200
3.4.2.5 eNOS knockdown induced VWF release from HUVECs..... 202
3.4.3 Discussion..... 204
4. Summary, General Discussion, and Conclusion 209
4.1 Summary..... 209
4.2 General discussion..... 221
4.2.1 Limitations of this work..... 226
4.2.2 Future studies 227
4.3 Conclusion 229
References..... 230

1. Introduction

1.1 Multiple myeloma

Multiple myeloma (MM) is a heterogeneous blood cancer that affects terminally differentiated plasma cells creating abnormal immunoglobulins (Figure 1.1). (1) The disease is clinically characterized by several symptoms known collectively by the acronym CRAB, Calcium elevation, Renal failure, Anemia, and Bone lesions. They are attributable to the underlining neoplastic plasma cell clone processing. (2) In addition, most patients produce monoclonal immunoglobulin heavy chains (M-protein) or light chains, which can be detected in the patient's bloodstream or urine. (2) MM is characterized by the different monoclonal proteins secreted by the malignant plasma cells. (3) However, about 15-20 % of MM patients secrete only a monoclonal free light chain, and fewer than three percent of them do not secrete any monoclonal proteins. (3)

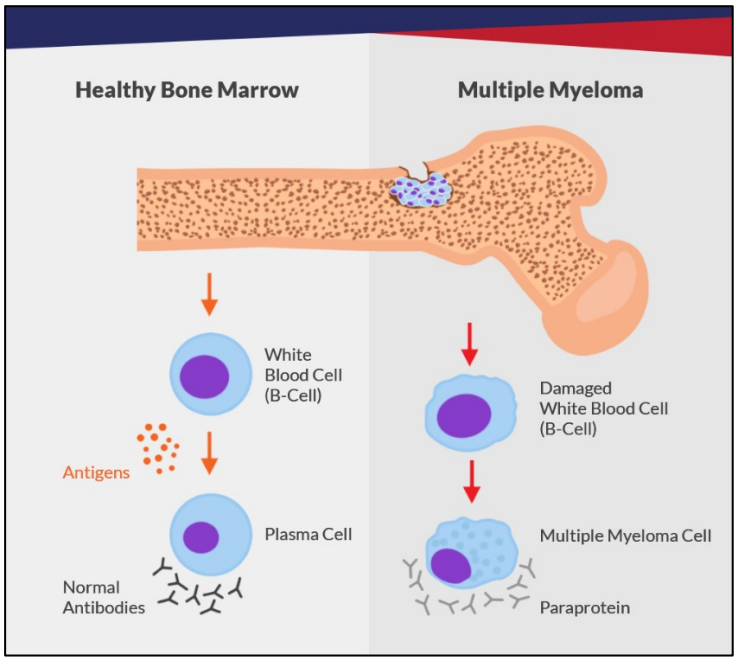


Figure 1.1: Multiple myeloma. Multiple myeloma cells are irregular plasma cells that accumulate in the bone marrow and create tumours in the bone. Normal plasma cells produce antibodies as a part of the immune defence mechanism against various pathogens. Malignant plasma cells produce non-functional and harmful immunoglobulin or M-protein. This abnormal alteration of these cells' behaviour leads to end-stage organ damage, resulting in various associated complications. The figure is taken from (Grandin, Journal of cardiac failure, 2015). (4)

MM accounted for approximately 2% of all cancer cases and was the 19th most common cancer in the UK in 2016-2018. It is considered the second most common blood cancer, with a five-year survival rate of 52.3%. (5) Globally, the disease accounts for the second-highest haematological malignancy in adults in Western countries such as the UK, USA, and Australia, and its occurrence rate is two to three times higher in black populations than in Caucasian populations. It primarily affects male and older populations, where the median age at diagnosis is 69–70 years. (2)

MM typically begins as smouldering MM or monoclonal gammopathy of unknown significance (MGUS), where both are defined as an asymptomatic clonal plasma cell disorder, and both are considered multiple myeloma precursors. (6) Smouldering MM is distinguished from Monoclonal gammopathy of undetermined significance (MGUS) by a significantly increased risk of progression into the malignant phase. (6) This distinction is vital in providing appropriate clinical care, prognostic evaluation, management, and counselling. (7)

New biomarkers have been developed to identify patients at high risk of developing MM from the MM precursor groups. (7) The diagnosis of MM requires evidence of the presence of 10% or more clonal plasma cells on bone marrow biopsy, in addition to one or more of the International Myeloma Working Group (IMWG) criteria myeloma defining events. (8) These include conventional CRAB features attributable to a plasma cell clonality, as well as three additional biomarkers: a serum-free light chain (FLC) ratio of ≥100 (providing elaborate FLC level is ≥100 mg/L), bone marrow that contains ≥60% plasma cells, and magnetic resonance imaging (MRI) investigation showing more than one focal lesion. (8)

Molecular classification of MM is essential in providing optimal management (8) as molecular subgroups of MM correlate with distinctive variations in disease presentation and prognosis. (8) The cause of the development of MM is not yet fully understood. During progression from multiple myeloma precursor to multiple myeloma, the abnormal genetic events in MM cells (MMCs) are somatic mutations and chromosomal abnormalities. (9) Class-switch recombination is the most abundant chromosomal translocation among these abnormalities, and abnormal V (D) J rearrangement may also be involved in disease development. Two major classifications are used to identify MM patients. Primarily, most of these patients can be categorized into one of three sub-clusters: initial immunoglobulin heavy chain (IgH) translocations, trisomies (40%), or a combination of both. (10) In addition to molecular

sorting based on definite genetic abnormalities, patients with MM may also be assembled into two sub-groups according to ploidy status evaluated by karyotyping. These groups are the non-hypodiploid group (up to 44/45 chromosomes) and the hypodiploid group (more than 46/47 chromosomes). (10) These events are counted as the beginning or main events, suggesting that the development of myeloma can follow at least two distinct pathways. (11)

However, the involvement of all these genetic abnormality events alone was not found to be sufficient for myeloma progression, as they have also been found to exist at the non-malignant-MGUS stage. (9) Both hypodiploidy and IgH translocations are found in 45% and 50 % of MM, respectively. (12) In contrast, almost five percent of patients do not express either IgH translocations or hypodiploidy. (12) In general, all these classifications are critical in predicting the prognostic impact, relapse of the disease and selecting treatment approaches (selection of drugs, the extent of therapy, aggressiveness of the treatment, etc.).(9)

1.2 Desynchronized cytokine production in multiple myeloma

The interplay between MMCs and the bone marrow microenvironment (hematopoietic and non-hematopoietic stromal cells) is essential for the progression and development of myeloma. (13) These cells secrete several factors that play a role in the proliferation, persistence and migration of MMCs and are also involved in bone damage. (14) The interaction between MMCs and stromal cells can be linked to a process known as cell adhesion mediated drug resistance (CAM-DR). (15) This process is best described as a survival mechanism utilized by MMCs to maintain their survival and avoid cytotoxic drugs' impact. Additionally, some features produced by the stromal cells are associated with angiogenesis, leading to a worse outcome. (16) Myeloma cells and the bone marrow (BM) environment encourage various mediators' as autocrine or paracrine release. (17) Indeed, the BM microenvironment in MM patients displays high levels of human growth factor (HGF), IL-6, TNFα, IL-1β, and cytokines stimulated by interferon-γ (IFN-γ). (17) Many of these cytokines support MM development and progression. (17)

The immune system also has a vital role in MM progression, tumour growth and produces many pro-inflammatory cytokines that are elevated in the serum of MM patient's, such as IL-15, TNF-α, IL-17, IL-1β, IL-18, IL-6, IL-22, IL-12, IL-23, IL-16, IL-17, and IFN-γ.(18) Tumour growth is associated with inflammation, and an escalation in pro-inflammatory cytokine quantities can maintain the progression of neoplasia. (18) Cytokines discharged by T lymphocyte subsets, and plasma cells can generate an environment in the BM that promotes cancer cell development. (19) Prabhala *et al*. have also reported a significant reduction in the number of BM Treg cells. (19) These cells were stated as dysfunctional and unable to suppress T lymphocyte growth, which progressively reduced as the disease progressed. (19)

1.3 Current treatments for multiple myeloma

Although MM is a treatable disease, it is not considered curable. (15) The current treatments for myeloma seek to control the disease, improve survival rates, and enhance the quality of life. Complete remission (CR) is an important goal for patients, and it is possible to achieve this by combining a variety of new classes of drugs. (20) These include immunomodulatory agents, which are combined with traditional treatments such as chemotherapy, thalidomide, anthracyclines, corticosteroids, alkylating agents, etc. (15)

Currently, there are two main MM treatment strategies: intensive and non-intensive treatment. (21) The former differs from the latter in using a higher dosage of the anti-myeloma therapy and is frequently followed by stem cell transplantation to achieve final disease remission. (21) However, this is a less common approach to treating MM since it is only appropriate for younger patients, which does not align with the median age of the MM population. (21) Early treatment of the disease in the first stage is, like most cancers, considered critical. (22)

Despite extended survival rates resulting from the development of more potent MM-targeting treatments, eventually, most patients will die from reaching the end-stage of their disease and some form of treatment-related complications. (22) Disease development and consequent relapses are defined by sub-clonal progression and gradually resistant disease, making successful treatment extremely challenging. (23)

It has been widely documented that generating an optimal level of response is essential in achieving an MM cure and that maintaining a consistent state of remission

is vital. Therefore, after administering the selected drug(s), response assessment and monitoring of therapy in MM is required and should be conducted using the International Myeloma Working Group (IMWG) uniform response criteria. (20) The basis of monitoring involves quantifying M protein levels by serum protein electrophoresis (SPEP) and urine protein electrophoresis (UPEP). (24) In general, however, the clinical management of elderly patients with myeloma remains challenging since most have pre-existing comorbidities that pose challenges to the treatment approaches and precise evaluation of many clinical and social factors. (25) In the past two decades, myeloma has conventionally been correlated with poor patient outcomes, reflected in a median general survival rate of only three years. (20) Nevertheless, the median survival rate has improved across all age groups following the introduction of novel therapeutic agents; the proteasome inhibitors (PIs). (24) This group of drugs acts by directly inhibiting proteasome function in multiple myeloma cells (MMCs), leading to the accumulation of mis-folded proteins in the cellular cytosol, thus activating apoptosis. (24)

Fundamentally, survival rate improvement has been achieved with the subsequent improvement of second and third generations PIs, immunomodulatory drugs, and recent therapy options such as monoclonal antibodies. (24) Elotuzumab (Empliciti) is a monoclonal antibody that binds to the SLAMF7 protein, located on myeloma cells and assists the immune system in attacking the cancer cells. The use of the second-generation PIs, carfilzomib (CFZ), has improved patient outcomes in elderly myeloma patients and significantly increased survival rates. (26)

1.4 The ubiquitin-proteasome system (UPS).

Proteasomes are protein complexes that degrade damaged or unneeded proteins by cleaving peptide bonds through a chemical reaction known as proteolysis(27). There are two primary forms of the human proteasome, the constitutive proteosome and the immune-proteosome, whose expression is induced by inflammatory cytokines. (28) In eukaryotes, the proteasomes are located in the cytoplasm and nucleus. (29) The constitutive 26S proteasome is a large, ~2.5 MDa, multi-protein, multi-catalytic ATP-dependent protease complex that functions as the degrading arm of the ubiquitin system (Figure 1.2). It functions as the main pathway for controlled degradation of the membrane, cytosolic and nuclear proteins in all eukaryotic organisms. (27) It is the

most abundant proteasome in mammals, and it is composed of two 19S regulatory cap subunits and one core catalytic 20S protein subunit. (29)

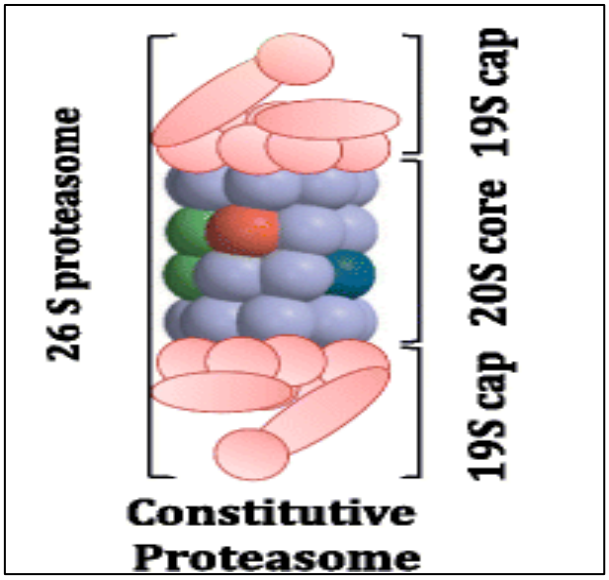


Figure 1.2: The two main components of the 26S constitutive proteasome. The proteasome comprises two 19S regulatory caps, where the ubiquitinated-protein recognitions and the de-ubiquitination occur. The other part of the 26S proteasome is the 20S proteasome, where protein degradation occurs. The figure was taken from (Schweitzer, Proceedings of the National Academy of Sciences, 2016). (30)

The 20S core consists of two outer rings, each of seven α units that function as a docking point for the regulatory cap (Figure 3). (27) The ends of the 20S core are closed by the N-termini of the α-subunits, frequently defined as the 'gate'. (31) 26S-mediated protein degradation is ATP-dependent, where the six ATPases present in the regulatory cap are the only ATP hydrolyzing proteins in the proteasome. (32) The 19S subunits of the regulatory particles are divided between two sub-structures, the 'lid' and the 'base complexes' (Figure 1.3). (32) The lid comprises the Rpn11 subunit with deubiquitinating action, and the ring of AAA-ATPases is found on the base. (33) The ATPases C-termini are drilled into pockets and found between the α-subunits of the core particle. This leads to the gate's opening by a translocation of the α tails. (34) The two β rings are the inner rings, each composed of seven β units (Figure 3). There are three proteolytic subunits (β1, 2, and 5) with different substrate activity and specificity (Figure 3). (34) These substrate specificities are β5 binding to chymotrypsin-like, β2 binding to trypsin-like and β1 binding to caspase-like substrates (Figure 3). (35) The binding of ATP to the 19S ATPase subunit is required to associate the 19S and 20S subunits, and the degradation of ubiquitin and unfolded proteins requires ATP

hydrolysis. (31) The ubiquitin-binding sites and multiple ATPase active binding sites are found in the 19S subunit, where polyubiquitinated and unfolded proteins are recognized. (29) These are subsequently transferred to the inner two rings of the 20S subunit, where proteolysis by the proteolytic 20S occurs. (36)

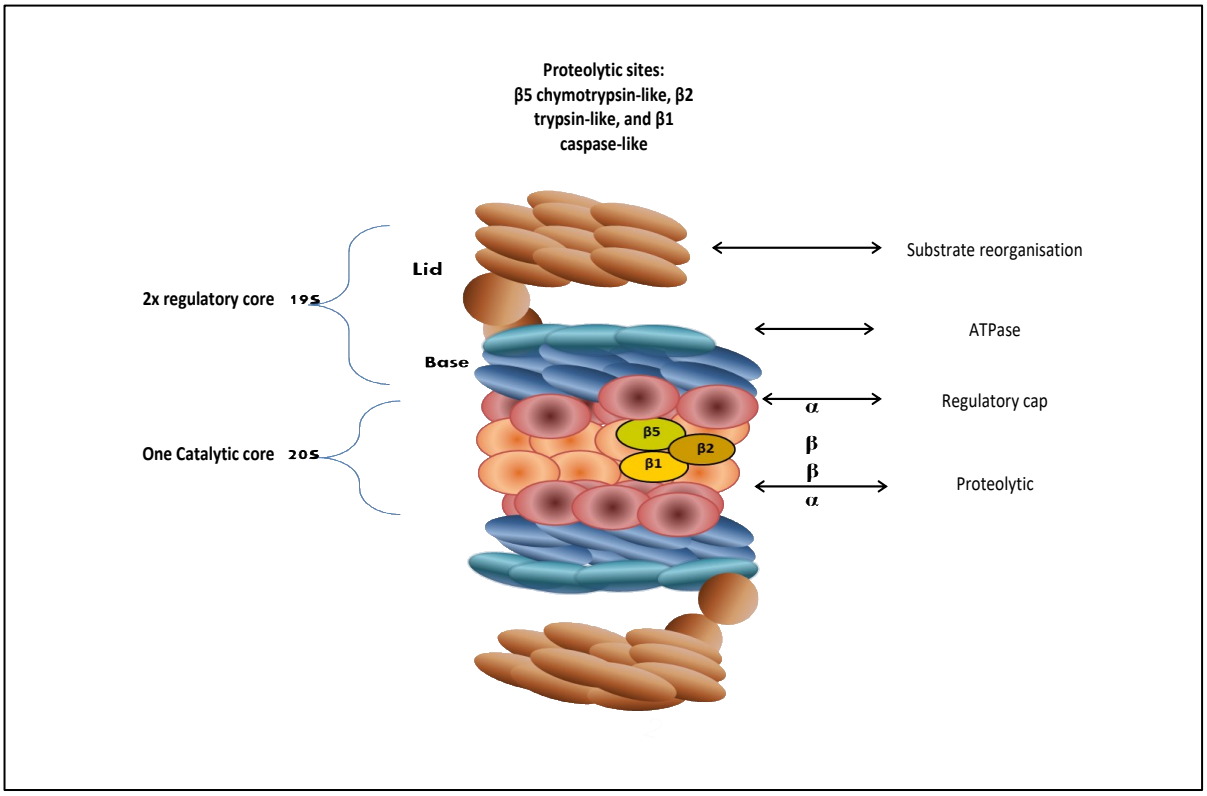


Figure 1.3: The anatomy of the 26S proteasome. The 19S core is part of the P26 regulatory core and is composed of lid and base. The 20S core is formed of two outer rings, where each is composed of seven α units that function as a docking point for the regulatory cap. The two β rings are the inner rings, where each is composed of seven β units. There are three proteolytic subunits (β1, 2, and 5) with different substrate activity and specificity. These substrate specificities are β5 binding to chymotrypsin-like, β2 binding to trypsin-like and β1 binding to caspase-like substrates. The figure was prepared by (Ahmed Hjazi, 2021)

Cells maintain efficient and adjustable systems to discard terminally misfolded proteins and avoid toxic effects. (33) This practice starts with detecting a substrate in the ER lumen and terminates its degradation by the cytoplasmic proteasome. This process is termed Endoplasmic Reticulum-Associated Degradation (ERAD). (29)

ERAD is initiated by exporting the misfolded protein, partially unfolded through the Sec61 translocon, an aqueous ER membrane channel. (28) This exportation causes

the target protein to be targeted by ubiquitin, a small regulatory protein found in most tissues of eukaryotic organisms, via a process known as ubiquitination. (36) Ubiquitination involves three main steps; activation, conjugation, and ligation. (33) These are performed by ubiquitin-activating enzymes (E1s) (118 kDa), ubiquitin-conjugating enzymes (E2s) (18.6 kDa), and ubiquitin ligases (E3s) (~8.5 kDa), respectively. (36) Initially, the ubiquitin molecules are activated and transferred to the E2 ubiquitin-conjugating enzyme by E1. Then the substrate is identified and conjugated to the ubiquitin chain by E3 ubiquitin-ligase. (28) Once a single ubiquitin molecule tags a protein, this promotes the ligation of the lysine residues of the protein substrate to the following ubiquitin molecule, which creates a polyubiquitin chain. (10) The last lysine-48 linked polyubiquitination chain is targeted for proteasome degradation of the tagged protein and flags it up to the abundantly expressed cytosolic ATPase, p97 (VCP). (28) With the assistance of accessory proteins such as Np14 (NPLOC4) and Ufd1 (UFD1L), and by consuming the mechanical force that results from ATP hydrolysis, the protein is extracted from the Esc61 translocon into the cytosol by P96. (10) The polyubiquitin chain directs the targeted substrate to the 26S proteasome by P97 to approach ERAD. (10) De-ubiquitination phases occur between translocation from the ER lumen and proteasomal consumption involving the de-ubiquitinating enzymes (DUB). (35) This enzyme plays a critical role in recycling and reversing the ubiquitin conjugation through the ubiquitin-proteasome pathway, dislocating the proteins from the ER membrane and feeding the ERAD substrate into the protostome. (28) The ERAD process yields fragmented peptides recycled into single amino acids for further protein synthesis (Figure 1.4). (10)

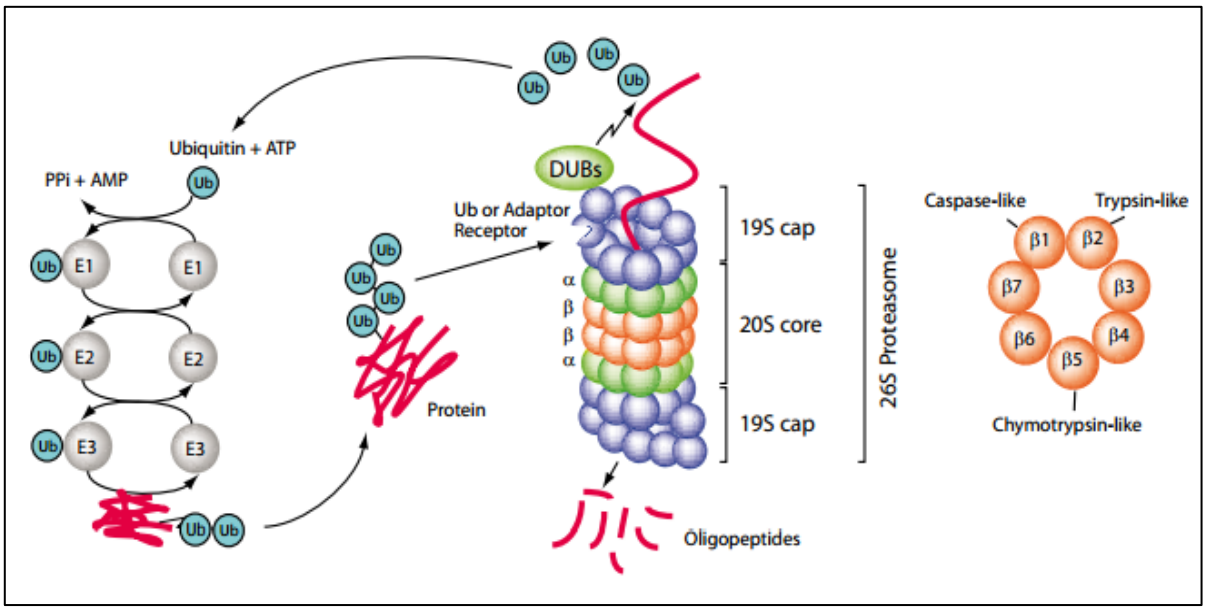


Figure 1.4: The ubiquitin-proteasome system (UPS). Misfolded protein is released from ER-membrane channel Sec61, followed by serial recruitment of three cytosol ubiquitination enzymes. E1- Ubiquitin activation, E2- Ubiquitin conjugation, and E3- Ubiquitin ligase bind substrate to the Ubiquitin chain. The conjugated protein is then transferred to the recognition site of the 26S proteasome, the 19S cap, where it is transferred through the cylinder system into the 26S proteasome catalytic site, which is made up of the 20S core and the outer two α rings whose role is to sustain a "gate" through which proteins enter the barrel. The inner two rings are made up of seven β subunits that include three to seven protease-active positions where the protein binds to the corresponding binding site β subunits, caspase-like, trypsin-like, and chymotrypsin-like. This process generates protein fragments and amino acids that can be re-used by the cell to create new proteins. This system of ubiquitination and proteasomal degradation is recognized as the ubiquitin-proteasome system. The figure was taken from (Auner, British journal of haematology, 2015). (10)

1.5 ER stress and the unfolded protein response (UPR)

The ER is an essential regulator of proteostasis and provides a network of interconnected quality control practices in the cell that sustains the functional proteome. (37) Disturbance of ER homeostasis due to redox or calcium balance fluctuations, elevated protein synthesis, and gathering of misfolded proteins cause ER stress. (38) The unfolded protein response (UPR) is a collection of phylogenetically conserved signalling pathways that sense impairment of the ERs protein-folding capacity, monitor the ERs conditions, communicate the gene expression program of eukaryotic cells, and control the ER lumen status. (35) It is elaborately integrated with

other cell physiology mechanisms to maintain the cellular homeostatic balance. (38) This response activates intracellular signal transduction pathways when the cell undergoes ER stress. (35)

Membrane and secreted proteins mature and fold in the ER lumen before they are released extracellularly, are expressed on the cell surface, or delivered to other endomembrane system components. (37) The accumulation of misfolded or unfolded proteins in the ER lumen activates the UPR. (39) It aims to resolve this stress by three significant actions: degrading misfolded proteins, halting protein translation, and increasing expression of molecular chaperones, which play a role in protein folding. (39)

Three principle components of UPR branch signal transducers have been identified (ATF6, PERK, and IRE1)(10) (Figure 5). These are transmembrane ER-resident proteins that continually monitor the ER-folding conditions. (10) They use a unique transduction mechanism and operate in parallel. (10) Their ER luminal domains detect the raised level of misfolded proteins and transmit adapting downstream signals with their cytosolic domains. (37) These three UPR sensors depend on BiP (Binding immunoglobulin Protein)/GRP78, an essential ER chaperone, to detect misfolded proteins. (40) BiP varies between monomeric and oligomeric states. However, the unmodified monomeric state of BiP is exclusively for association with unfolded proteins. Under basal conditions, BiP binds to these sensors' luminal domains, thus inhibiting their activation. (25) However, BiP dissociates from the sensors and strongly binds to the exposed hydrophobic domains of proteins when they accumulate in the ER. (25) These sensors' subsequent phosphorylation and activation initiate signalling pathways to establish an adaptive cellular response that allows cells to cope with protein misfolding (Figure 1.5). (25)

Firstly, activation of Inositol requiring protein-1 alpha (IRE1) (by auto-phosphorylation), which features endoribonuclease activity, leads to translation of a stable and active transcription factor, XBP1. (41) XBP1 is cleaved in the Golgi apparatus by protease S2P and S1P before translocation into the nucleus; thus, nucleus-specific transcriptional programs are activated. (41) The activation of this protein enhances cellular adaptation, including upregulation of genes that encode

proteins with diverse functions in the UPR, rising ER folding capacity, ER volume, and ERAD (Figure 1.5). (40)

Secondly, similar to XBP1, activated Activating Transcription Factor-6 (ATF6) is cleaved in the Golgi before entering the nucleus. (42) The ATF6α cytosolic domain (ATF6f) transcriptionally upregulates genes behaving as ER-resident chaperones, such as BiP, P58 and protein 94 (GRP94) and ERAD components to help in the correction of ER stress. (43) Thus, ATF6 and IRE1 are generally involved in transcriptional upregulation of ERAD components and increase the cells capacity to degrade and fold proteins (Figure 1.5). (40)

Thirdly, activated Protein kinase RNA-like ER kinase (PERK) (activated by dimerization and auto-phosphorylation) acts differently from the earliest UPR sensors through a transitional response. (43) Activated PERK phosphorylates Ser51 of eukaryotic transitional initiation factor alpha subunit (eIF2a), causing transitional protein suppression by a general inhibition of cellular mRNA transcription. (44) This suppression considerably reduces protein-folding demand, thus restoring ER homeostasis. (45) However, this inhibition does not last permanently, as eIF2α phosphorylation triggers the translation of particular mRNAs to produce proteins that reverse the suppression mechanism. (45) These include activating transcription factor 4 (ATF4), which triggers the production of growth-arrest and DNA damage-inducible protein 34 (GADD34). (45) The activation of these proteins provides a negative feedback loop to suppress general protein translation by dephosphorylation of eIF2α that restores protein production. (45)

In addition, active ATF4 targets another transcription factor known as the C/EBP Homologues Protein (CHOP) that works together with ATF4 to induce protein biosynthesis (46). Thus, the initial phase of general protein translation inhibition is rapidly resumed, restoring cellular protein homeostasis (Figure 1.5). (46)

These sensor pathways activate downstream signalling to resolve the ER stress and restore cellular protein homeostasis. (10) This is achieved by increasing the ER's clearance capacity by autophagy and ERAD, decreasing folding load, and increasing folding capacity. (10) Together, these serve as feedback loops that diminish ER stress, improve antioxidant responses, and activate amino-acid metabolism to re-establish homeostasis within the ER lumen (Figure 1.5). (44)

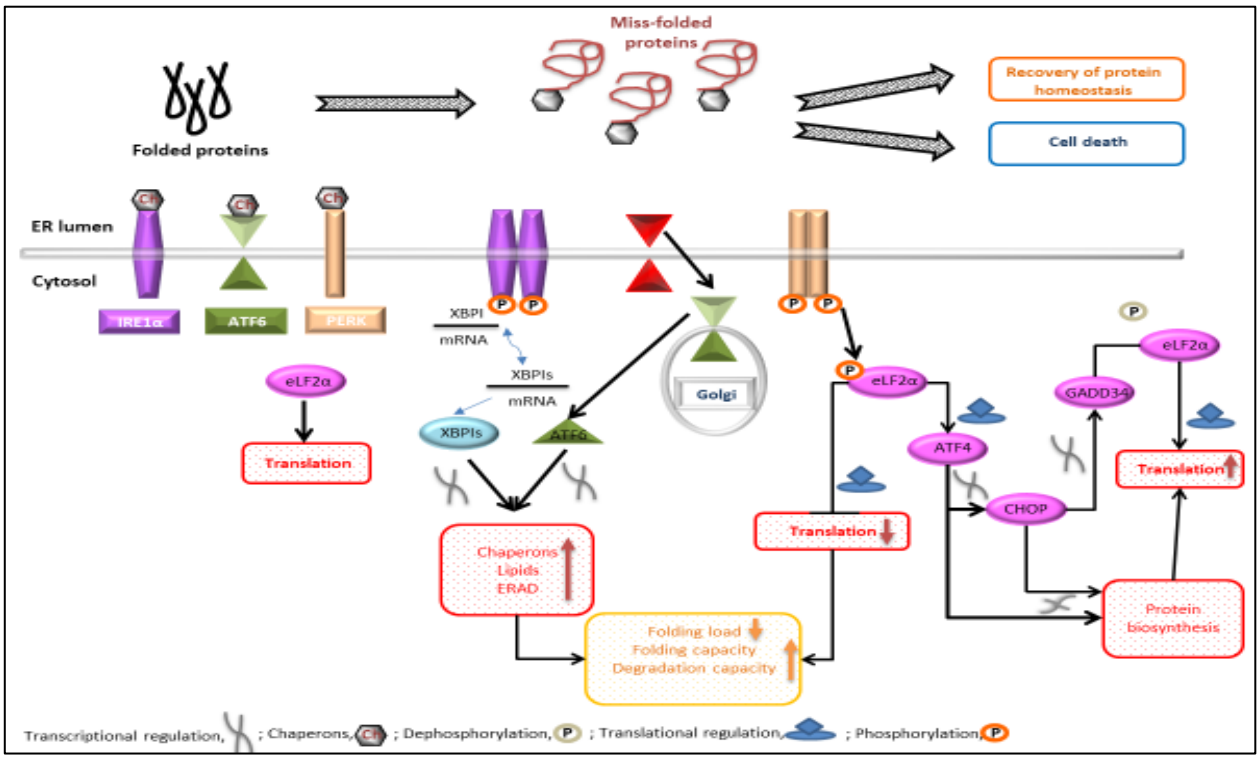


Figure 1.5: The Unfolded Protein Response (UPR). As a result of the accumulation of misfolded protein in the ER-lumen, BiP dissociates from the three ER-resident sensors (ATF6, PERK, and IRE1α) and binds to the misfolded protein, allowing the activation of these sensors and the initiation of upstream signalling to resolve the ER stress. The diagram summarizes the principal UPR signalling cascade and the resultant possible outcomes. The figure was taken from (Auner, British journal of haematology, 2015). (10)

Under conditions of prolonged ER stress, the UPR goal shifts from supporting cellular survival to one that induces apoptosis by changing its signalling towards a "terminal UPR" that ultimately drives the cell into apoptosis. (Figure 6)(47) There is still uncertainty about whether one or multiple alternative mechanisms leads to cellular death by ER stress. (10) Several pieces of evidence suggest that a diverse program of pro-apoptotic signals activates the cell death machinery if ER stress cannot be resolved. (48) One possibility is that proteins downstream of the three UPR branches provide opposing signals and that the relative timing of their initiation alters the balance between apoptosis and cytoprotective effects as ER stress persists. (49) Persistent or unresolved ER stress beyond the restoration of protein homeostasis is correlated with increased pro-inflammatory and a pro-apoptotic cell status. PERK and IRE1α are the two principal UPR receptors involved in this process. (50) IRE1α binding to TRAF2

and ASK-1 leads to the activation of the inflammatory signalling molecule p38 MAPK and activates the pathway of JNK signalling; hence, procaspase four is enabled, resulting in apoptosis. (50) In addition, IRE1α enhances the activation of several pro-death and pro-inflammatory proteins such as caspase-2. (48) CHOP induces apoptosis by overexpressing Bim, a pro-apoptotic molecule, and directly inhibiting Bcl-2, an anti-apoptotic molecule. This triggers an apoptotic cascade due to the ER release of cytochrome C into the cytoplasm. In addition, PERK induces CHOP activation, which induces GADD34 upregulation that mediates the dephosphorylation of elf-2α. This restores protein synthesis and, as a result, the build-up of the unfolded and misfolded protein inside the ER lumen, leading to proteotoxicity and oxidative stress. (50) Ca2+ depletion of the ER store induces both Bac and Bcl2 activation, which initiates cellular apoptosis. (49) The limited impact of single apoptosis-associated ER stress machinery's involvement on cell survival suggests that combinatorial mechanisms are involved in cellular death when the ER is irreversibly damaged. (49)

It has also been reported that there is a correlation between the release of multiple pro-inflammatory factors and the activation of the UPR(Figure 6). (51) IRE-1α is the most prominent UPR effector shown to regulate pro-inflammatory signals transcriptionally, but PERK and ATF6 are involved to a lesser extent in the process. (50) This regulation is primarily accomplished through transcription factors Activator Protein-1 (AP-1) and NF-kB. (50) The activation of NF-kB stimulates the expression of the effector enzymes and key pro-inflammatory cytokines of the immune response, such as cyclooxygenase, Il-6, and TNF-α. (52) It has been reported that when Human Umbilical Vein Endothelial Cells (HUVECs) show overexpression of ATF-6, this correlates with induction of severe ER stress. (53) HUVEC apoptosis is enhanced by activating caspase 3, 9 and 12, through ATF-6 overexpression. (53) In addition, ATF-6 overexpression reduces the level of anti-apoptotic while simultaneously increasing the level of pro-apoptotic molecules (Bcl-2 and Bax, respectively), which leads to the phosphorylation of JNK and CHOP, thus inducing apoptosis of the affected cell. (53) Furthermore, the PERK-ATF4 pathways were reported to induce reactive oxygen species (ROS) production, combined with a reduction of antioxidants, which characterize another significant pathway of ER stress that promotes cell death. More recently, the role of the most ER-bound effector, IRE-1α, was also studied in

correlation to atherogenesis. (54) This study revealed that using an IRE-1α inhibitor prevented the production of mitochondrial ROS and the expression of several pro-atherogenic genes (Figure 6). The correlation between ER stress and atherogenesis in glycated HDL contribution was recently examined. (55) These studies highlighted the vital role of ER stress in the progression of atherosclerosis through different actions, such as apoptosis of macrophages and vascular endothelial cells and activation of pro-apoptotic caspases. (52) The authors reported that macrophage apoptosis was prevented when PERK or CHOP was silenced or when Phenybutyric Acid (PBA) was used. (56) Moreover, XBP-1 expression was significantly upregulated in the endothelial cells (EC) isolated from atherosclerotic lesions compared to the normal aorta (56), suggesting an association between ER stress and atherosclerosis (Figure 1.6).

Overall, there is still uncertainty about the definitively associated mechanisms connecting the intrinsic cellular apoptotic pathways and ER-stress-induced UPR signalling pathways. However, it is well established that various cells exhibit a discrepancy in UPR signalling pathways' involvement in cell death. (10) Generally, the consequence of ER stress is determined by the cell type, duration, and extent of proteotoxic stress. (10)

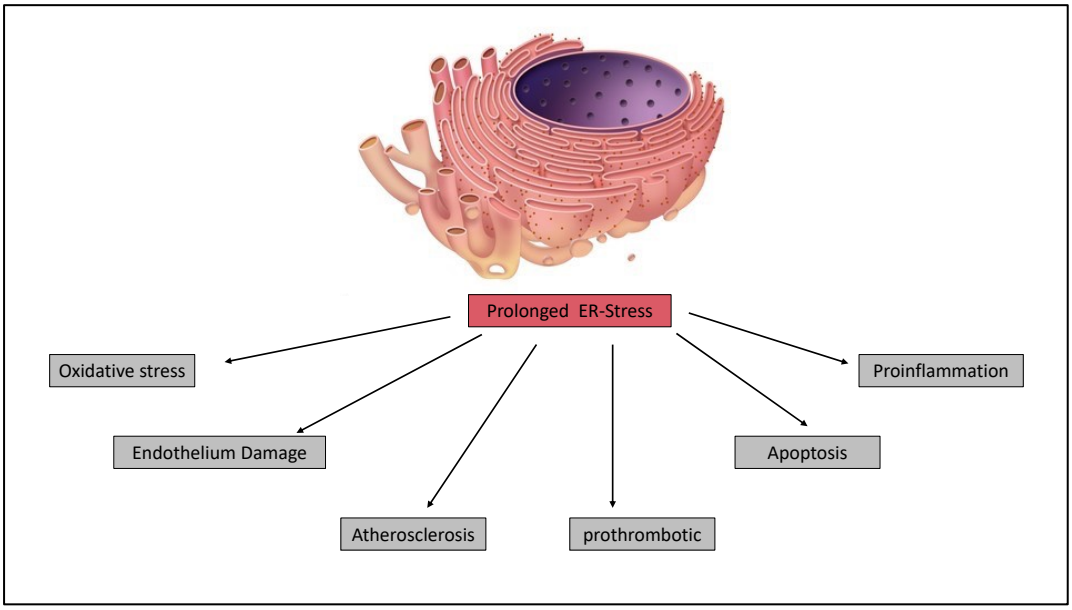


Figure 1.6: Consequences of prolonged ER stress. The ER has different pieces of machinery to sense the cellular proteostasis status and adapt to various cellular alterations. Among these, the UPR is an effective ER defence mechanism to resolve ER stress activation. However, if this mechanism fails to resolve ER stress, different levels of cellular damage can occur due to prolonged ER stress. The figure was prepared by (Ahmed Hjazi, 2021)

1.6 Proteasome inhibitors (PIs)

The introduction of proteasome inhibitors (PIs) as a therapeutic agent for multiple myeloma has advanced management and survival for plasma cell cancers. (57) Optimization of dosing schedules and steady adaptation with toxicity profiles have informed the recent use of proteasome inhibitors as significant components of numerous treatment regimens. Mainly, the PIs target the secretory feature of multiple myeloma cancer cells (MMCs). (58) Cancer cells typically have greater demand for proteasome activity than normal cells, making them more sensitive to the pro-apoptotic consequences of proteasome inhibition. (58) These facts make proteasome inhibition a tractable therapeutic candidate in oncology. (59) Generally, proteasome inhibitors target ERAD in multiple myeloma cells (MMCs). (60) They inhibit the proteasome 26S in particular, which leads to impaired proteolysis activity. (60) Once this occurs, a cellular selective mechanism is activated to resolve the harmful impact of this inhibition, known as the unfolded protein response (UPR). (61) However, if this mechanism fails to achieve the aimed purpose, it will eventually trigger the cell to undergo apoptosis. (62)

PIs are a therapy that enhances survival and quality of life and provides a significant therapeutic response, particularly in poor-prognosis multiple myeloma patients. (63) Currently, three proteasome inhibitors (PIs) are licenced to treat multiple myeloma. (63) The first-class PI, Bortezomib (BTZ), treats both newly diagnosed and relapsed/refractory MM (RRMM); CFZ, a second-generation PI, treats RRMM as both a monotherapy and in combination with other anti-myeloma agents; and the third generation PI Ixazomib, which is considered the first oral PI, treats RRMM (Figure 1.7).(64) Based on their active moiety and chemical structure, PIs can be categorized into three clusters: boronates, salinosporamides, and epoxyketones. (63)

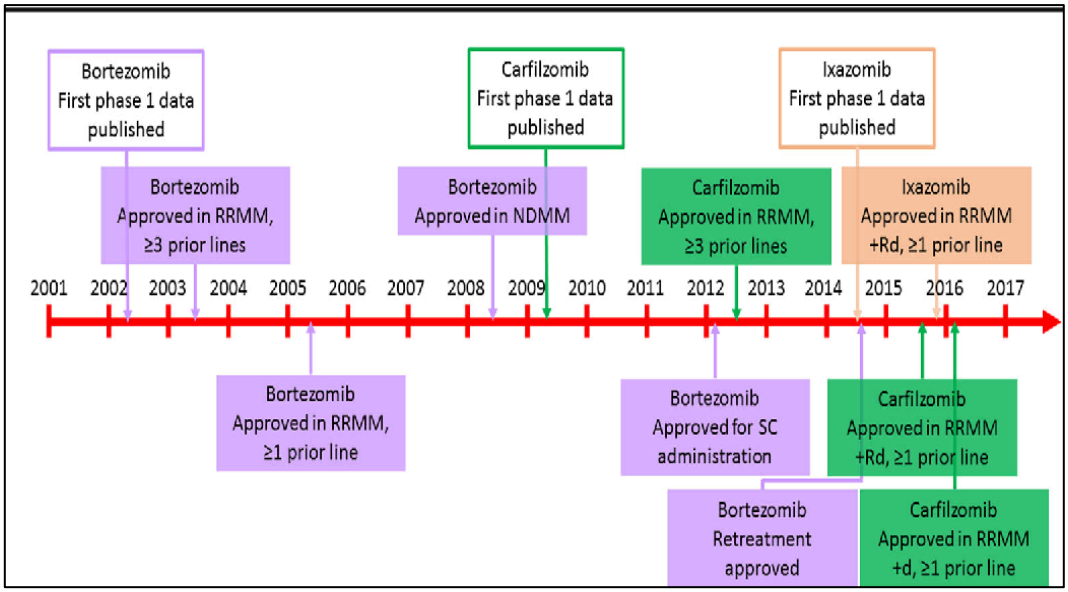


Figure 1.7: Timeline of the proteasome inhibitor approval for clinical usage. Timeline of the three FDA-certified proteasome inhibitors in MM showing dates of original publications and authorizations. RRMM, relapsed/refractory multiple myeloma NDMM, newly diagnosed multiple myeloma; Rd, lenalidomide, d, dexamethasone. This figure was adapted from. The figure was taken from (Gandolfi, Cancer and Metastasis Reviews, 2017) (57)

1.6.1 Boronate and Salinosporamides

1.6.1.1 Bortezomib (BTZ) is a dipeptidyl boronic acid-based chemical structure drug. It was approved by the Food and Drug Administration (FDA) for treating multiple myeloma in 2003. (65) The drug reversibly binds to the proteasome and targets the caspase-like and chymotrypsin-active sites, with marginal influence on trypsin-like activity. (65) Results from the phase III VISTA trial suggested an almost one-third reduction of risk of death amongst MM patients who were administrated BTZ plus melphalan and prednisone (VMP) compared with those treated with melphalan (MP) alone. (66) Additionally, *in vitro* studies have revealed that BTZ improves the sensitivity of MMCs to standard drugs and overwhelms those cells with chemotherapeutic agent resistance. (67) Usually, the drug is administered with other MM main treatments (cyclophosphamide and/or dexamethasone) to develop its maximum effectiveness. (68)

Several mechanisms could describe the cellular toxicity effect of this drug. These include suppressing tumour survival pathways, obstructing tumour metastasis, and inhibiting tumour growth and angiogenesis. (69) BTZ directly induces apoptosis of

tumour cells and constrains the stimulation of NF-κB in cells and in the tumour microenvironment. (69) It also diminishes adherence of myeloma cells to the bone marrow microenvironment and inhibits the expression and intracellular signaling of IL-6 in myeloma cells. (69) In addition, BTZ suppresses the expression of proangiogenic mediators and apoptotic regulators. (69)

However, a recent meta-analysis reported by Xiao *et al*. revealed that the prevalence of all grades and high-grade BTZ-associated cardiotoxicity was 3.8% and 2.3%, respectively. (70) In addition, reported side effects were seen with the usage of BTZ in MM patients. (70) These side effects range from mild side effects, such as dizziness and nausea, to more serious adverse events such as neuro/nephro toxicity(71), so that prolonged usage of BTZ treatment is restricted by the development of BTZ resistance and treatment-generated peripheral neuropathy. (71)

6.1.2 Ixazomib is a natural lactone composite drug derived from the marine bacterium *Salinospora tropica.* (57) Ixazomib is an irreversible PI that slightly disturbs the caspase-like activity only within the proteasome. (72) This effect provides an exclusive effectiveness and safety profile and does not display cross-resistance with other PIs.(72) The activation of caspase-8–mediated signalling pathways are mainly the Ixazomib-induced apoptosis mechanism. (73) *In vitro* studies have proved the antitumour capability of this drug against multiple myeloma cells, other hematologic malignancies, and solid tumours. (73)

1.6.2 Epoxyketones

1.6.2.1 CFZ (PR-171) is an irreversible epoxyketone PI structurally and mechanistically similar to BTZ. (74) The FDA approved this drug to treat multiple myeloma in 2012. (74) According to the initial drug studies, approval was given for a 27mg/m2 dosage of CFZ twice weekly in a two consecutive-day pattern as a monotherapy (75), and current guidelines now recommend human clinical drug dosage ranging from 20 to 75 mg/m^2 and can exclusively give it intravenously. (75) Recently, the outcome of two landmark studies, the Aspire and Endover CFZ clinical trials, have led to the combined usage of CFZ with dexamethasone, or lenalidomide plus dexamethasone in the European Union and the USA.(76) Currently, a 56mg/m2 CFZ dose combined with dexamethasone is the CFZ twice-weekly standard protocol

based on the recommendations of the ENDOVER study findings.(76) However, the difficulty of intravenous infusion of the drug twice weekly is a significant burden for healthcare providers and patients. For this purpose, recent studies have recommended using a more accessible once-weekly dosing standard instead. (77) This establishes an essential milestone for future research using 70mg/m2 of CFZ once weekly in clinical practice. (77) The usage of CFZ requires evidence of disease progression within the last two months of administering the last therapy and a clinical history of two previous treatments. (77) The drug is rapidly metabolized extrahepatically in approximately 30 to 60 minutes after IV infusion, thus providing advantageous minimal renal side-effects in contrast to the first-generation PIs.(78)

Similar to BTZ, CFZ obstructs both the constitutive and immunoproteasome and has comparable effectiveness against the β5 and LMP7 subunits. (78) In addition, it also shows potent inhibition of the caspase-like activity of the β1 subunit and trypsin-like inhibitory activity of the β2 subunit of the 20S proteasome. (78) Studies have revealed robust inhibition of the β5 subunit chymotrypsin-like activity that is superior to BTZ. (78) The irreversible binding and the broader site selectivity interactions of CFZ enhance its inhibitory effect and overcome BTZ resistance. (79) Indeed, CFZ-survival rates in RRMM were significantly higher than in the BTZ group. (6) This could indicate a superior effect of CFZ among these patients. (80) Moreover, there was a significant enhancement of the RRMM survival rate when CFZ and dexamethasone were combined compared to the usage of BTZ plus dexamethasone. (81) A high dose of CFZ can induce sufficient β5/ β2 subunit inhibition, which is more effective than the B5/B1 subunit inhibition produced by BTZ.(82)

Additionally, it was proved that the β5/β2 co-inhibition achieved by CFZ was more effective in treating primary cells and refractory MM cell lines than the same BTZ inhibition profile. (83) The randomized phase three ENDEAVOR study showed that CFZ-treated patients had advanced rates of more significant responses, explained by meaningfully extended progression-free survival than the BTZ-group. (84) According to Kyprolis *et al*. there was an almost 25% improvement of partial response (tumour reduction) and 48% higher overall response to therapy in the CFZ group compared to the BTZ group. (85) Notably, the wide dose range of CFZ can establish easy and safe β2 inhibition titration levels. (86) Thus, this can maximize the CFZ level tolerated level in the clinic. (10) Together, these advantageous features contribute to advanced treatment response to CFZ.

The specific mechanisms by which CFZ promotes cell death and its specificity for MMCs are only partly understood. Generally, the chronic induction of ER stress by CFZ in MMCs shifts the regular UPR cytoprotective function to be apoptotic. (87) However, there is still uncertainty about whether single or multiple alternative mechanisms leads to cellular death by prolonged ER stress. (88) One potential possibility is that proteins downstream of the three main UPR branches initiate apoptosis as ER stress persists. (88)

PERK and IRE1α are two principle UPR receptors involved in this process. The binding of IRE1α to TRAF2 and ASK-1 activates the inflammatory signalling molecule, p38 MAP kinase, and activates the JNK signalling pathway. (10) This activation leads to the subsequent activation of the procaspase-4 pathway that results in cellular death. (10) PERK activation induces cellular death by different mechanisms. (10) Activation of PERK leads to activation of eIF2α by phosphorylation, which activates the ATF4 transcriptional factor. Subsequently, ATF4 activates CHOP, a pro-apoptotic transcriptional factor, which initiates GADD34 expression. (10) GADD34 activation mediates the dephosphorylation of elf-2α, thus restoring protein synthesis and, as a result, the build-up of the unfolded and misfolded protein inside the ER lumen. (10) This toxic accumulation of misfolded proteins in the ER lumen leads to oxidative stress. (89) In addition, CHOP induces apoptosis by overexpressing the pro-apoptotic molecule Bim and directly inhibiting the anti-apoptotic molecule Bcl-2(10). This overexpression triggers the initiation of the intrinsic apoptotic reaction cascade due to the ER release of cytochrome C into the cytoplasm. (10) The activation of the second primary ER stress receptor, IRE1α, enhances pro-apoptotic proteins and pro-inflammatory pathways such as caspase-2. (47) The suppression of NF-kB activity that leads to inhibition of cytokine-dependent survival pathway and cell adhesion disturbance could also be proposed as alternative mechanisms to induce MMCs death by CFFZ. (10) It was observed that CFZ activates the downstream UPR-apoptotic signals, caspases 9, 3 ,and 8, suggesting intrinsic and extrinsic caspase pathways. (90). All these mechanisms suggest the ability of CFZ to induce cancer cell death with the involvement of different cellular mechanisms.

1.7 CFZ associated cardiovascular complications

Although the continued development of cancer-targeting therapies has revolutionized oncology, many of them are associated with significant cardio-vascular toxicity. (90) Cardiovascular adverse events (CVAEs) involve cardiovascular diseases, such as heart failure, hypertension, cardiac arrhythmias, ischemic events, and thrombosis, and this collection of medical complications, which are considered the most dangerous CFZ-associated side effects in MM (91), have been gradually increasing since the initial approval of the drug for the treatment of MM(92) (Figure 1.8).

	Hypertension		Cardiac failure		Ischemic heart disease		Dyspnea	
	All grades	Grade ≥3	All grades	Grade ≥3	All grades	Grade ≥3	All grades	Grade ≥3
Phase 3 studies								
ASPIRE[37†]								
KRd group (n=392)	14.3	4.3	6.4	3.8	5.9	3.3	19.4	2.8
Rd group (n=389)	6.9	1.8	4.1	1.8	4.6	2.1	14.9	1.8
ENDEAVOR[31§]								
Kd group (n=463)	25	9	<9	<6	<3	<2	28	5
Vd group (n=456)	9	3	<4	<3	<4	<3	13	2
FOCUS[40]								
Carfilzomib group (n=157)	15	3	5	2			15	1
CS±cyclophosphamide group (n=158)	6	0	1	1			9	0
Phase 2 studies[38*]								
Carfilzomib (n=526)			7.2	5.7	3.4	1.3		

Figure 1.8: Different CFZ-cardiovascular associated events in patients with relapsed/refractory multiple myeloma. Three landmark studies, ASPIRE, ENDEAVOR, and FOCUS data, showed that CFZ was associated with an increased rate of various cardiovascular complications, including hypertension, cardiac failure, ischemic heart disease, and dyspnea. These outcomes were when the CFZ was used alone or combined with lenalidomide, or dexamethasone compared to BTZ. K: carfilzomib; R: lenalidomide; d: dexamethasone; V: bortezomib; CS: corticosteroids. This figure is adopted from. The figure was taken from (Bringhen, Haematologica, 2018).(93)

A systematic review and meta-analysis showed that, among 2594 patients, 18.1% developed varieties of CVAEs and that CFZ–associated hypertension was significantly higher in MM patients than those treated with BTZ. (94) In another study, CFZ caused severe cardiotoxicity, with up to 7.2 % of patients developing treatment-emerging heart failure. (95) Waxman *et al*. performed a retrospective analysis of 2,594 MM patients and showed that 18.1% of CFZ-treated patients experienced all-grade CVAEs.(95)

Among 526 patients who received CFZ monotherapy, 7.2% and 22.1% demonstrated signs of cardiac failure and CVAEs during treatment, respectively. (96) Taken together, these findings suggest a higher rate of CFZ-associated cardiac side effects compared to BTZ.

The CFZ dosage and infusion time are considered principal cofactors in drug-associated CVAEs(97), and it has been proved that a higher proportion of cardiovascular complications occur with a higher dosage of the drug. (97) Similarly, a shorter drug infusion rate of 2-10 min was significantly correlated with increased risk of the CFZ-associated CVAEs compared to a 30-minute optimal drug infusion time. (97)

Research has recognized that risk factors, such as age and obesity among MM patients, are linked to cardiovascular disease. (98) However, clinical studies argue that patient-related risks, such as lifestyle and age, and disease-related risks, such as amyloidosis, renal impairment, and anemia, also need to be considered before making conclusions about drug safety. (98). In agreement, some studies found that MM patients have higher comorbidities at baseline, leading to higher CVAE rates. (99) Indeed, according to Bringhen *et al*., there were raised events of cardiovascular complications of MM patients at reference point compared to non-MM patients. (98) This correlation suggests that multiple myeloma patients are considered an increased-risk population for cardiovascular diseases. Among 32,193 MM patients in a retrospective study, almost 66 percent suffered cardiac events during baseline. (99) Thus, making a judgment about cardiac drug toxicity is extremely challenging in the presence of all these contrasting facts.

1.8 The potential impact of CFZ on the endothelium

Various mechanisms could be proposed to link endothelial dysfunction (ED) to CFZ exposure. These include cellular inflammation, apoptosis, induction of pro-thrombotic factors, and oxidative stress resulting from diminished Nitric Oxide (NO) production and a decrease in NO bioavailability. (6) Current findings have determined that CFZ activates MM cell apoptosis by enhancing ER stress. (78) Therefore, it is assumed that CFZ unfavourably affects ECs via a comparable pathway. (78) ER stress in

endothelial cells ultimately leads to endothelial damage. This results in an increased risk of pro-inflammatory and pro-thrombotic activation of the endothelium. (78)

Several adhesive and signalling inflammatory mediators are involved in all stages of atherosclerosis, the foundation of several cardiovascular diseases, including activation of vascular endothelium, early lesion formation, lesion progression, and plaque rupture. (100) The expression of cytokines, growth factors, and tissue factors also contributes to the inflammatory response of the endothelium (100), and there are documented links between these pro-inflammatory alterations and the activation of the UPR. For instance, the most prominent UPR effector, IRE-1α, stimulates pro-inflammatory signalling through NF-kB. (101) Mitochondrial ROS production, atherogenic chemokines, and cytokine upregulation are prevented using an IRE-1α inhibitor. (102)
NO's role has also been examined in ER stressed endothelium, where endothelial nitric oxide (eNOS) mRNA and protein expression was significantly diminished. (103) The expression and activity of eNOS were also reduced in coronary artery endothelium when ER stress was induced by tunicamycin. (104) Furthermore, it has been shown that increasing ROS in the vasculature causes endothelium dysfunction. (105) This is caused by reducing NO bioavailability that ultimately leads to oxidative stress. (105) Viewed collectively, these mechanisms could explain the proposed damage impact of CFZ on the endothelium. Primarily, the potential ER stress activation in the endothelium by CFZ could lead to the failure of the UPR to resolve the stress. Thus, the endothelium could potentially be activated, causing oxidative stress, pro-inflammatory cytokine production and pro-thrombotic factor recruitment, which in turn results in endothelium damage. This potential damage could be translated into a variety of CFZ-associated cardiovascular side effects.

1.9 The endothelium & endothelial dysfunction

1.9.1 Physiological endothelium

The vascular endothelium is advantageously located on the inner lining of the vasculature known as the intima. (106) It possesses diverse metabolic, immunologic, and secretory roles (107) and responds to several hormones, vasoactive factors, and

neurotransmitters. (106) This interaction significantly contributes to controlling vasomotion, inflammation, thrombosis, and platelet aggregation, maintaining the blood vessel's steady state and functionality. (108) The endothelium releases numerous vasoactive factors to maintain fine vascular tone(109), and regular blood flow is maintained by controlling various endothelium-derived substances' release and expression. (110) Primarily, these can be vasoconstrictive factors such as thromboxane A2 (TXA_2) and endothelin-1 (ET-1), or vasodilatory factors such as nitric oxide (NO), which is essential for protecting blood vessels from injury and maintaining normal haemostasis (110), prostacyclin (PGI_2), and endothelium-derived hyperpolarising factor (EDHF). (109)

1.9.1.1 Prostacyclin and Thromboxane A2

Thromboxane A2 and prostacyclin, also called prostaglandin I2 are endothelium-derived prostanoids, and their synergistic actions regulate vascular function. (109) Cyclooxygenase (COX) enzymes stimulate their production, of which there are two isoforms COX-1 and COX-2. (111) ECs constitutively express COX-1, whereas they express COX-2 when the endothelium is impaired and exposed to inflammatory cytokines. (112) PGI_2 receptors are found on both platelets and vascular smooth muscle cells (113), and PGI_2 binding activates the IP receptor in both cell types. (113) This activation results in the inhibition of platelet aggregation and smooth muscle relaxation. (114) It was reported that residual vessel dilation was caused by increased PGI_2 synthesis when nitric oxide (NO) was blocked. (115) This suggests that PGI_2 has a compensatory action in the dilation of the vessel apart from NO vasodilation action. (115)

On the other hand, TXA_2 causes vasoconstriction and platelet aggregation, in contrast to the PGI_2 function. (116) Similarly to prostacyclin, thromboxane receptors are found in platelets and smooth muscle. (116, 117) The binding between thromboxane and thromboxane-prostanoid (TP) receptors in the platelet trigger platelet aggregation. (116) Similar binding in the smooth muscle leads to increase intracellular Ca^{2+} levels that result in vasoconstriction. Altogether, the equilibrium activity of TXA_2 and PGI_2 aids to sustain homeostasis in the healthy vessel. (117)

1.9.1.2 Endothelin-1

Endothelin-1 (ET-1) is a very effective vasoconstrictor factor secreted by the endothelium. (109) Three endothelin-1 isoforms, ET-1, ET-2, and ET-3, are found in the human body. (109) However, the endothelium only releases the first isoform ET-1.(109) The endothelium release and production of this hormone is stimulated by inflammatory signals such as interleukins and TNF-α and is reduced by PGI_2 and NO. (118) ET-1 receptors have been described in endothelial cells (ET-B1) and smooth muscle cells (ETA and ET-B2). (119) In common with thromboxane, endothelin-1, causes vasoconstriction by increasing the intracellular $Ca2^+$ concentration. (119) The endothelium ET-B1 receptor activation then triggers vasodilatation by prompting the release of NO and PGI_2.(120)

It has been shown that under endothelial dysfunction (ED) conditions, there is an upregulation of endothelium ET-B2 receptors and smooth muscle receptors, thus enhancing vasoconstriction. (121) The influence of each receptor on the vasculature has been studied in healthy participants and patients with heart disease. (121) Notably, there was vasodilation induction in ED participants when the ETA receptors were blocked. (121) While in healthy applicants blocking ETB receptors cause vasoconstriction. (121)

Apart from its vasoactive consequences, ET-1 also triggers smooth muscle cell proliferation and initiation of inflammation in the vessel. (122) Attachment of ET-1 to ETA receptors stimulates macrophages, enhances neutrophil-vessel wall connections, and promotes free radical concentrations, all of which lead to endothelium dysfunction. (122) In addition, a correlation between ETA receptor inhibition in diseased vessels and the reduction of reducing atherosclerosis has been described, suggesting that ETA receptors function during ED. (123) ET-1, therefore, contributes to the pathogenic processes in the cardiovascular system by possessing both proliferative and inflammatory effects. (124) It reverses NO's effect at a different molecular level. (109) It reduces NO's release by inhibiting eNOS, producing superoxide anions (O2), a potent free radical that further reduces NO bioavailability. (109) It also increases reactive oxygen species (ROS) production by activating NADPH oxidase. (109)

1.9.1.3 Endothelium-Derived Hyperpolarizing Factor (EDHF)

(EDHF) is a still-unknown vasodilator substance that hyperpolarises smooth muscle by creating a negative charge on the cell membrane. (125) The agonist's stimulation triggers EDHF release by the endothelium. NO, and PGI2 is also involved in vessel dilation by hypopolizration. (126) However, inhibition of these substances was insufficient to achieve the complete absence of vessel hypopolizration, suggesting a third factor in this process. (127) Three factors describe membrane hyperpolarisation, stimulation of endothelial receptors, and the subsequent rise in Ca^{2+} levels triggers K+ efflux from the cell. (128) This causes the smooth muscle to release K+, causing hyperpolarisation. (128) The smooth muscle cell membrane potential modification decreases intracellular Ca2+ levels, causing smooth muscle relaxation. (128)

1.9.1.4 Nitric Oxide (NO)

NO is the most crucial endothelium-derived substance that acts as a vasodilator on the smooth muscle. (109) It is also considered a critical regulator of endothelial oxidative stress resulting from reactive oxygen species (ROS) and inflammation. (109) The enzyme nitric oxide synthase (NOS) stimulates NO production by converting L-arginine into NO. (109) Three isoforms of NOS exist, the macrophage or inducible isoform (iNOS), the neuronal isoform (nNOS), and the endothelial isoform (eNOS), which yields nitric oxide in the vasculature. (109)

NO production begins when inactive eNOS is connected to the protein caveol, found in the caveola, a small invagination in the cell membrane. (129) When Ca^{2+}intracellular levels increase, eNOS disconnects from caveolin and activates. (129) The ER release of Ca^{2+} that triggers the detachment of eNOS from caveolin is caused by NO agonists. (130) These include acetylcholine (ACh), adenosine diphosphate (ADP), bradykinin (BK), substance P, thrombin, and adenosine triphosphate (ATP). (131) Once intracellular Ca^{2+} stocks decrease, a signal is sent to the membrane receptors to open Ca^{2+} channels permitting extracellular Ca^{2+} into the cell. (132) Lastly, Ca^{2+} molecules that enter the cell bind to the protein calmodulin located in the cellular cytosol. (132) This binding initiates the structural change of calmodulin, which allows it to bind to eNOS.(133) Finally, eNOS converts L-arginine into NO, released from the endothelium as a gas or accompanying other molecules. (133) The phosphorylation of eNOS is

another mechanism the cell employs to regulate NO production. (134) This occurs via protein kinases such as cyclic guanosine-3', 5-monophosphate (cGMP) protein kinase-dependent Ligand protein kinase (Figure 1.9). (134) eNOS phosphorylation at some specific phosphorylation sites, including Ser-116, regulates the basal secretion of NO from endothelial cells. (135) Moreover, eNOS phosphorylation improves eNOS interaction with caveolin-1 and diminishes the vascular responsiveness of intact aortic rings, controlling vascular tone. (136) In general, increased eNOS phosphorylation correlates with improved endothelial NO release.

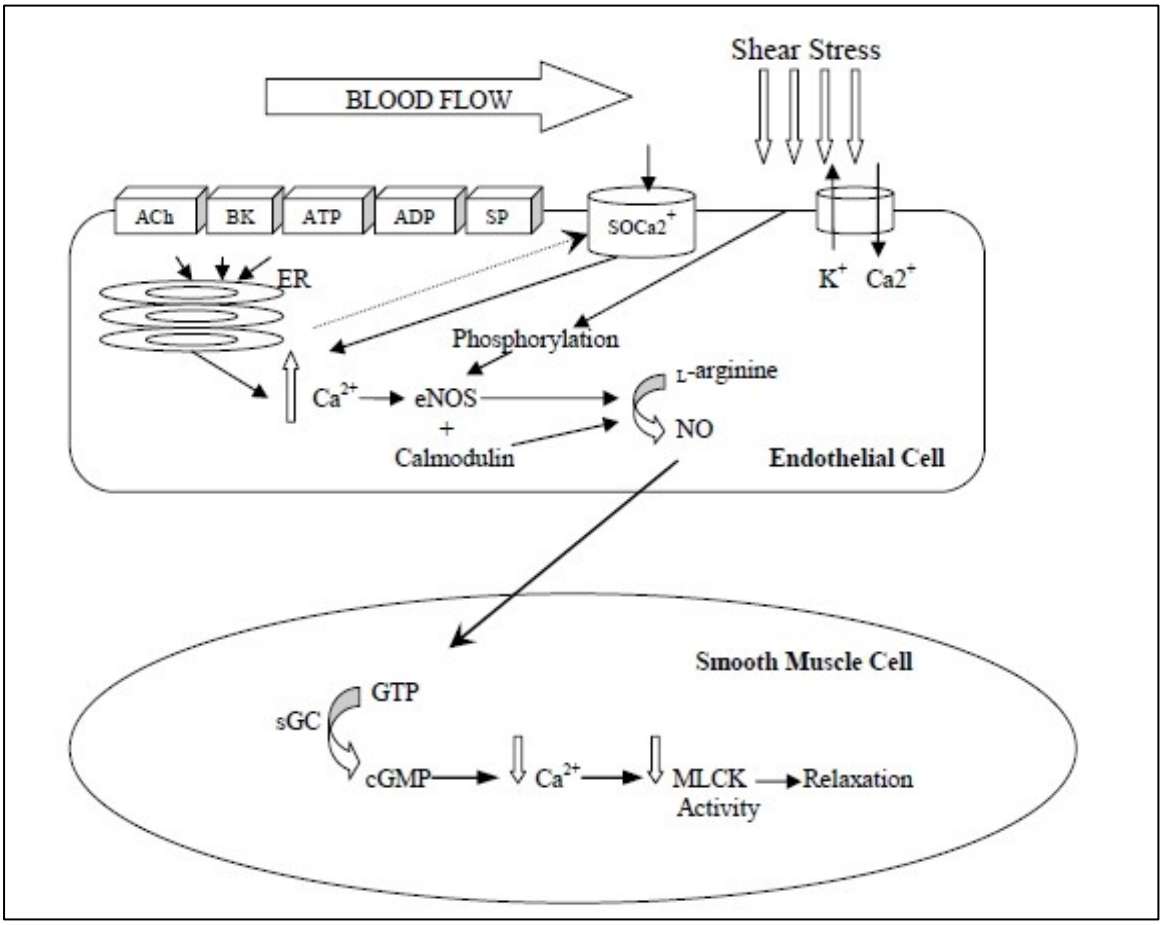


Figure 1.9: Nitric oxide production in the endothelium, and its influence on the vascular smooth muscle cell. ATP= adenosine triphosphate; ACh=acetylcholine; SP= substance P; BK= bradykinin; ADP= adenosine diphosphate; NO= nitric oxide; SOCa2+= store-operated Ca2+ channel; sGC= soluble guanylyl cyclase; cGMP= cyclic guanosine-3', 5-monophosphate; ER= endoplasmic reticulum; MLCK= myosin light chain kinase. *The Ca2+ stores depletion of the endoplasmic reticulum a signal is directed to SOCa2+ channel which permits extracellular Ca2+ into the endothelial cell. The figure was taken from (Danial, British Journal of Haematology, 2015). (124)

Once created, NO diffuses into the bordering smooth muscle through the endothelial cell. (137) This reduces smooth muscle tension by recruiting soluble guanylyl cyclase enzyme (sGC). (137) Further, it also aids to rebuild Ca^{2+} stores in the sarcoplasmic reticulum, which reduces smooth muscle cell contraction. (138) These mechanisms constantly operate and maintain the basal vasodilator tone achieved by NO.(138). It was reported that a dose-dependent escalation in blood pressure was observed due to the vessels constricting, which was inverted when NO was administered. (138) These outcomes indicate NO's significance in maintaining resting vasodilator tone.

Apart from vasodilatation, NO downregulates platelet adherence and aggregation to the endothelium and plays a significant role in anti-inflammatory and anti-thrombotic functions. (139) In addition, it prevents the adhesion of leucocytes and blocks mRNA translation of a variety of adhesion molecules such as intercellular adhesion molecule (ICAM-1), P-selectin, and vascular cell adhesion molecule (VCAM-1). (140) Thus, this prevents leukocyte attachment to the endothelium and further activation of inflammatory response. (141) It had been reported that there was significant induction of P-selectin when NO was inhibited. (142) NO can also inhibit the production of various immuno-modulatory cytokines (e.g., IL-1, L-12) by macrophages. (143) Nitric oxide production by the endothelium is also physiologically significant in maintaining basal systemic and coronary tone, particularly at the base of the arterioles (resistance vessels) in the vascular circulation. (144) In the average coronary circulation, NO maintains both arteriolar dilator and basal epicardial tone. (144)

The endothelium functions as a barrier to limit the transportation of components between the lumen of blood vessels and the interstitium. (144) The penetrability of this barrier, which is vital for homeostatic balance, is also regulated by NO.(144) Lastly, it has been reported that NO has a remarkable anti-oxidative effect. (145) This was demonstrated by the amplification of the antioxidant ability of plasma by the administration of NO donors. (145) In addition, the ability of NO to eliminate O2- has been recognized both *in vitro* and *in vivo*. (146) These facts significantly highlight the broad spectrum of NO activities in the endothelium.

1.9.2 Endothelium Dysfunction (ED)

The endothelium forms a vital segment of the vasculature and supports an athero-protective environment *via* the function of endothelial cell-derived vasoactive factors. (147) Altered vascular homeostasis is known as endothelial dysfunction (ED)(147) and occurs when the endothelium fails to maintain normal function. This phenomenon, in turn, occurs during the initial and late stages of different cardiovascular events. (148) ED is mainly characterized by the four following features. Firstly, a reduction in NO bioavailability resulting from decreased NO production and increased generation of reactive oxygen species (ROS). (149) Secondly, failure to mediate vasodilation(149). Thirdly, overproduction of adhesion molecules, growth factors, inflammatory molecules (e.g., cytokines), ROS, chemokines, and altered (excessive or impaired) angiogenesis(149). Lastly, enhanced thrombosis and disrupted fibrinolysis. (107) The activated endothelium facilitates the formation of the inflammatory microenvironment by enhancing monocyte adhesion, rolling and diapedesis across the vessel wall via interaction with adhesion molecules. (149) Leukocyte infiltration to the site of infection or injury is a notable feature of inflammation, which NO can strongly influence. (109) Inhibition of NO production results in a noticeable rise in leukocyte adherence to the endothelium and subsequent atherosclerosis and may cause various cardiovascular diseases to develop. (150) The activated endothelium itself also releases inflammatory cytokines such as interleukin-6 and TNFα, , which amplify the inflammatory response. (151) In general severe ED leads to the elimination of NO release, which modifies the agonists' function from vasodilation stimulator to vasoconstriction influencer. (152) All these effects of endothelial dysfunction are essential in developing a variety of ED-associated disorders. (153) These include systemic hypertension, pulmonary hypertension, congestive heart failure, etc., all of which are associated with diminished endothelium functions. (153)

1.10 Coagulation and Haemostasis

1.10.1 Introduction to the coagulation system

The coagulation system is a complex, connected system that primarily maintains the fluidity of blood in the cardiovascular system while permitting the rapid development

of blood clots to avoid haemorrhaging following vessel damage. (154) Thrombus development is the end goal of a sequence of enzymatic reactions and protein interactions, commonly referred to as the Coagulation Cascade. (154) The system's main elements are platelets, coagulation factors, inhibitors, the vessel wall, and the fibrinolytic system. (154) The initial activation of the coagulation system occurs when the vessels are damaged, and the endothelium lining the blood vessel is exposed to the bloodstream, thus stimulating the activation of the coagulation process. (155) This primarily involves two broad and central haemostatic systems: the primary and the secondary coagulation pathway. (155) Prior to creating fibrin inside a clot, primary haemostasis, arising from the activity of platelets, occurs, yielding a platelet plug. (155) Secondary haemostasis describes the creation of a fibrin scaffold, which is essential to steady the platelet plug created by the proteolytic coagulation cascade at the injury site. *In vivo*, two routes eventually end in thrombin development, and hence the cleavage of fibrinogen to fibrin as a part of the secondary haemostasis. (155) The 'Extrinsic pathway' or the 'Tissue Factor pathway' is the primary pathway for inducing blood clotting. (155) Stimulation of this pathway produces a 'thrombin burst', which eventually leads to platelet aggregation, fibrin development and stabilisation, and the prevention of fibrinolysis. (156) The second pathway is the 'Intrinsic pathway' or 'Contact Activation', which initiates with the establishment of a core complex of collagen via high molecular weight kininogen (HMWK), Factor XII (FXII) and prekallikrein. (156)

1.10.2 Primary haemostasis

1.10.2.1 Introduction to Primary haemostasis

Primary haemostasis is the phrase used for the instant plug development upon damage of the vessel wall, which is accomplished by vasoconstriction, platelet adhesion, and aggregation (Figure 1.10). Generally, primary haemostasis contains two main components: vasculature (VWF and other coagulation regulators) and platelets. (157) The blood vessel wall has an essential capacity to constrict when damaged, causing reduced blood flow to the injured area. (157) This is physiologically valuable in that it both reduces blood flow to a wounded area and permits blood to be "rerouted". (158) Thus, the body can continue to deliver blood supply to the tissue.

(159) The fibrin construction is not compulsory for haemostasis at this step. (159) Primary haemostasis is, however, only temporarily efficient. (159); haemorrhage may begin without secondary haemostasis supporting the platelet plug by creating a stable fibrin clot. (159)

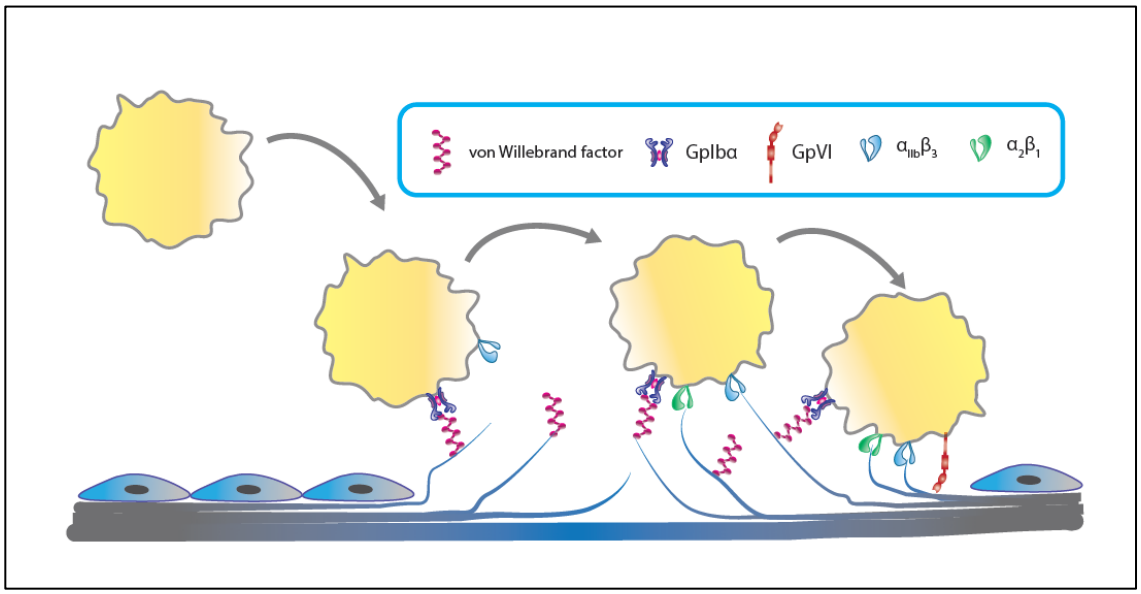


Figure 1.10: Graphic sketch of platelet adhesion to the injured vessel wall. The adhesion of platelets is essential following vascular injury. It is usually described as the first step by which single platelets bind to the cellular and extracellular matrix components of vessel walls such as VWF and tissues through specific membrane receptors, initially in the exposed sub-endothelium, interaction between GP Ib-IX-V complex and subendothelial VWF A1 domain. This process leads to platelet reduction, firm adhesion to sub-endothelium, change in the shape of platelets, and platelet recruitment (platelet-to-platelet adhesion, or aggregation). As a result, thrombus forms, stopping haemorrhages and allowing wounds to heal. The figure was taken from (Versteeg, New fundamentals in haemostasis. Physiological reviews, 2013) (160).

1.10.2.2 The sequence of events of primary haemostasis

As platelets circulate, they can interact with endothelial cells, which form a barrier to the underlying sub-endothelial matrix. (161) Under normal conditions, endothelial cells secrete nitric oxide (NO), and prostacyclins function as effective negative controllers of platelet adhesion and activation by delivering repressing signals to guarantee that platelets stay in a latent state. (161) Upon vessel injury, the endothelial barrier is disturbed, revealing pro-thrombotic surfaces that contain the Tissue Factor (TF), Von Willebrand factor (VWF), and collagen. (161) As blood is revealed to hydrophilic injury

surfaces, accumulation of plasma-borne VWF and fibrinogen on the extracellular matrix delivers other sites of interaction. (162) The initial adhesion of platelets to the place of the wound is chiefly facilitated by collaborations between the platelet surface glycoprotein GPIbα and immobilized VWF, with additional binding locations for VWF on platelets offered by $\alpha_{IIb}\beta_{III}$. (162) Consecutive reinforcement of the connections between collagen, VWF, GPIbα and $\alpha_{IIb}\beta_{III}$ obstructs the original rolling movement of platelets on pro-thrombotic surfaces and permits other collagen receptors to bind such as GPVI and $\alpha_2\beta_1$. (163)The functional significance of VWF-GpIbα connections for haemostasis is demonstrated by the severe bleeding phenotype shown in people with von Willebrand disease type 3 and Bernard Soulier syndrome, which is linked to the lack of VWF and GpIb, respectively. (163) Three central receptors facilitate platelet adhesion; the integrin receptors (GPVI and α2β1) bind directly to collagen, and the hetero-tetrameric receptor (GPIb-IX-V) binds to VWF. (159) The third receptor is fundamentally expressed on platelets and is observed as a complex of two glycoproteins (GPIb and GPIX). (164) The VWF interaction with platelet is described in detail below in (Section 1.12).

According to existing models, platelets are involved in this process in several steps. (165) These include releasing a mixture of bio-active elements created de novo or stored in intracellular granules, mechanically engaging other platelets to the thrombus, accelerating and focussing the coagulation response, and shaping the overall thrombus environment to establish distinctive zones with heterogeneous arrangement and function. (166) The primary stimulatory sign provoking these reactions in single platelets adhering to the injured vessel wall is believed to be facilitated by collagen receptors, of which GPVI is commonly found to be the most important. (166) With the continuing collection of a three-dimensional thrombus, various G protein-coupled receptors on the platelet surface are stimulated in response to diffusible platelet agonists inside and across the thrombus, thereby motivating further platelet enrolment and thrombus progression (Figure 11). (166)

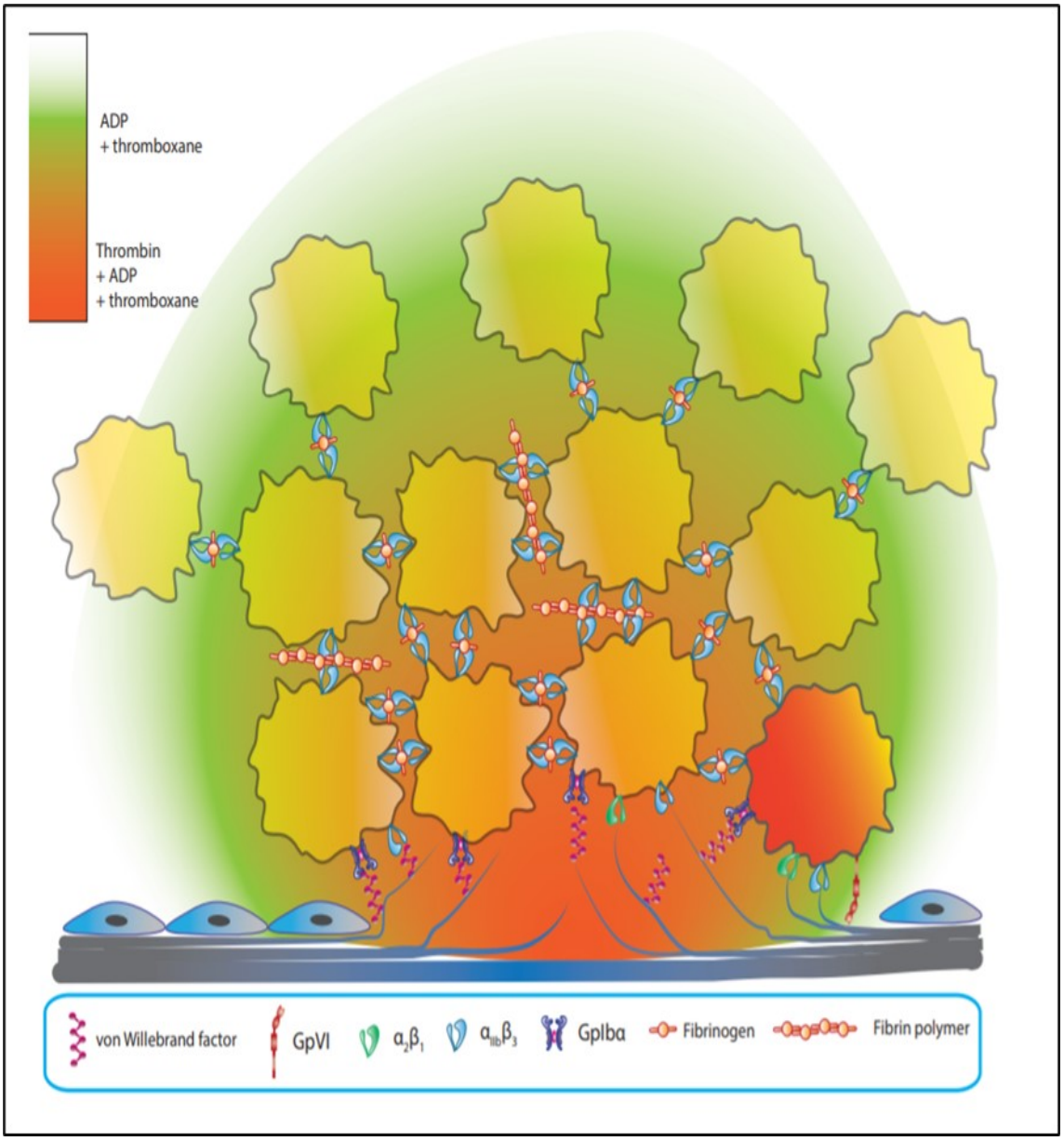


Figure 1.11. Graphic illustration demonstrating the heterogenic construction of a haemostatic plug. In the deepest levels of the thrombus, platelets obtain several powerful signals from collagen via receptors α2 β1 and GPVI, from thrombin via receptors PAR4 and PAR1 and from paracrine agonists via TPα and P2Y12. A section of platelets (coloured red) creates a connection with collagen turning procoagulant, fixing coagulation factors and hastening thrombin production, while most turn effectively pro-aggregatory by initiating αIIbβ3 to combine fibrinogen and fibrin. The two latter activities diminish thrombus permeability, restricting the distribution of thrombin to the external surface of the thrombus. In the thrombus skeleton, platelets are subjected to minimal intensities of small-scale sized agonists such as ADP and thromboxane A2 and rapid amounts of thrombin. These inadequate inducements are appropriate to deliver fractional initiation of αIIbβ3 but insufficient to stimulate granule excretion or P-selectin exposure. The figure was taken from (Versteeg, New fundamentals in haemostasis. Physiological reviews, 2013) (160).

Simultaneously, accumulating of negative feedback loop inhibitory signals' avoid extreme thrombus creation. (166) With the creation of a monolayer of platelets that covers the pro-thrombotic external surface of an injured vessel wall, collagen-triggered signalling via the integrin $\alpha_2\beta_1$ and glycoprotein GPVI occur, thus causing activation of phospholipase Cγ (PLCγ) 2 initiating an extended surge in intracellular calcium levels. (159) Consequently, platelets undergo a distinctive shape modification with pseudopodia creation, increasing their surface area and robust aggregatory action. (167) Synchronized stimulation by thrombin is acknowledged to enhance the procoagulant platelets interaction on collagen surfaces, perhaps related to amplified intracellular calcium mobilization. (167) The platelet granules discharge and the enhanced development of thrombin on procoagulant platelet membranes causes prompt stimulation of adjacent platelets and enrolment by gathering platelets into the thrombus through the interaction of $\alpha_{IIb}\beta_{III}$ and to a minor level GPIbα with fibrinogen. (168)

Platelets store various substances in granular stores named α-granules (alpha granules), δ-granules (dense granules) and lysosomal granules, enclosing diverse sets of hemostatically active elements that are secreted upon stimulation by a calcium-dependent exocytotic mechanism. (168) In response to platelet activation, α-granules release additional pro-haemostatic proteins such as VWF, Factor XI, Factor V and prothrombin, enhancing platelet adhesion and clotting at the site of the wound. (168) Merging of α-granules with the platelet membrane through exocytosis additionally reloads platelets with other membrane proteins, improving their pro-haemostatic and pro-inflammatory action. (169) α-granule exocytosis also delivers proteins essential in platelet-neutrophil interactions such as CD40L and P-selectin to the platelet surface. (169) Other α-granule derived proteins include growth factors such as PDGF, anti-angiogenic factors such as angiostatin and platelet factor IV, proteases such as MMP-2, angiogenic factors such as VEGF, and cytokines such as TNF-α. (169)
Dense granules are rich in serotonin and ADP, molecules classified as platelet agonists. (170) They, therefore, function as additional platelet activators and recruiters. (170) Dense granules also contain calcium required for platelet activation and secondary haemostasis. (171) Current studies have revealed that dense granules also function as a store for short-chain polyphosphate. (171) Polyphosphates have

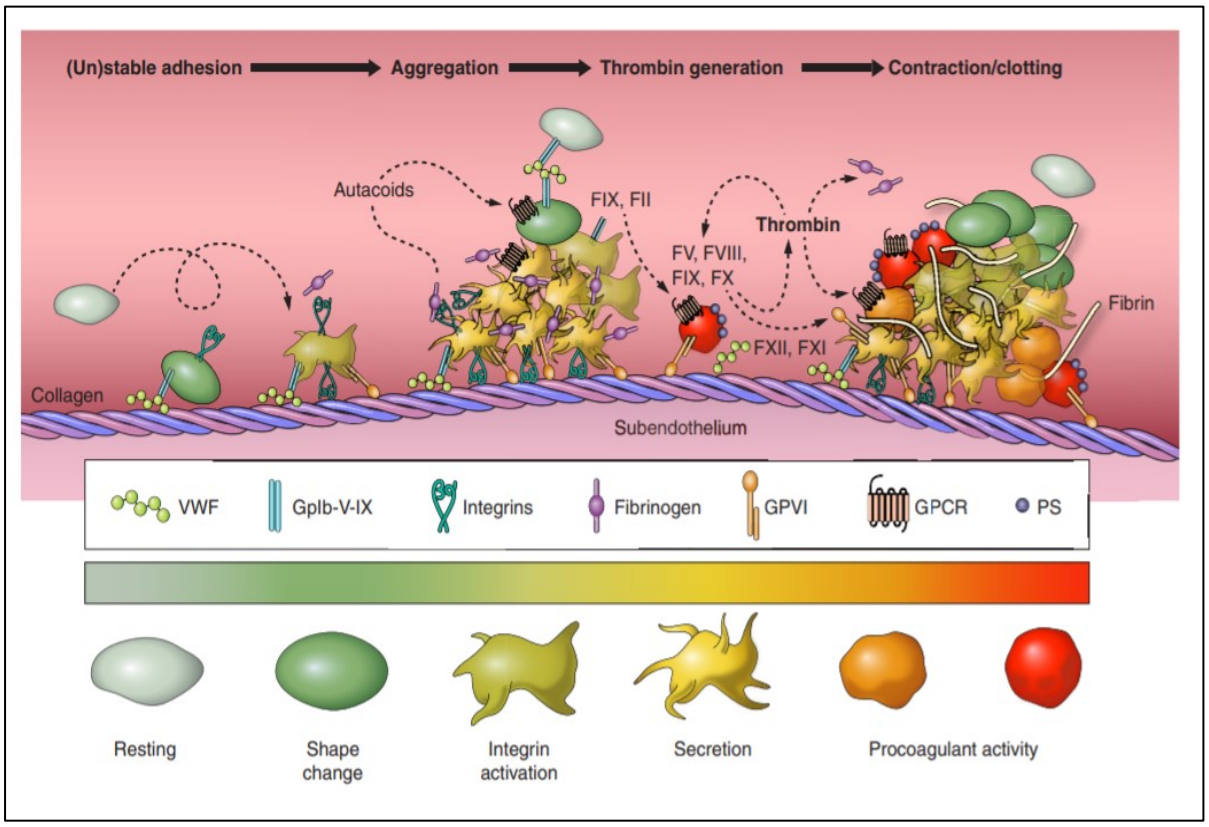
been proved to have numerous functions in haemostasis. (172) They also exhibit procoagulant ability by stimulating Factor V activity in the common pathway(171).

Consequent to the release of the granules, platelet membrane phospholipids (phosphatidylcholine) is hydrolyzed by active phospholipase A2, yielding arachidonic acid. (173) This is the primary substrate for subsequent reactions involving numerous enzymes (e.g., COX-1, cyclo-oxygenase,) which generate eicosanoids, specifically thromboxane A2, which are potent platelet agonists. (174) Upon activation, platelets adhere dynamically to the internal membrane leaflet and expose the phosphatidylserine. (175) Exposed phosphatidylserine provides the surface where the coagulation cascade occurs. (176) It is the binding site for coagulation factors and expands their action, thus encouraging fibrin formation. (177) Platelet membrane PS is reversed to the outside when platelets are triggered, permitting coagulation factors to attach to the activated platelet. (177) Activated platelets also release microparticles supplemented with PS from their membrane surfaces. (178) These microparticles expand the platelet surface area, thus delivering a bigger surface where the fibrin development can proceed. (178)

Activated platelet-derived agonists (ADP, thromboxane A2) and active coagulation factors (thrombin) trigger further platelet recruitment to the site of vessel damage. (179) This happens by a mechanism known as “outside-in signalling”, which stimulates other platelets. (179) This mechanism requires facilitator molecules, such as guanine exchange factors (GEF) and G proteins. Two key platelet receptors for agonists are involved in the process as well. (179) These are Protease-activated receptors (PAR) which binds to several agonists, such as thrombin, and P2Y12, a receptor for ADP.(180) Integrin, GPIIb/IIIa, also known as αIIbβ3 or CD41/61, is the fibrinogen receptor on platelets. (181) It is usually present on platelet surfaces but binds only fibrinogen on stimulated platelets. (181) Once platelets are stimulated, intracellular signalling triggers a conformational change of the fibrinogen receptor outside the platelet. (182) This structural change in the fibrin receptor allows other platelets to bind to fibrin, forming platelet aggregates. (182) This is collectively known as Inside-out signalling (stimulation of the fibrinogen receptor). (183) At the very end of this process, platelet aggregation occurs, where it is facilitated primarily by fibrinogen, which attaches to stimulated platelets' fibrinogen receptor (GPIIb/IIIa). (184) This adheres the platelets together, thus constructing the primary plug (Figure12). (184) This adherence stimulates them to release substances that lead to

the activation and aggregation of more platelets. (185) They also release components that inhibit activation of the anticoagulant system. (185) Assembly of coagulation factor complexes on the platelet surface significantly intensifies fibrin formation (the propagation stage of secondary haemostasis). (186) The platelet plug is adequate to prevent bleeding from nearly all small blood vessels in response to daily events such as minor trauma. (184) However, this plug must be stabilized and enhanced to stop haemorrhage in larger vessels or after more severe injury(184), which is achieved through secondary haemostasis.

Figure 1.12: The primary platelet plug. Endothelial damage reveals subendothelial matrix proteins



Von Willebrand factor (VWF) and collagen to circulating platelets. Platelets stick to VWF via surface receptors or collagen and become stimulated via intracellular signalling. Once stimulated, platelets alter shape and experience phospholipid metabolism, generating platelet agonists such as thromboxane A2 (TXA2) and producing platelet agonists such as ADP. These initiate and engage naive circulating platelets. The fibrinogen receptor (GPαIIbβ3 or GPIIb/IIIa) is triggered by inside-out signalling. Once activated, it connects fibrinogen, which joints with additional platelets, creating a platelet plug. This is adequate to prevent haemorrhage in tiny blood vessels (e.g., mucosal vessels) but is inadequate in bigger vessels or with a severe wound. The figure was taken from (Versteeg, New fundamentals in haemostasis. Physiological reviews, 2013) (160).

1.10.3 Secondary haemostasis

1.10.3.1 Introduction to secondary haemostasis

The intricacy of the coagulation system is defined by the presence of two controverting natural selection requirements: (1) to guarantee substantial production of thrombin when required to prevent bleeding; and (2) to remove excessive coagulation to avoid thrombosis and sustain sufficient perfusion of tissues. (168) The complicated equilibrium between these two functions has led to the development of numerous intensification stages on the one hand, in which sequential proteolytic reactions result in an exponential growth in thrombin production and to a multitude of controlling machinery and negative feedback loops on the other, to boundary and restrict clot formation to the location of vascular damage. (168) Secondary haemostasis is an enzymatic cascade that ultimately results in fibrin generation from thrombin cleavage of fibrinogen. (187) Fibrin monomers are subsequently cross-linked to form a stable fibrin clot that stabilises the primary platelet plug. (187) Conventionally, this process has been classified into three individual pathways: intrinsic (contact activation pathway), extrinsic (tissue factor derived pathway), and common pathway. (188)

1.10.3.2 The Tissue factor pathway (the extrinsic pathway)

Theoretically, tissue factor-driven coagulation can be grouped into three individual stages: initiation, amplification and propagation. (189) In the initiation phase, subendothelial cell-expressed TF is stimulated and interacts with blood procoagulant components, creating a complex with FVII, which is activated to its functioning from FVIIa. The TF-FVIIa complex stimulates FX and FIX (Figure 13). (190) While this complex is still bound to the membranes of TF-expressing cells, FXa next attaches to and triggers FV to generate the prothrombinase complex, causing the transformation of minor quantities of prothrombin to thrombin (FIIa). (191) The trace quantity of thrombin generated during the initiation phase leads to the release of FVIII from VWF and activates it to FVIIIa. (192) Factor VIIa interacts with FIXa on the platelet exterior. In the presence of calcium, this complex activates other FX to FXa. (190) FVIIIa-FIXa alongside calcium is referred to as the ‘tenase’ complex, which is crucial for the intensification and propagation of thrombin production. (192) The TF-VIIa complex can also activate FIX directly, known as “the alternate” pathway. FIXa can contribute to the amplification stage of thrombin production (Figure 1.13). (192)

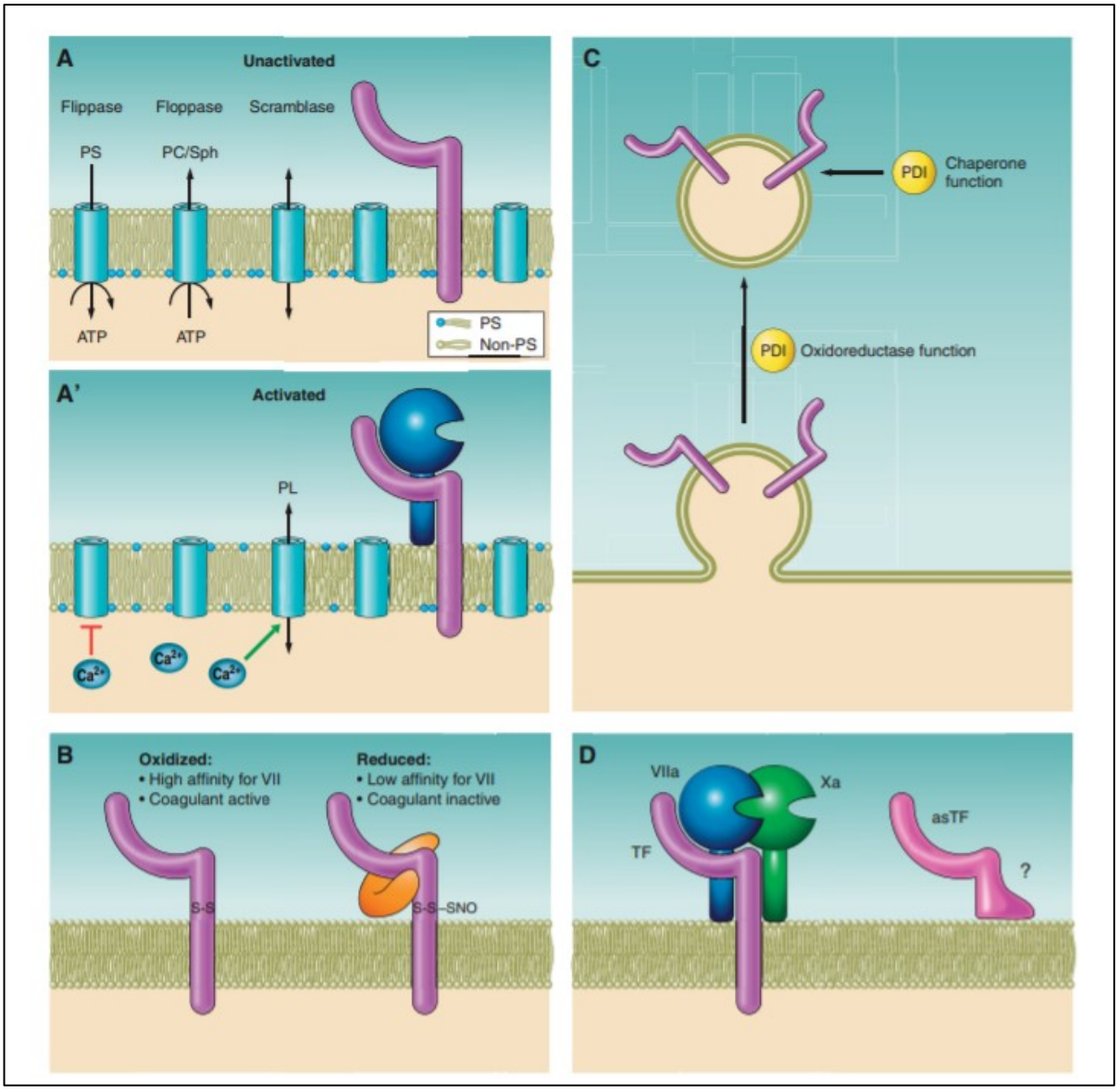


Figure 1.13: Regulation of TF activity. A: stimulated introduction of phosphatidylserine (PS). In relaxing situations, TF-exposing cells sustain a non-symmetrical membrane structure, causing minimal PS subjects in the external membrane circular and high contents in the internal leaflet. This irregularity is sustained in ATP-supported internal transfer of PS by flippase and external transfer of non-PS by floppies. In response to stimulus, calcium transients will prevent flippase and promote the non-discriminating lipid carrier scramblase, causing PS to reveal and the formation of a negatively charged exterior that operates to attach coagulation factors. **B:** TF disulphide control. TF is reserved on the cell exterior in an inoperative situation in the course of PDI- and/or nitric oxide (NO)-determined diminution of the TF allosteric disulphide. **C:** circulatory cells, such as stimulated monocytes, PDI-dependently discarded TF-positive MPs. **D:** MPs or TF on the cellular exterior may synergize with ordinarily cleaved TF to enrich TF procoagulant action. The figure was taken from (Versteeg, New fundamentals in haemostasis. Physiological reviews, 2013) (160).

The development of the ‘tenase’ complex leads to substantial production of FXa, which attaches to FVa, most of which is secreted from the α-granules of procoagulant platelets to produce the prothrombinase complex. (191) In the presence of calcium, the prothrombinase complex generates a ‘Thrombin Burst’, which results in a high localised concentration of thrombin resulting in rapid generation of fibrin. (191) The thrombin generated in the propagation stage persists in initiating platelets, FV, FVIII and FXI, leading to further thrombin production. (193) Additionally, thrombin initiates FXI, which through the initiation of FIX additional influences to thrombin production. (194)

The enormous quantities of thrombin produced via propagation and amplification yield the fibrin clot and concurrently inhibit its dissolution (inhibition of fibrinolysis). (195) Two stages are involved in fibrin formation; firstly, the construction of a soluble fibrin network by polymerising fibrin monomers. (195) Secondly, Factor XIII stabilization of the fibrin network via crosslinking (195). The duplex structure of α, β, and γ chains form the backbone structure of fibrinogen. (196) Each group of chains is connected at one end, creating a molecule comprising two-terminal ends: a primary (linked) E domain and (D domains). (196) Initially, thrombin cleaves fibrinogen at the E domain to create soluble fibrin. (196) This cleavage results in releasing small peptides from the terminal end of the β and α chains of fibrinogen, named fibrinopeptide A.(196) This cleavage (particularly fibrinopeptide A) leads to covalent links between each fibrin monomer's terminal (D) ends. (197) Thus, resulting in long fibrils (fibrin polymer) formation by the spontaneous association of soluble fibrin. (197) Each polymer is also linked lightly with bordering polymers. (197) Following this, thrombin activate the enzyme FXIII, which stabilises the fibrin polymer network. (197) The neo-epitope D-dimer is formed when the γ chains of each fibrin monomer's terminal (D) ends are crosslinked with the help of factor XIIIa. (197) These crosslinks connect to the following fibrin polymers across their α chains, creating a three-dimensional crosslinked system. (198) Meanwhile, this process triggers a fibrinolysis inhibitor, named thrombin-activatable fibrinolytic inhibitor (TAFI). (198) Thus, while the fibrin clot is forming, fibrinolysis is constrained, inhibiting the breakdown of the clot. (198) Fibrin-stabilizes and integrates the primary platelet plug, which is crucial for the platelet plug interaction with the damaged blood vessel. (198)

At different phases in this process, initiated coagulation factors suspended in plasma or bound to endothelial cells are continuously inactivated by circulatory antithrombotic

substances such as antithrombin (inhibits thrombin and FXa)(199), tissue factor pathway inhibitor (TFPI) (constrains FXa). (200) In an advanced phase, activated protein C (APC) (inhibits FVa, FVIIIa); however, association into building complex attach to the platelet membrane presents defence from these inhibitors. (201) Moreover, the “bursts” of thrombin production accomplished in the locality of procoagulant platelets with efficient prothrombinase and tenase complexes cause the initiation of factor XIII and TAFI, shielding the emerging fibrin fibbers from deactivation by plasmin. (202) All these mechanisms are discussed in detail below (Section 10.4)

In conclusion, the coagulation system defined above displays that thrombin is created in two diverse stages of coagulation, primary in minutes response with minor effects for fibrin development and following in the propagation stages in a powerful burst of action in which all accessible fibrinogen is hastily polymerized.

1.10.3.3 The contact pathway (the intrinsic pathway)

Similar to the former pathway, the intrinsic pathway is triggered by damage inside the vascular system and is initiated by exposed endothelium content, platelets, collagen, or other negatively charged elements. (203) It involves factors XII, XI, IX, and VIII; the Hageman factor or factor XII (FXII) can activate blood clotting through a cascade of proteolytic reactions known as the intrinsic pathway of coagulation. (203) Upon its exposure to the endothelium matrix leading to the autocatalysis of a small volume of FXII into FXIIa, thus forming the intrinsic Xase. Next, FXIIa cleaves plasma kallikrein (PK), which communally convert other FXII into FXIIa.(204) In a prototypical cascade of proteolytic effects, FXIIa progresses to activate FXI to be FXIa, which in turn activates FIXa, thus leading to the development of the tenase complex after connection with FVIIIa.(205) In this chain of actions, the intrinsic coagulation pathway eventually congregates with the extrinsic coagulation pathway in the development of the prothrombinase complex (the common pathway). (205) The prothrombinase complex catalyzes the photolytic cleavage of prothrombin (FII) to thrombin (FIIa). (205) Thrombin, as the terminal coagulation protease, stimulate the creation of insoluble fibrin via the cleavage of soluble fibrinogen monomers and initiation of the transglutaminase FXIII as described earlier. The intrinsic pathway can besides be stimulated by factors of the extrinsic and common pathways. (205) Cross-activation is considered to be significant for the constant initiation of coagulation as an action of the

TF; FVIIa complex is constrained by tissue factor pathway inhibitor. (206) According to Josso *et al*. defined the capability of the TF, FVIIa complex to activate FIX competently. (205) (Figure 1.14). In summary, activation of both the tissue factor or the contact pathways, thus the coagulation cascade is preserved in a pro-thrombotic situation by until it is inhibited by the fibrinolysis pathways or by the exogenous anticoagulants

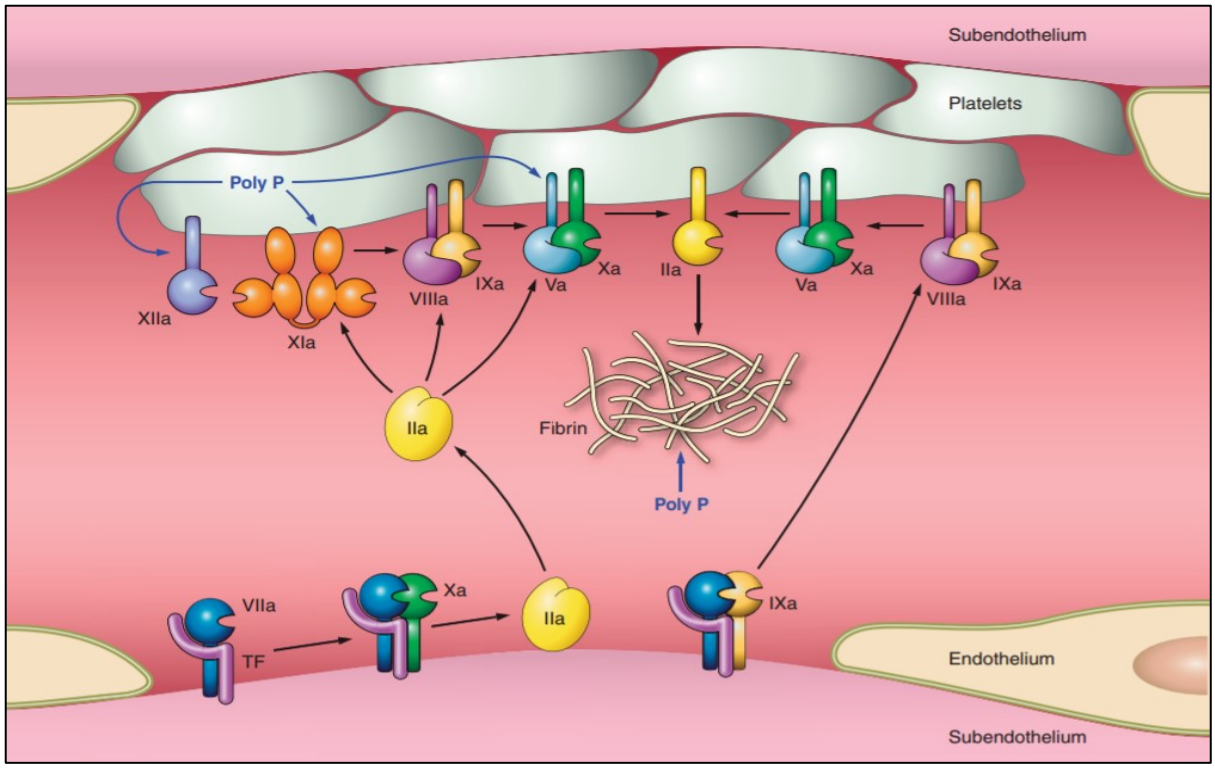


Figure 1.14: The coagulation cascade. In the cell-based model, fibrin creation and thrombin production progress on cell surfaces. In the induction stage of thrombin production, plasma FVII connects to the subendothelial fibroblasts tissue factor (TF). This binding autoactivates FVII and the TF-FVII complex creating the “extrinsic pathway”, which triggers FX on fibroblast membranes. The extrinsic pathway is rapidly reversed by tissue factor pathway inhibitors and yields only a minor quantity of thrombin. The small quantity of thrombin produced by the extrinsic pathway later intensifies its creation on phosphatidylserine (PS)-rich surfaces of stimulated platelets by triggering FXI, FV of the intrinsic pathway and FVIII, the common pathway cofactor. FXIa subsequently triggers FIX, making a vigorous “intrinsic pathway” complex with FVIIIa on the platelet surface. The activated PS-enriched platelet surface propagates thrombin, creating a “thrombin burst”. It is crucial for creating crosslinked fibrin from fibrinogen by cleaving fibrinogen to soluble fibrin, activating factor XIII, which crosslinks fibrin while constraining fibrinolysis. The created fibrin strictly intercalates and connects to the platelet plug, founding a steady fibrin clot. The figure was taken from (Villiers, British Small Animal Veterinary Association, 2016) (207).

1.10.4 The coagulation inhibitors

substantial works have been made in the latest years to establish the suppressor tools of the coagulation process. (208) Primary, circulating protease inhibitors, such as heparin cofactor II, anti-thrombin, C1 inhibitor, and tissue factor protease inhibitor (TFPI), defaecate stimulated coagulation factors by confronting their active sites. (208) The second anticoagulant approach is delivered by the enzyme-based protein C/protein S pathway. (209) Remarkably, the latter is involved in endothelial-based routes of coagulation deactivation (Figure 1.15). (209)

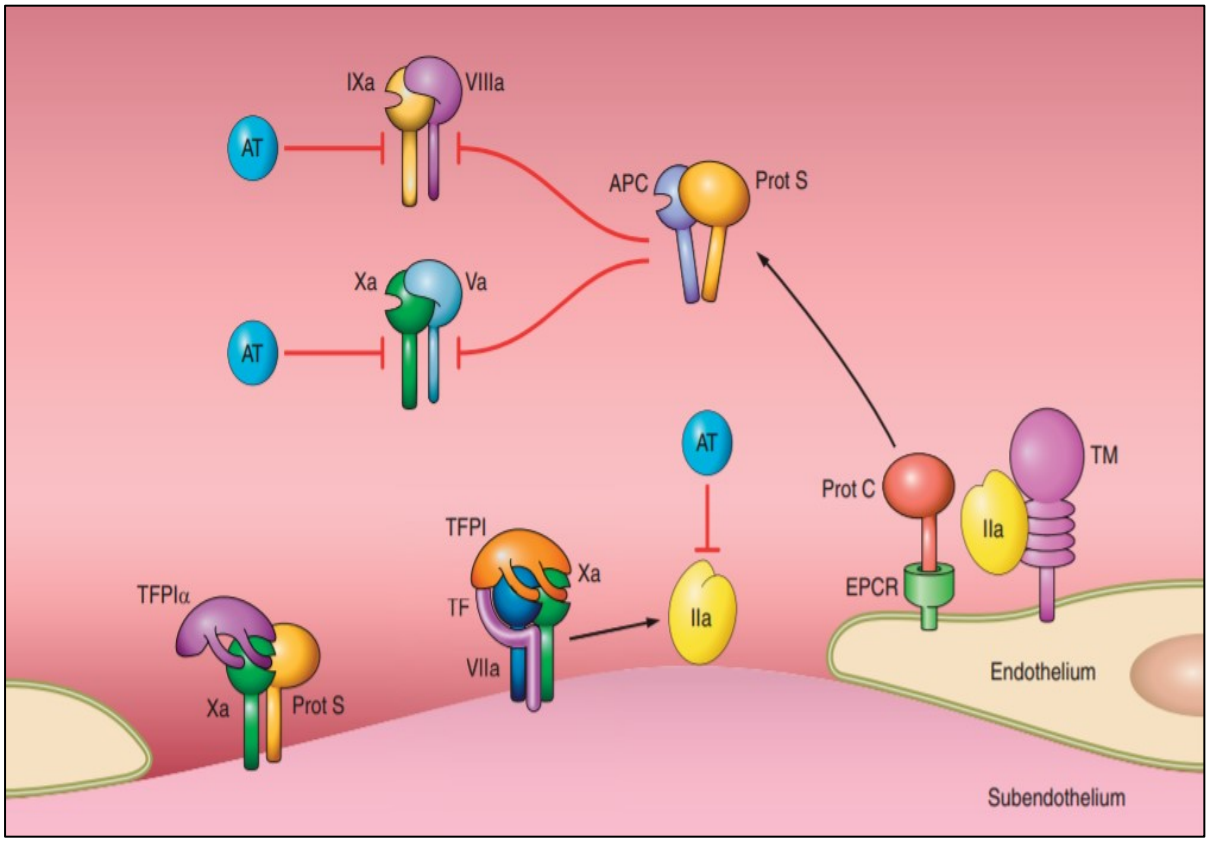


Figure 1.15: Negative regulation of the coagulation cascade. TFPI attaches to the TF-FVIIa-FXa complex or FXa to constrain the coagulation act. Protein S could also combine with TFPIa to additional prevent FXa action. Produced thrombin at adequate quantities attaches to thrombomodulin and is introduced to protein C in a building complex with EPCR, later which protein C is initiated (APC). APC in compound with its cofactor protein S later disables FVIIIa and FVa. Antithrombin (AT) creates an additional management level as it obstructs the function of thrombin, FX and FIXa. This figure was adapted from.The figure was taken from (Versteeg, New fundamentals in haemostasis. Physiological reviews, 2013). (160)

1.10.4.1 The protein C/protein S pathway

Since the 1980s, it has been well-known that activated protein C (APC) in a compound with protein S creates proteolytic deactivation of FVIIIa and FVa, hence suppressing prothrombinase and tenase actions. (210) Protein C is a 420-amino acid anticoagulant mediator with a remarkable homology to the vitamin K-dependent procoagulant factors. (211) Its complete activation requires protein C cleavage to activated protein C (APC) and interaction with its cofactor, protein S, a vitamin K-dependent protein (635 amino acids). (211) It contains a thrombin-sensitive region, NH2-terminal phospholipid-binding Gla domain, two laminin G-type domains which synergistically with FV target FVIIIa, and four EGF-like domains that are essential for protein S attachment. (211) As a result of thrombin concentration upregulation during the coagulation process, it attaches to the endothelial transmembrane protein, thrombomodulin. (212) Once this complex forms, thrombin proteolytically cleaves and triggers protein C attachment to adjacent endothelial protein C receptor (EPCR). (212) Protein C activates after cleavage at Arg169, thus eliminating the activation peptide. (212)

There is a suggestion that attachment of thrombomodulin to thrombin is not firmly requisite for protein C stimulation, though its cleavage is exceptionally slow in the lack of thrombomodulin. (86) Due to the substantial endothelial surface area in capillary beds, the initiation of protein C in these tiny vessels is reasonably practical. (213) However, protein C attachment and presenting it to the thrombin-thrombomodulin complex require supplementary Endothelial cell protein C receptor (EPCR) in larger vessels, where the endothelial surface area-blood volume ratio is low. (213) According to *in vitro* study, the existence of EPCR improves APC formation by 6-fold. (213) This is consistent with the hypothesis that the attachment and stimulation of protein C are endothelial cell membrane-dependent processes. (210) On the endothelial cell membrane, APC-protein S complex proteolytically cleaves FVa and FVIIIa, which are ordinarily membrane-bound as well. The structural requirements for this cofactor inactivation have been studied in detail. (214) Both FV and FVIII are characterized by an A1-A2-B-A3-C1-C2 domain structure. (215) The A domains shape into a globular structure with the B domain. The B domain of both factors is eliminated during the initiation of the cofactors by FXa or thrombin. (215) While the A domains cooperate with FIXa and FXa, respectively, the inactivation complex of protein S with APC

cleaves FVa at, Arg679, Arg506 and Arg306 are leading to broad downregulation of prothrombinase action. (216) Protein S moreover exhibits anticoagulant action in the lack of APC by numerous mechanisms, i.e., by challenging with prothrombin for direct attachment to FVa, by constraining FXa, or by encouraging the FXa-TFPI interaction (111, 119, 120). Thus, this pathway is considered as one of the key endothelia cells natural anticoagulant systems.

1.10.4.2 Coagulation protease inhibitors

Anti-thrombin and TFPI are the most widely studied among numerous plasma proteins that apply negative regulatory control on the coagulation process. (217) Antithrombin is a serpin inhibitor (an acronym for serine protease inhibitor), while TFPI is a Kunitz-class protease inhibitor that restricts coagulation induction. (218) TFPI is present on the microvascular endothelium and platelets, where it remains linked to the cell surface. (219) Only 20% of the circulatory TFPI is lipid-free, while the remaining is associated with lipoproteins. (219) In human plasma, three TFPI isoforms, developing from unconventional splicing, have been recognised, TFPIα, TFPIβ, and TFPIδ.(220) Two different manners are used by TFPI to inhibit the coagulation process: interaction with the temporary TF/FVIIa/FXa complex and direct inhibition of free FXa.(220) The second domain of TFPI blocks FXa action, while the first domain of TFPI inactivates TF/FVIIa complex. (221) Lately, protein S has been recognized as a significant cofactor for TFPI-dependent inhibition of FXa by intensifying the attraction of TFPI for FXa in a procoagulant phospholipid-dependent means, however not TF/FVIIa, at low procoagulant stimuli. (222) However, it is notable that the TFPI/protein S does not inhibit thrombin production in the existence of elevated TF concentrations, except adequate APC at subsequent points in coagulation is created to slow down thrombin production. (223)

Antithrombin (earlier antithrombin III) is considered one of the greatest significant inhibitors of thrombin creation and function. (160) This is demonstrated by its great affinity concerning three main coagulation proteases, i.e., thrombin, FXa, and FIXa. In clinical practice, the heterozygous deficit in antithrombin presents a 10-fold advanced risk of venous thrombosis; however, absolute homozygous absence has undoubtedly not been detected in humans, perhaps since it is fatal. (224) Antithrombin-deficient

mice likewise die in utero, supporting the concept that broad antithrombin deficiency is contrary to life. (225)

Serpins (serine protease inhibitors) similar to antithrombin belong to a kind of protease inhibitors separate from Kunitz-type inhibitors. (226) They show a classic extended reactive centre loop (RCL) dependent on protease attack. (226) Subsequently to cleavage, the protease covalently associates to the cleaved RCL, and the RCL joins into the core body of the serpin. (227) The direct impact of these actions, the serpin implements a hyper stable configuration, the protease catalytic domain is distorted, and the protease assembly is disordered, implementing a zymogen-like state. (228) The anti-thrombin's biological deactivation of coagulation proteases is intensely enriched by heparin. (226) Long-chain heparins role interacts with antithrombin and thrombin or protease FXa, FIXa, thus delivering these factors organized in intimate proximity. (229) In summary, all these coagulation regulation mediators and others coagulation regulator provide a negative regulation of the coagulation cascade, thus maintaining a normal coagulation response

1.11 Fibrinolysis and the control of blood coagulation

1.11.1 The fibrinolysis system

In general, a series of cascading reactions involving cell surfaces (platelets and endothelial cells), enzymes, and coagulation proteins, function collectively to make thrombin the principal enzyme in coagulation and the dominant factor in the generation of a fibrin clot. (154) The fibrinolytic system works in parallel and ensures that this physiological clot will be resolved at a particular time point. (155) Taken together, the structures and the balance between the coagulation and the fibrinolysis systems maintain the efficiency of the haemostatic system. (155) Once the injured blood vessel starts to heal, the generated thrombus is broken down by plasmin action. (230) In this process, the zymogen plasminogen is converted into active plasmin on the cell surfaces or the surface of the fibrin clot. (230) Proteolysis of fibrin generates soluble fibrin degradation products (FDPs), some of which have chemotactic and immunomodulatory functions. (230) Fibrin plays a critical part in haemostasis as the end-product of both the coagulation cascade and the fibrinolysis. (231) Many factors

greatly influence fibrinolysis efficiency, including the rate of thrombin generation, clot structure, the overall biochemical environment, fibrinogen isoforms and polymorphisms, and thrombus-associated cell reactivity. (230) Similar to the coagulation system, controlling the fibrinolytic system involves a wide range of cofactors, inhibitors, and receptors (Figure 1.16). (230) Fibrinolytic action can be created either on the cells that demonstrate profibrinolytic receptors or on the surface of a fibrin-comprising thrombus. (230) The coagulation and fibrinolytic systems are well controlled and integrated, thus assuring balanced haemostasis. (230)

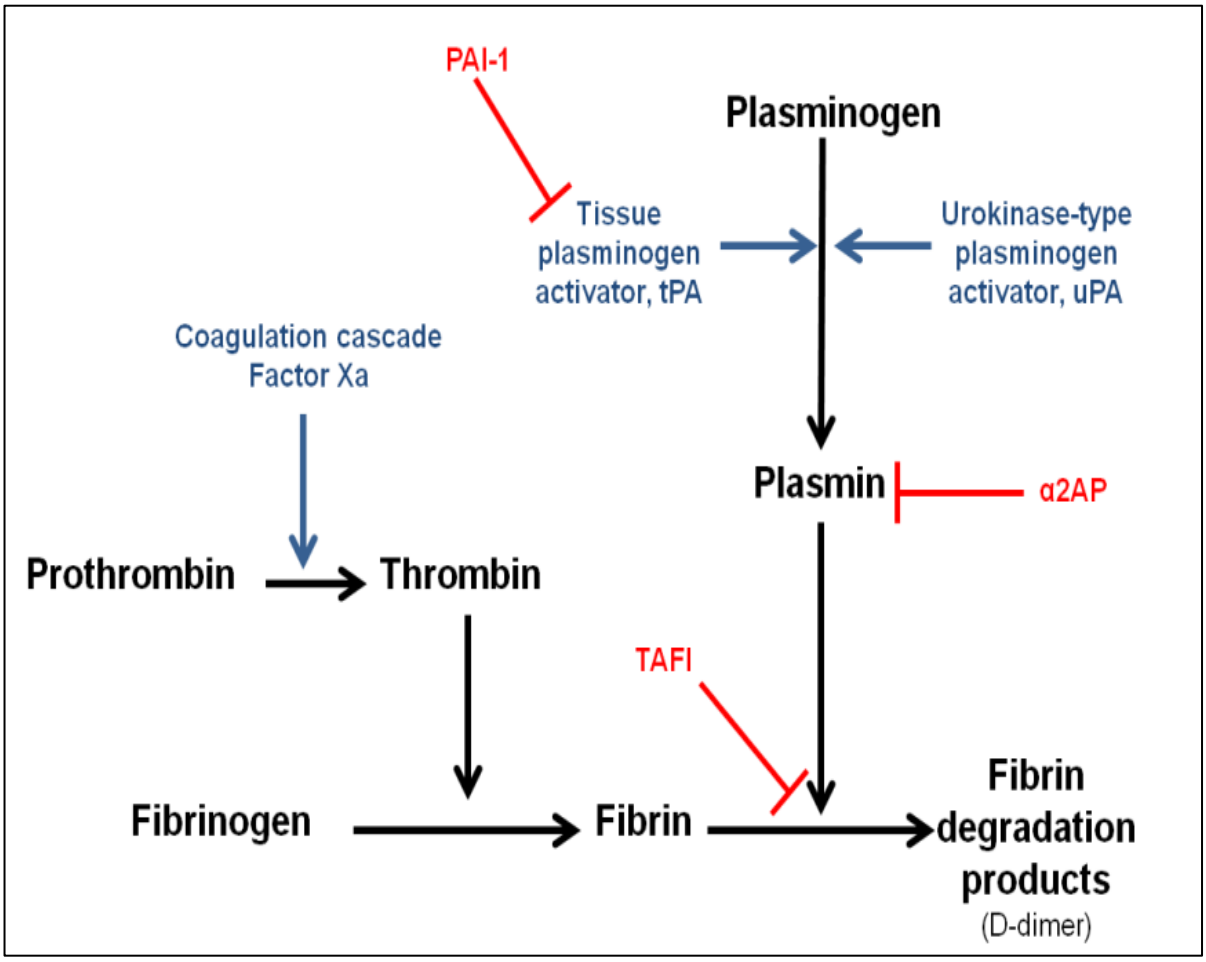


Figure 1.16: Fibrinolysis. Both urokinase-type plasminogen activator (u-PA) and tissue plasminogen activator (t-PA) convert Plasminogen to plasmin. Plasmin is the crucial enzyme accountable for the lysis of the fibrin clot. Direct plasmin inhibition via alpha-2-antiplasmin (α2AP) or indirect inhibition via thrombin activatable fibrinolysis inhibitor (TAFI) and plasminogen activator inhibitor-1 (PAI-1) are controlling the fibrinolysis system *in vivo.* The figure was taken from (Quinsey, The international journal of biochemistry & cell biology, 2004). (218)

1.11.2 Clot structure and fibrin formation

Fibrinogen is a soluble protein of 340-kDa size, found in the circulation at 2–4 mg/mL concentrations. (192) It consists of three different disulphide-linked polypeptide chains (Aα, Bβ, and γ) composing of two-protein sets. (192) Fibrin monomers are created from fibrinogen by the action of Thrombin. (192) A disulphide-linked trinocular protein defines the developing monomer whose C- and N-termini join at the D - and E nodules, respectively. (192)

In a stepwise fashion, the assembly of fibrin fibres is processed latterly. Factor XIIIa is responsible for the formation of fibrillar aggregates by cross-linking Fibrin at lysine residues. (192) This formation is combined with red blood cells, and platelets deliver structural integrity to the developing thrombus. (192) Circulatory flow and turbidity assist protofibril assembly and fibrin polymerization by adjusting the fibres as the rising thrombus forms. (232)

Several factors impact clot stability, including platelet numbers, pH, and local calcium concentration. Stability is also somewhat dependent on the geometry of the fibrin network and fibrin fibre diameter. (192) The concentration of local thrombin also influences clot structure, as elevated thrombin concentrations create more stable clots. (192) Soft clots are more vulnerable to fibrinolysis and bleeding, whereas solid clots are more tolerant but may encourage thrombosis. (192)

Thrombus development is based on the isoform structure of the fibrinogen pool rather than the total fibrinogen concentration. (233) Clot structure, thus, indicates the complex interaction of many elements varying from the efficiency of thrombin generation to polymorphisms in fibrinogen itself, the responsiveness of cells, such as platelets, and the biochemical environment. (233) These factors describe fibrin clot construction, which is also a critical factor in the effectiveness of clot lysis. (233)

1.11.3 Regulation of fibrinolysis

Plasmin is the initial fibrinolysin initiated from plasminogen by any of the two main serine proteases, urokinase-type plasminogen activator (u-PA) and tissue plasminogen activator (t-PA). (233) Whereas t-PA is produced and secreted by endothelial cells, u-PA is generated by macrophages, urinary epithelium, and

monocytes. (233) These proteases have extremely short half-lives in the blood circulation (4–8 minutes) because of elevated concentrations of specialized inhibitors. (233), which are crucial to avoid extra unregulated plasminogen or plasmin activator activity. (234) Examples of the coagulation inhibitors, three fibrinolysis crucial serpins; plasminogen activator inhibitor-2 (PAI-2), plasminogen activator inhibitor-1 (PAI-1) and α2-antiplasmin (A2AP)(234). When plasmin is attached to fibrin, it is protected from A2AP inhibition, allowing fibrinolysis to progress. (235) Correspondingly, the plasminogen activators u-PA and t-PA are quickly constrained by PAI-1, which is distributed into the circulation from platelets, endothelial cells, and other cells. (235)
The non-serpin fibrinolysis inhibitor Thrombin activated fibrinolysis inhibitor (TAFI) is stimulated by thrombomodulin-associated thrombin. (236) TAFI is classified as a carboxypeptidase that deletes arginine residues and C-terminal lysines on fibrin, thus reducing the number of accessible plasminogen attachment sites, slowing plasmin production, and steadying clots. (236)

1.11.4 Clot-based fibrinolysis

Fibrinolysis occurs on fibrin surfaces (key activation sites for fibrinolysis) by modulating the binding of plasmin and plasminogen. (237) Upon binding of plasmin to fibrin, A2AP protects plasmin from inhibition, allowing the activation of fibrinolysis, while initially, fibrin bind A2AP to prevent the clot fibrinolysis. (238) Because both fibrinogen and fibrin encourage the transformation of plasminogen to plasmin, they enable their destruction. (239) Alterations in fibrin clot formation correlate with differences in fibrinolysis rates so that denser clots with lesser pores and other tightly loaded fibres lyse more slowly than clots with more significant pores and more lightly loaded fibres. The interruption in fibrinolysis volume in densely bursting clots with thinner fibres is probably due to a mixture of mechanisms, counting diminished in the infiltration of the fibrinolytic enzymes into the core of the clot, as well as the decreased attachment of t-PA and plasminogen to densely loaded, thin fibres. Fibrin removal is additionally accelerated by delivering new binding sites for plasminogen, as C-terminal lysine residues become unprotected at an expanding rate during fibrinolysis. (239)

1.11.5 Cell surface fibrinolysis

The surfaces of the fibrin thrombus and the endothelial cells offer a protected, safe place for maintaining u-PA, plasmin, and t-PA, from soluble circulating inhibitors. Numerous cell surfaces involving a u-PA receptor (uPAR), plasminogen receptors, and the annexin A2 complex connect plasminogen and its activators on monocytes, endothelial cells, and several other cell types. (237) Some receptors, such as the transmembrane plasminogen receptor (PlgR-KT) and uPAR, could regulate other non-fibrinolytic acts, such as catecholamine release and cell-matrix adhesion. (240)

Annexin A2, an essential element of cell-based fibrinolysis, is a part of the calcium-binding protein annexin family that plays various physiologic roles. (241) On the surface of monocytes and endothelial cells, annexin A2 creates a heterotetrameric structure with additional proteins. Additionally, plasminogen and t-PA bind to the profibrinolytic p11 receptor (S100A10). (242) The (annexin A22-S100A10) complex substantially supports the t-PA-dependent initiation of plasmin separately from fibrin. (243) Therefore, the annexin A2 complex inhibition function could increase thrombosis risk by damaging fibrinolysis (Figure 1.17). (243)

1.11.6 Fibrin degradation products

Plasmin thrombus degradation generates fibrin degradation products (FDPs). (244) Several FDPs, including fibrin degradation dimers, monomers, and fibrinopeptide B, are released due to this process. (244) The level of D-dimer indicates the degree of plasmin and thrombosis fibrin polymers cleaving activity. (244)

A few FDPs demonstrate thrombus regulatory capacity, such as artificial peptides delivered from degradation product fibrin B knob, which has been proved to diminish the fibrinolysis. (245) The mechanism behind this is not yet clear, but according to previous studies, it is improbable that FDPs apply any amplification of target-specific feedback inhibition. (246)

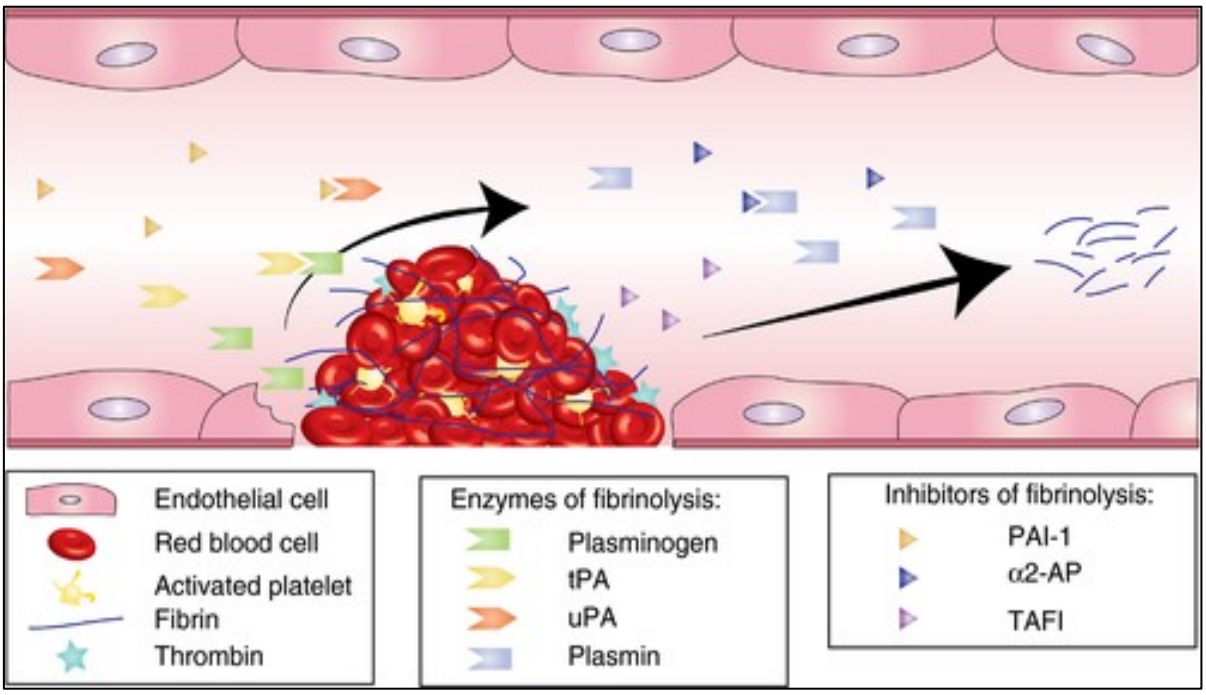


Figure 1.17: Overview of fibrinolysis. PAI-1, plasminogen activator inhibitor type 1; t-PA, tissue-type plasminogen activator; α2-AP, α2-antiplasmin; u-PA, urokinase-type plasminogen activator; TAFI, thrombin-activatable fibrinolysis inhibitor. The figure was taken from (Kanji, International Journal of Molecular Sciences, 2021) (247).

1.12 VWF and the endothelium

1.12.1 Introduction to VWF

Mature VWF is a multimeric protein composed of matching subunits linked by disulphide bonds forming dimers of almost 500kD. (248) These dimers are linked together to create multimers of several sizes that may be up to 1μm in length. (248) VWF is encoded by a gene located on the short arm of chromosome 12 and includes 52 exons and 180kb. (248) Only megakaryocytes and endothelial cells produce and store VWF, respectively, which stabilises FVIII in the blood circulation. (248) This activity is achieved by developing a non-covalently bound VWF-FVIII complex which locates FVIII to a platelet plug and consequent clot formation. (248)

VWF and its platelet counterparts, integrin αIIbβ3 and the receptors glycoprotein Ibα (GPIbα), are considered the main elements in primary haemostasis. (249) The GPIbα receptor is located on the platelet surface in an active form that does not require stimulation to bind VWF. (249) The GPIbα–VWF interaction leads to immediate platelet arrest. Thus, intracellular signalling arises, and the platelets become stimulated. (250) This causes structural rearrangement and the employment of other

receptors, which ends up in primary haemostasis followed by secondary haemostasis and robust clot formation (sections 1.9 and 1.10). (250) The natural role of VWF is exceptional in its capacity to encourage platelet–platelet and platelet–surface interactions under the most adverse environments of high velocity/high shear flow. (251)

1.12.2 The potential correlation between VWF and endothelium dysfunction

VWF release from the endothelium results in platelet adhesion and aggregation, part of the physiological haemostasis. However, this activity can extend beyond controlling wound healing and develop various vascular-associated pathological events. Several experimental and clinical reports propose that a high level of VWF reflects endothelium injury or endothelial dysfunction. (252) A high level of VWF may be a valuable indirect marker of atherosclerosis and/or thrombosis. (252) The association between ischaemic heart disease and VWF levels is well known, indicating the involvement of endothelial dysfunction in the pathogenesis of coronary artery disorders. (253) For example, amplified VWF concentrations are observed in patients with earlier myocardial infarction. (254) There is also a correlation between the clinical severity of angina and VWF level. (254) According to Bridges *et al*. a substantial upregulation in VWF levels was confirmed in patients who were re-perfused at 90 minutes after thrombolytic treatment. (255) Therefore, endothelial dysfunction could result from re-perfusion in acute myocardial infarction. (255) There was a significant reduction of VWF level following 24 hours post-thrombolysis therapy (t-PA). (256) According to Progetto *et al*. the VWF level was an essential indicator for atherothrombotic incidents in patients with angina pectoris. (257) Similarly, 3043 patients with angina pectoris in a prospective multicentre study showed that VWF, tissue plasminogen activator, and fibrinogen levels were independent indicators of acute coronary syndromes after two years of follow-up. (258) Experimental and clinical data proposes a connection between acute arterial thrombosis and upregulated VWF levels as well. (259) For example, amplified VWF level is a vital independent indicator to recognize diabetes mellitus risk factors in patients with myocardial infarction. (260) Furthermore, the origin and progress of atherosclerotic plaques itself may be promoted by enriched secretion of VWF in response to inflammation, thus causing local recruitment of platelets.

(261) Diabetes, a well-established atherosclerosis risk factor, has a robust connection with VWF levels, and several reports have stated a positive correlation between diabetes and VWF. (262) The increased levels of VWF may be accredited to endothelial cell destruction following the release of VWF into the blood circulation or, instead, to raised insulin levels, which have a significant positive association with VWF.(262) The level of VWF was three times higher than the standard value in patients with visible angiographic intracoronary thrombosis. (263) In a prospective analysis of myocardial infarction survivors, a raised concentration of VWF was observed as well. (264) The precise means by which VWF raises the cardiovascular risk in patients with post-myocardial infraction or angina is unknown. Amplified endothelial damage in coronary artery disease could be due to greater levels of VWF and amplified thrombin generation. (265) The augmented levels of VWF may intensify the risk of thrombogenesis in patients with pre-existing vascular comorbidities. (265)

Amplified VWF levels have also been confirmed in patients with inflammatory vascular disease, including vasculitis, giant cell arteritis Sjogren's syndrome, polyarteritis nodosa, and Felty's syndrome. (266) For example, it was demonstrated that increased VWF levels in all patients with Raynaud's phenomenon involved patients with and without connective tissue disease or atherosclerosis. (267) Patients with Raynaud's phenomenon and systemic sclerosis also have amplified VWF, mainly if the diffuse disease was present. (268) Among 74 rheumatoid arthritis patients in the Wallberg-Jonsson study, there was a significant increase in VWF after two years of monitoring. (269) It should be noted that the VWF level was found to be amplified in multiple myeloma patients. (270) All these facts indicate a clear association between VWF and endothelium damage with the potential involvement of pro-thrombotic and pro-inflammatory processes and others (Figure 1.18).

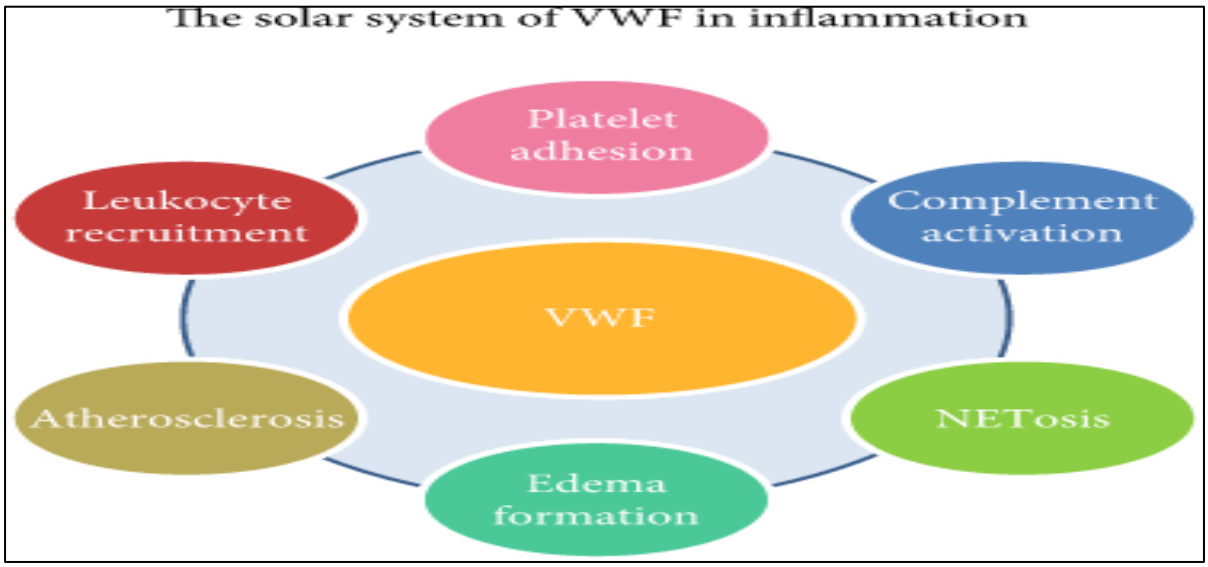


Figure 1.18: The "solar system" of vascular inflammation mediated by VWF. VWF is considered the centre of the vascular inflammation "solar system". It is also the principal among various inflammatory pathways circles in its "gravitational field." VWF enhances platelet and leukocyte enrolment in inflamed tissue, alters vascular penetrability and develops oedema. This encourages inflammation and atherosclerotic plaque formation and delivers a stimulating surface for complement initiation and NETosis. These processes may result in organ failure, tissue injury, and thrombo-inflammatory disorders. The figure was taken from (Mannucci, New England Journal of Medicine, 2004). (271)

1.12.3 Synthesis, storage, and secretion of VWF

Weibel–Palade bodies store VWF, rod-shaped organelles originating from the Golgi apparatus. (272) Endothelial cells manufacture VWF as -pro-VWF, i.e., the pro-peptide, a signal peptide, and the mature VWF subunit. (272) Following multimerization and dimerization of pro-VWF, it is transferred to the storage granules and, later, undergoes signal peptide removal. (273) Two forms of VWF are secreted by the endothelium:1) molecules secreted directly upon creation, or 2) through a controlled route in which stored mature VWF molecules are discharged after encouragement by secretagogues. (273) The VWF secretion can either be luminal or apical into the basolateral compartment or the circulating blood or abluminal into the subendothelial environment. (274)

It is commonly anticipated that VWF stored within Weibel–Palade bodies are collections of the giant multimeric species, i.e., ultra-large VWF, which typically is not detected in a healthy individual's blood. (275) Their organized discharge at damage

locations would provide the maximum thrombogenic forms of VWF directly where required. (276) Ultra-large VWF is cleaved by the metalloproteinase ADAMTS-13 to eliminate them from circulation. (276) In response to numerous agonists of biological relevance, such as oestrogens, histamine, fibrin and thrombin, endothelial cells release their VWF stock. (276) This secretion from Weibel–Palade bodies possibly occurs whenever the haemostatic mechanism is triggered. (276)

1.12.4 Platelet α-granules contain VWF

The additional storage location for VWF is inside the platelet α-granules, including 20% of the absolute VWF existing in the blood. (277) Numerous additional significant particles are found in the platelet α-granules, including fibrinogen, fibronectin, and thrombospondin (Section. 9.3.2.2). (278) The platelet α-granules VWF content typically also comprises the ultra-large VWF multimers. (277) Once platelets are stimulated by agonists such as adenosine diphosphate (ADP), thrombin and collagen, they secrete their granule contents; this ensures the availability of ultra-large VWF multimer at sites of vascular damage. (279) The equivalent discharge of ultra-large VWF multimers from bordering endothelial cells guarantees the existence of the most haemostatically operative multimers at the vessel wall in the vascular lesion. (280) It is unlikely that VWF released from storage stock is bound to factor VIII. (280) Whilst the primary attachment of FVIII to circulating VWF may assist in locating it at a site of vascular injury, its subsequent detachment from VWF may be a requirement for its stimulation and role as a clotting factor. (280)

1.12.5 Interactions of VWF with coagulation proteins

The larger VWF multimers seem to bind favourably to fibrin, irrespective of whether the latter is cross-linked or not. (281) This binding is followed by covalent cross-linking of fibrin α-chain with the VWF multimers. (281) Moreover, VWF seems to enhance platelet adhesion to fibrin clot and platelet incorporation into polymerizing fibrin. (282) Aside from VWF, αIIbβ3 and GPIbα are involve in the platelet adhesion to fibrin in flowing blood. (283) Once the coagulation mechanism is activated, VWF functions as a cofactor accelerating the light chain cleavage by FVIII. (284) This event leads to

FVIII/VWF complex dissociation. (285) The VWF protects FVIII from the inhibitory activity of protein C when they form a complex. (285) Thus, the balance of anticoagulant and pro-coagulant factors is preserved.

1.12.6 VWF-mediated primary haemostasis

VWF has an essential function in primary haemostasis where it facilitates platelet adhesion to injured vascular subendothelium and consequently platelet aggregation (Figure 1.19). After vascular damage, VWF domains A1 and A3 connect precisely to fibrillar collagen type I and III. (286) This binding prompts signals that involve platelet activation. (286) These signals activate protein kinase C and tyrosine kinases and promote cytosolic Ca_{2+} influx. (161) They can be seen under static conditions and are also related to platelet activation under high shear stress conditions. (161)

Once VWF is restrained in subendothelial connective tissue, it primarily facilitates platelet adhesive interactions exposed to rapid blood flow. (159) Two separate platelet receptors are located on the platelet membrane for VWF, the integrin αIIbβ3 (GPIIb-IIIa complex) and the glycoprotein GPIbα in the GPIb-IX-V complex. (159) Binding between platelet GpIb receptor and the A1 domain of restrained VWF ends in initial adhesion, characterized by a constant surface translocation of the platelets. (251) This practise eventually results in stable platelet adhesion by collaborating with the platelet collagen receptors GpIa/IIa38 and GpVI.(287) Thus, stimulation of the platelet αIIbβ3 receptor complex and conclusively platelet aggregation. (287)

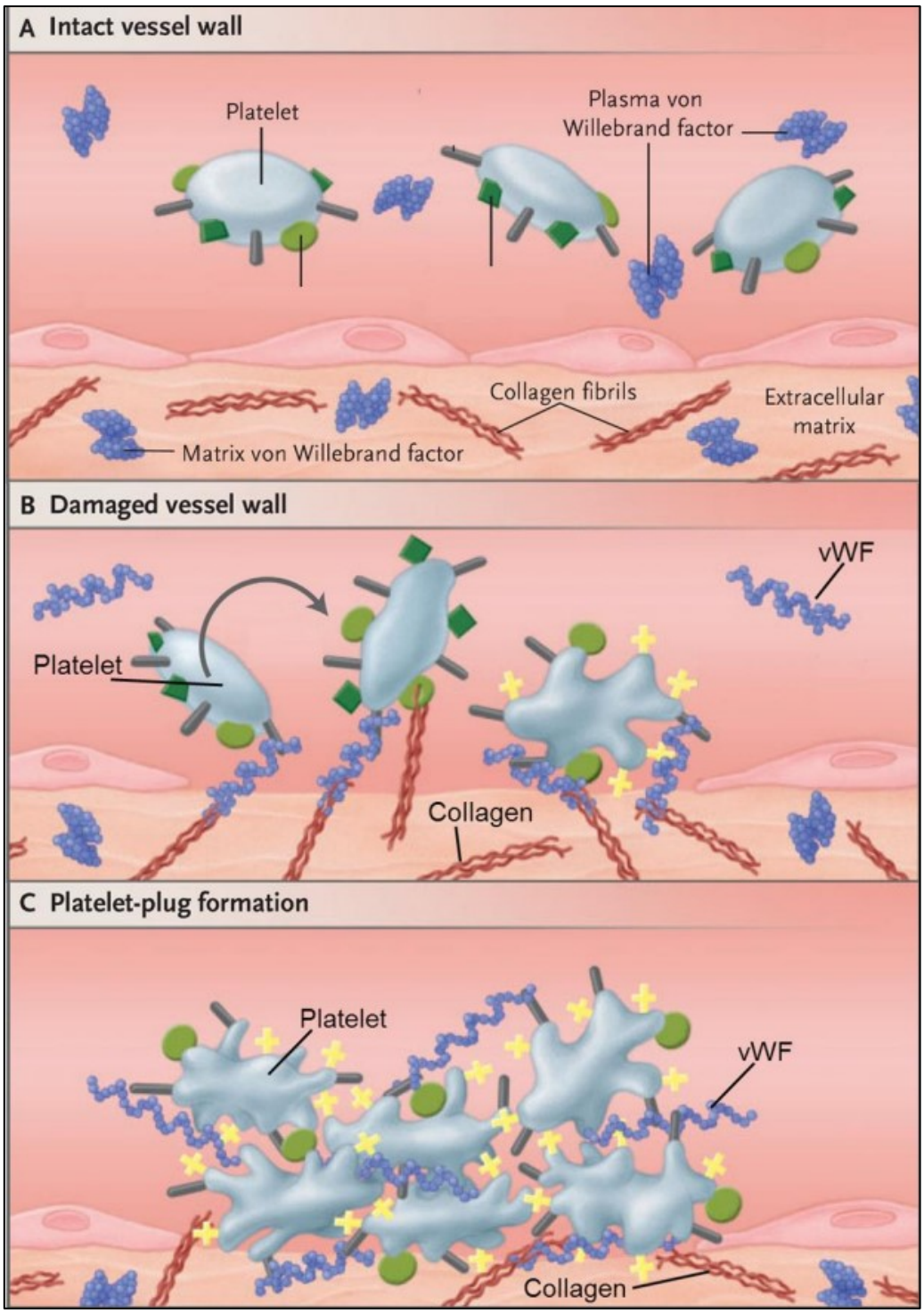


Figure 1.19: VWF mediated primary haemostasis. (A). The primary reaction of coagulation proteins to vessel damage. VWF is stretched by expansion shear force in the vessel and attaches to platelets, FVIII and collagen (**B**). Platelet plug development is accomplished once a sufficient amount of platelets, VWF and related coagulation proteins attach to cover the vessel wall (**C**), the end product of the platelet clot formation. The figure was taken from (Mannucci, New England Journal of Medicine, 2004). (271).

1.13 Hemostatic abnormalities in MM patients

MM patients have a raised risk of arterial and venous thrombosis (162) and have various haemostatic defects, including both thrombosis and abnormal bleeding. (163) Among 157 MM patients and 34 MGUS patients, 25% of them showed an abnormal prolonged prothrombin test (PT), time indicating hypo-coagulation tendency. (164) The upregulation of D-dimer and the development of autoantibodies such as lupus anticoagulant (LA) and anti-prothrombin antibodies in MM patients were correlated with the hyper-coagulation pattern of this disease. (165,166) Generally, it is widely accepted that multiple myeloma is linked to an increased risk of venous thromboembolism (VTE). This can occur in deep veins of the arm, leg, groin, and others, which can travel through the circulation to develop deadly pulmonary embolism. (162)

There are at least four potential causes for hypercoagulability in MM patients: procoagulant autoantibody production, inflammatory cytokines impact on the endothelium, interference of immunoglobulins on fibrin structure, and developed resistance against activated protein C (APC). (167) Furthermore, endothelium injury, either by chemotherapy or tumour cells, may prompt thrombosis. (167) This damage could cause upregulation of adhesion molecules, thus permitting adhesion to cellular blood elements (platelets, neutrophils, lymphocytes, and tumour cells). (167) However, other non-MM-related comorbidities could also be involved in this adverse situation. (162) and the roots behind thrombotic complications in MM patients are still not fully addressed in the majority of cases. (167) Chemotherapy may be considered the chief inducer of thrombotic abnormalities rather than a specific abnormality. (168) This is because thrombotic events become more prevalent after treatment. (168) Patients are particularly at risk to develop thrombosis when using immunomodulatory treatments such as Thalidomide. (169) Almost 30 % of these patients may acquire venous thrombosis if not provided with suitable prophylaxis. (162)

Interestingly, even with the considerable adverse events reported with the usage of BTZ in MM therapy, treatment with BTZ showed some protective effects, such as diminished thrombotic risk (288). However, the molecular foundation for this finding remains unknown. It was widely accepted to be associated with a protective effect on

the endothelium. (289) Cell-based experiments revealed that BTZ enhances expression of the transcription factor Kruppel-like factor 2 (KLF2) in several cell types, including HUVECs, which may explain the mechanism behind the anti-thrombotic effect of BTZ. (290) Moreover, experiments in GL-K2-KO mice demonstrated a chondroprotective effect associated with BTZ usage. (290) Can *et al*. claimed that the usage of BTZ was associated with a significant protective influence on the uterus of ovariectomized rats via the suppression of NF-κB activity. (291) An animal study also showed that BTZ had a neuroprotective effect in retinal ischemia-reperfusion damage via the inhibition of NF-κB related inflammatory pathways. (292) Considering all these observations indicate that BTZ has a significant protective effect at several levels.

The administration of CFZ in clinical practice has shown a remarkable enhancement of MM therapy. (293) However, numerous publications have reported that its use has been associated with severe adverse events, including various cardiovascular complications. (294) CFZ usage in MM was associated with an increased risk of thrombotic microangiopathy (TMA). (170) In addition, the use of this drug was correlated to the development of Venous Thromboembolism VTE. (171) Overall, haemostatic abnormalities in these patients are correlated to an unfavourable prognosis. As most patients with thrombotic complications are asymptomatic, their early diagnosis and treatment will enhance their prognosis. Similarly, there have been growing reports of CFZ-associated cardiovascular adverse events (CAVEs), involving heart failure, ischemic events, cardiac arrest, cardiac arrhythmias, and severe hypertension.(94, 295) However, the root behind these adverse events is still poorly understood. There is now a clear need to study the impact of CFZ on the endothelium in order to understand the basis of the CFZ-associated adverse events, which is investigated in this study.

2. Research hypothesis and aims

The introduction of CFZ as a treatment option for multiple myeloma has significantly enhanced the survival rate of RRMM. It is well established that CFZ induces MMC death by proteasome inhibition, resulting in persistent ER stress and activation of the terminal UPR. (3) However, the association of CFZ treatment with increased cardiovascular side effects suggests that CFZ may be causing endothelial cell damage. (296) Although comprehensive studies have been performed to investigate this issue, there is still uncertainty about the role of CFZ in endothelium damage. *Therefore, this study aims to investigate the potential off-target impact of CFZ to establish whether CFZ-mediated proteasomal inhibition in endothelial cells results in endothelial damage*. This damage could increase the risk of thrombus formation, oxidative stress, and the release of inflammatory cytokines from the damaged endothelium, which could explain the mechanism behind these complications. There are no approaches to avoid CFZ-associated cardiovascular complications in patients. However, based on the European Myeloma Network recommendations, it is crucial to estimate and attempt to decrease the cardiovascular risk at baseline before administering the drug to MM patients. (297) The study of the effect of CFZ on endothelial cells is fundamental to understanding the pathways responsible for cardiovascular complication development and their prevention.

This project aims to study the hypothesis that CFZ cardiovascular complications result from endothelial cell (EC) dysfunction and is due to the impact of CFZ on proteasome function in ECs so that CFZ induces EC inflammation, apoptosis, impaired homeostasis, and impairs production and bioavailability of NO resulting in the induction of oxidative stress.

2. Materials and Methods

2.1 Cell culture and passage

All tissue culture work was performed using aseptic techniques in accordance with good laboratory practice under a Class II Laminar Flow Hood, and all cells were cultured at 37°C with 5% CO_2 in a LEEC Culture Safe CO_2 Precision 50 Incubator (LEEC, UK).

Human umbilical vein endothelial cells (HUVECs, Lonza, Basel, Switzerland) acquired from pooled donors were selected as the endothelial cell standard model to examine the effect of CFZ on the endothelium. HUVECs were grown and maintained in Lonza Endothelial Cell Basal Medium-2 (EBM™-2, Lonza, Basel, Switzerland) supplemented with 5ml of 500µg/ml penicillin/streptomycin, 50ml of Fetal Bovine Serum (FBS, Sigma Aldrich, UK) and Endothelial Cell Growth Medium supplemented according to manufacture instructions (EGM™ -2 SingleQuots™, Lonza, Basel, Switzerland). The EGM™-2 supplements contain Fibroblast Growth factor, Recombinant analogue 3-Insulin-like growth factor, Hydrocortisone, Endothelial Growth Factor, Gentamycin sulphate/Amphotericin-1000, Vascular Endothelial Growth factor, Ascorbic acid, and Heparin. The addition of these supplements denotes EBM-2 becoming EGM-2. In all experiments, HUVECs were cultured on surfaces that had been coated with attachment factor (AF) (Gibco, UK) for at least 20mins at 37°C. To revive frozen HUVECs, cells were rapidly thawed, and the entire vial was transferred to a T75 flask with 11ml of EGM-2 media and incubated overnight. The next day, media was changed daily until the cells reached 100% confluency. To split the cells, media was removed from the confluence monolayer cells, and the attached cells were washed twice with 1x sterile phosphate-buffered saline (PBS) (8 mM Na_2HPO_4,2.7 mM KCl,137 mM NaCl, and 2mM KH_2PO_4) (ThermoFisher Scientific, UK). Cells were detached from the flask by incubation with 1ml of 1x TrypLE™ Express Enzyme (ThermoFisher Scientific, UK) for 1 minute at 37°C. Once cell detachment was confirmed by microscopic examination, trypsin was neutralised with 3ml of EGM™-2 media. Cells were then collected in a 15ml falcon tube (Thermo Scientific™, UK), centrifuged at 1400 rpm for 5 minutes at room temperature. The supernatant was discarded, and the cell pellet was resuspended in EGM™-2 media. Cells were re-

seeded into the planned cell culture plates and cultured under the conditions described above.

2.2 Treatment of HUVECs with CFZ

CFZ was purchased from Stratetch (Cambridge, UK) and resuspended with 1ml of sterile Dimethyl sulfoxide (DMSO, Sigma Aldrich, Missouri, UK), yielding a 2μM final stock concentration. 10μl aliquots were stored according to the manufacture's recommendation at -20°C. HUVECS were cultured in either 6 or 48-well plates and were stimulated with designated concentrations of CFZ and, in some experiments, 20ng/ml of stated cytokines for denoted times. In all experiments, HUVECs were cultured until they reached 100% confluence. The medium was changed on the day of drug stimulation, and the cells were re-incubated for 1 hour at 37°C. Afterwards, the cells were treated with 750nM CFZ (or in some experiments as noted varying concentrations of CFZ) for 60mins. As a control, some cells were non-drug stimulated, and some cells were incubated with an equivalent concentration of the DMSO vehicle. Following the 60mins incubation, the medium was discarded, and cells were washed twice with sterilised 1x PBS buffer and added 2ml of fresh EBM-2 media. The cells were left to recover for designated time periods up to 48 hours and were imaged using light microscopy. Subsequently, the cells were harvested with either protein lysis or RNA lysis buffer as described below (section 2.3.1 and 2.4.1, respectively), using a cell scraper (Carl Roth, Karlsruhe, Germany) and transferred into Eppendorf tubes and stored at -80°C until further investigations were conducted.

2.2.2 Treatment of HUVECs with multiple doses of CFZ

To assess the impact of multiple CFZ doses on HUVECs, cells were initially treated with CFZ for 1 hour as described, and the following removal of the drug was allowed to recover for 24 hours. Subsequently, the same process was repeated to administer a second drug dose. After the 24-hour recovery time, the media was removed from the cells and incubated with fresh EGM-2 media for 1 hour. 750nM CFZ was added for 1 hour, then the cells were washed twice with PBS and then incubated with fresh EGM-2.

2.2.3 Stimulation of HUVECs with inflammatory cytokines

The cytokines TNFα and IL-1β were purchased from Abcam (Cambridge, UK) and were obtained as liquids, both with a stock concentration of 20µg/ml. To investigate how CFZ could enhance or decrease the effects of inflammatory stimuli on HUVECS, cells were cultured and treated with CFZ as described. Following CFZ treatment, some cells were treated with either 20ng/ml TNFα or 20ng/ml IL-1β or a combination of both cytokines for designated time points.

2.2.4 CFZ treatment of Human embryonic kidney 293 (HEK 293) and multiple myeloma (OPM-2) cells

HEK293 cells were routinely grown in our laboratory and were available for use. OPM-2 cells were kindly supplied by Dr Wayne Mitchell. HEK293 cells were maintained in Minimum Essential Media (MEM) (Gibco, UK). OPM-2 cells were maintained in RPMI-1640 media (Gibco, UK). Both cell culture mediums were supplemented with 1000 U/mL penicillin, 10mg/ml streptomycin (Sigma-Aldrich, UK), 10ml L-L-glutamine (Sigma-Aldrich, UK), and 10% heat-inactivated FBS (Sigma Aldrich, Missouri, UK). $2x10^5$ of each cell line were cultured in a 6-well plate in a humidified incubator at 37°C, 5% CO_2 and maintained until they reached 100% confluency. Afterwards, CFZ was added as described in (Section 2.2.1); the media cells were harvested; the protein and genomic RNA content were collected and stored at -80°C for further investigations to be conducted.

2.3. Western blotting

2.3.1 Cell harvesting and extraction of total protein

Total cellular protein was extracted from cells using cold Radio- Immunoprecipitation Assay (RIPA) lysis buffer (150 mM NaCl, 1.0 mM EDTA, 0.1% (w/v) SDS and 0.01% (w/v) sodium azide, 50 mM Tris HCl, 1.0% (v/v) NP-40, 0.5% (w/v) Sodium Deoxycholate, pH 7.4) (Thermo Scientific™, UK) supplemented with one tablet of Pierce Protease Inhibitor Tablets (Thermo Scientific™, UK). The lysate was left on ice for 30 minutes, with vortexing and pipetting to assist the lysis. The tubes containing the protein lysate were centrifuged (13000 rpm, 15 minutes, 4°C), the pellet was

discarded, and the supernatant containing proteins was stored at -80°C until further investigations were conducted.

2.3.2 Measuring total protein concentration

Cellular protein lysate vials were retrieved from the -80°C freezer and defrosted at room temperature. According to the manufacturer's instructions, the Pierce Bicinchoninic acid assay (BCA) Protein Assay (Thermo Fisher Scientific, UK) was used to quantify the total protein concentration in the samples. The assay principle is based on creating a robust, purple-coloured copper /BCA complex. The protein concentration was calculated using the absorbance readout of the samples against a standard curve employing the linearity equation obtained from the standard curve plot (y=ax+b). The standard curve was prepared in a two-fold dilution, using 2mg/ml Albumin diluted with distilled water (dH_2O). 2µl of the standard curve, blank (dH_2O), and samples were loaded in a 96-well microplate (Thermo Fisher Scientific, UK) in duplicate. Subsequently, 200µl of (A+B) reagents mixture was prepared using 1:50 B: A ratio and added to each well. This step was followed by 30 minutes of incubation at 37°C in a shaking incubator (Thermo Fisher Scientific, UK). The absorbance was measured at 562nm using a Quant Biotek™ microplate spectrophotometer and Gen51 11 software (Quant Biotek™, UK). The data were extracted from the machine, analysed by Excel (Microsoft Office, 2019), and presented as µg/ml.

2.3.3 SDS-page gel electrophoresis and Western Blotting

2.3.3.1 SDS-page gel electrophoresis

20µg of protein lysate was diluted with a variable amount of dH_2O to a final volume of 30µl and 4x LDS loading buffer (6% sodium dodecyl sulphate (SDS), 200mM Tris-HCl pH 6.8, 7.5%v/v 2-mercaptoethanol, 2 mM EDTA, 0.02 % bromophenol blue, 10 % glycerol) (Invitrogen™ Novex™NuPAGE®, UK). Proteins were denatured at 75°C for 15 minutes using a dry bath system heating block (STAR LAB, UK) and then left to cool before loading them into the running system. Protein fractionation was completed by loading 20µl of the denatured protein mixtures and 5µl of CozyHi™ Prestained Protein Hyper ladder (highQu, Kraichtal, Germany) onto their corresponding wells 4-12% precast polyacrylamide gel (ThermoFisher, UK). The SDS-PAGE gels were loaded into a life technology electrophoresis tank filled with 1X Bolt™ MES SDS

Running Buffer (25 mM Tris base, 250 mM glycine, 0.1 % (w/v) SDS) (ThermoFisher, UK). Protein electrophoresis was conducted by connecting the tank to the ENDURO™ Power supply (GeneseeScintific, USA) programmed for 35 minutes at 200V. Subsequently, the Trans-Blot ® Turbo ™ Transfer System RTA Transfer Kit (Bio-Rad, UK) was used at 25 V for 15 minutes to transfer the proteins onto nitrocellulose membranes with 0.45µm pore size in transfer buffer (24 mM Tris base, 193 mM glycine, 20 % (v/v) methanol).

2.3.3.2 Western Blotting

When the protein transfer was completed, the membrane containing proteins was blocked using 5% (w/v) bovine serum albumin (BSA) (ThermoFisher, UK) in 0.1% Tris Buffered Saline Tween buffer (0.1% TBS-Tween) (900ml of dH_2O, 100ml of 10x TBS, 1ml of TWEEN™20) (TWEEN™20, Sigma Aldrich, UK) at room temperature (RT) for 1hr on a tube shaker (Benchtop Centrifuge Tube Shaker, Green BioResearch, UK). Next, the blocked nitrocellulose membranes were sliced based on the molecular size of the interested protein. The nitrocellulose membrane pieces were incubated with the corresponding primary antibodies diluted in a 5% BSA-TBST mixture overnight at 4°C on a tube shaker. Primary antibodies, the molecular size of each protein, animal source, company, catalogue number, and respective dilutions used are detailed in (Table. 2.1).

Antibody	Source	The molecular size of the target protein	Antibody Dilution	Antibody stock Concentration	Company	Cat. Number
GAPDH	Mouse	37 kDa	1/1000	2mg/ml	Abcam	ab105430
p-IRE1α	Rabbit	130 kDa	1/1000	100μg/ml	Cell Signaling Technologies (CST)	3294
CHOP	Mouse	32 kDa	1/1000	100μg/ml	CST	2895
Ubiquitin	Rabbit	8 kDa	1/1000	100μg/ml	CST	3933
BiP	Rabbit	75 kDa	1/1000	200μg/ml	CST	3183
PERK	Rabbit	125 kDa	1/1000	100μg/ml	CST	3129
p-eLF2α	Rabbit	37 kDa	1/1000	200μg/ml	CST	3398
ATF4	Rabbit	49 kDa	1/1000	100μg/ml	CST	11815
P58	Rabbit	58 kDa	1/1000	100μg/ml	CST	2940
TM	Rabbit	75 kDa	1/1000	100μg/ml	Abcam	Ab109189
ICAM1	Mouse	74 kDa	1/1000	100μg/ml	Abcam	Ab2213
TF	Rabbit	80 kDa	1/1000	100μg/ml	Abcam	Ab211016
VWF/HRP	Rabbit	230 kDa	1/1000	100μg/ml	Dako	P0226

Table 2.1: Western Blotting Primary antibodies.

Subsequently, the membranes were washed at room temperature five times for 5 minutes in 100ml 0.05% TBS-Tween Buffer pH 7.5 (900ml of dH_2O, 100ml of 10x TBS, 0.05 % (v/v) Tween 20). The membranes were then incubated at room temperature for 1 hour with their animal-sourced matched horseradish peroxidase-conjugated anti-Immunoglobulin G antibodies (HRP-conjugated) (Table. 2.2). Afterwards, the membranes were washed as described earlier to remove excess secondary antibodies. Finally, Supersignal ™ West Pico Plus Chemiluminescent Substrate kit (ThermoFisher Scientific, UK) was used to develop the membrane, using the BIO-RAD ChemiDoc MP Imaging System (BIO-RAD, UK). The protein volumes were obtained using Image Lab Software (Bio-Rad, UK). All proteins were normalised against the

housekeeping protein Glyceraldehyde 3-phosphate dehydrogenase (GAPDH) to calculate the fold change difference of each protein.

Antibody	Source	Dilution	Concentration	Company	Cat. Number
Anti-Mouse IgG	Goat	1/2000	1mg/ml	Dako	P0448
Anti-Rabbit IgG	Goat	1/2000	1mg/ml	Dako	P0447

Table 2.2: Horseradish peroxidase (HRP)-conjugated secondary antibodies.

2.4. Quantitative Real-Time Polymerase Chain Reaction (qRT-PCR)

2.4.1 Harvesting Cellular RNA lysate

Total cellular RNA content was harvested using BL+TG buffer (1% 1-Thioglycerol, 4M Guanidine thiocyanate, 0.01M Tris pH 7.5) obtained from the ReliaPrepTM RNA Cell Miniprep System (Promega, USA). The volume of BL+TG buffer was used as follows: if the cells were harvested from 6-or 48-well plates, 500µl and 100µl of the buffer were used, respectively. The lysate was transferred into the corresponding labelled Eppendorf tubes. The lysate was left on ice for 30 minutes and vortexed every five minutes. Finally, the lysate was stored at -80^{o}C until further processing and investigation.

2.4.2 Extracting total Cellular RNA and sscDNA synthesis

Cellular RNA lysate vials were retrieved from the -80^{o}C freezer and defrosted on ice. The total cellular RNA lysate was extracted using ReliaPrepTM RNA Cell Miniprep System (Promega, USA). 100% Isopropanol has added to the RNA lysate if the cells were harvested from 6-, 48-well plates, 170µl and 35µl of 100 % Isopropanol were used, respectively. The solutions in each tube were vortexed for 5 seconds, and the content of each tube was transferred into the corresponding labelled ReliaPrepTM Minicolumn inserted into collection tubes. Subsequently, the tubes were centrifuged at 13,000×g, 20°–25°C for 30 seconds. This centrifugation setting was applied to all the steps of the total RNA extraction apart from the spinning time required. The liquid in the collection tubes was discarded, and 500µl of RNA wash solution diluted with 95 % ethanol was added to the minicolumn, followed by centrifugation for 30 seconds.

The liquid in the collection tubes was discarded, and 30µl of freshly prepared DNase I incubation mix (24µl of Yellow Core Buffer + 3µl 0.09M $MnCl_2$ +3µl of DNase I enzyme) was applied directly to the membrane inside the column to each tube. The tubes were incubated at room temperature for 15 minutes, followed by washing them with 200µl of column wash solution re-suspended with 95% ethanol and centrifuged for 15 seconds. The liquid in the collection tubes was discarded, and 500µl of RNA wash solution was added to the minicolumn and centrifuged for 30 seconds. Subsequently, the minicolumns were transferred into new collection tubes, and 300µl of RNA wash solution was added to the minicolumn and centrifuged for 2 minutes. Lastly, the minicolumns were moved into a 1.5ml elution tube, 30µl of Nuclease-Free Water was added to the membrane of each minicolumn tubes and centrifuged for 1minute. The minicolumns were discarded, and the elution tubes containing the purified RNA were stored at –80°C until further processing. The RNA concentration (ng/µl) was determined using NANODROP 1000 (Thermo Scientific, UK) at 260 nm absorbance, and the degree of protein and reagent contamination was determined using the 260/280 and 260/230 ratio, respectively. According to the manufacturer's protocol, cDNA was prepared using the iScriptTM cDNA synthesis kit (iScript™ cDNA Synthesis Kit Bio-Rad, UK). An equivalent amount to 1000ng of RNA was aliquoted in a 20µl final volume reaction mix as indicated in (Table. 2.3). The cDNA synthesis reaction was conducted on MultiGene OPTIMAX Thermal cycler (Applied Biosystem, UK) and programmed as detailed in (Table. 2.4).

Component	**Volume per reaction,** µl
5x iScript Reaction Mix	4
iScript Reverse Transcriptase	1
Nuclease-free water	Variable
RNA templet (1000 ng of total RNA)	Variable
Total volume	20

Table 2.3: cDNA synthesis reaction mix components.

Reaction step	**Time**
Priming	5 minutes at 25°C

Reverse transcription	20 minutes at 46°C
RT inactivation	1 minute at 95°C
Optional step	Hold at 4°C

Table 2.4: cDNA synthesis reaction mix protocol.

2.4.3 Real-time Quantitative PCR (RTq-PCR)

RTq-PCR was performed to analyse a panel of genes using primers purchased from (Eurofins Genomics, France) with a 20nM concentration of both forward and reverse primers per reaction. All primer sequences were taken from previous publications, listed in (Table. 2.5). The prepared cDNA was diluted in 1:10 with RNase free water yielding a 100ng final sample concentration before preparing the standard curve. The standard curve was prepared by pooling an equal volume of cDNA from each test sample, and then a five-point, 1:4 serial dilutions with RNase free water were prepared, including a blank. The RTq-PCR reaction mix for each sample was prepared as follows: 5µl of PowerUp™ SYBR™ Green Master Mix (Applied Biosystems, UK) was added to 2µl of the primers cocktail along with 0.5µl of free nuclease water. Two µl of each cDNA sample were loaded in MicroAmp Fast 96-Well Reaction Plate 0.1mL (Applied Biosystems, USA) followed by adding 9µl of the reaction mix. No template controls were run by adding 2ul of ddH_20 followed by 9ul of the reaction mix. The cDNA amplification was conducted in the Applied Biosystems StepOnePlues machine (Applied Biosystems, USA). The thermocycler machine's cycling was programmed as follows: denaturation at 95°C for 10 minutes followed by 40 annealing/extension cycles at 95°C for 3 seconds, and 60°C for 30 seconds. Three technical repeats were loaded for each sample, and gene expression was quantified following the standard curve method. Primer dimer development was identified by analysis of melt curves. Wells were omitted from the experiment if either no peaks were identified beyond the threshold or several peaks above the threshold were observed at different temperatures. GAPDH was used as a housekeeping gene for normalisation test samples against untreated/DMSO control cells. Fold Change of mRNA expression was calculated using the RQ values described in (298) GAPDH expression was established to be stable in the numerous stress conditions examined, with slight changes in the gene quantity values that were not correlated a particular experimental condition. The data were analysed with GraphPad Prism (V 9.1.2) and Excel (Microsoft Office, 2019).

Primer sequences for RT-qPCR		
Gene	**Forward primer** (5'-3')	**Reverse primer** (5'-3')
GAPDH (298)	TCTGCTCCTCCTGTTCGACA	AAAGCAGCCCTGGTGACC
CHOP (299)	AGCAGAGGTCACAAGCACCT	TTCATGCTTGGTGCAGATTC
PERK (300)	GATCCGGTTCCTTGGTGTCA	CCATGCTTTCACGGTCTTGG
eLF2α (301)	AGCAGAGGTCACAAGCACCT	TTCATGCTTGGTGCAGATTC
ATF4 (302)	AGATGACCTGGAAACCATGC	AGGGATCATGGCAACGTAAG
BiP (303)	GCCGTCCTATGTCGCCTTC	TGGCGTCAAAGACCGTGTTC
IRE1α (304)	CGGGAATTCGGCCGAGTCCTCGCCATG	CAAGCGGCCGCCTTTCCCAACTATCACCACGCT
TF (305)	GCCAGGAGAAAGGGGAAT	CAGTGCAATATAGCATTTGCAGTAGC-
TM (306)	CCCAACACCCAGGCTAGCT	GATGTCCGTGCAGATGAAACC
VWF (307)	GCAGTGGAGAACAGTGGTG	GTGGCAGCGGGCAAAC
tPA (308)	TGGTGTGGGATCTGCGTACA	CCTCCACTCCATACAGGGTCA
EPCR (309)	CAACTTCAGGATGTTGACAA	CTACAGCCACACCAGCAAT
TFPI (310)	CAATGGGACTATGATGGCCCTTCA	AATCATAGTGAAAACACCTTATAG
eNOS (311)	TGGACCTGGATACCCGGAC	TGGTGACTTTGGCTAGCTGGT
PS26 (312)	CGTTCACTCCAGACTGGGAAAG	CGGTCGTGAATAGGTGTCAGCT

Table 2.5: Primer sequences for qRT-PCR. Forward primer sequences (5'-3') and reverse primer sequences (5'-3') are shown for primer sets, which amplify the cDNA of the indicated proteins.

2.5 Enzyme-Linked Immunosorbent Assay (ELISA)

2.5.1 VWF ELISA

An "In house" ELISA was used to measure the soluble VWF protein concentration. Initially, a VWF capture antibody solution was prepared using polyclonal rabbit anti-human VWF (Dako, UK) diluted 1:1000 in carbonate-bicarbonate coating buffer (1 Litter of distilled water, 0.64 g Sodium Carbonate (Na_2CO_3), 3.7 g Sodium Bicarbonate

($NaHCO_3$)) to give a final concentration of 3 µg/ml. Subsequently, 100µl of the capture antibody was loaded to each well of a Greiner Bio One™ 96 Well ELISA plate (96-well plate) (Star Lab, UK). The plates were incubated for 60-90 minutes at room temperature or overnight at 4°C. Plates were washed three times with 0.1% PBS-T buffer. After, wells were blocked using 2% (w/v) BSA in PBS-T buffer for 90 minutes at room temperature. A seven-point standard curve was prepared to dilute normal human control plasma (Technoclone, UK) from 1:40 serially. Samples were diluted accordingly. Following washing, 100µl of each sample was loaded in duplicate and plates were incubated either at room temperature for 90 minutes or at 4°C overnight. Subsequently, the washing procedures were repeated. Afterwards, 100 µl of polyclonal rabbit anti-human VWF-HRP conjugated antibody diluted 1 in 2000 (final concentration 1µg/ml) diluted in PBS-T was added to each well and incubated for 45mins at room temperature. The washing steps were repeated, and sigma colourfast reagent was prepared by mixing SIGMAFAST™ OPD tablets (Sigma-Aldrich, UK) with ddH_2O. The substrate was loaded into the 96-well plates, and once sufficient colour changes were observed (typically 2mins), the reaction was stopped using 50µl of 2M Sulfuric Acid (H_2SO_4, Sigma-Aldrich, UK). Finally, the plate was read at 492 nm in the microplate reader. The standard curve was plotted in Excel, and the equation for straight line; y = mx+b, was used to calculate the concentrations of the analysed samples.

2.5.2 ICAM-1 and Ang2 ELISA

Levels of soluble ICAM-1 and Ang2 were measured using the human ICAM-1/CD54 DuoSet ELISA kit and the Ang2 DuoSet ELISA kit, both from R&D Systems, UK). Both ELISA's were performed exactly as specified by the manufacturer.

2.6 Immunofluorescence staining

2.6.1 Immunofluorescence staining for Actin and VWF

Cells were cultured essentially as described in (Section 2.1) except a 13mm glass coverslip was placed in each well and coated with attachment factor before cells were seeded in the wells. Following the experiment, media was removed, and cells were washed twice with PBS. Cells were fixed in the dark for 20 minutes at room temperature

with 1ml of 4% paraformaldehyde (PFA) (40g PFA powder, 0.5% Triton X-100, 1000ml 1X PBS, PH 6.9 - 7.4) (Sigma Aldrich, UK). PFA was discarded, and the cells were washed three times with PBS and incubated with 20mM NH_4Cl for 20mins. Following washing twice with PBS, HUVECs were then permeabilised by incubating with 1ml of 0.1% Triton-X (Sigma Aldrich, UK) at room temperature for 4 minutes and then washed twice with PBS. For actin fibres, cells were stained with Alexa Fluor™ 584 Phalloidin (Abcam, UK) diluted 1 in 1000, and for VWF cells were stained with anti-VWF-FITC antibodies (Abcam, UK). Both were diluted in PBS with 1%(w/v) BSA and incubated for 60mins at room temperature in the dark, then moved into the fridge overnight. The Fluoroshield Mounting Medium with DAPI (Abcam, UK) was used to mount the stained cells under a glass coverslip. Cells were visualised and imaged using an EVOS M5000 microscope (Invitrogen, UK).

2.7 Flow cytometry

2.7.1 ICAM-1 flow cytometry

The cells were cultured as described in (Section 2.2.1**)**; adherent cells were washed twice with PBS and detached using the trypsin enzyme. The light microscope was used to confirm the detachment of the cells by examining cell forms under the light microscope. The trypsin was neutralised with EBM-2 media, and the detached cells were transferred into labelled Eppendorf tubes centrifuged for 5 minutes at 1500 rpm, 4°C. Supernatants were discarded, and cells were resuspended as following: **1)** test samples were resuspended in a solution composed of 1:40 FITC-conjugated anti-human CD54 antibody (BioLegend, California, USA) diluted in 39µl of 0.5% BSA-PBS solution (0.25g BSA to 50mL 1 x PBS (sterile); **2)** unstained negative control cells were resuspended in a solution composed of 39 µl of 0.5% BSA-PBS solution only.

The cells were then transferred to 96 well polypropylene plate, 8mm round-U base (ThermoFisher Scientific, UK). The plate was foiled with aluminium and incubated for 20 minutes in the cold room. Later, the plate was spun down at 1500 rpm, 4°C, for 5 minutes, using Thermo Scientific M-20 Microplate Swinging Rotor (Cole-Parmer, UK). The supernatant was discarded, and 100µL of 0.5% BSA:1xPBS was used to resuspend cells in each well. After aliquoted cells were transferred to polypropylene FACS tubes (Corning, New York, USA), cells were pipetted thoroughly to ensure sample homogeneity. The cells were further diluted with 100µl of 0.5% BSA:1x PBS if

they were to be processed immediately, or with 4% PFA if they were to be processed the next day. The BD Accuri™ flow cytometer (BD Biosciences, California, USA) was used to run the cells at slow speed for 2 minutes. The gating of cells was on side light scatter alongside forwarding light scatter applied to eliminate unwanted debris. Subsequently, single cells gating was used to eliminate doublets/clusters cells; the threshold for positive FITC/ CD54 staining was obtained by gating unstained cells control. FLOWJO software (BD Bioscience, UK) was used to analyse the raw data. GraphPad Prism 9.0 was used to perform statistical analysis and generate figures.

2.7.2 Annexin-V and Propidium Iodide (PI) apoptotic flowcytometry

Cell preparation and harvesting were conducted as described in (Section 2.7.1). The dead cells (zombie) control was prepared by incubating the cells with 20-30µl DMSO for 20-30 minutes. Test samples and zombie samples were resuspended in a solution composed of 39µl 1x binding buffer (Abcam, UK) and 5µl Annexin V-FITC, 5µl PI and 1µl SYTOX Green dye (Abcam, UK). The unstained negative control cells were resuspended in a solution composed of 39µl 1x binding buffer only. After the cells were transferred to polypropylene FACS tubes and incubated in the dark for 5 minutes at room temperature. Stained cells were analysed by flow cytometry, and raw data were analysed as described in (Section 2.7.1).

2.8 Small interfering (si) RNA transfection

All siRNAs (BiP, eNOS, and scrambled control) were purchased from Santa Cruz (California, USA) and prepared according to manufacturer instructions. HUVECs were seeded in AF coated plates, and siRNA transfection was performed once the cells were 80% confluence. RNAiMAX transfection agent was used according to manufactures instructions. Initially, preliminary experiments were performed to determine the optimal concentration of siRNA. After optimisation, 20nM was selected as a standard concentration for all the transfection procedures. A transfection complex was prepared for each well of a 6-well plate: in **tube A**, 15µl of Lipofectamine™ RNAiMAX (Thermo Fisher Scientific, UK) was diluted with 150µl of Opti-MEM® Medium (Gibco, UK). In **tube B**, 8 µl of each siRNA stock (20nM) were diluted with 150µl Opti-MEM® Medium. For each well of the 48-well plate, a transfection complex was prepared as follows: in the **tube, A** 1.35µl of Lipofectamine™ RNAiMAX was

diluted with 22.5µl of Opti-MEM® Medium. In **tube B**, 0.6µl of each siRNA stock (20nM) was diluted with 22.5µl Opti-MEM® Medium. Both tubes were mixed gently by inverting them a few times, and the mixture from tube B was transferred to tube A. The solution was mixed gently and incubated at room temperature for 5 minutes. 250 µl of the siRNA transfection reagent was then transferred into each well of the 6-well plate. According to the planned experiment, the plates were then re-incubated for 24-48 hours, and then cells were stimulated with DMSO, CFZ or CFZ plus cytokines. Once the experiment finished, the media and cells were harvested, the protein and genomic content were collected and stored at -80°C for further investigations.

2.9 Functional studies on HUVECS

2.9.1 Turbidity assay

Turbidity assays were performed to study the formation of fibrin clots on the endothelium following drug and cytokine treatment. The method utilizes a spectrometer to measure the absorbance of light through a growing fibrin clot, where absorbance increases as the clot become denser. The time between the assay starting and the formation of the first fibrin aggregates is known as the lag time; therefore, the lower the lag time, the more pro-thrombotic active the cells are. HUVECs were cultured in a 48-well plate as described in (Section 2.2.5) and were either non-treated or treated with DMSO, CFZ, TNFα or both CFZ and TNFα. Each well was loaded with 100µl plasma for each reaction, then the reaction started by adding 100µl HEPES/NaCl buffer pH7.5 supplemented with 20mM $CaCl_2$ to give a final $CaCl_2$ concentration of 10mM in each well. The 48-well plate was immediately read using the microplate reader at 405nm for 30-minutes/30-second measurement interval (Figure 2.1). The data were extracted from the machine, analysed by Excel, and presented as absorbance curve and lag time using GraphPad Prism 9.0.

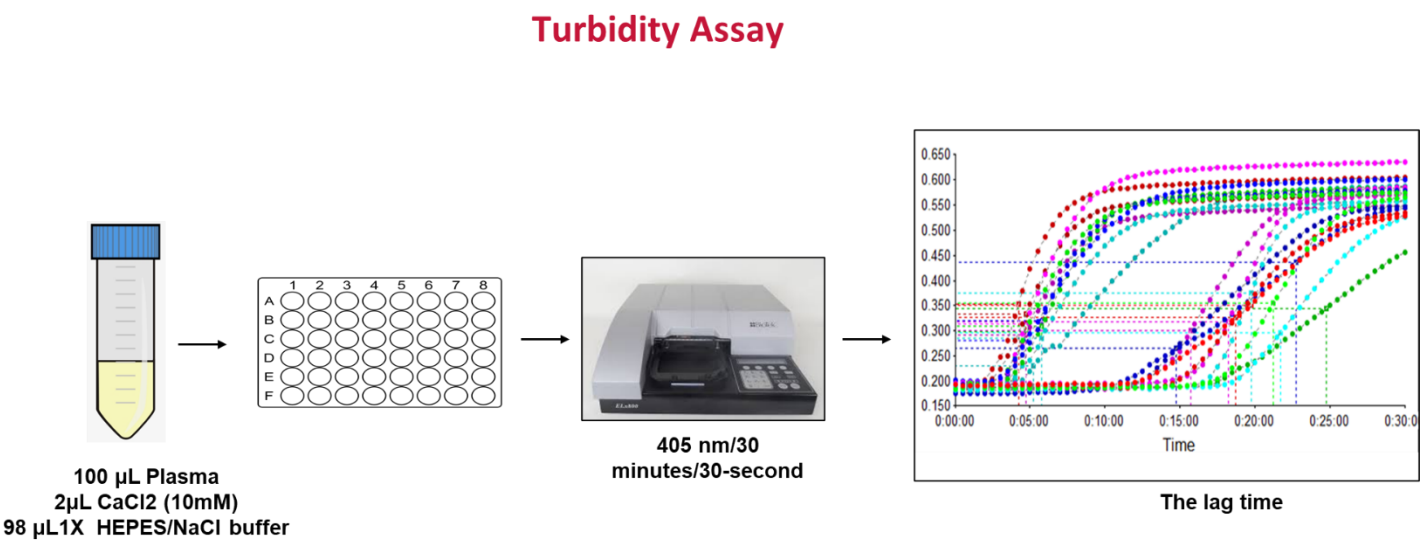


Figure 2.1: Schematic illustration of the turbidity assay. The figure was prepared by (Ahmed Hjazi, 2021)

2.9.2 Factor X activation assay

The principle of this assay is to measure the activation of Factor X on the HUVECs surface. The assays utilise purified proteins and eliminate the need for plasma. In brief, following treatment of the cells with drug, cytokine or both, cells are incubated with FVIIa, which complex with cell surface tissue factor to convert FX to FXa. Therefore, if the cells express more TF on their surface, it will bind more FVIIa and activate more factor X. The generation of Xa can then be monitored by the cleavage of a fluorogenic factor Xa specific peptide substrate. The cells were cultured and treated in 48-well plates as described in (Section 2.2.5). HUVECs were washed once with 1x PBS, and the cells in each well were then incubated with 2.5nM FVIIa diluted in reaction buffer (50mM HEPES, 122mM NaCl, 5mM $CaCl_2$, pH 7.4) yielding a final volume of 100µl and incubated at 37°C for 60mins. Following this, cells were washed three times in washing buffer (50mM HEPES, 122mM NaCl, pH 7.4) and then incubated with 175nM human factor X (Enzyme Research Laboratories, Swansea) diluted in reaction buffer in a final volume of 100µl and re-incubated at 37°C for 20 minutes. After 20mins 90µl of the reaction was removed and added to a 96 well plate. Finally, 40µl of the substrate solution was added to each well (0.2mM S-2765 chromogenic substrate diluted in 50mM HEPES, 122mM NaCl pH7.4), and the plate was immediately read at 405nm

for 30 minutes/30-second measurement interval. The data were analysed as described in (Section 2.9.2) (Figure 2.3).

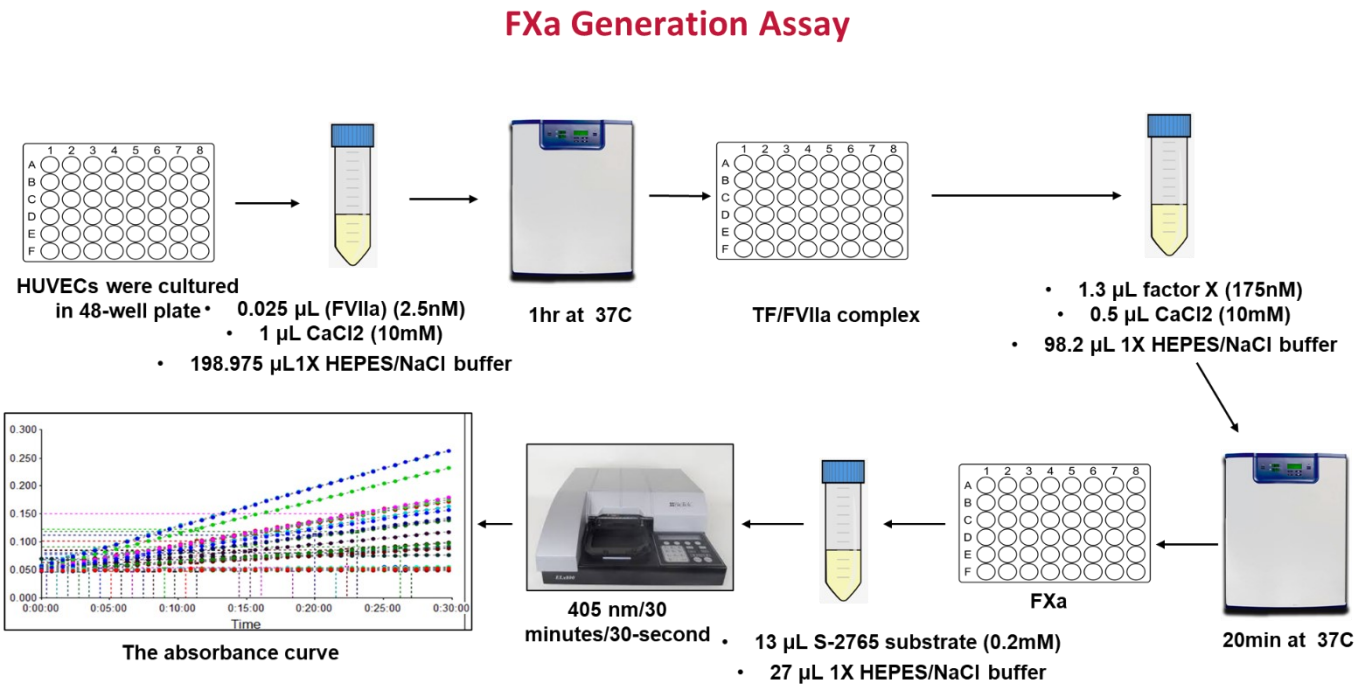


Figure 2.2: Schematic illustration of Factor X Human Chromogenic Activity Assay. The figure was prepared by (Ahmed Hjazi, 2021)

2.9.3 Activated Protein C (APC) generation Assay

In its activated state, Protein C is important as an anticoagulant, which is derived from zymogen protein C. It is activated when it interacts with the thrombomodulin-thrombin complex, thus generating APC. The generation of APC can then be monitored by the cleavage of a fluorogenic APC specific peptide substrate. The cell was cultured in a 48-well plate as described in (Section 2.2.5). Cells were washed once with 1x HEPES/NaCl buffer. After, 100µl of reaction buffer (0.9µl of protein C, 10µl of 1:10 thrombin diluted in HEPES/NaCl, and 90µl of 1X HEPES/NaCl buffer) was added to each well apart from the blank wells. 100µl of 1x HEPES/NaCl buffer were added to the blank wells. The plates were incubated for 60 minutes at 37°C. Another 96-well plate was prepared for the next step by adding 4µl of Hirudin (thrombin inhibitor) (Sigma Aldrich, UK) to each well. Once the incubation finished, 90µl of cells

supernatant from the 48-well plate was transferred to the correspondent labelled wells of the 96-well plate. The 96-well plate was incubated for 10 minutes at 37°C. Once the incubation finished, 10µl of S-2360 substrate (Chromogenix, Sweden) was added to each well. The absorbance of the plates was read using the Microplate reader at 405nm for 60 minutes/30-second measurement interval (Figure 2.4). The data were analysed as described in (Section 2.9.2) and presented as absorbance curve and endpoint absorbance figure par.

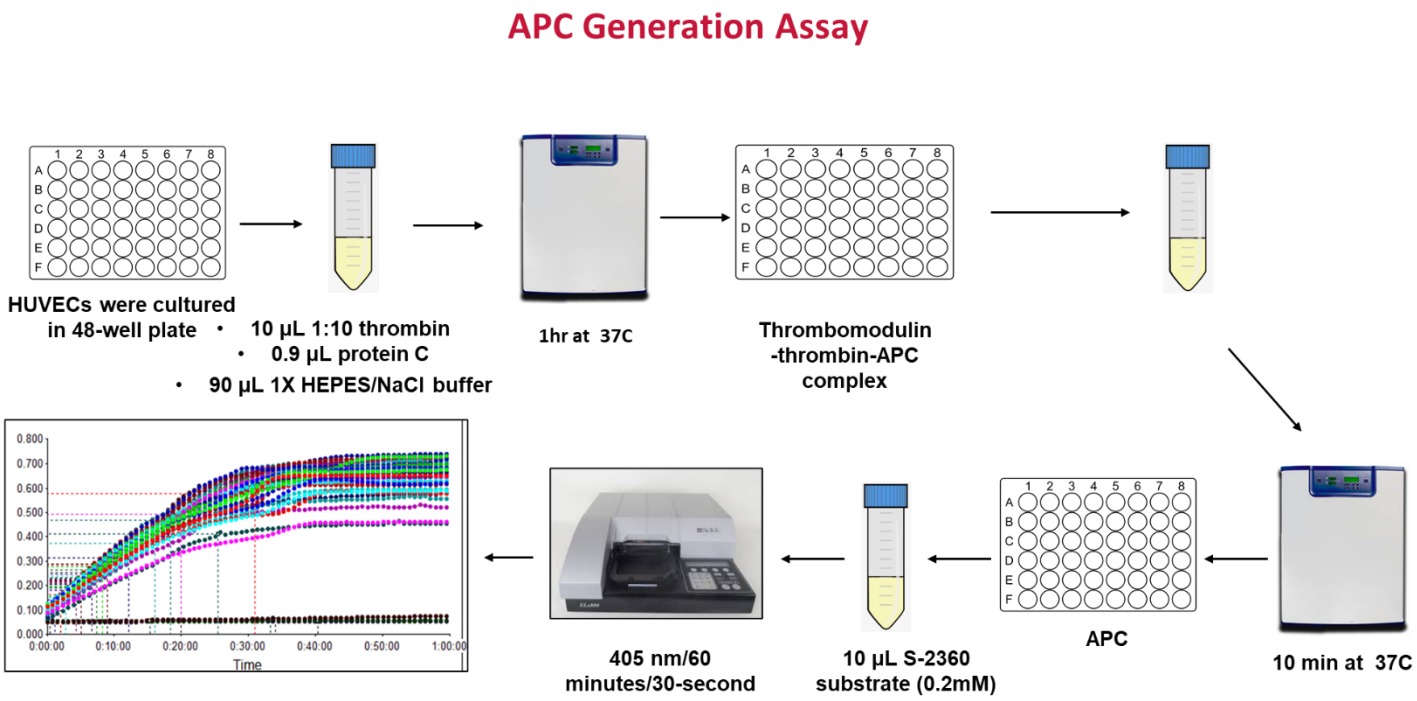


Figure 2.3: Schematic illustration of Activated Protein C (APC) generation Assay. The figure was prepared by (Ahmed Hjazi, 2021)

2.9.4 Microfluidic perfusion assays

2.9.4.1 Cell culture

Microfluidic flow assays were performed to assess the effect of CFZ on endothelial function under physiological conditions of shear stress. Von Willebrand factor (VWF) is a major endothelial-derived glycoprotein involved in

haemostasia. The release of VWF by endothelial cells occurs following endothelial damage or activation, which allows interactions with circulating platelets. In this assay, the formation of VWF-strings on endothelial cells is measured in a physiologically relevant environment. HUVECs were trypsinised from a 100% confluence T-75 flask using 1ml of trypsin enzyme, then neutralized with 4ml of EBM-2 medium. Cells were collected in a sterile 15ml tube (Thermo Fisher Scientific, UK), centrifuged at 1500rpm, at room temperature for 5 minutes and resuspended with 1ml of EBM-2 medium. From this, 100µl of cells was added to Ibidi single-channel $I^{0.4}$ Ibidi coated flow chambers. From a typical confluence T75, this equates to approximately 100,000 cells. The Ibidi slides comprise a single channel of 400µm high coated with an undisclosed adherent surface. The cells were left to attach for 1 hour at 37°C, 5% CO_2. Following this, each reservoir on either side of the channel was topped up with 60µl of EBM-2 medium and incubated overnight. Typically, within 24-48 hours, the cells had formed a monolayer and were ready for use. On the day of the experiment, the cells were washed once with PBS and then incubated with fresh EGM-2 for 1 hour. Following this, the cells were incubated with either DMSO or 750nM CFZ for 1 hour. The cells were washed and incubated with fresh EGM-2 with or without 20ng/ml TNFα (overnight) after the drug incubation. After the overnight incubation, the slides were assembled under a fluorescent microscope and perfused with washed red blood cells and labelled platelets as described in the following sections.

2.9.4.2 Preparation of washed platelets and red blood cells

Solutions required for this section were prepared in advance and listed in (Table 2.6).

Solution	Components	Final Concentration	Company	Storage
Platelet wash buffer	1mM $MgCl_2$, 100mM NaCl, 36mM Citric acid, 5mM KCl, 5mM glucose, 2mM $CaCl_2$, pH 6.5 (with NaOH pellets)	N/A	Prepared in the lab	4°C
Ethylenediaminetetraacetic acid (EDTA)	Stock solution	(500 mM, pH 8.0)	Cayman Chemicals, USA	4°C
Acid Citrate Dextrose (ACD)	71 mM citric acid, 111 mM glucose, 85 mM sodium citrate, pH 4.5	N/A	Prepared in the lab	4°C
HEPES-Tryrodes buffer	10mM HEPES, 2.68mM KCl, 11.9mM $NaHCO_3$, 137mM NaCl, 0.42mM NaH_2PO_4 ,1.7mM $MgCl_2$, 5mM glucose, pH7.4	N/A	Prepared in the lab	4°C
saline solution	450mg NaCl in 50ml H_2O	0.9% (w/v)	Prepared in the lab	Room temperature
Dihexyloxacarbocyanine Iodide (DiOC)	Stock solution	5µM	Bio Legend®, USA	-20°C
Prostaglandin E_1 (PGE1)	Stock solution	100µM	Sigma Aldrich, UK	-20°C
Apyrase	Stock solution	1mg/ml	Sigma Aldrich, UK	-20°C

Table 2.6: Flow assay solutions

HEPES-Tyrodes buffer, ACD, and platelet wash buffer were pre-warmed to room temperature before use. Blood was collected from a healthy donor into a 50ml tube containing 10% v/v ACD. Blood was centrifuged for 15 minutes at 120g, with no break at 20-25°C. The resulting platelet-rich plasma (PRP) was transferred carefully dropwise using a plastic pasture pipette to a fresh 15ml tube, and the RBCs were kept in the original 50ml tube. 100nM PGE1, 100mU Apyrase, and 10%v/v ACD were added to the PRP tube, and an equal volume of 0.9% saline was added to the RBCs tube, and this was gently inverted 2-3 times to mix. Both tubes were centrifuged for 15 mins at 1200g, with no brake. Once the centrifugation finished, the top layer of the PRP tube containing platelet-poor plasma was transferred into another 15ml tube and stored at -20°C for future use. The platelet pellet was carefully and slowly resuspended in 14ml of a solution containing platelet wash buffer, 3.5mg/ml BSA, 100nM Prostaglandin E1, 0.7µl DiOC and 100mU Apyrase. The supernatant was discarded from the RBCs tube, and the RBCs were carefully mixed with an equal volume of 0.9% saline. Both tubes were centrifuged for 12 min at 1200g, with no brake. Following this, the supernatant of the platelet tube was discarded, and the pellet was carefully resuspended with 1ml of HEPES/Tryodes buffer. The RBCs supernatant was discarded and washed a final time with 0.9% saline. Following the last RBC wash, the supernatant was discarded, and the washed RBCs were resuspended to the original starting volume of blood with HEPES/Tryodes buffer, and the 1ml washed and labelled platelet solution was added to the resuspended RBCs.

2.9.4.3 Perfusion over HUVECS

The washed RBCs and platelet mixture prepared in (Section 2.9.5.1) were drawn into a 10ml BD PlastiPak™ Syringe (BD Emerald™, UK) and mounted onto a Harvard syringe pump (World Precision Instruments, UK). An inlet tube was connected to the syringe and placed into one side of the Ibidi slide. A waste tube was connected to the other side of the slide. The RBC/platelet mix was then perfused through the channel at a defined volumetric flow rate of 800µl/min to give an approximate wall shear rate of $100s^{-1}$. Platelet capture to VWF was visualized in real-time using an OLYMPUS CKX41 microscope connected to a Lumen 200 Fluorescence Illumination System. Live images were captured after 3mins perfusion using QCapture Pro software. The VWF string bodies were counted manually using the ImageJ particle counter, and GraphPad Prism 9.0 was used to perform statical analysis and create the figures.

2.9.5 Leukocyte adhesion assay

The interaction between endothelium and leukocytes is essential for the inflammatory response. In this assay, the adhesion between endothelial cells and leukocytes is measured under shear stress conditions. As described earlier, cells were cultured and treated in Ibidi single channel I0.4 Ibidi coated flow chambers. The perfusion assays were performed similar to described above, except whole blood drawn into 10% v/v ACD was directly treated with DiOC to label platelets and white blood cells. Whole blood was perfused at $100s^{-1}$ through endothelial cells, and leukocyte adhesion was recorded in real-time. The relative difference in size between leukocytes and platelets allowed for easy differentiation between the two.

2.10 Statistical analysis

GraphPad Prism Version 9.0 (GraphPad Software, La Jolla, CA, USA) was used to analyse all the data. Data was compared to untreated or vehicle (DMSO) control and presented as a mean ± standard error of the mean (SEM). Three or more independent experiments ($n \geq 3$) with three technical repeats for each experiment were conducted, unless stated in the result. The multiple comparisons and the p-values of the data involving two independent variables were analysed by One-way or Two-way ANOVA followed by Tukey's multiple comparisons post hoc test. P values of less than 0.05 were considered as a significant difference between groups. p values are indicated in figure legends, *$p < 0.05$, **$p < 0.01$ and ***$p < 0.001$ and ****$p < 0.0001$.

3. Results

3.1 CFZ did not induce ER stress in HUVECs

3.1.1 Introduction

Multiple myeloma (MM) is the malignant transformation of plasma cells that collect in the bone marrow, leading to marrow failure and bone destruction. (313) The disease is more frequent in older people and found twice as frequently in black people than white people. (104) The mean age of patients with MM is 61 years for women (79% > 70 years) and 62 years for men (75% > 70 years). The root causes of this disease are not yet fully understood, and its extent, clinical course, sensitivity to drugs and complications differ widely among patients. (104) Treatment of MM has notably improved during the past decade. The expansion in the number of active drugs has created several potential drug combinations that can be used as first-line drugs and in relapsed settings. (314) In addition, a greater understanding of the cellular disease mechanisms have emerged as a foundation for new combinations of treatments and drug development. (56) According to the Surveillance Epidemiology and End Results database, there was a significant increase in the five-year survival rate between 1975 (25%) – 2005 (34%) due to the administration of advanced and more effective treatment regimens. (315) Even though MM is usually sensitive to numerous cytotoxic treatments, both as a primary treatment and in the management of relapsed disease, responses to the drugs are transient; therefore, the cure of MM is hugely challenging with existing approaches. (315) The current drawbacks of MM treatment approaches can lead to disease relapse and are refractory to all available treatments. Therefore, developing a new, more effective, and a well-tolerated class of MM drugs is essential. (316)

The 26S proteasome plays a vital function in cellular homeostasis in ubiquitin-dependent protein turnover involving misfolded targets and obsolete proteins, stress response, apoptosis, cell-cycle progression and DNA repair. (10) Thus, the proteasome has emerged as a vital tool for cancer treatment with the authorisation of bortezomib (BTZ), a first-class reversible proteasome inhibitor (PIs) for (RRMM). (316) Nevertheless, BTZ has been found to be ineffective among some MM patients and

others who developed drug resistance, which became an essential trigger to establish other PIs with superior activity.

CFZ is a novel, evaluated, irreversible epoxomicin-related second-generation PI. This agent effectively binds and exclusively inhibits the 26S chymotrypsin-like β-subunit of the immunoproteasome and proteasome activities. (317) This inhibition leads to an accumulation of ubiquitinated substrates within the cellular cytosol, resulting in ER stress and the activation of the unfolded protein response system. (317) Prolonged activation of this system and failure of the cells to restore normal protein production ultimately leads to apoptosis. Programmed cell death was associated with mitochondrial membrane depolarization, the activation of both intrinsic and extrinsic caspase pathways, the activation of c-Jun-N-terminal kinase, and the release of cytochrome c. (317) CFZ has significantly advanced the management of relapsed and/or refractory MM patients, involving those intolerants to bortezomib. (318) Significantly increased response rates have been confirmed with CFZ as a single treatment or combined with corticosteroids, immunomodulators and alkylating agents, including in patients who have failed various prior treatments. (318) CFZ also demonstrates substantial potential as a frontline MM treatment, supporting response and survival rates. (318) Importantly, CFZ has presented improved effectiveness than bortezomib and shown effectiveness against bortezomib-resistance in the clinic and bortezomib-resistant MM cell lines. (319) CFZ also has overwhelming resistance to other standard treatments and has operated synergistically with dexamethasone to increase cancer cell death. (319) However, the usage of CFZ in MM has been associated with an increased risk of serious adverse events. Various cardiovascular complications were reported among such events, including hypertension, myocardial infarction, ischemic heart disease, and angina. (320) Among 60 MM patients treated with CFZ, 12% (95% confidence interval, 3.8%-20%) were diagnosed with cardiovascular risk complications. (321) They experienced ≥20% reversible left ventricular ejection fraction (LVEF), which is a principal indicator of cardiac dysfunction. The incidence of LVEF reduction was 5% at three months, 8% at six months, 10% at 12 months and 12% at 15 months. (321)

In this results chapter, I hypothesised that the cytotoxic effect of CFZ against MM cancer cells could be an off-target effect against the human vascular endothelium. Therefore, I investigated the potential ability of CFZ to inhibit proteasome function within endothelial cells, thus causing the activation of ER stress in the endothelium.

3.1.2 Results

3.1.2.1 Carfilzomib causes a distinct morphological change in HUVECS and induces protein ubiquitination.

In order to investigate the initial hypothesis that CFZ alters and damages endothelium function similarly to its ER stress effect against MMCs, HUVECs were cultured under static conditions and exposed to CFZ in concentrations equivalent to those found in the plasma of patients undergoing anti-MM treatment 500-2000 nM (750 nM of CFZ was selected as standard dosage for one hour), and the pharmacokinetic half-life of the drug was 1 hour. Initially, light microscopy revealed a progressive morphological change. Cells appeared 'stretched' in CFZ treated cells in the 24 hour recovery period after drug treatment (Figure 3.1.1 D), suggesting structural rearrangement of F-actin stress fibres and possible activation of the endothelium; while after a 48-hour recovery period, the cells had almost returned to a similar appearance as that of untreated and DMSO treated cells; a normal 'cobblestone' cell morphology, indicating cell recovery (Figure 3.1.1, A, B, C, E). Next, it was investigated if CFZ induces proteasome inhibition of endothelial cells. Ubiquitin is a protein implicated in the regulation of misfolded protein degradation through ERAD mechanisms. (322) The build-up of ubiquitinated chains triggers the ERAD by the proteasome. HUVECs were treated with 750nM of CFZ for 1 hour, followed by removal of the drug and replacement with fresh media. Cell lysates were harvested at selected time-points (0hr, 24hr and 48hr). Western blotting was used to compare the ubiquitination levels of CFZ treated cells compared to non-treated and DMSO controls. The immunoblotting results obtained across three biological repetitions indicated that ubiquitination was significantly up-regulated in CFZ-treated cells after 24 hours compared to the controls, which is consistent with the role of the drug as a proteasome inhibitor (Figure 3.1.2 A&B). Taking all these observations together, CFZ demonstrated an evident potent ability to inhibit proteasome function in HUVECs; however, this was a transient effect, since the ubiquitination level and the cell morphology almost returned to a comparable level and appearance as the control cells after 48 hours of recovery.

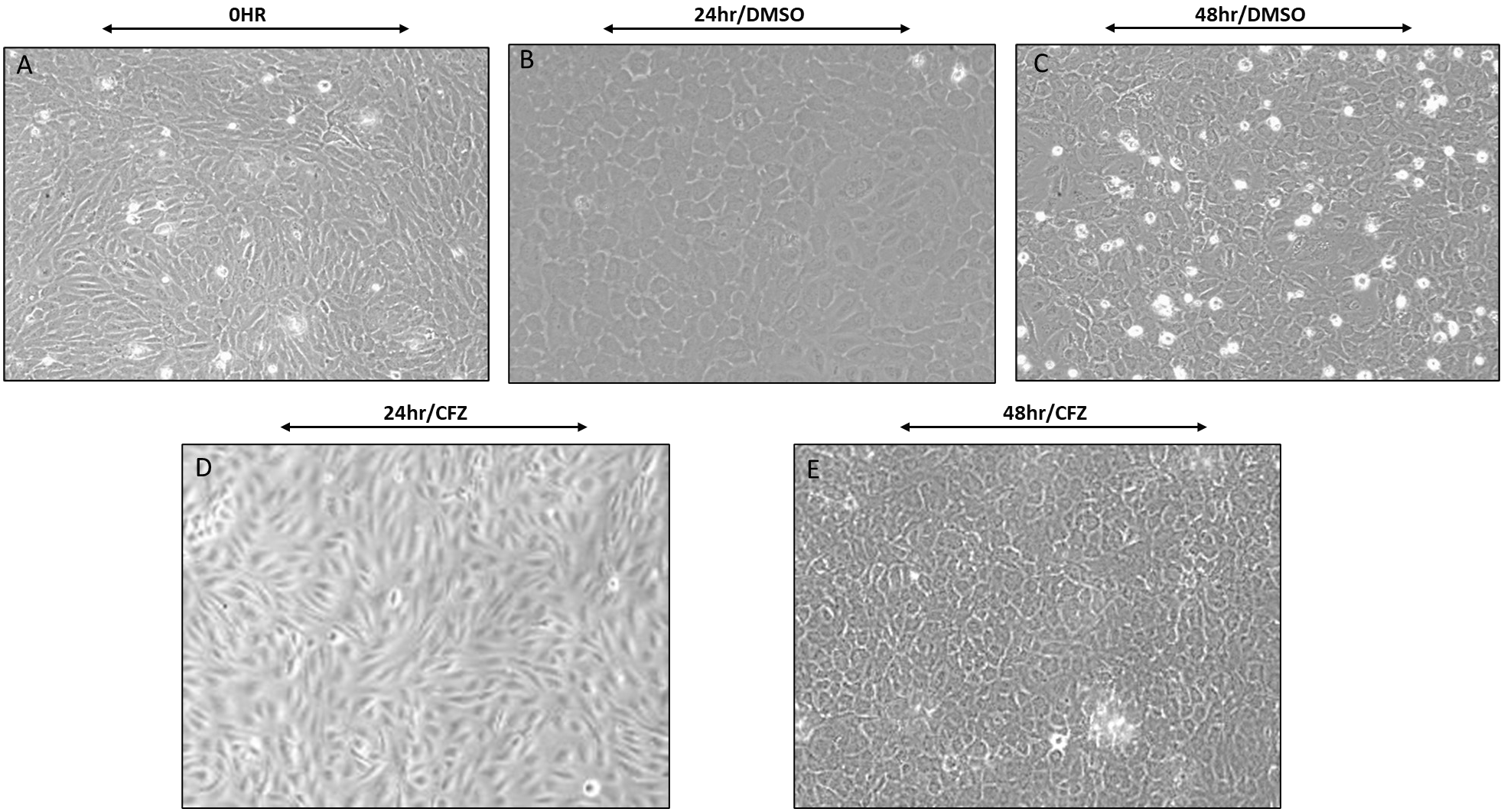


Figure 3.1.1: CFZ induces a morphological change in HUVECs. HUVECs were treated with 750nM of CFZ and DMSO for 1 hour, followed by washing the cells with PBS and replacing them in fresh EBM-2 medium. Morphological observation using a light microscope (10X objective). DMSO, Dimethyl sulfoxide; CFZ, carfilzomib.

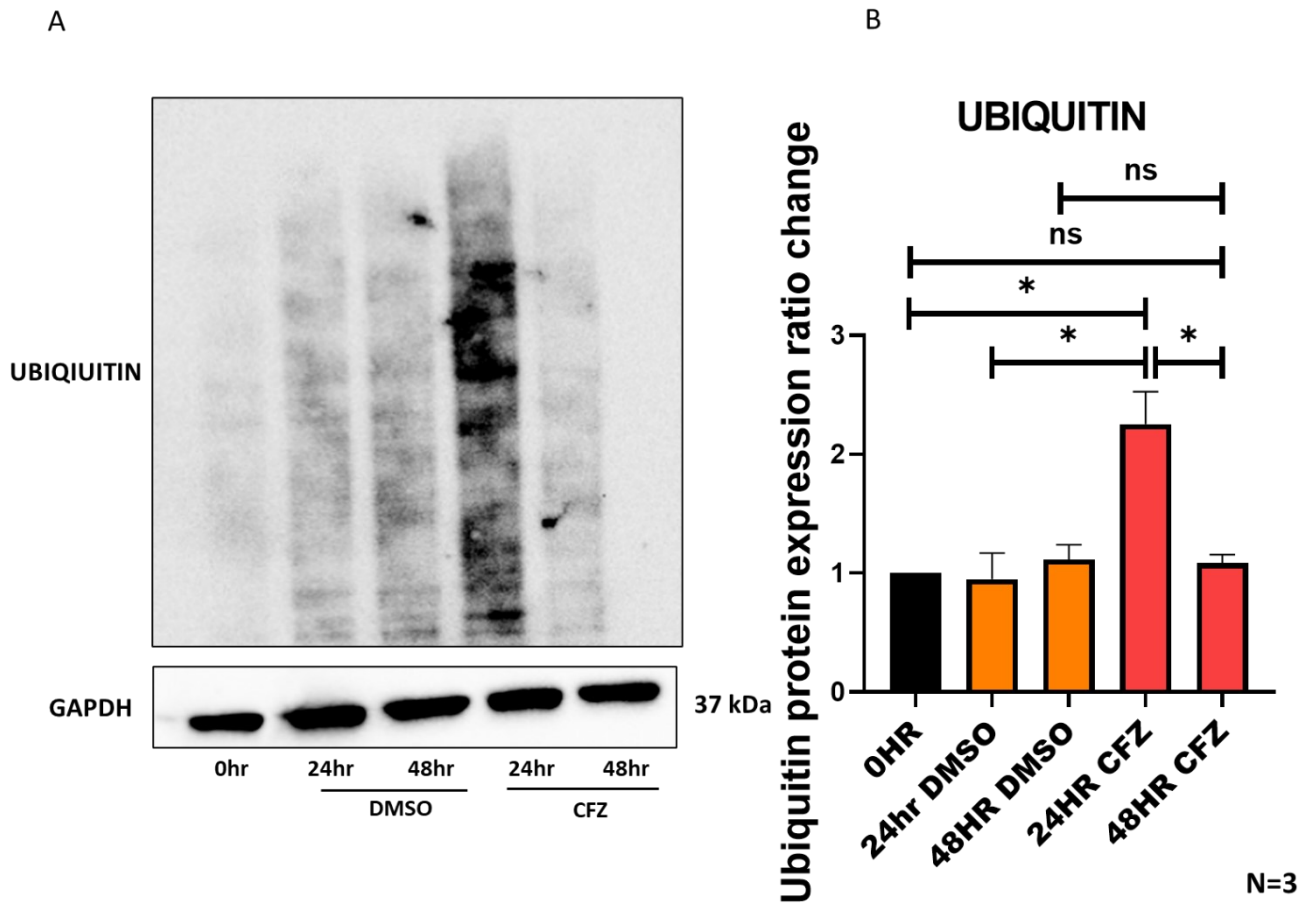


Figure 3.1.2: CFZ induced proteasome inhibition in HUVECs. HUVECs were treated with 750nM of CFZ and DMSO for 1 hour, followed by washing the cells with PBS and replacing them in fresh EBM-2 medium. Cells were then harvested to extract protein after 0hr, 24hr and 48hr. Western blot was used to determine the extent of ubiquitination. A) Western blot analysis of ubiquitin-protein level expression. B) Density quantification of Western blots. DMSO, Dimethyl sulfoxide; CFZ, carfilzomib. Three technical repeats were performed in one experiment, and the quantification of data was normalised to GAPDH levels and presented as the mean ± SEM. The data represented the average of three independent experiments. The expression trends of ubiquitin between CFZ and DMSO cells were compared using one-way ANOVA. Significant: *P < 0.05, **P < 0.01, ***P < 0.001.

3.1.2.2 Carfilzomib did not induce ER stress in HUVECs

Since CFZ resulted in changes in HUVEC morphology and ubiquitination, the ability of CFZ to indue ER stress was investigated. HUVECS were treated with CFZ for one hour as described (Methods 2.2.1). Cells were left to recover for 24hr, and 48hr and then cells were collected for gene and protein expression analysis using a panel of known ER stress markers (BIP, PERK, IRE1α, ATF6, CHOP, and ATF4) using qPCR (Figure 3.1.3) and immunoblotting (Figure 3.1.4), respectively. Interestingly, the data obtained showed that CFZ did not induce ER stress in HUVECS at any tested time points. This was revealed by a relative expression of all tested ER stress markers between CFZ treated cells compared to the untreated and the vector-DMSO controls. These data show that despite the induction of ubiquitination, at least at this dose of CFZ, ER stress is not induced in HUVECs. Thus, the morphological alteration observed in HUVECs could be sourced from an off-target effect of CFZ on HUVECs, leading to endothelial activation or cellular structural rearrangements.

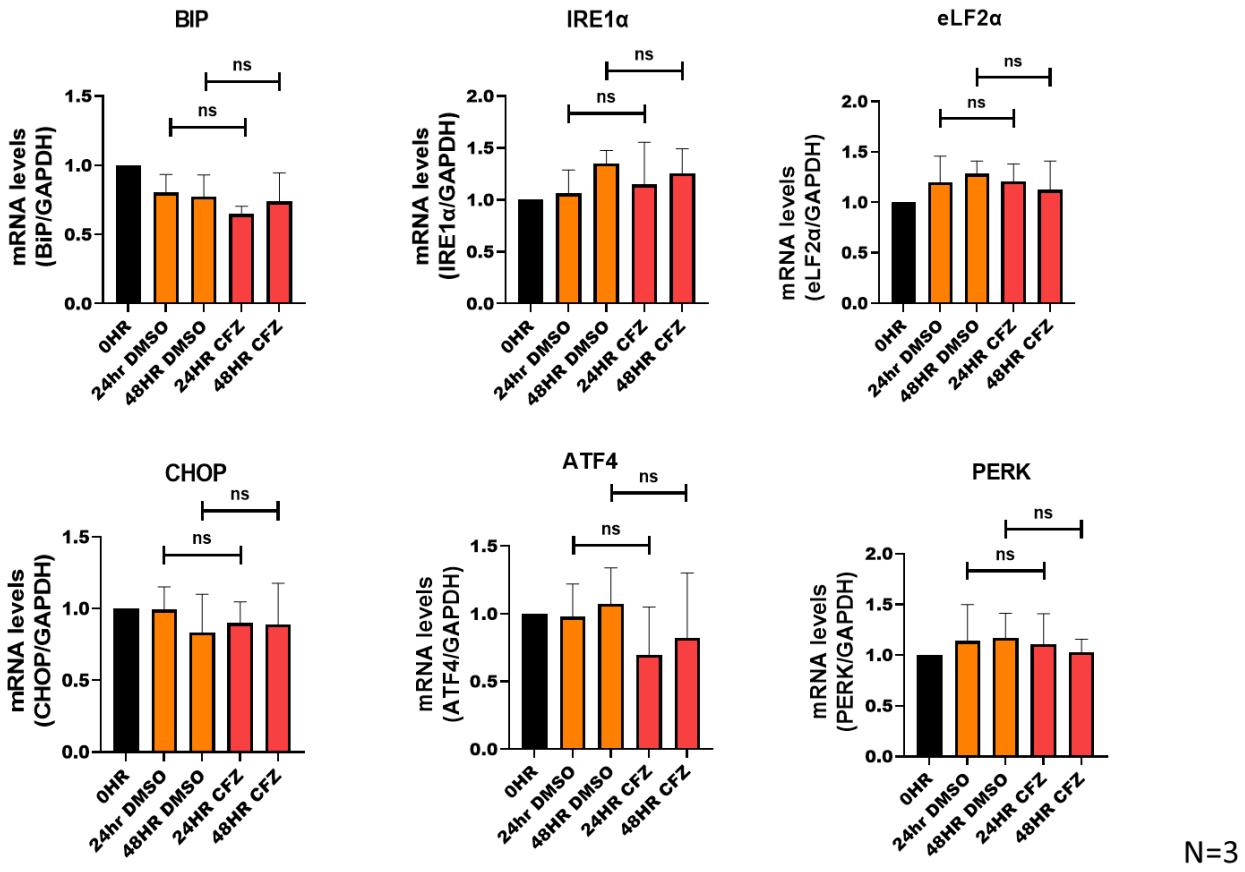


Figure 3.1.3: CFZ did not induce ER stress in HUVECs. HUVECs were treated with 750nM of CFZ and DMSO for 1 hour, followed by washing the cells with PBS and replacing them in a fresh EBM-2 medium. Cells were harvested to extract RNA at 0hr, 24hr and 48hr. cDNA was prepared from RNA to quantify mRNA expression using q-PCR. The expression level of mRNA of principal ER stress markers (BIP, PERK, eLF2α, ATF4, CHOP, and IRE1α) in CFZ treated HUVECs and controls. DMSO, Dimethyl sulfoxide; CFZ, carfilzomib. Three technical repeats were performed in each experiment, and the quantification of data was normalised to GAPDH levels and presented as the mean ± SEM. The data represent the average of four independent experiments. The expression trends of mRNA between CFZ and DMSO cells were compared using one-way ANOVA. Significance: ns, non-significant; *P < 0.05; **P < 0.01; ***P < 0.001.

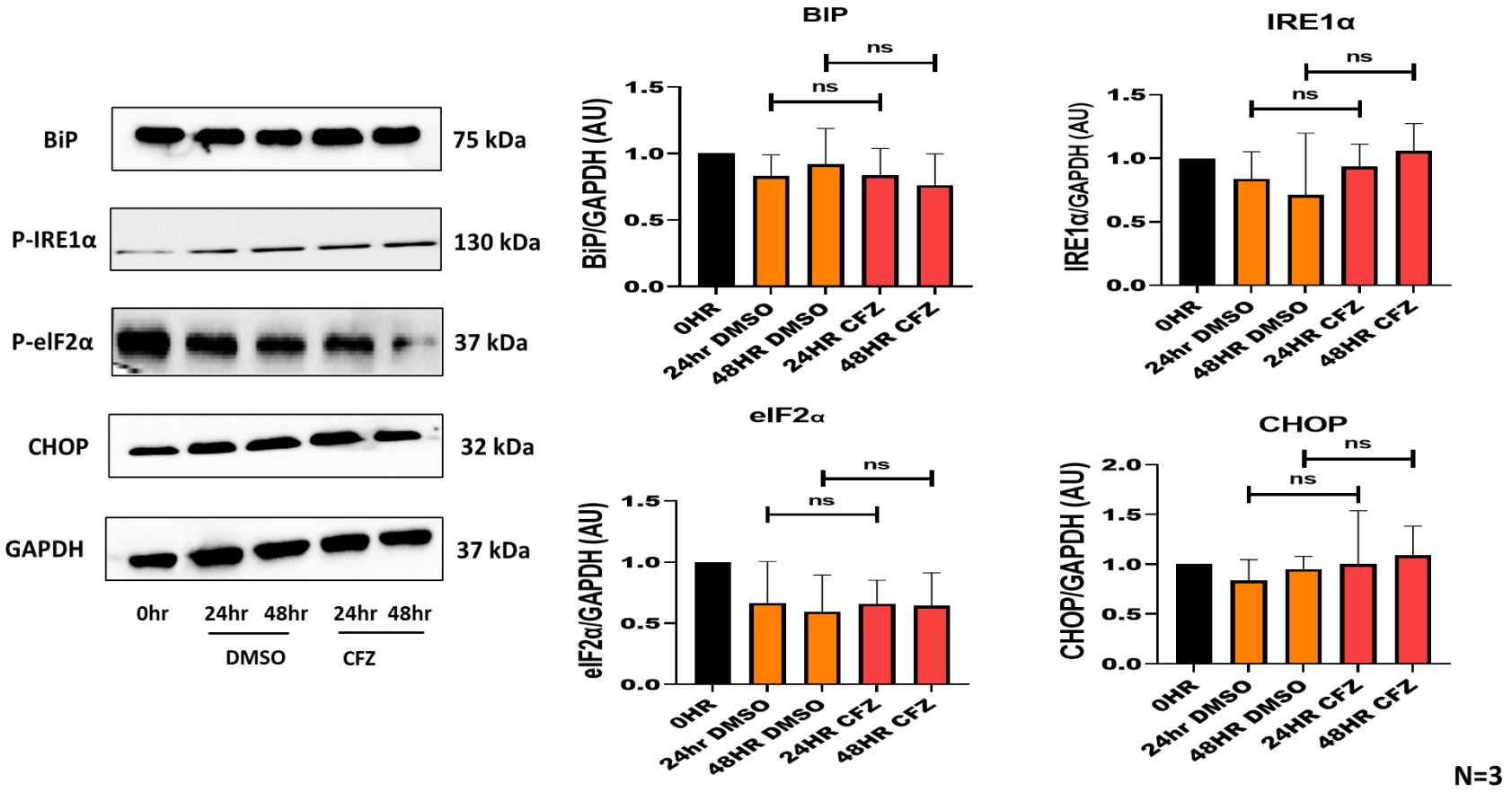


Figure 3.1.4: ER stress protein expression of CFZ treated HUVECs compared to controls. HUVECs were treated with 750nM of CFZ and DMSO for 1 hour, followed by washing the cells with PBS and replacing them in a fresh EBM-2 medium. Cells were harvested to extract protein at 0hr, 24hr and 48hr. Western blot was used to determine the protein level. Western blot bands of BiP (75 kDa), CHOP (32 kDa), eIF2α-p (37 kDa), IRE1α-p (130 kDa) and GAPDH (37kDa) and Density quantification of Western blots. DMSO, Dimethyl sulfoxide; CFZ, carfilzomib. Three technical repeats were performed in each experiment, and the quantification of data was normalised to GAPDH levels and presented as the mean ± SEM. The data represents the average of three independent experiments. The expression trends of protein species between CFZ and DMSO cells were compared using one-way ANOVA. Significance: ns, non-significant; *P < 0.05; **P < 0.01; ***P < 0.001.

3.1.2.3 Tunicamycin induced ER stress in HUVECs

Since the data obtained showed that CFZ could not induce ER stress in HUVECS, experiments were repeated alongside tunicamycin (TM), a known inducer of ER stress in endothelial cells. (313) TM is a naturally occurring antibiotic that stimulates ER stress in cells by preventing the biosynthesis of N-linked glycans, which results in the accumulation of misfolded proteins in the ER, thereby inducing ER stress. (104) To confirm that TM could induce ER stress in endothelial cells, HUVECs were treated with 10µg/ml of tunicamycin for 24 hours, followed by the removal of the drug and replacement with fresh media; some cells were treated with 750nM of CFZ and DMSO as described earlier. At selected time-points (0hr, 24hr and 48hr) during recovery, the cells were harvested, and cell lysates were collected. Gene expression analysis of a panel of known ER stress markers (*BIP, PERK, IRE1α, ATF6, CHOP*, and *ATF4*) were monitored using qPCR and some of them were confirmed using immunoblotting.
As expected, tunicamycin induced ER stress in HUVECs at all the tested time points. In addition, there was an apparent morphological change in TM treated cells, with cells appearing more "stretched" and elongated and clear patches lacking cells were visible, indicating a potential correlation between ER stress and morphological alteration in HUVECs (Figure 3.1.5). qPCR data demonstrated a significant increase in the ER stress gene expression profiles for all genes tested on tunicamycin-treated HUVECs compared to untreated, DMSO-treated controls and CFZ-treated HUVECs (Figure 3.1.6). This finding was further confirmed by a Western blot analysis (Figure 3.1.7). This data shows tunicamycin induced ER stress on HUVECs, but CFZ did not achieve this throughout the investigated experimental conditions.

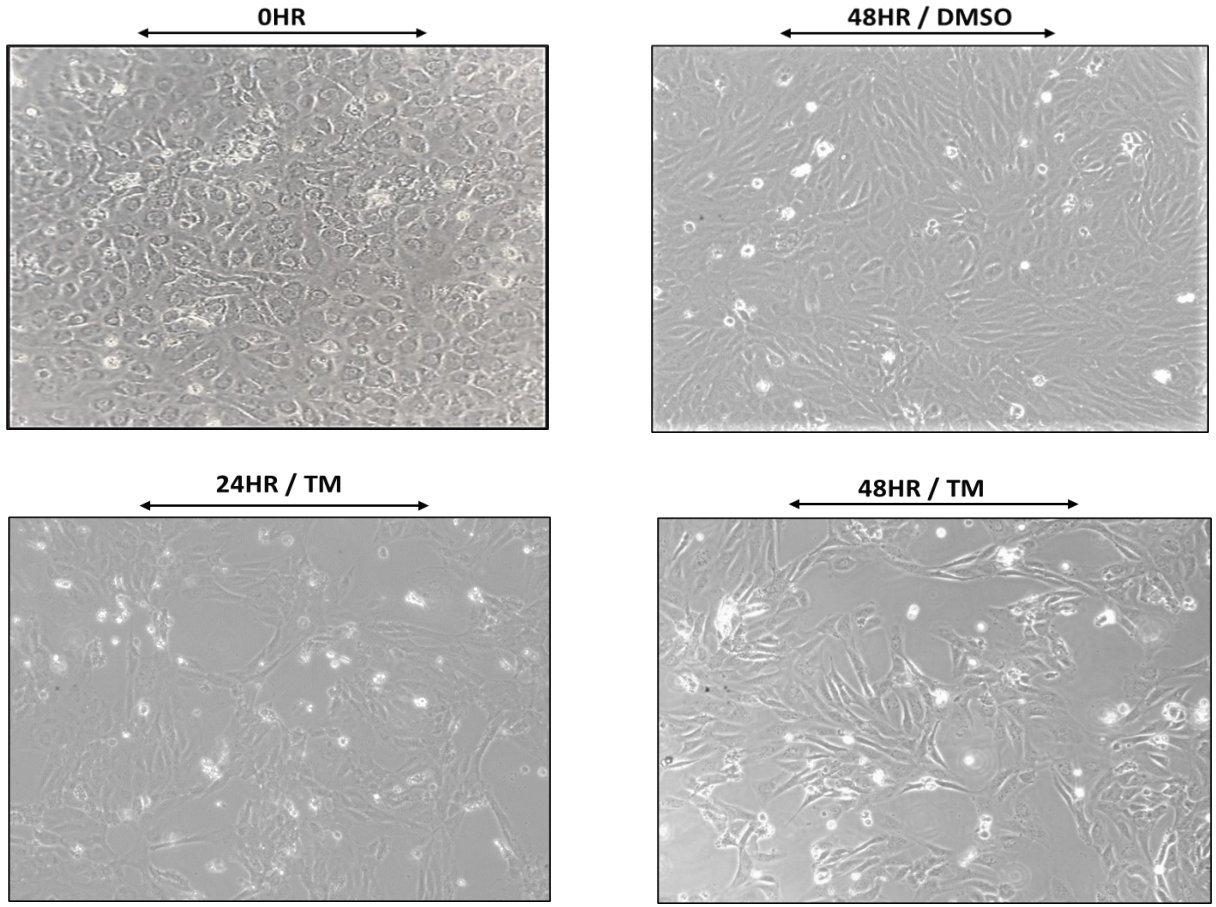


Figure 3.1.5: Tunicamycin treatment induces a morphological change in HUVECs. HUVECs were treated with 750nM of CFZ, DMSO for 1 hour and 10µg/ml tunicamycin for 24 hours, followed by washing the cells with PBS and replacing them in a fresh EBM-2 medium. The morphological observation was conducted using a light microscope (10X objective). DMSO, Dimethyl sulfoxide; CFZ, carfilzomib; TM, tunicamycin

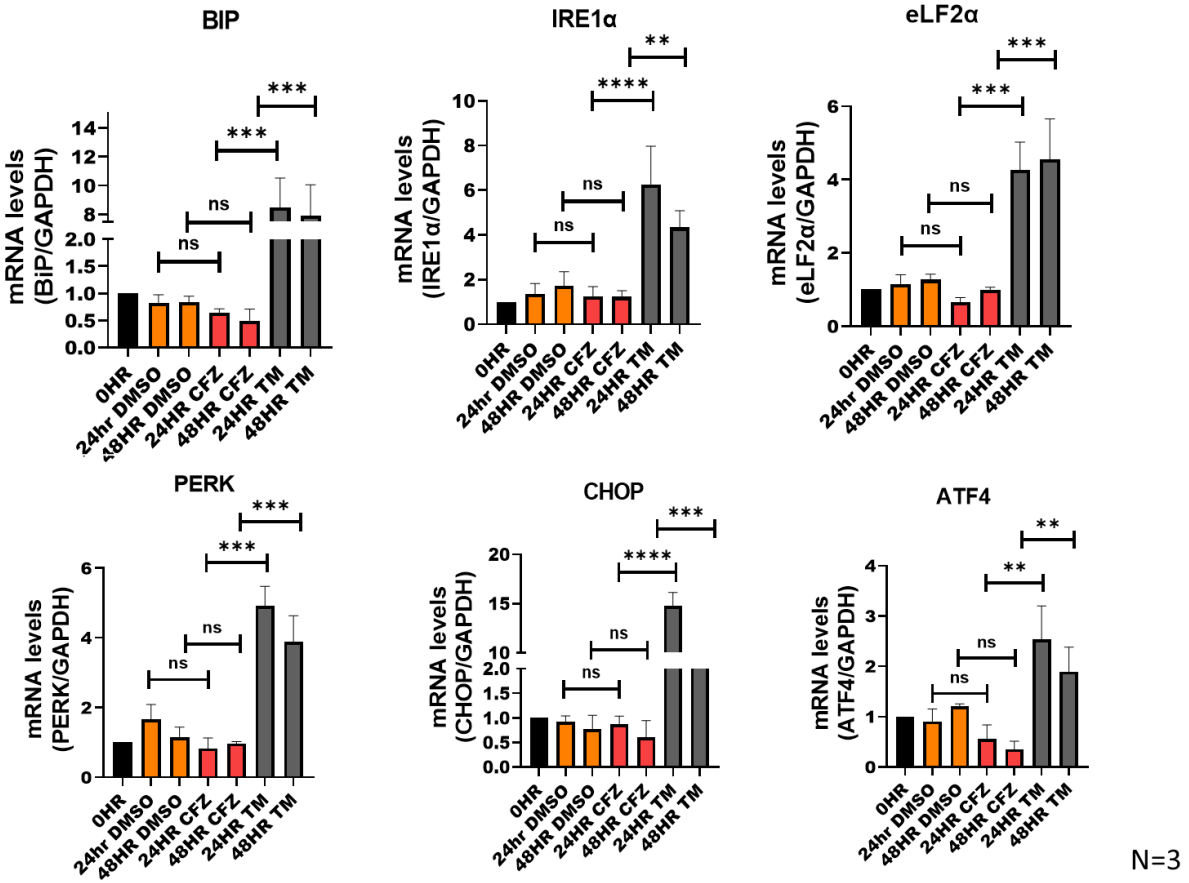


Figure 3.1.6: Tunicamycin treatment induces ER stress in HUVECs. HUVECs were treated with 750nM of CFZ, DMSO for 1 hour and 10µg/ml tunicamycin for 24 hours, followed by washing the cells with PBS and resuspending them in a fresh EBM-2 medium. Cells were harvested to extract RNA at 0hr, 24hr and 48hr. cDNA was prepared from RNA to quantify mRNA expression. q-PCR, the expression level of some of the principal's ER stress mRNA markers (BIP, PERK, eLF2α, ATF4, CHOP, and IRE1α) in tunicamycin, treated HUVECs. DMSO, Dimethyl sulfoxide; CFZ, carfilzomib; TM, tunicamycin. Three technical repeats were performed in one experiment, and the quantification of data was normalised to GAPDH levels and presented as the mean ± SEM. The data represented the average of three independent experiments. The expression trends of mRNA between CFZ and DMSO cells were compared using one-way ANOVA. Significance: *P < 0.05; **P < 0.01; ***P < 0.001; ****P < 0.0001.

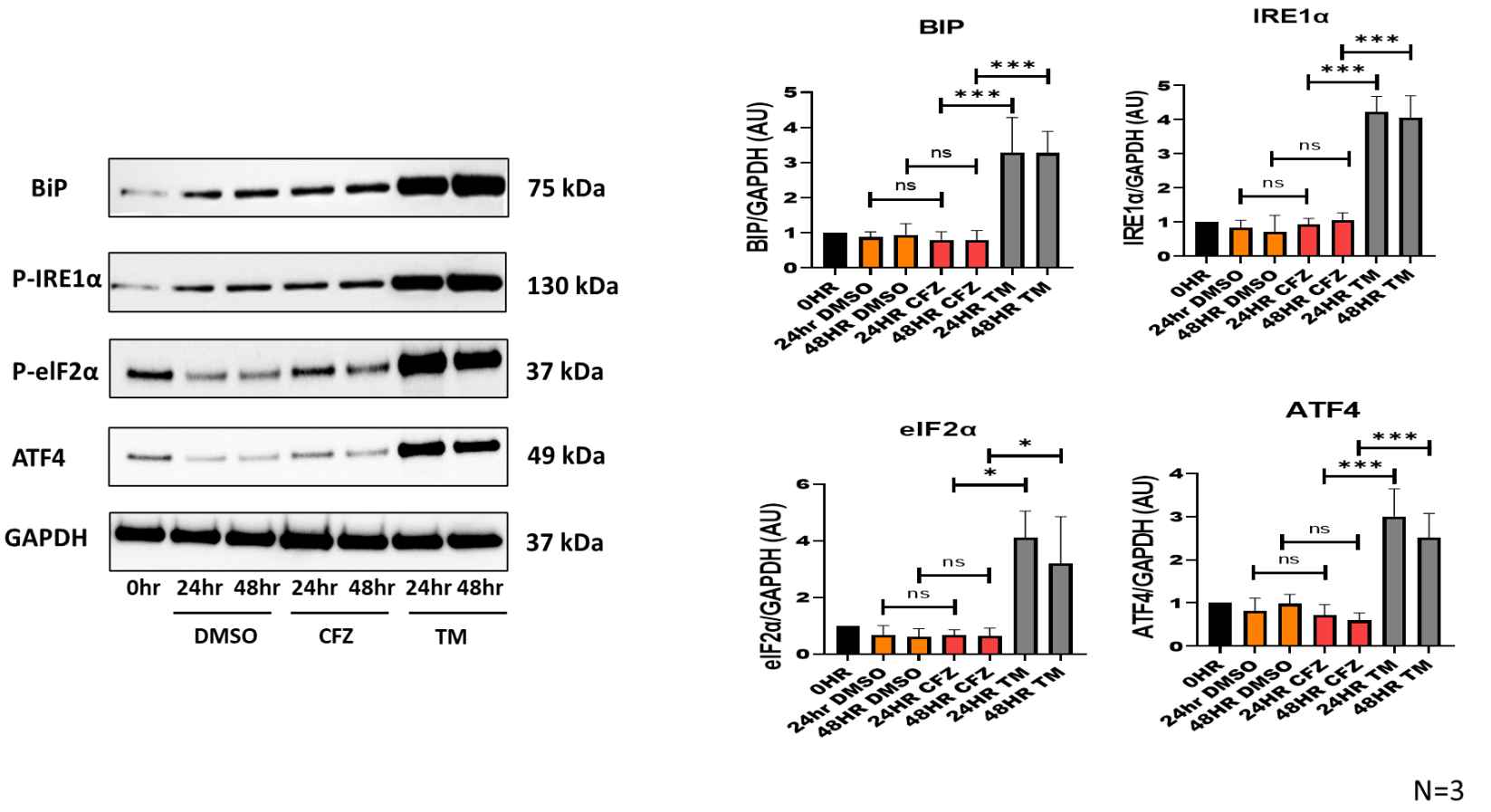


Figure 3.1.7: ER stress protein expression of tunicamycin treated HUVECs compared to CFZ treated HUVECs and controls. HUVECs were treated with 750nM of CFZ and DMSO for 1 hour and 10 µg/ml tunicamycin for 24 hours, followed by washing the cells with PBS and replacing them in a fresh EBM-2 medium. Cells were harvested to extract protein at 0hr, 24hr and 48hr. Western blot was used to determine the protein level. Western blot bands of BIP (75 kDa), ATF4 (49 kDa), eLF2α-p (37 kDa), IRE1α-p (130 kDa), and GAPDH (37 kDa) and Density quantification of Western blots. DMSO, Dimethyl sulfoxide; CFZ, carfilzomib; TM; tunicamycin. Three technical repeats were performed in one experiment, and the quantification of data was normalised to GAPDH levels and presented as the mean ± SEM. The data represented the average of three independent experiments. The expression trends of protein species between tunicamycin and CFZ cells were compared using one-way ANOVA. Significance: *P < 0.05; **P < 0.01; ***P < 0.001; ****P < 0.0001.

3.1.2.4 Repeated dosing of Carfilzomib did not induce ER stress in HUVECS

In clinical practice, CFZ is administered intravenously over a 28-day treatment cycle over two consecutive days each week. (314) Since treating HUVECS with one dose of CFZ did not induce ER stress, it was investigated if two consecutive days of HUVECs stimulation with CFZ could induce ER stress. The cells were stimulated twice with 750nM of CFZ for 1hr treatment over two consecutive days, followed by 24 hr recovery after each CFZ treatment (Methods 2.2.2). Interestingly, whereas a single dose of CFZ resulted in increased ubiquitin expression 24 hours post-recovery but a return to normal levels after 48 hours, the second dose of CFZ maintained increased ubiquitination after 48 hours (Figure 3.1.8A). This finding indicates that stimulating HUVECs with CFZ in similar conditions to the clinical setting enhances the proteasome inhibition ability of CFZ in the endothelium. However, this accumulation of proteasome inhibition in the endothelium was not adequate to trigger the induction of ER stress. The expression of the principal ER stress marker, BiP, was comparable to both non treated and vehicle (DMSO) control cells either after a single pulse or double pulses with CFZ (Figure 3.1.8B). Hence, these data indicate that even though two consecutive days of stimulation with CFZ increased ubiquitin expression in endothelial cells, it did not induce ER stress activation in HUVECs, implying the potential ability of HUVECs to escape the pathological impact of CFZ under the presented experimental conditions.

BiP is an essential ER chaperone to detect misfolded proteins(323). Under basal conditions, BiP binds to the three ER stress sensors' luminal domains (IRE1α, ATF6, and PERK), which inhibits their activation. (324) However, BiP dissociates from the sensors and strongly binds to the exposed hydrophobic domains of the proteins when they accumulate in the ER. (325) The phosphorylation and activation of these sensors initiate pathways signals to establish an adaptive cellular response, which resolves ER stress and restores cellular protein homeostasis. From this point onwards, BiP was selected as the main marker to demonstrate ER stress unless indicated in the text.

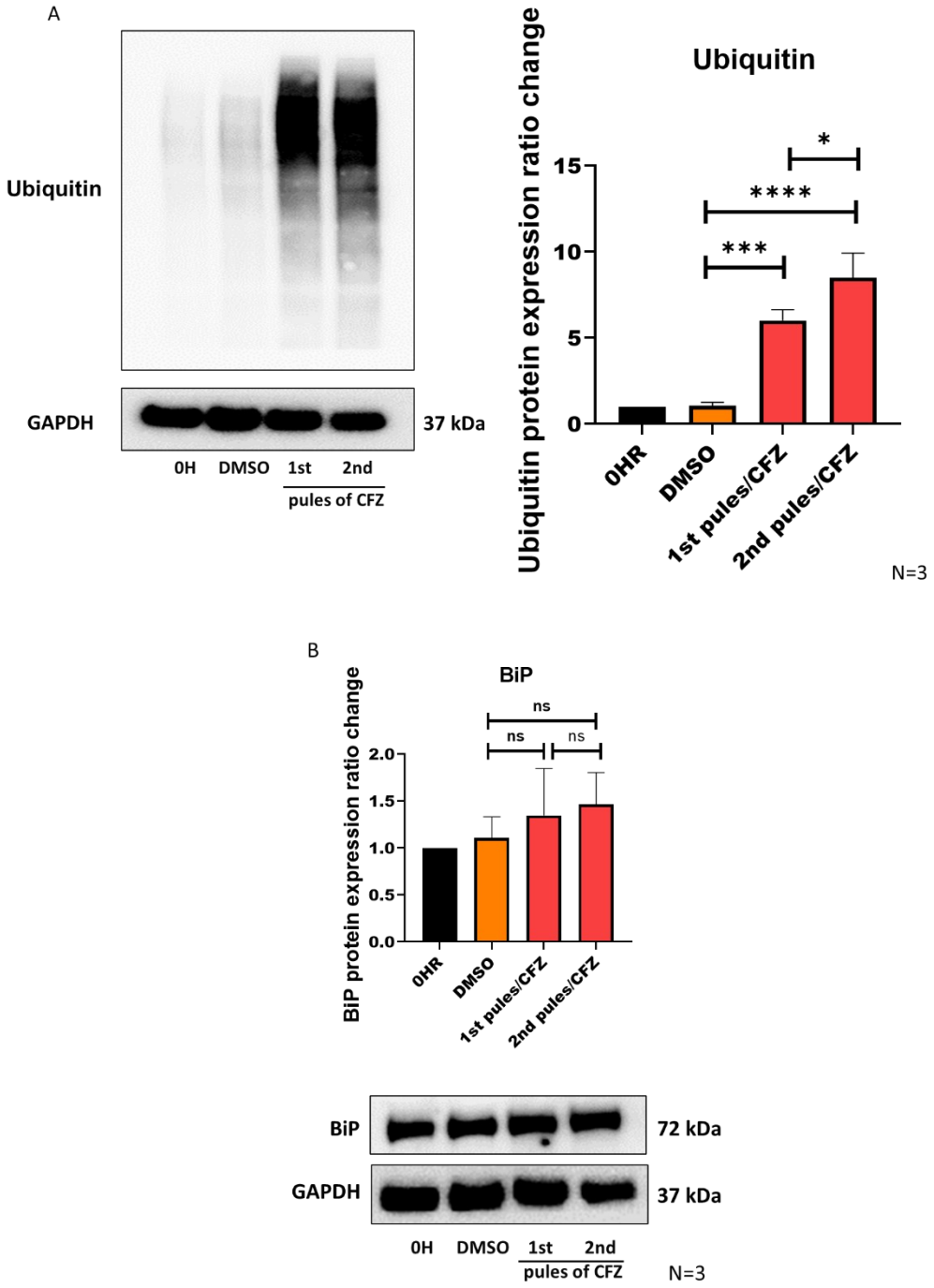


Figure 3.1.8: Carfilzomib did not induce an accumulative effect on the endothelium. HUVECs were treated twice with 750nM of CFZ and DMSO for 1 hour for two consecutive days, followed by washing the cells with PBS and replacing them in a fresh EBM-2 medium and left to recover for 24 hours after each CFZ treatment. Cells were harvested to extract protein at 0hr, 24hr after the 1st and 2nd DMSO or CFZ treatment. Western blot was used to determine the protein level. A) Western blot analysis of ubiquitin-protein level expression and Density quantification of Western blots. B) Western blot bands of BIP (75 kDa) and GAPDH (37 kDa) and density quantification of Western blots. DMSO, Dimethyl sulfoxide; CFZ, carfilzomib. Three technical repeats were performed in one experiment, and the quantification of data was normalised to GAPDH levels and presented as the mean ± SEM. The data represented the average of three independent experiments. The ubiquitin and BiP protein expression trends between 0hr, DMSO and CFZ cells were compared using one-way ANOVA. Significant: *P < 0.05; **P < 0.01; ***P < 0.001; ****P < 0.0001.

3.1.2.5 Increasing concentrations of CFZ did not induce ER stress in the endothelium

Since there was no induction of ER stress in the endothelium either with a single or double dosage of 750nM CFZ, it was hypothesised that higher doses might be required to induce ER stress in HUVECS. For this purpose, cells were treated with three different concentrations of CFZ; 750nM, 1500nM and 3000nM for 1hr, followed by a 24hr recovery. While 1500nM represents the higher end of the predicted available plasma concentration of CFZ when injected, 3000nM represents a very high plasma dosage. Interestingly, there was no induction of ER stress in the endothelium among all the concentrations applied to the cells (Figure 3.1.9). This was revealed by comparable BiP protein expression in the CFZ treated cells compared to non-treated, and DMSO controls. This finding indicates that CFZ cannot trigger the activation of ER stress in the endothelium, even with the usage of a higher concentration of the drug.

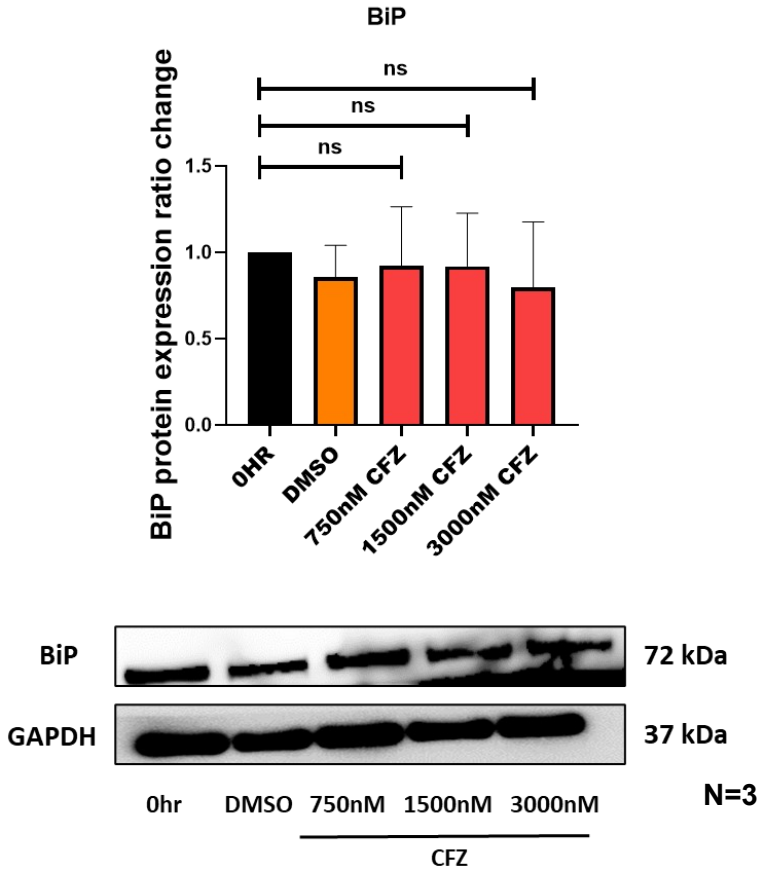


Figure 3.1.9: Higher concentration of CFZ did not induce stress in the endothelium. HUVECs were treated with 750nM, 1500nM and 3000nM of CFZ and DMSO for 1 hour, followed by washing the cells with PBS and resuspending them in a fresh EBM-2 medium. Cells were harvested to extract protein at 0hr, 24hr and Western blot was used to determine the extent of ER stress. Western blot analysis of BiP protein level expression and density quantification of the Western blot was conducted. DMSO, Dimethyl sulfoxide; CFZ, carfilzomib. Three technical repeats were performed in one experiment, and the quantification of data was normalised to GAPDH levels and presented as the mean ± SEM. The data represented the average of three independent experiments. The expression trends of BiP protein expression between 0hr, DMSO and CFZ cells were compared using one-way ANOVA. Significant: *P < 0.05; **P < 0.01; ***P < 0.001; ****P < 0.0001.

3.1.2.6 Carfilzomib potentially induced ER stress in HUVECs at earlier recovery time points

Since none of the earlier experiments showed that CFZ could induce ER stress, and since there was an apparent morphological alteration of HUVECs at 24hr post CFZ treatment, it was hypothesised that CFZ might be inducing ER stress that was resolved 24 hours post-treatment and therefore not detectable in the previous experiments. To investigate this, the cells were treated with 750 nM of CFZ for 1 hour, washed with PBS and resuspended in fresh EBM-2 medium for nine selected recovery time points (1hr, 2hr, 4hr, 6hr, 8hr, 10hr, 12 hr, 24hr, and 48hr, respectively). The light microscope observation showed a progressive morphological change in CFZ treated cells. The morphological alteration of HUVECs started after 1-hour recovery and lasted up to the 24hr recovery point. These morphological abnormalities were recorded as the cells became elongated and 'stretched', more apparent than at the 10hr and 12hr HUVECs recovery time points (Figure 13.1.0, E&F). However, this morphological change became less pronounced at 24 hours and almost returned to normal at 48 hours (Figure 3.1.10, H&I). In general, the control cells appeared to form a typical 'cobblestone' pattern, while the CFZ treated cells appeared more elongated and 'stretched' throughout the assay, indicating a potential cytoskeleton rearrangement/activation of the endothelium that progressed through the assay. Concerning the ubiquitin expression, there was a gradual upregulation of the ubiquitin expression in the CFZ treated HUVECs, which started from 1-hour recovery and reached the peak at the 8-hour recovery time point, followed by the gradual reduction of ubiquitination expression until the cells reached complete recovery at 48 hours (Figure 3.1.11). Equivalently, an increase of the *BiP* gene was observed within 24 hours in the CFZ treated HUVECs. There was a significant induction of the *BiP* gene between 2hr-10hr post-treatment recovery (Figure 3.1.12, A). However, in stark contrast to the previous observations, the Western blot analysis of BiP protein expression showed that there was a significant upregulation of this protein in the CFZ treated HUVECs that started from the 2-hour recovery point and persisted for at least 48 hours, indicating sustained ER stress activation in the endothelium (Figure 3.1.12, B). It was clear that the BiP protein expression in this experiment was majorly opposed to the earlier finds, thus indicating conflicting data, which was resolved later in this chapter.

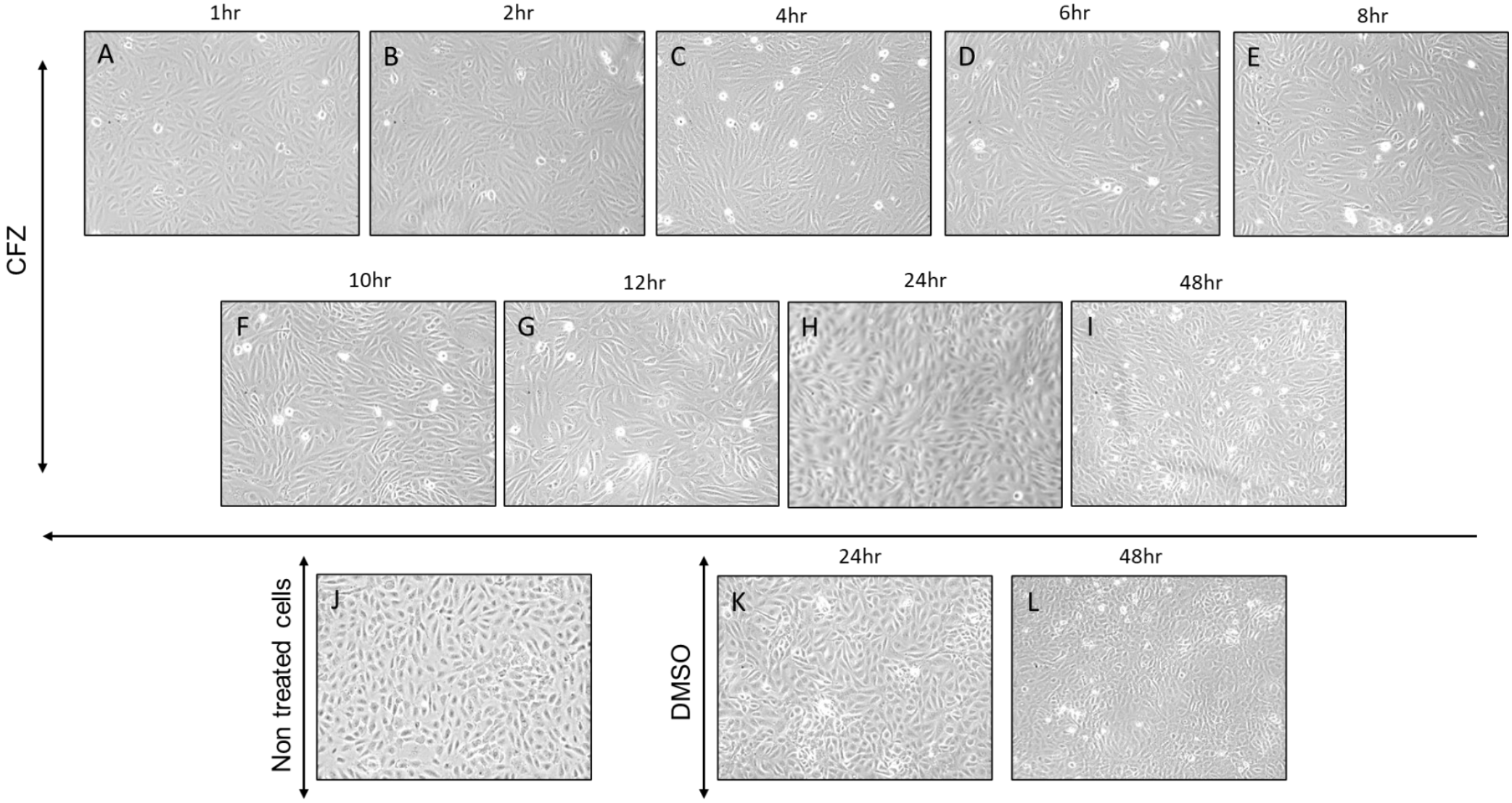


Figure 3.1.10: CFZ induced morphological change at early recovery time points in HUVECs. HUVECs were treated with 750nM of CFZ and DMSO for 1 hour, followed by washing the cells with PBS and replacing them in a fresh EBM-2 medium. Cells were harvested to extract protein at 0hr, 24hr and 48hr. Morphological observation using a light microscope (10X objective). DMSO, Dimethyl sulfoxide; CFZ, carfilzomib**.**

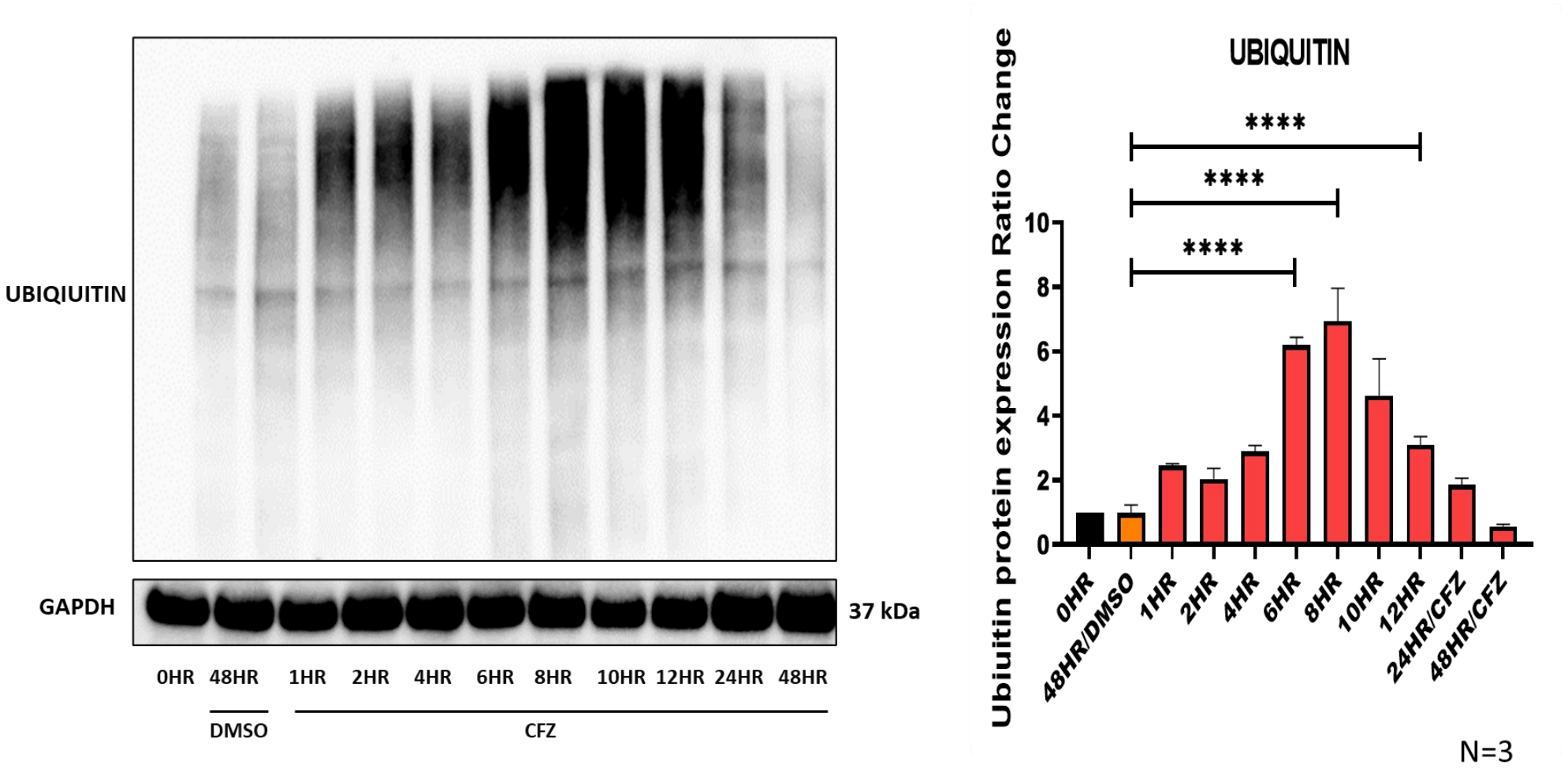


Figure 3.1.11: CFZ induced ubiquitin expression at early recovery time points in HUVECs. HUVECs were treated with 750nM of CFZ and DMSO for 1 hour, followed by washing the cells with PBS and replacing them in a fresh EBM-2 medium. Cells were harvested to extract protein at 0hr, 24hr and 48hr. Western blot analysis of ubiquitin-protein level expression and Density quantification of Western blots. DMSO, Dimethyl sulfoxide; CFZ, carfilzomib. Three technical repeats were performed in one experiment, and the quantification of data was normalised to GAPDH levels and presented as the mean ± SEM. The data represented the average of three independent experiments. The expression trends of ubiquitin between CFZ and DMSO cells were compared using one-way ANOVA. Significant: *P < 0.05, **P < 0.01, ***P < 0.00

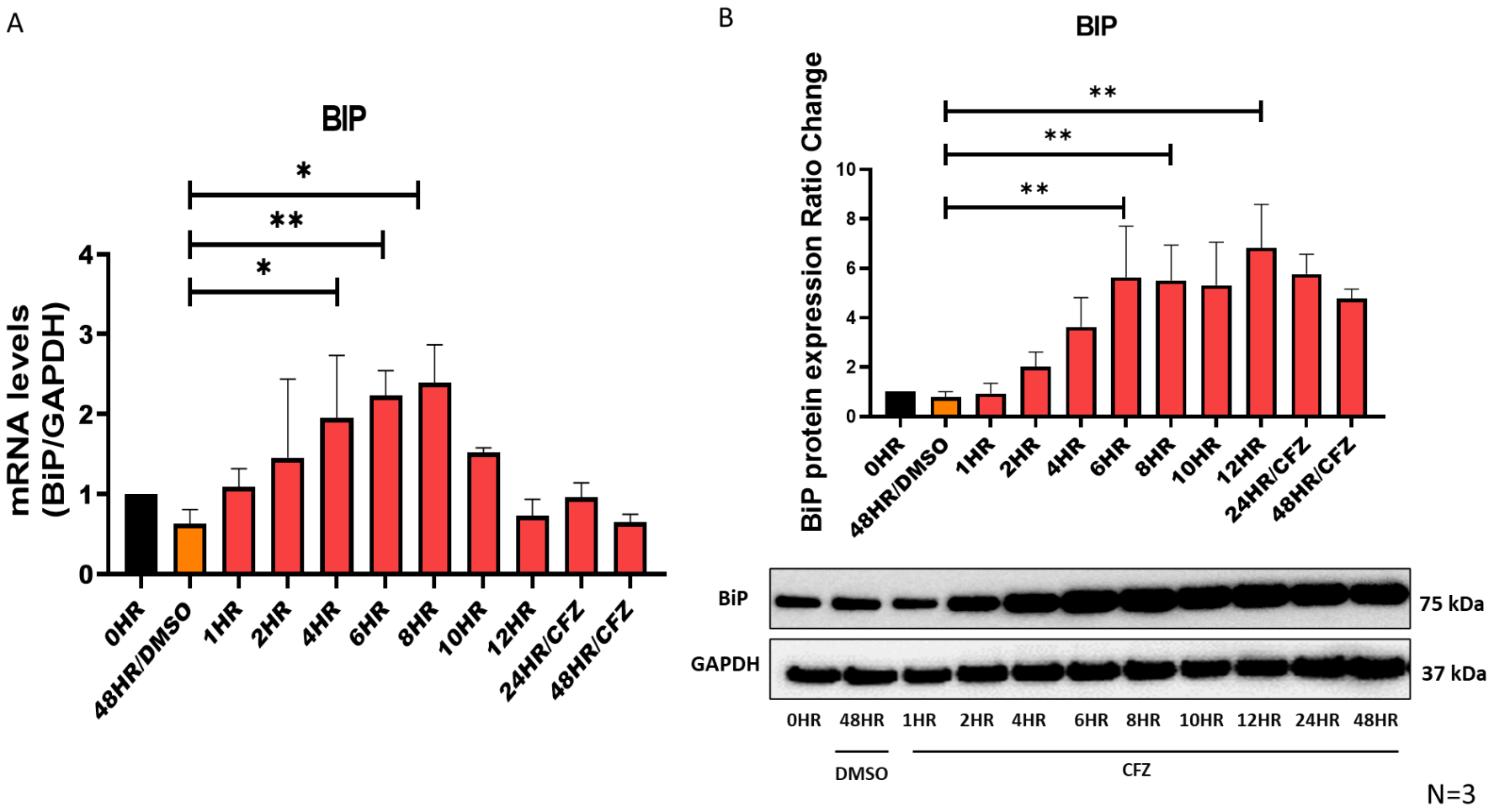


Figure 3.1.12: Emerged conflicting BiP protein expression in CFZ treated HUVECs. HUVECs were treated with 750nM of CFZ and DMSO for 1 hour, followed by washing the cells with PBS and replacing them in a fresh EBM-2 medium. Cells were harvested to extract protein at 0hr, 24hr and 48hr. qPCR and Western blot were used to determine the extent of BiP expression. A) The expression level of mRNA of BIP in CFZ treated HUVECs and controls**.** B) Western Blots analysis of BiP protein expression and density quantification of Western blots. DMSO, Dimethyl sulfoxide; CFZ, carfilzomib. Three technical repeats were performed in one experiment, and the quantification of data was normalised to GAPDH levels and presented as the mean ± SEM. The data represented the average of three independent experiments. The expression trends of BiP protein and gene expression between CFZ and DMSO cells were compared using one-way ANOVA. Significant: *P < 0.05, **P < 0.01, ***P < 0.001.

3.1.2.7 CFZ mediated BiP expression was dependent on the confluence of HUVECs.

Previously obtained data showed a conflict in BiP protein expression. Earlier findings showed no induction of BiP protein expression at either 24hr or 48hr recovery; however, later experiments showed significant induction of BiP at these time points. To explain the potential cause of this conflicting data, two possibilities were identified. Initially, it was hypothesised that the differences were due to different batches of drugs being used for experiments. Therefore, I conducted an experiment where HUVECs were treated in parallel for 1 hour using "new" and "old" batches of CFZ. The cells then were re-suspended in a fresh EBM-2 medium and left to recover for 24 hours. However, there was no remarkable morphological diversity in the pattern of the CFZ effect in morphology among both batches of the drug. Both batches showed the same appearance of HUVECs alteration where the cells were stretched and elongated, indicating cytoskeleton rearrangement or activation of HUVECs (Figure 3.1.13A). In agreement, the Western blot analysis showed that there was no induction of BiP expression in both 'the old' and 'the new' batches of the drug (Figure 3.1.13B), indicating that both batches of drug used in this study were similar, and this did not account for the observed conflicting data.

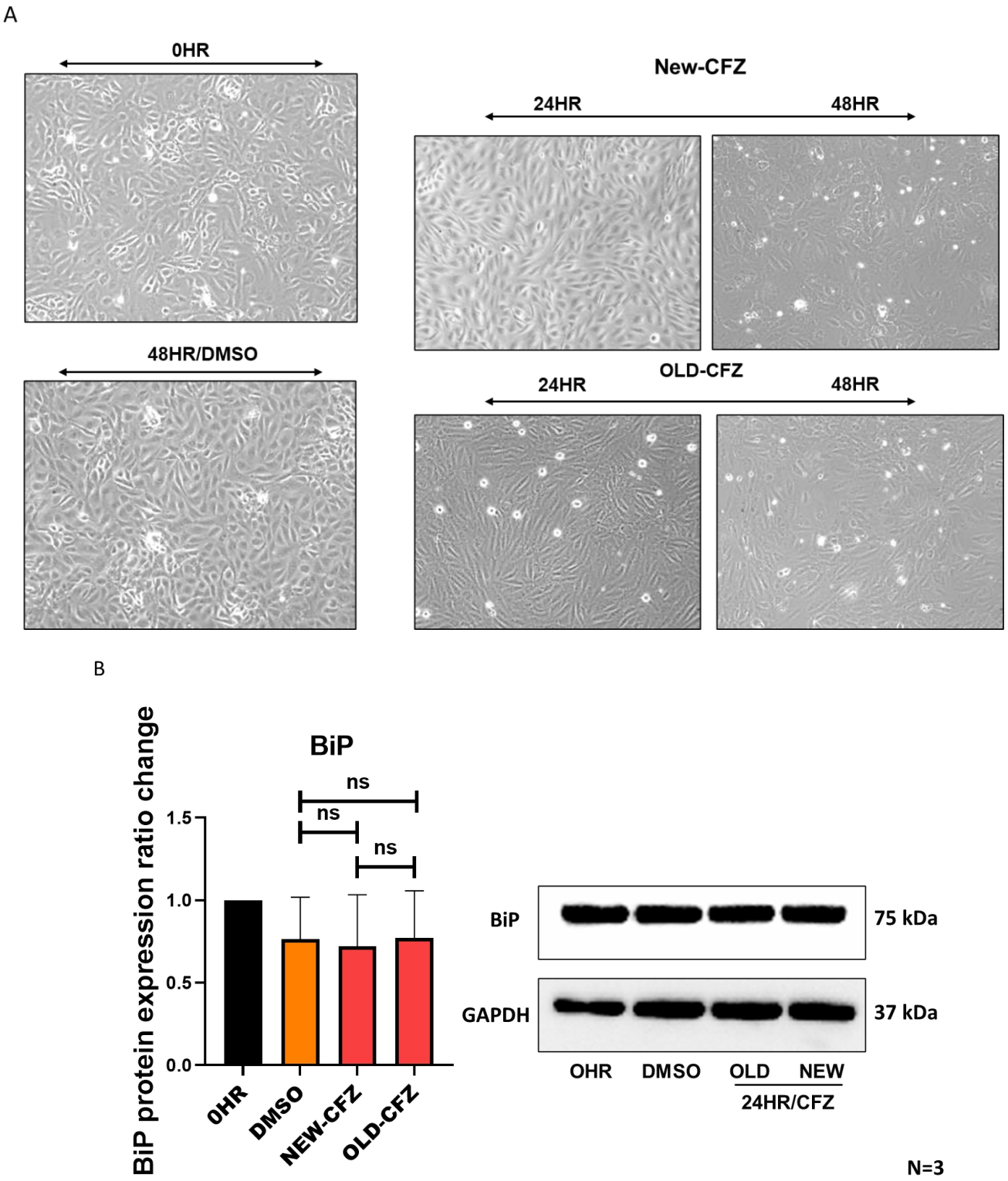


Figure 3.1.13: The "new" and "old" batches of CFZ did not induce BiP expression in HUVECs. HUVECs were treated with 750nM of CFZ and DMSO for 1 hour, followed by washing the cells with PBS and replacing them in a fresh EBM-2 medium. Cells were harvested to extract protein at 0hr, 24hr and 48hr. A) Morphological observation using a light microscope (10X objective). B) Western blot analysis of BiP-protein level expression and density quantification of Western blots. DMSO, Dimethyl sulfoxide; CFZ, carfilzomib. Three technical repeats were performed in one experiment, and the quantification of data was normalised to GAPDH levels and presented as the mean ± SEM. The data represented the average of three independent experiments. The expression trends of BiP between CFZ and DMSO cells were compared using one-way ANOVA. Significance: *P < 0.05, **P < 0.01, ***P < 0.001

To further investigate the cause of the conflicting data, the starting morphology of the HUVECS was re-analysed. Therefore, it was hypothesised that sub-confluent cells were more rapidly growing with increased protein demands that render them susceptible to proteasome inhibition. To investigate this further, a direct comparison between the effect of CFZ on (70-80%) and 100% confluent cells was performed. As before, cells were treated with 750nM CFZ for 1 hour, resuspended in fresh EBM-2 medium and then left to recover for 24 hours.

Considerably, it was noted that when the starting confluency of the cells was below 100% (70-80%), this correlated with a substantially more significant morphological change and elongation (Figure 3.1.14). In addition, there was more intense ubiquitination expression in the 80% confluent cells, indicating higher ubiquitination of cytosolic proteins, thus demonstrating more protein-producing demand (Figure 3.1.15A). Equally, there was a significant upregulation of BiP expression in the 80% confluent HUVECs only (Figure 3.1.15B). Conversely, I found that the cells were 100% confluent in all experiments when BiP was not up-regulated. Together, these observations indicate that in sub-confluent HUVECS, CFZ can induce ER stress; however, CFZ has limited effects in confluent cells. This data also resolves the conflicting data that was seen in previous experiments.

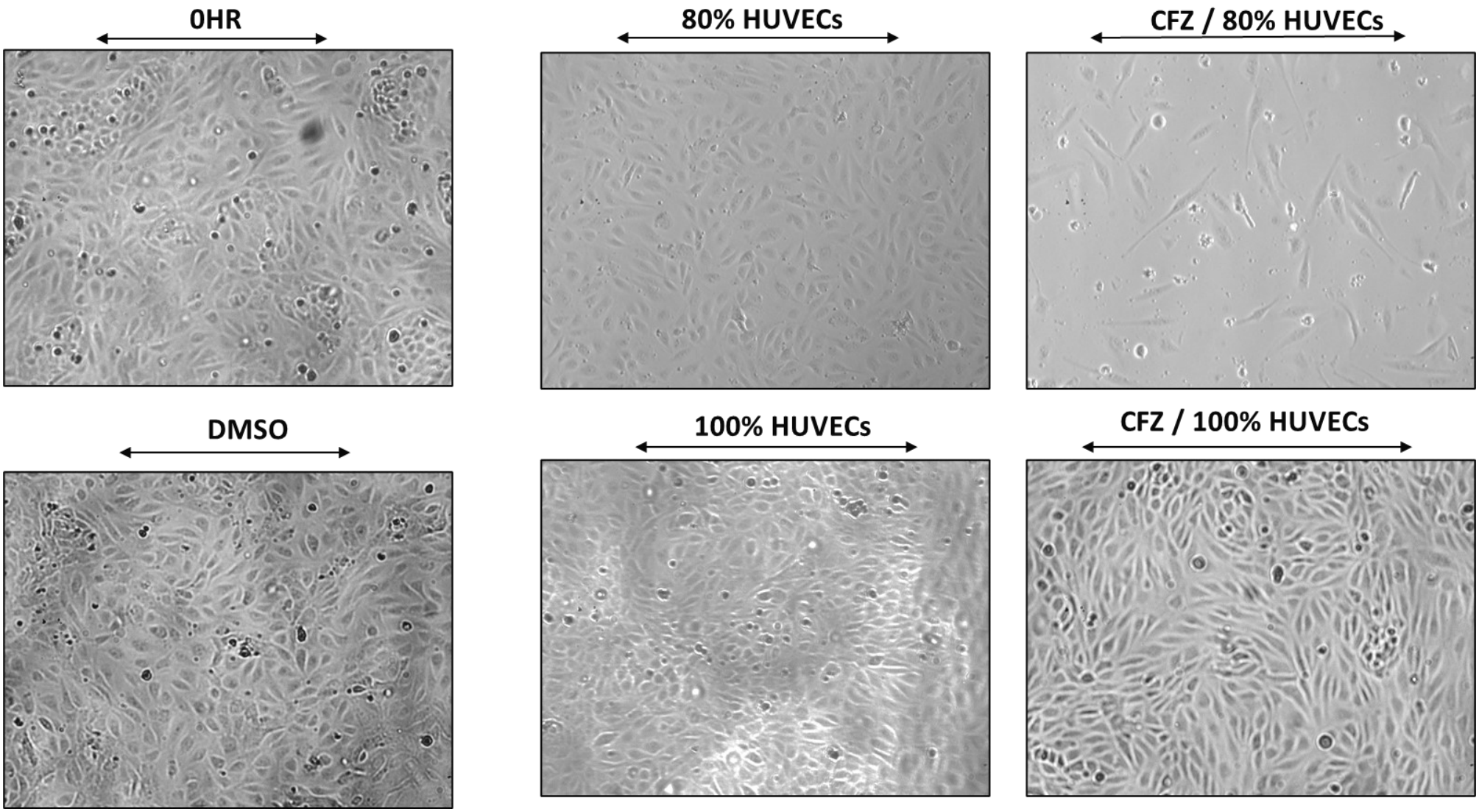


Figure 3.1.14: CFZ induces more morphological alterations in 80% confluence HUVECs. HUVECs were cultured in two different confluences, 80% and 100%; then, cells were treated with 750nM of CFZ and DMSO for 1 hour, followed by washing the cells with PBS and replacing them in a fresh EBM-2 medium. Morphological observation using a light microscope (10X objective)**.** DMSO, Dimethyl sulfoxide; CFZ, carfilzomib

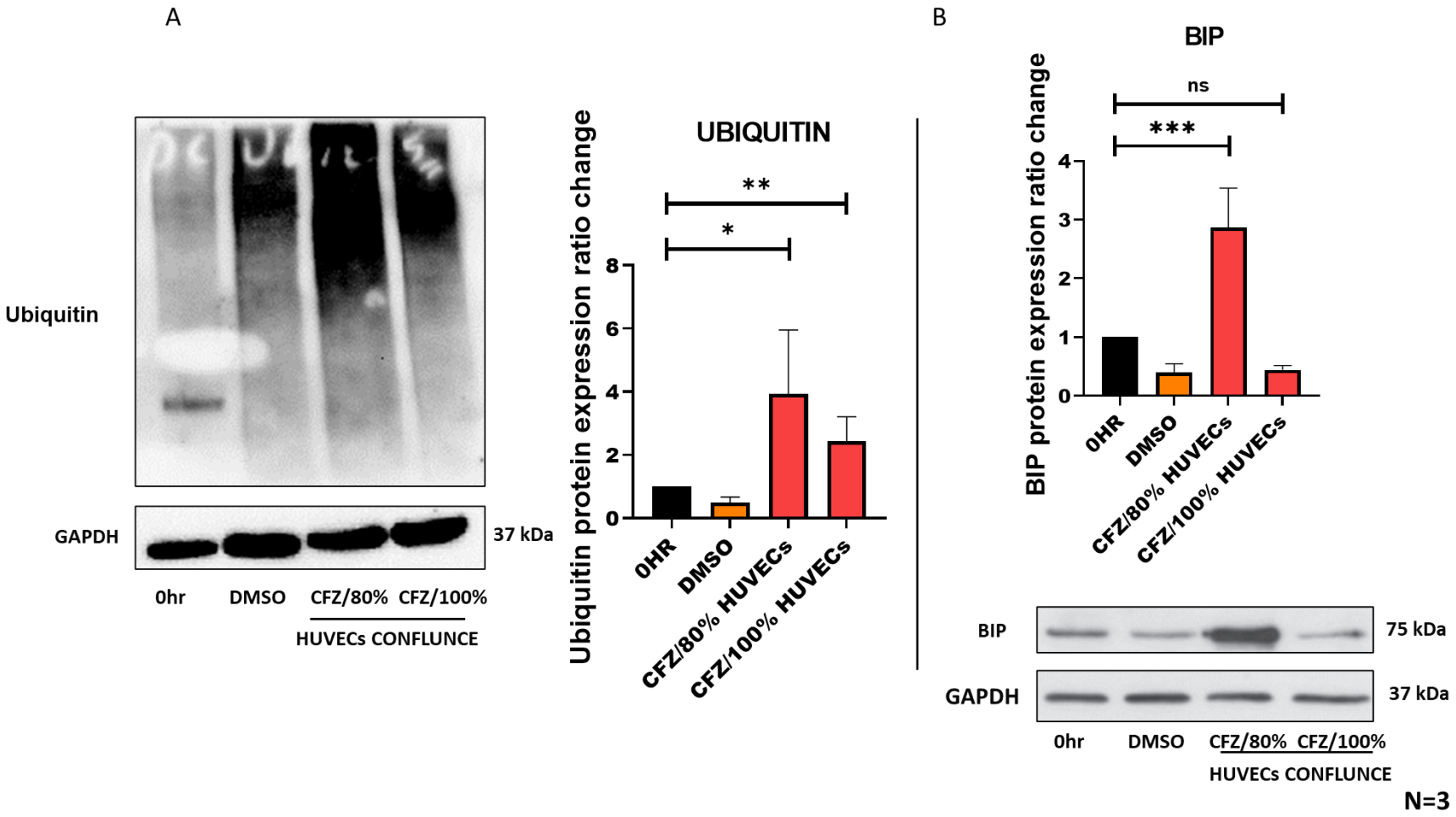


Figure 3.1.15: CFZ induced BiP upregulation in 80% confluence HUVECs, but not 100% confluence HUVECs. HUVECs were cultured in two different confluences, 80% and 100%; then, cells were treated with 750nM of CFZ and DMSO for 1 hour, then washed with PBS and replaced in a fresh EBM-2 medium. Cells were harvested to extract protein at 0hr and 24hr. A) Western blot analysis of ubiquitin-protein level expression and density quantification of Western blots. B) Western blot analysis of BiP protein level expression and density quantification of Western blots. DMSO, Dimethyl sulfoxide; CFZ, carfilzomib. Three technical repeats were performed in one experiment, and the quantification of data was normalised to GAPDH levels and presented as the mean ± SEM. The data represented the average of three independent experiments. The ubiquitin and BiP protein expression trends between CFZ and DMSO cells were compared using one-way ANOVA. Significant: *P < 0.05, **P < 0.01, ***P < 0.001

3.1.2.8 CFZ did not induce apoptosis in either 80% or 100% confluent HUVECs

Even though our findings showed the lack of CFZ ability to induce ER stress in fully confluent HUVECs, a considerable morphological alteration was seen during the experiments. Therefore, I inquired if other mechanisms could cause endothelium damage by CFZ, such as cellular apoptosis. For this purpose, the expression of well-known apoptotic markers (Annexin-V and PI) were investigated using flow cytometry. The cells and the experiments were conducted as described in (Methods 2.7.2). As a positive control, some cells were treated with 20-30µl of DMSO for 20-30 minutes to prepare “zombie” cells. Interestingly, flow cytometry revealed that the percentage of each apoptotic or combined marker was similar in CFZ treated HUVECs compared to untreated and DMSO controls regardless of the starting confluency of the cells (Figure 3.1.16,17). However, as expected, the “zombie” cells showed significant expression of both apoptotic markers than CFZ treated cells (Figure 3.1.16,17). These findings indicated the absence of apoptosis triggered by CFZ in the endothelium. Taken together, these findings show that CFZ did not induce apoptosis of HUVECS in these experiments.

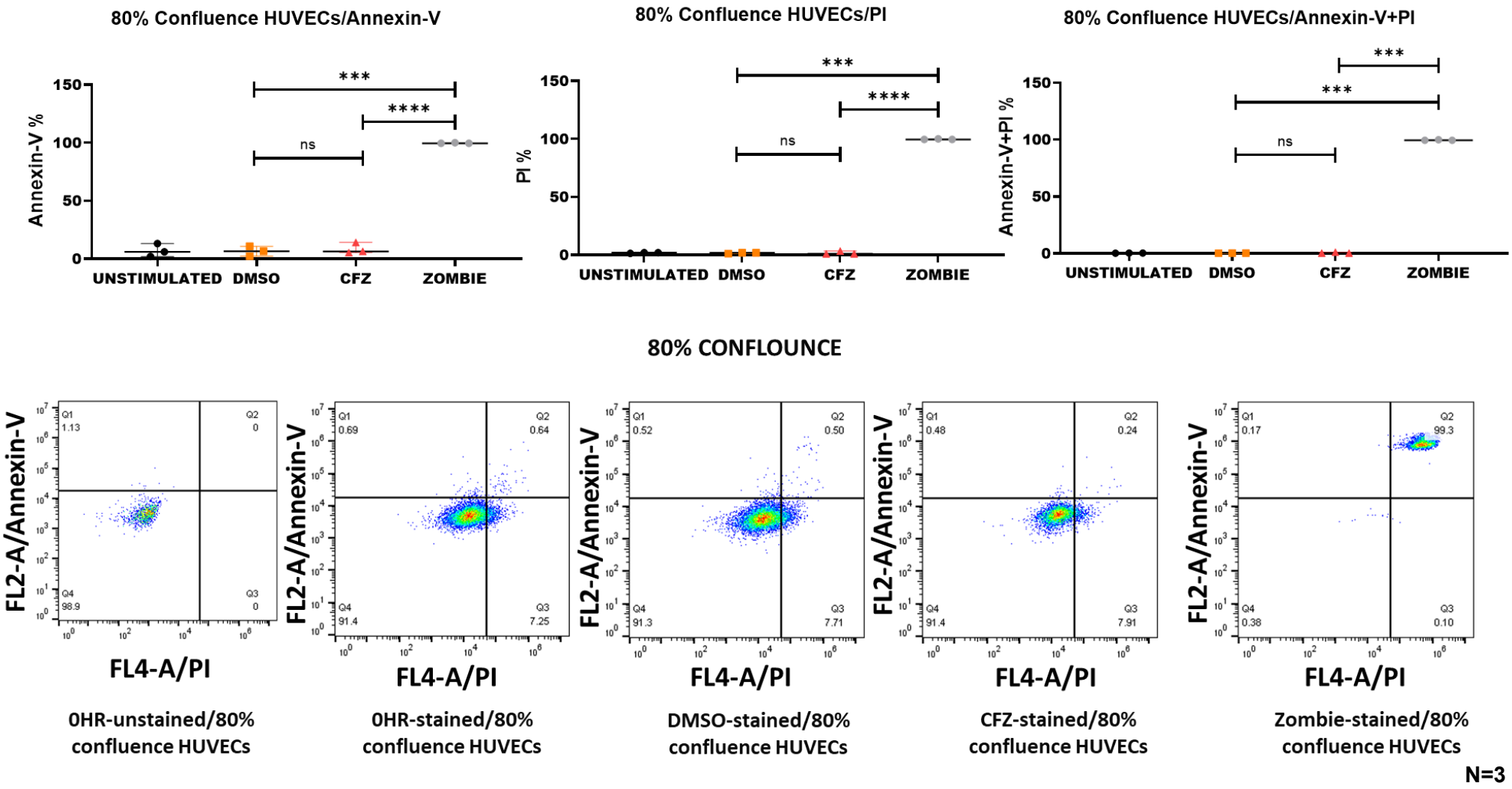


Figure 3.1.16: CFZ did not trigger apoptosis in 80% confluence HUVECs. HUVECs were cultured to 80% confluence; then, cells were treated with 750nM of CFZ and DMSO for 1 hour, washed with PBS and replaced in a fresh EBM-2 medium for 24hr. Annexin-V and PI flow cytometry analysis for 80% confluence cells. DMSO, Dimethyl sulfoxide; CFZ, carfilzomib. The data represented the average of three independent experiments. The expression trends of Annexin-V/PI between CFZ and DMSO cells were compared using one-way ANOVA. Significant: *P < 0.05, **P < 0.01, ***P < 0.00

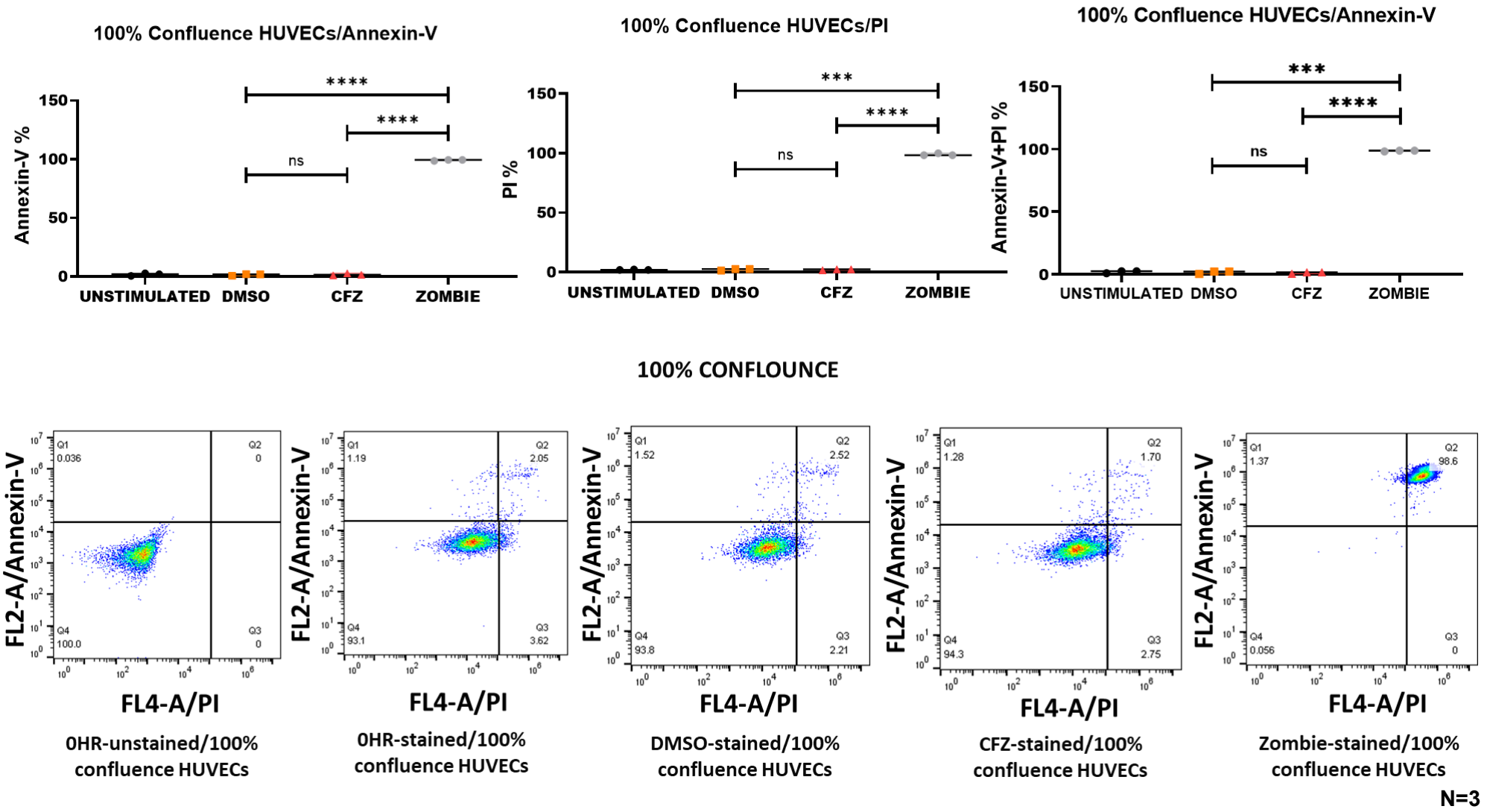


Figure 3.1.17: CFZ did not trigger apoptosis in 100% confluence HUVECs. HUVECs were cultured in 100% confluences; then, cells were treated with 750nM of CFZ and DMSO for 1 hour, washed with PBS and replaced in a fresh EBM-2 medium for 24hr. Annexin-V and PI flow cytometry analysis for 100% confluence cells. DMSO, Dimethyl sulfoxide; CFZ, carfilzomib. The data represented the average of three independent experiments. The expression trends of Annexin-V/PI between CFZ and DMSO cells were compared using one-way ANOVA. Significant: *P < 0.05, **P < 0.01, ***P < 0.001

3.1.2.9 CFZ did not induce ER stress in human embryonic kidney 293 (HEK293) cells but did induce ER stress in multiple myeloma cells (OPM-2)

According to the data obtained in this chapter, I have found no evidence to support the hypothesis that CFZ induces ER stress in HUVECs. Therefore, I hypothesised that CFZ could induce ER stress in cancer cells since they overgrow with more protein-demanding cells (10) but not in non-malignant cells. It is widely accepted that CFZ induces ER stress in multiple myeloma cancer cells *in vitro*, including the OPM-2 cell line. (317) Therefore, to validate and to compare the drug been used in my assays; the HEK293 cell line, one of the most popular and easy to grow cell cultures, was selected as a non-malignant negative control cell and the OPM-2 cell line, which originated from the malignant cells of a multiple myeloma patient, as a positive control to check the ability of the drug to induce ER stress.

For this purpose, the cells from each cell line were treated with 750nM CFZ/ DMSO for 1 hour, washed and re-suspended in a fresh medium and left to recover for 24 hours (Methods 2.2.4). Consistent with my HUVECs findings, the data obtained showed that CFZ remarkably altered the HEK293 cell morphology, similarly indicating a cytoskeleton rearrangement (Figure 3.1.19). However, in agreement with my previous findings, there was no induction of BiP expression in HEK293 cells after a 24-hour recovery (Figure 3.1.20). In contrast, there was a significant induction of ER stress in the OPM-2 cells, which is consistent with the literature (Figure 3.1.20). (320)

Taken together, these data suggest that CFZ induced ER stress in high protein-demanding cells, such as sub-confluence HUVECs and cancer cells such as OPM-2 cells, but not in non-malignant cells that have a regular protein turnover, such as fully confluence HUVECs and HEK293 cells.

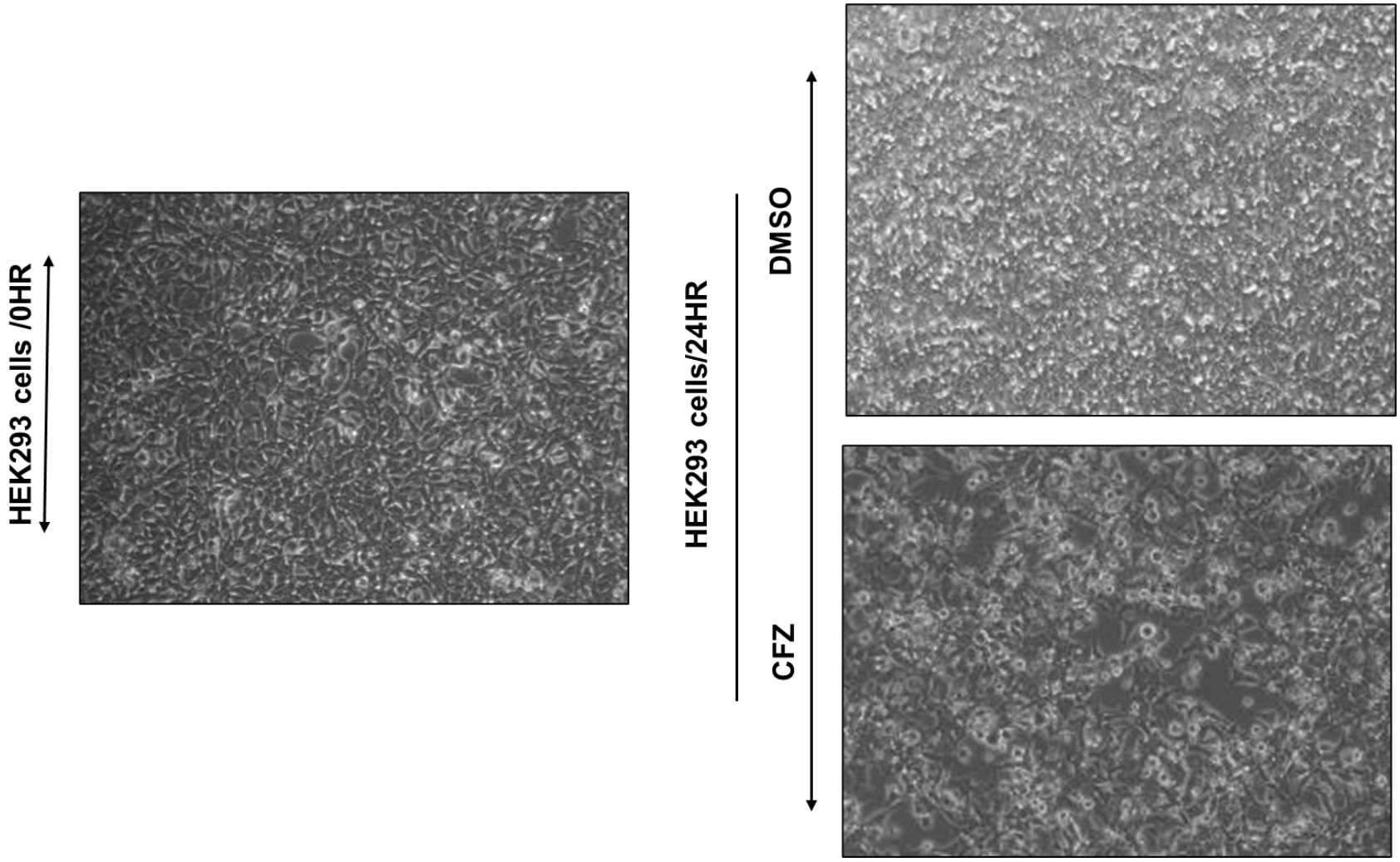


Figure 3.1.19: CFZ induced morphological change in HEK293 cells. HEK293 cells were cultured up to 100% confluency; then, cells were treated with 750nM of CFZ and DMSO for 1 hour, washed with PBS and replaced in a fresh medium. Morphological observation of HEK293 cells using a light microscope (10X objective). DMSO, Dimethyl sulfoxide; CFZ, carfilzomib.

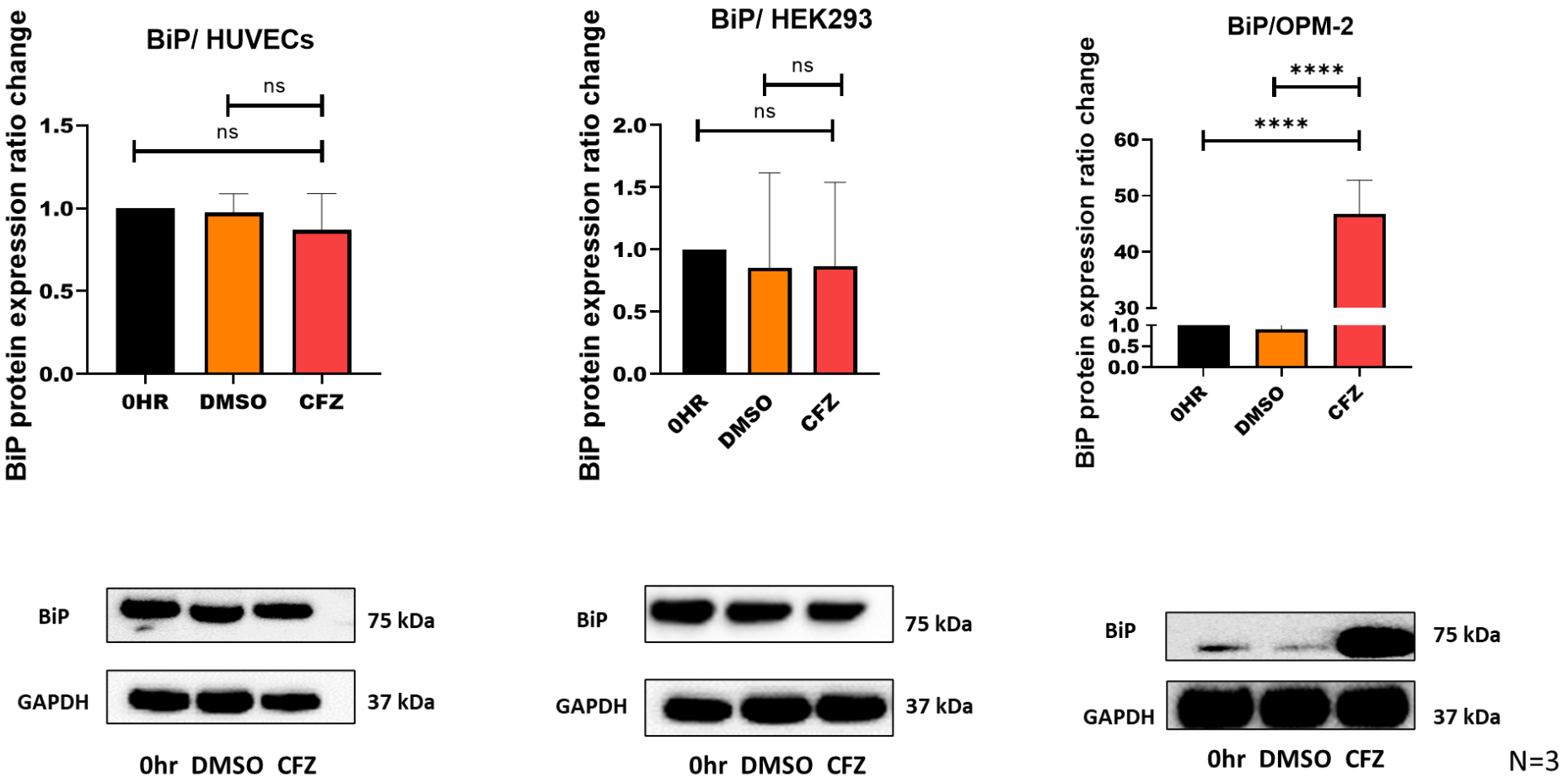


Figure 3.1.20: CFZ did not induce ER stress in HUVECs or HEK293 cells but induced ER stress in OPM-2 cells. HEK293 and OPM-2 cells were cultured up to 100% confluency; then, cells were treated with 750nM of CFZ and DMSO for 1 hour, then washed with PBS and replaced the cells in a fresh medium. Cells were harvested to extract protein at 0hr and 24hr. Western blot analysis of BiP protein level expression and density quantification of Western blots. DMSO, Dimethyl sulfoxide; CFZ, carfilzomib. Three technical repeats were performed in one experiment, and the quantification of data was normalised to GAPDH levels and presented as the mean ± SEM. The data represented the average of three independent experiments. The expression trends of BiP protein between CFZ and DMSO cells were compared using one-way ANOVA. Significant: *P < 0.05, **P < 0.01, ***P < 0.00

3.1.2.10 CFZ did not induce de novo proteasome synthesis in HUVECs

The proteasome is an integral part of the ER-associated degradation system. It is will-established that some cells have the capacity to initiate *de novo* proteasome synthesis in response to ER stress activation or when there is the accumulation of the mis-folded proteins in the cellular cytosol. (321) In this process, cells produce more proteasome subunits to expand the proteasome expression for the misfolded proteins, thus preventing the lethal consequences of prolonged ER stress activation. (321) The data indicated a significant increase in ubiquitination expression, but CFZ induced no ER stress. Therefore, I asked if HUVECs could recruit a mechanism to avoid the induction of ER stress, such as a *de novo* proteasome synthesis. (321) In order to investigate this, the cells were treated as described earlier (section 3.2.1). Both Western blot and qPCR data showed no de novo proteasome synthesis induction. This was revealed by the relative expression of PS20 in all treated and non-treated conditions (Figure 3.1.21A&B), implying that the endothelium did not utilise this mechanism to avoid the induction of ER stress by CFZ.

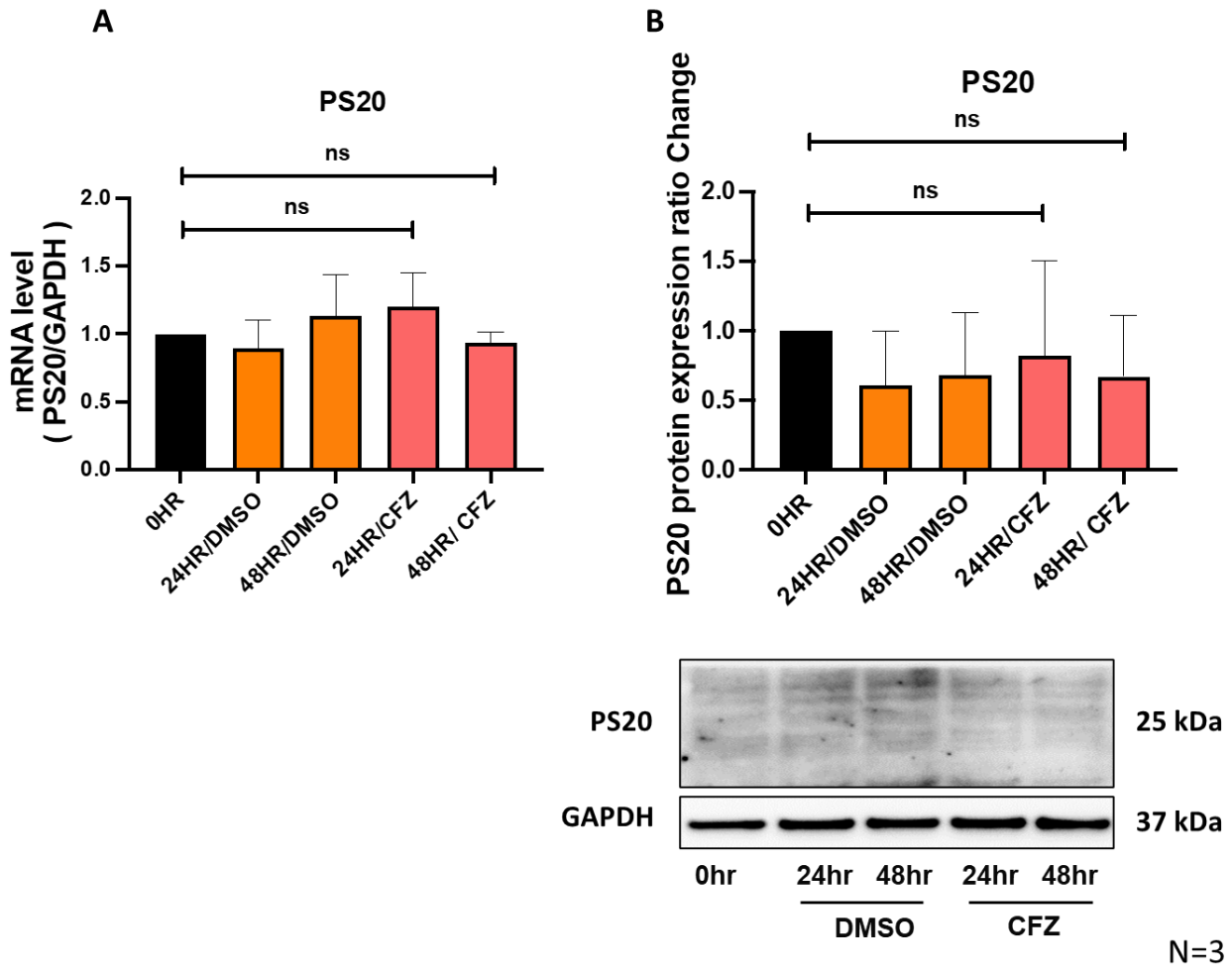


Figure 3.1.21: CFZ did not induce de novo proteasome synthesis in HUVECs. HUVECs were treated with 750nM of CFZ and DMSO for 1 hour, followed by washing the cells with PBS and replacing them in a fresh EBM-2 medium. Cells were harvested to extract protein at 0hr and 24hr. A) The expression level of mRNA of PS20 in CFZ treated HUVECs and controls. B) A Western blot analysis of PS20-protein level expression and density quantification of Western blots. DMSO, Dimethyl sulfoxide; CFZ, carfilzomib. Three technical repeats were performed in one experiment, and the quantification of data was normalised to GAPDH levels and presented as the mean ± SEM. The data represented the average of three independent experiments. The expression trends of PS20 between CFZ and DMSO cells were compared using one-way ANOVA. Significant: *P < 0.05, **P < 0.01, ***P < 0.001.

3.1.3 Discussion

Since CFZ induces ER stress in MMCs, it was initially hypothesised that similar effects would be seen in HUVECs, which has not yet been addressed. Endothelial cells are essential regulators of vascular permeability and immunity; hence, examining the effects of CFZ on the endothelium is of crucial importance. Therefore, this chapter aimed to investigate how CFZ may impact the endothelium by focusing on whether CFZ could induce ER stress in endothelial cells. HUVECs were used since they are considered a standard endothelial model, are relatively easy to grow compared to other endothelial cell types, and are also easy to obtain and economical. (326) In order to attempt to mimic the *in vivo* situation as closely as possible, HUVECs were treated with a single or double 750nM dose of CFZ or with different concentrations of CFZ (750nM, and 1500nM) for 1 hour, thus mimicking equivalent to the minimal and maximal concentration that is found in MM patient serum and the estimated clinical exposure of average drug half-life, respectively. (3) In a rat model, study data showed that CFZ was rapidly cleared extrahepatically, via epoxide hydrolysis and peptides cleavage, with a half-life of 30-60 minutes. (327) In agreement, it is widely accepted that the CFZ is rapidly cleared from the patient serum after IV infusion with a half-life ≤1 h in patients.(90)

In this chapter, two main findings were observed in CFZ treated HUVECs: 1) treating the cells with one or two doses of CFZ and high clinical doses of CFZ did not induce ER stress or apoptosis in the confluent HUVECs, though there was a visible change in the morphology of treated cells. 2) Treating sub-confluent HUVECs with 750nM of CFZ induced a significant induction of BiP expression, thus indicating ER stress. However, sub-confluent HUVECs do not adequately mimic the physiological state of the endothelium that forms a confluent luminal monolayer structure in the human vascular system.

Initially, to investigate the hypothesis that CFZ induces ER stress in HUVECs, I first examined the core functional ability of CFZ to inhibit the proteasome function in my selected cell model. This was achieved by comparing the level of ubiquitination expression between CFZ treated and untreated cells and DMSO controls. Effective inhibition of the proteasome function could cause prolonged proteotoxic endoplasmic reticulum stress. (328) The data showed an almost three-fold increase in the ubiquitination level in CFZ treated HUVECs compared to controls at 24 hours only. This increased expression of ubiquitin at 24 hours indicated the drug's ability to induce proteasome inhibition in HUVECs, which resulted in an accumulation of misfolded protein in the ER lumen. However, the decreased expression of ubiquitin at 48 hours indicated the rapid recovery of proteasome activity.

Interruption of ER homeostasis due to a build-up of misfolded proteins can lead to ER stress. (100) To determine if CFZ could induce ER stress in HUVECs, the expression of a panel of ER stress markers were investigated. We aimed to maximise the chance to identify any potential ER stress activation by selecting a wide range of ER stress screening markers. These included BIP, PERK, IRE1α, ATF6, CHOP, and ATF4, which were examined at the beginning of this study. Interestingly, the qPCR and western blot data showed that CFZ did not induce any of these ER stress markers in HUVECs at the 24hr and 48hr recovery after treatment with CFZ for 1 hour.

To confirm that my assays were sensitive in detecting ER stress, assays were repeated following the treatment of HUVECs with tunicamycin, a known ER stress inducer. (329) Tunicamycin is an antibiotic that inhibits the attachment of precursor sugar structures to newly synthesised proteins within the ER, resulting in an accumulation of misfolded proteins and ER stress. (329) Consistent with the literature, treatment of HUVECs with tunicamycin induced the upregulation of ER stress markers; however, no increase was observed with CFZ treated cells in the same experiments. This data indicates that under the conditions of the assays used, CFZ could not induce ER stress in HUVECs. (329)

Since CFZ did not induce any of the selected ER stress markers, the key ER stress regulator BiP was selected as the principal ER stress marker to be investigated in the subsequent experiments. Indeed, this selection was consistent with several articles that considered BiP the key ER stress markers since it controls the activation of the three main proteins of the unfolded protein response (PERK, IRE1α, ATF6). This was clearly stated by Vitale et al. when they claimed that the alteration of BiP expression is defining the ER stress. (330) In another way, induction of BiP could be considered as the early signs and the regulator of the ER stress response; therefore, I decided to screen all my experiments for ER stress by using BiP as a principle marker and followed with other markers if an ER stress activation was observed.

In clinical practice, CFZ is typically administrated over two consecutive days each week for three weeks, followed by a recovery week in a 28-day cycle for the treatment of MM. (331) The first cycle dose is 20mg/m^2, but if the beginning dose is tolerated, the dosage will be amplified to 56mg/m^2 for the residual cycles. (331) Interestingly, exposure to an accumulative dosage of CFZ over two consecutive days showed an enhanced proteasome inhibitory effect. The ubiquitination expression was progressively up-regulated, reaching a peak after 48 hours, not found in the single dosage experiment. However, this effect was inadequate in inducing ER stress in the endothelium since BiP induction was not induced in the CFZ accumulative

experiment. Also, my data showed that increasing concentrations up to 3000nM of CFZ could not achieve ER stress activation in the endothelium. In summary, all these data showed that CFZ did not induce ER stress activation in HUVECs.

Various hypotheses could explain the reasons behind these outcomes. Firstly, it is widely accepted that cancer cells have a sensitive dependence on the degradative feature of protein homeostasis because of their fast cell cycle, hyperactive protein synthesis, and several genomic mutations, which often result in defective proteins and an imbalance in protein levels. (329) Therefore, the high protein demand of cancerous cells, unlike normal cells (HUVECs), combined with the disruption of protein production that results from proteasome inhibition by CFZ, could result in fatal ER stress, which seems improbable in HUVECs. (16)

Secondly, when CFZ impairs ERAD, which is considered one of the central cellular processes to control normal protein production and turnover; however, HUVECs could utilise and activate other mechanisms to degrade unwanted proteins, such as autophagy. (3) This mechanism is considered a complementary proteocatabolic method to compensate for proteasome inefficiency. (3) Terminally or misfolded non-functional cytosolic proteins that the UPS does not rapidly destroy can form toxic and proteolysis-refractory masses. (332) These are moved in a microtubule-dependent pattern towards the centrosome, forming aggresomes that are selectively immersed and transported to the lysosome by the autophagic machinery. (332) Thirdly, the load vs capacity model predicts that cells can avoid the harmful impacts of proteasome inhibition by attenuating the protein load in the cytosol. (333) This could be another mechanism utilised by the endothelium to escape from the effect of proteasome inhibition caused by CFZ. (333) Lastly, it could be that the experiment time exposure (1hr) was not adequate to induce ER stress in HUVECs. However, prolonged exposure of the cells to the treatment is not physiologically relevant since it is well known that the drug half-life in MM patients ranges between 30-60 minutes; therefore, it was not approached in my experimental setting. (297)

Interestingly, while CFZ could not induce ER stress, it did induce a distinct morphological change in treated HUVECS. Under normal *in vitro* culture conditions, a monolayer of HUVECS assumes a "cobblestone" like appearance. (334) However, following CFZ treatment, the HUVECS took on a stretched conformation. Several studies had reported a similar morphological appearance when the endothelium was activated. According to Stroke *et al*. endothelial cells become more elongated and stretched in response to TNF-α stimulation. (335) Activated ECs have shown a

structural rearrangement, including significant reorganisation of the cytoskeleton F-actin and aligned alongside the central axis of the cells, which is linked to enhanced cell stiffness and contractility. (336) Another author claimed a functional link between the cytoskeleton dynamic and ECs morphology during an activation response of HUVECs. (337) In general, the morphological change observed in this chapter indicated a noticeable effect of CFZ on HUVECs, such as structural rearrangement and EC activation, which is investigated in the next chapter.

The earlier data indicated no induction of ER stress-mediated by CFZ; however, there was an evident morphological alteration of HUVECs after CFZ treatment, particularly at 24 hr recovery. Thus, I hypothesised that a potential earlier ER stress induction could occur without being detected by the former experiments. The data obtained from the time-course assay indicated a time-dependent increase of ubiquitinated proteins and a progressive morphological change within 24 hours after the initial CFZ treatment in HUVECs. Surprisingly, CFZ was established to stimulate a significant upregulation of BiP protein expression, which initiated at 2 hours and lasted up to 48 hours of recovery post an initial one-hour CFZ treatment in HUVECs. Thus, the upregulation in ubiquitinated protein levels and elevated BiP expression imply ER stress is achievable in HUVECs within one CFZ treatment. However, this finding flagged conflicting data; this related to BiP protein expression at 24 hours and 48 hours in this assay and previous experiments. While the former experiments indicated no induction of BiP expression after a 24 hour and 48-hour recovery, the time course assay showed a lasting induction of ER stress in HUVECs after 1 hour of CFZ treatment. According to the backward investigation of all the conducted experiments, various factors were identified that could cause this conflicting outcome, which was examined by a series of experiments. The conclusion obtained from these assays indicated that the variety of HUVECs confluency caused the conflicting outcome at the initiation of my experiments. My data showed that the CFZ could not induce ER stress when cells were in full confluence at the beginning of the experiment. However, this was not the case with sub-confluence cells, with significant induction of BiP, thus ER stress. However, the latter finding did not precisely reflect the well-known human endothelium's monolayer structure; thus, conducting a further investigation was not undertaken. (338) Sub-confluence and proliferating endothelial cells are present when the endothelium is actively proliferating in angiogenesis and wound healing situations. (339) This was reported by several studies where it has been reported that endothelial cells were not fully confluence during the process of vascular repair and angiogenesis. (340) The observed difference of ER stress induction between the confluent and sub-confluent cells could be that the actively growing cells are more sensitive to the effect of the proteasome inhibitors. (341) This could be supported by the fact that endothelial cells at the

growth phase require different proteins to cope with the different requirements of cellular growth. (341) Consistent, growing HUVECs duplicate every 1-2 days, during which they are highly active and proliferative (non-confluence cells). (342) On the other hand, it is widely accepted that a resting HUVEC monolayer has significantly less demands on protein production. (342) In general, it could be that the active growing cells are more sensitive to the effect of the proteasome inhibitors, which could explain the potent induction of BiP expression in the 80% confluence HUVECs, but not in fully confluent cells. Similar to this, Aldo *et al.* reported that BTZ induces an anti-angiogenesis effect in MM via direct and indirect impact on endothelial cells by inhibition of interleukin-6 (IL-6) and vascular endothelial growth factor (VEGF) secretion by the multiple myeloma patient-derived endothelial cells (MMECs). (343) In agreement, Politue *et al.* demonstrated that BTZ showed a significant anti-angiogenic effect in MM patients via interferes with the action of the endothelium VEGF autocrine and paracrine pathway; thus, altering angiogenesis of the malignant plasma tumour. Taken together, CFZ may exert part of its anti-myeloma effect through anti-angiogenic mechanisms, which will be interesting to study in the future. (344)

Taken all together, it could be that the induction of BiP expression in the time course assay occurred because the cells may have been less confluent. Working with HUVECs and judging the cell confluency is always widely discussed by the interested scientist. (345) Identifying the grading of HUVECs confluency requires some time and extensive expertise, particularly in higher grade confluency cells since it is very subjective. However, it the. most important that the source of the error has been identified and the conflicting incident was resolved in a scientific approach. Therefore, in summary, once the conflicted BiP expression data have been resolved, there was a lack of evidence supporting the hypothesis that CFZ mediate ER stress in the full confluence HUVECs. Therefore, potential alternative mechanisms were hypothesised later and examined to address the research question.

Among these proposed mechanisms, since CFZ induced an apparent morphological alteration, I hypothesised that CFZ could mediate apoptosis in a similar pattern as multiple myeloma cancer cells. However, there was no induction of apoptosis in the full confluence cells, which was in line with the previous findings indicating the lack of ER stress activation in these cells. Even though there was a significant induction of BiP expression stress in the 80% confluence HUVECs, there was no induction of apoptosis in these cells. Prolonged disturbance of ER homeostasis leads to the activation of the unfolded protein response - a set of pathways that monitor the diminishing of the ER protein-folding function and observe the ER's condition. (346) The activation of this

pathway resolves ER stress and restores normal homeostasis by involving three significant actions (88): expanding the expression of molecular chaperones, suppressing protein translation, and degrading misfolded proteins. (88) These actions are consequences of activating three principal ER stress transducers: ATF6, PERK and IRE1, which were all dependent on the BiP/GRP78, an essential ER chaperone to identify misfolded proteins. (41) The downstream signalling of these transducers aims to re-establish cellular protein homeostasis and resolve ER stress. (347) This is accomplished by expanding folding capacity, improving the ER's clearance capacity by ERAD and autophagy, and reducing the folding load. (347) All these together serve as a protective cellular mechanism to defend against the harmful impact of ER stress. Thus, this could explain why there was no activation of the apoptosis in the 80% confluence HUVECs when there was a significant induction of ER stress in the cells.

Lastly, in this chapter, I hypothesised that a similar CFZ effect would be found in non-malignant cells, but not cancer cells, since they are rapidly growing cells and more suitable to the harmful impact of proteasome inhibition. Therefore, I stimulated a non-malignant cell (HEK293) and a multiple myeloma cancer cell (OPM-2) with the same single dose concentration used in the HUVECs experiment. Interestingly, the data obtained supported and confirmed my latest hypothesis. I found no induction of BiP protein in CFZ treated HEK293 cells, indicating the absence of ER stress activation in these cells. On the other hand, there was a significant induction of BiP protein expression in the OPM-2 cells, indicating an activation of ER stress in the cancer cells, which agreed with the published literature. Mishima *et al*. reported an accumulation of protein aggregates and ubiquitinated proteins in the cytoplasm of MMCs caused by CFZ, leading to significant induction of ER stress and eventually to cellular death. (348) Similarly, CFZ was proved to induce a permanent inhibition to the β5 subunit of the 20S proteasome in OPM-2 cells, which led to ER stress activation. (10) In agreement with my result CFZ was found to lead to an upregulation of BiP expression in OPM-2 cells which agreed with the well-known fact of the cytotoxicity effect of CFZ against MMCs. (349) Moreover, it supports the proposed hypothesis that CFZ does not induce ER stress in the non-malignant cells since they are less dependent on protein production and turnover.

In conclusion, the results of this chapter led me to reject the initial hypothesis that CFZ induces ER stress activation in the endothelium. Alternative mechanisms, such as endothelium activation alteration of endothelium haemostasis, were then hypothesised and investigated in the second chapter.

3.2 CFZ induces cytoprotective and thrombo-protection effects in HUVECs

3.2.1 Introduction

Desynchronised cytokine phenomena classically demonstrate multiple myeloma (MM) with elevated circulating inflammatory cytokines found in MM patients(16). The interaction between MMCs and bone marrow stromal cells is essential for cancer cell survival and progression. (350) Among these, the inflammatory cells, macrophages, dendritic cells (DCs), and lymphocytes play a vital role in MM progression and tumour growth. (351) The myeloma cells and bone marrow environment triggers the autocrine or paracrine release of numerous mediators, which promote MM progress. (352) Among 79 newly diagnosed and 20 relapsed MM patients, their serum cytokine (IL-1, TNFα, IL-6, and VEGF) concentrations were significantly higher than control subjects ($P<0.001$). (353) According to Methap *et al*., the serum level of IL-6, IL-21, IL-1β, and TNFα were remarkably amplified in MM patients' serum compared to healthy controls. (354)

The human cardiovascular system is internally covered with a luminal mono-structural layer of squamous vascular endothelial cells. (355) The endothelium creates a bridge and barrier between circulating blood and other vessel wall and tissue components(355) and functions to maintain the finely tuned vascular system. (356) Indeed, the endothelium is considered an endocrine organ that secretes many mediators to maintain normal blood flow, control vascular contraction and relaxation, thrombosis and inflammatory activation. (357) It also strictly monitors and controls coagulation and the fibrinolysis system. (358) Among endothelium mediators, nitric oxide and prostacyclin are considered major endothelial cell-derived vasodilators, endothelium-derived relaxing factor (EDRF) as a relaxing factor, endothelin-1 and thromboxane A2 as vasoconstrictive factors.

When the endothelium fails to maintain normal haemostasis, reduced creation/availability of nitric oxide is found. This is known as endothelium dysfunction when there is a disparity in the relative involvement of endothelium-derived contracting and relaxing factors. (359) This initial pathologic step is involved in the prognosis of various types of endothelium dysfunction associated with cardiovascular

complications, such as hypertension, myocardial infarction, and acute coronary syndromes. (360)

Endothelial cells do not trigger platelet activation in a healthy vascular system, though these cells are in close contact. (361) Platelet activation is triggered by the discharge of substances from an activated or damaged endothelium. (361) The release of VWF from an injured endothelium, exposure of ICAM-1, VCAM-1, and P-selectin on the plasma membrane and the expression of chemokines and platelet-activating factors, all together stimulate a pro-coagulator and pro-inflammatory environment. (361) The pathological activation of these mechanisms leads to the formation of atherosclerosis, which eventually leads to damage of endothelium-dependent vasodilation mechanisms, which is the functional feature of endothelial dysfunction. (362)

An association between the enhanced incidence of venous thrombosis and MM has been reported. (363) This could be through direct damage to the endothelium by MMCs, alteration of physiological coagulation balance, or damage caused by the aggressive chemotherapies used in MM treatment. (363) In most cases, the mechanisms behind a thrombotic event in MM patients cannot be explained, but using chemotherapy in MM treatment may play a more significant role in thrombotic development than an individual abnormality since thrombotic events become more noticeable after starting treatment. (364) However, even before administering chemotherapy in MM patients, hypercoagulability in MM patients has been well documented. (365) There is evidence of damage to the fibrinolytic and anticoagulant pathways in MM patients. (365) An elevated/abnormal immunoglobulin, abnormal cytokine production, and activated protein C (APC) pathway resistance have been proposed as causative mechanisms of hypercoagulability in MM patients. (366) In addition, CFZ usage in MM has increased the risk of various thrombosis complications. Danhof *et al*. revealed that 25% of patients who received CFZ progressed with signs of congestive heart failure caused by thrombosis. (367)

Since, as described in chapter one, CFZ did not induce ER stress in the endothelium, **I hypothesised and investigated** if stimulation of HUVECs with pro-inflammatory cytokines and CFZ would induce ER activation in if this would pro-inflammatory and pro-thrombotic activation of the endothelium.

3.2.2 Results

3.2.2.1 Combined treatment with CFZ and cytokines induced morphological change and ubiquitination expression but did not induce ER stress in the endothelium

It is well known that MM patients have a significantly amplified level of pro-inflammatory cytokines, such as TNFα and IL-1β, in their serum. (368) Therefore, we hypothesised that the existing pro-inflammatory environment in MM patients could enhance CFZ cytotoxicity and induce ER stress or pro-thrombotic and pro-inflammatory activation in the endothelium.

For this purpose, I stimulated confluence HUVECs with 20ng/ml NF and/or with 20ng/ml IL-1β combined with CFZ or alone, followed by a one-hour treatment with 750nM CFZ. The cells were harvested after a 24hr or 48hr period following CFZ treatment or stimulation with the cytokines, followed by gene and protein expression analysis (Figure 3.2.1).

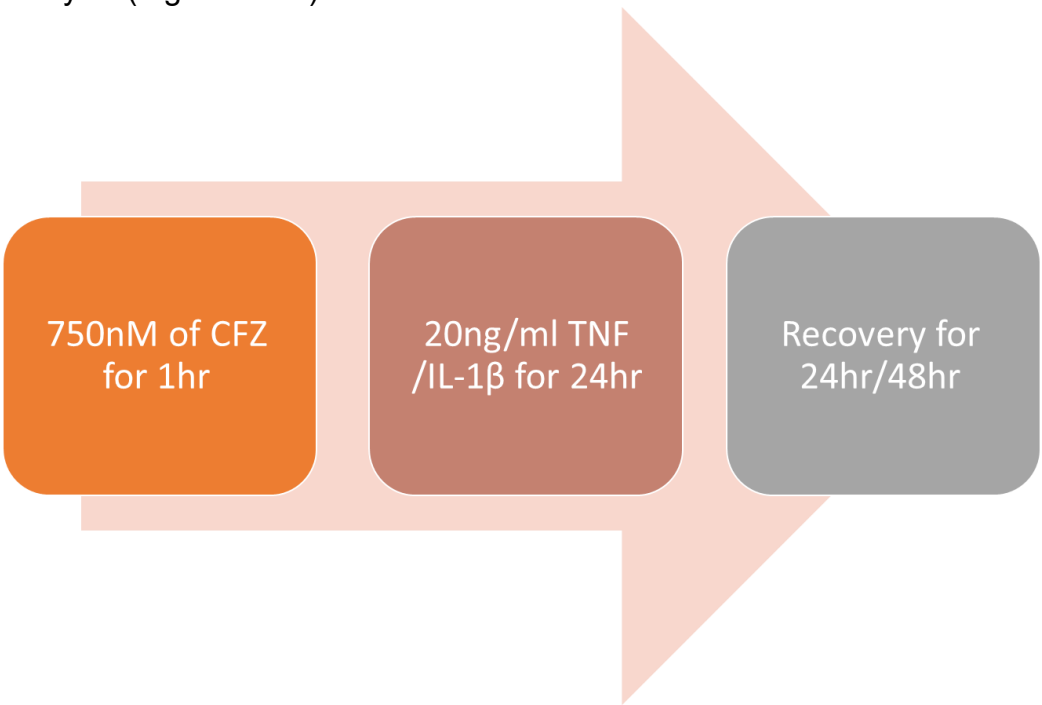


Figure 3.2.1: A schematic illustration of the experimental timelines

Tunicamycin was used as an ER stress positive control in this experiment. Interestingly the cytokine-stimulated (TNFα, IL-1β and TNFα + IL-1β) cells showed a noticeable morphological alteration; the cells were slightly “stretched” and elongated compared to the typical morphology found in the untreated and DMSO vehicle controls

(Figure 3.2.2), which was similarly observed in CFZ and CFZ+TNFα/IL-1β-treated HUVECs, indicating a potential activation of HUVECs in all conditions (Figure 3.2.3)

In order to test the hypothesis that cytokine stimulation of cells could enhance the ability of CFZ to induce ER stress, I investigated the ubiquitination level among all treated cells. Consistent with the earlier findings, CFZ showed an evident ability to inhibit proteasome function and revealed a significant two-fold increase of ubiquitin-protein expression in CFZ treated cells compared to the untreated control (Figure 3.2.4). This upregulation was also found in TNFα alone treated cells, suggesting an effect of TNFα on proteasome function (Figure 3.2.4). In contrast, tunicamycin and IL-1β did not induce ubiquitin expression, suggesting that neither can modulate proteasome activity. (Figure 3.2.4). This finding indicates that TNFα could enhance the ability of CFZ to inhibit the proteasome function of the endothelium.

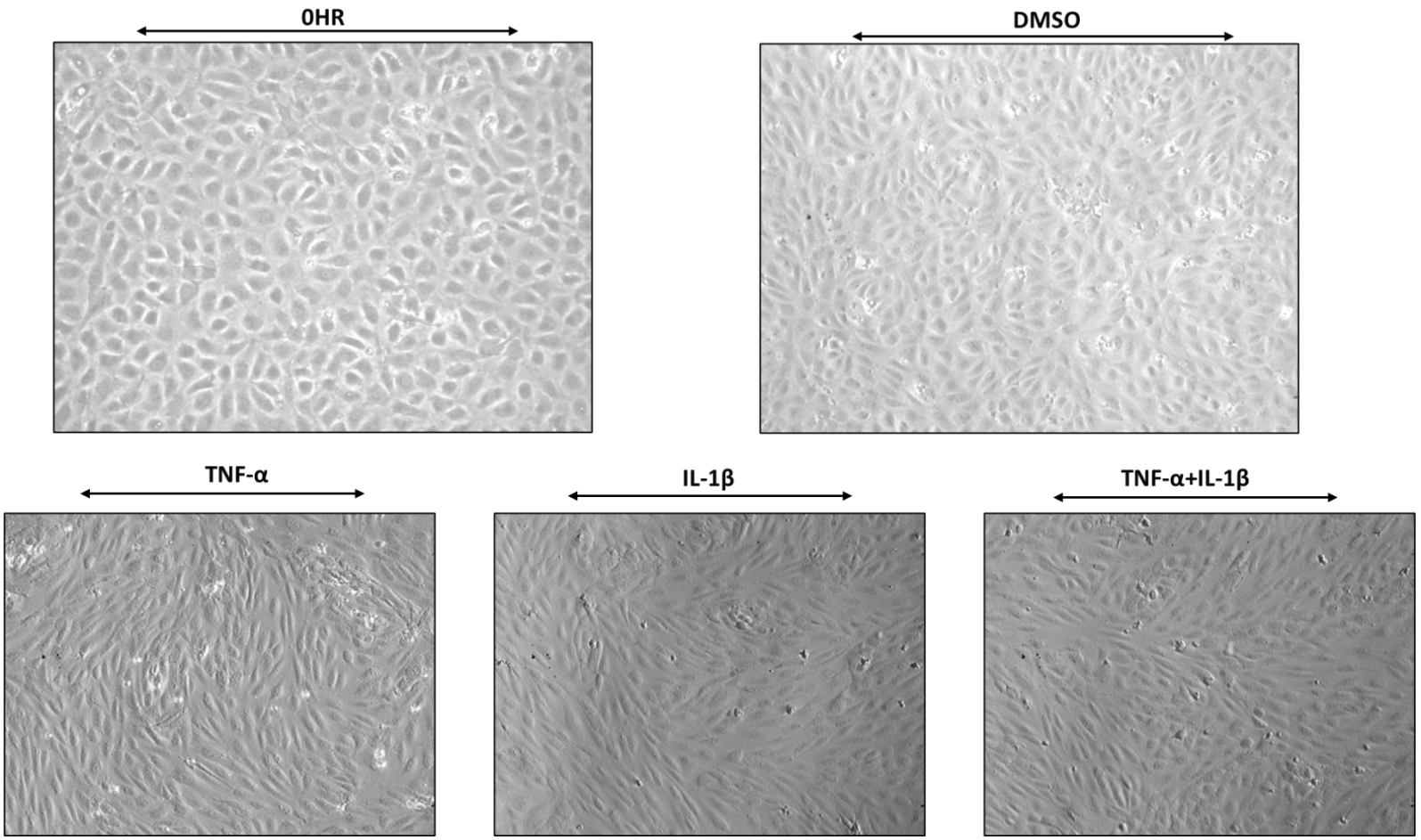


Figure 3.2.2: TNFα and IL-1β stimulation-induced morphological change in HUVECs. HUVECs were treated with 750nM of CFZ and DMSO for 1 hour, followed by washing the cells with PBS and replacing them in fresh EBM-2 medium. Some cells were stimulated for 24 hr with 20 ng/ml of TNFα and/or 20 ng/ml IL-1β after 1hr treatment with 750nM CFZ. The morphological observation was conducted using a light microscope (10X objective).

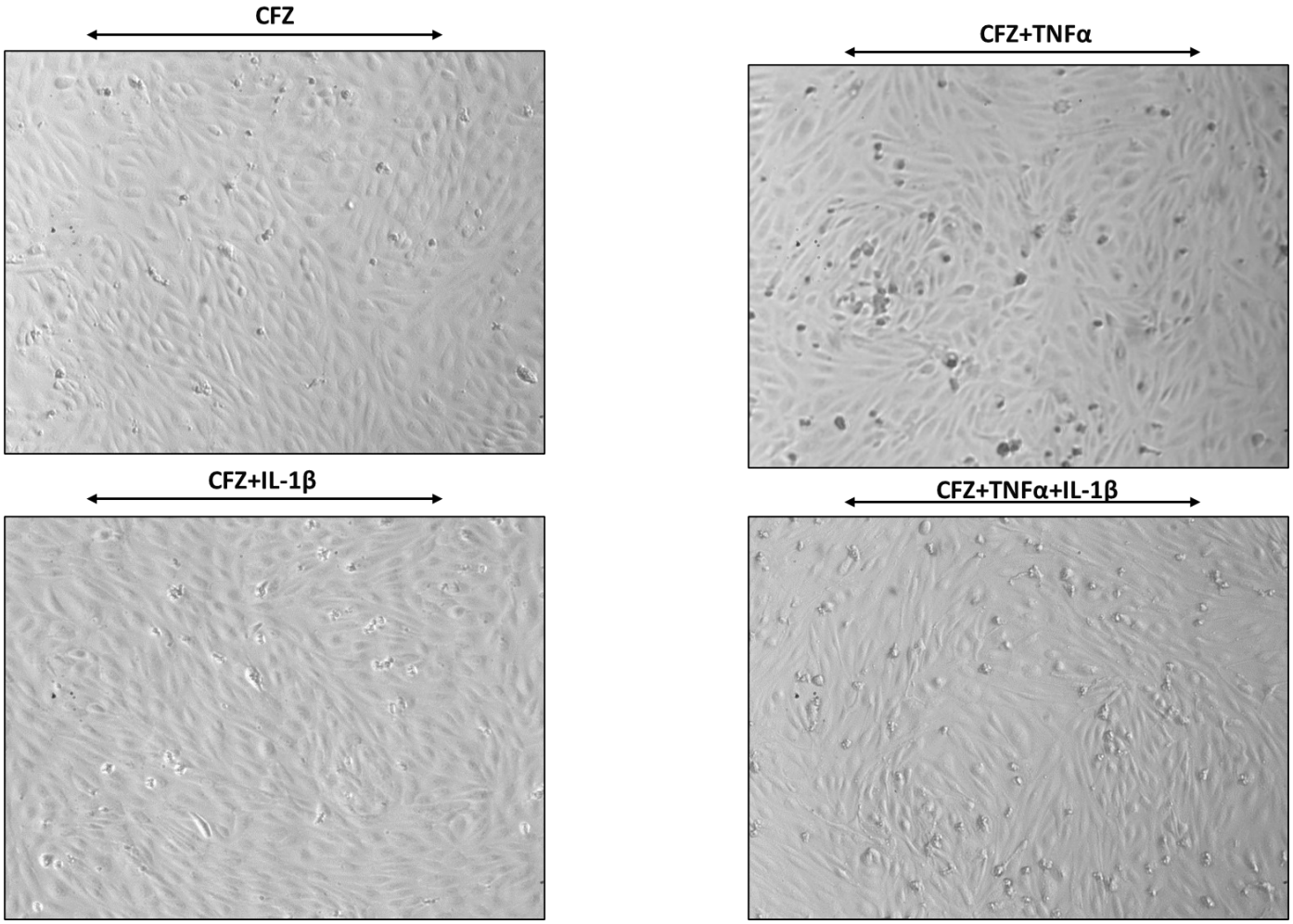


Figure 3.2.3: CFZ alone or combined with TNFα and IL-1β stimulation-induced morphological change in HUVECs. HUVECs were treated with 750nM of CFZ and DMSO for 1 hour, followed by washing the cells with PBS and replacing them in a fresh EBM-2 medium. Some cells were stimulated for 24 hr with 20 ng/ml of TNFα and/or 20 ng/ml IL-1β after 1hr treatment with 750nM CFZ. The morphological observation was conducted using a light microscope (10X objective).

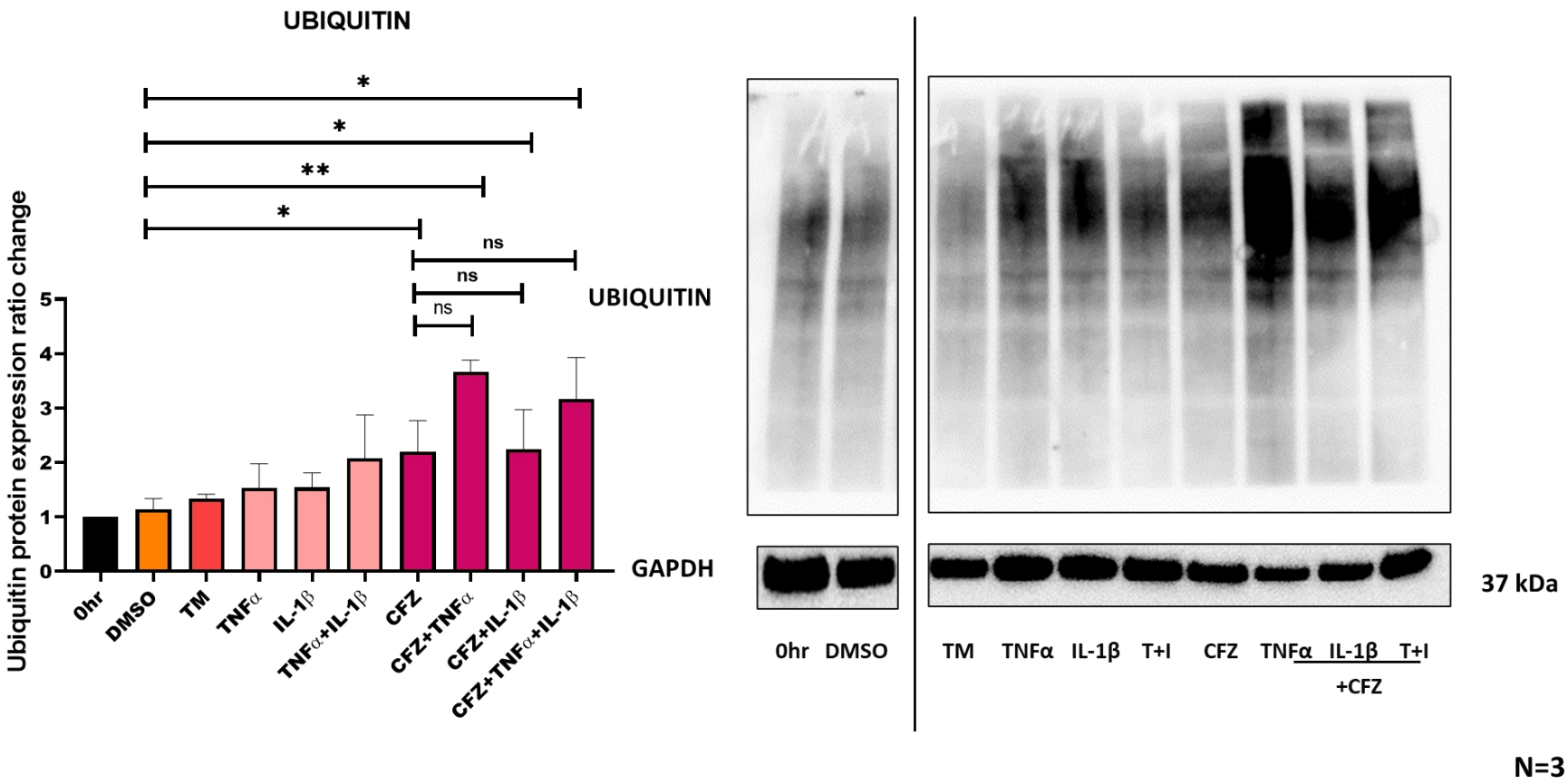


Figure 3.2.4: TNFα stimulation of HUVECs enhanced CFZ proteasome inhibition. HUVECs were treated with 750nM of CFZ and DMSO for 1 hour, followed by washing the cells with PBS and replacing them in a fresh EBM-2 medium. Some cells were stimulated for 24 hr with 20 ng/ml of TNFα and/or 20 ng/ml IL-1β after 1hr treatment with 750nM CFZ. Cells were harvested to extract protein at 0hr and 24hr. Western blot was used to determine the extent of ubiquitination. Western blot analysis of ubiquitin-protein level expression and density quantification of Western blot. DMSO, Dimethyl sulfoxide; CFZ, Carfilzomib; TM, Tunicamycin; TNFα, Tumour Necrosis Factor; IL-1β, Interleukin-1 β; T+I, TNFα+IL-1β. Three technical repeats were performed in one experiment, and the quantification of data was normalised to GAPDH levels and presented as the mean ± SEM. The data represents the average of three independent experiments. The expression trends of ubiquitin of all treated cells were compared using one-way ANOVA. Significance: *P < 0.05, **P < 0.01, ***P < 0.00.

To investigate if cytokine stimulation of HUVECs could enhance CFZ ability to induce ER stress in HUVECs, Western blot and qPCR were used to analyse the expression of protein and gene expression of the principal ER stress marker (BiP). In common with my previous findings, CFZ alone did not induce ER stress in HUVECs, while TM significantly induced ER stress (Figure 3.2.5 A, B). This was revealed by the significant induction of both gene and protein expression of BiP in the TM treated cells, while this was absent in the CFZ treated cells.

Interestingly, although TNFα alone showed an ability to enhance CFZ proteasome inhibition, it was insufficient to induce ER stress in the endothelium. This was revealed by a similar expression of the BiP gene, and protein in CFZ treated cells compared to CFZ+TNFα. These findings suggest that the cells can avoid the activation of ER stress even where there is significant inhibition of proteasome function (Figure 3.2.5 A, B). All these findings suggest that stimulation of the endothelium with cytokines does not trigger the activation of ER stress in the endothelium.

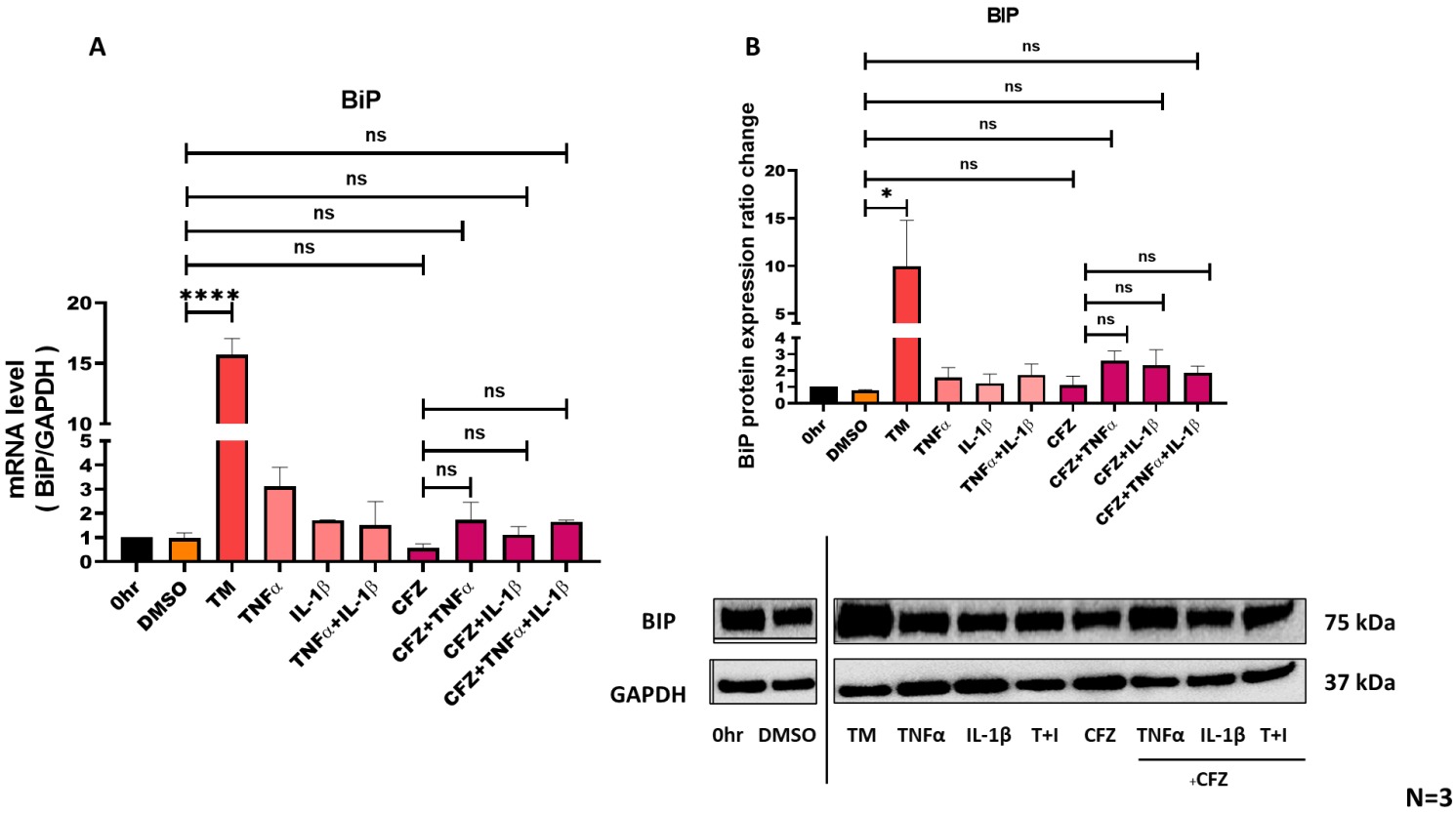


Figure 3.2.5: TNFα and IL-1β stimulation did not enhance CFZ to cause ER stress in HUVECs. HUVECs were treated with 750nM of CFZ and DMSO for 1 hour, followed by washing the cells with PBS and replacing them in a fresh EBM-2 medium. Some cells were stimulated for 24 hr with 20 ng/ml of TNFα and/or 20 ng/ml IL-1β after 1hr treatment with 750nM CFZ. Cells were harvested to extract protein at 0hr and 24hr. A) qPCR analysis of BiP gene-level expression. B) Western blot analysis of BiP protein level expression and density quantification of Western blot. DMSO, Dimethyl sulfoxide; CFZ, Carfilzomib; TM, Tunicamycin; TNFα, Tumour Necrosis Factor α; IL-1β, Interleukin-1 β; T+I, TNFα+IL-1β. Three technical repeats were performed in one experiment, and the quantification of data was normalised to GAPDH levels and presented as the mean ± SEM. The data represents the average of three independent experiments. The expression trends of BiP of all treated cells were compared using one-way ANOVA. Significance: *P < 0.05, **P < 0.01, ***P < 0.001

3.2.2.2 Prolonged stimulation with TNFα did not induce ER stress in HUVECs

There was a significant upregulation of ubiquitin expression and significant morphological changes in the CFZ combined with the TNFα-treated HUVECs. However, the previous experiment showed that a combination of CFZ and TNFα did not induce BiP expression. Therefore, I hypothesised that prolonged exposure of the endothelium to TNFα may trigger these cells beyond their protection mechanisms, thus inducing ER stress. For this purpose, cells were treated for 24-48 hours with 20 ng/ml TNFα. The cells were harvested, and the proteins and mRNA were collected at selected TNFα stimulation time points (24hr and 48hr) and after 1 hour of treatment with 750nM of CFZ.

Consistent with my previous findings (Chapter 1 and Figure 3.2.4), CFZ treatment induced a significant induction of ubiquitination at 24 hours, but this was not seen at 48h (Figure 3.2.6). A combination of CFZ and TNFα also showed significantly enhanced induction of ubiquitination compared to the controls and the CFZ treated cells at 24 hours only (Figure 3.2.6). This indicates that TNFα stimulation of the cells after a one-hour treatment with 750nM CFZ enhanced the CFZ proteasome inhibition. However, in common with data showed in chapter one, this effect was not permanent; in CFZ treated cells, ubiquitination expression almost returned to the baseline after 48 hours recovery, and interestingly, prolonged stimulation with TNFα did not induce ubiquitination, indicating the cells' ability to recover from the effect of TNFα stimulation (Figure 3.2.6).

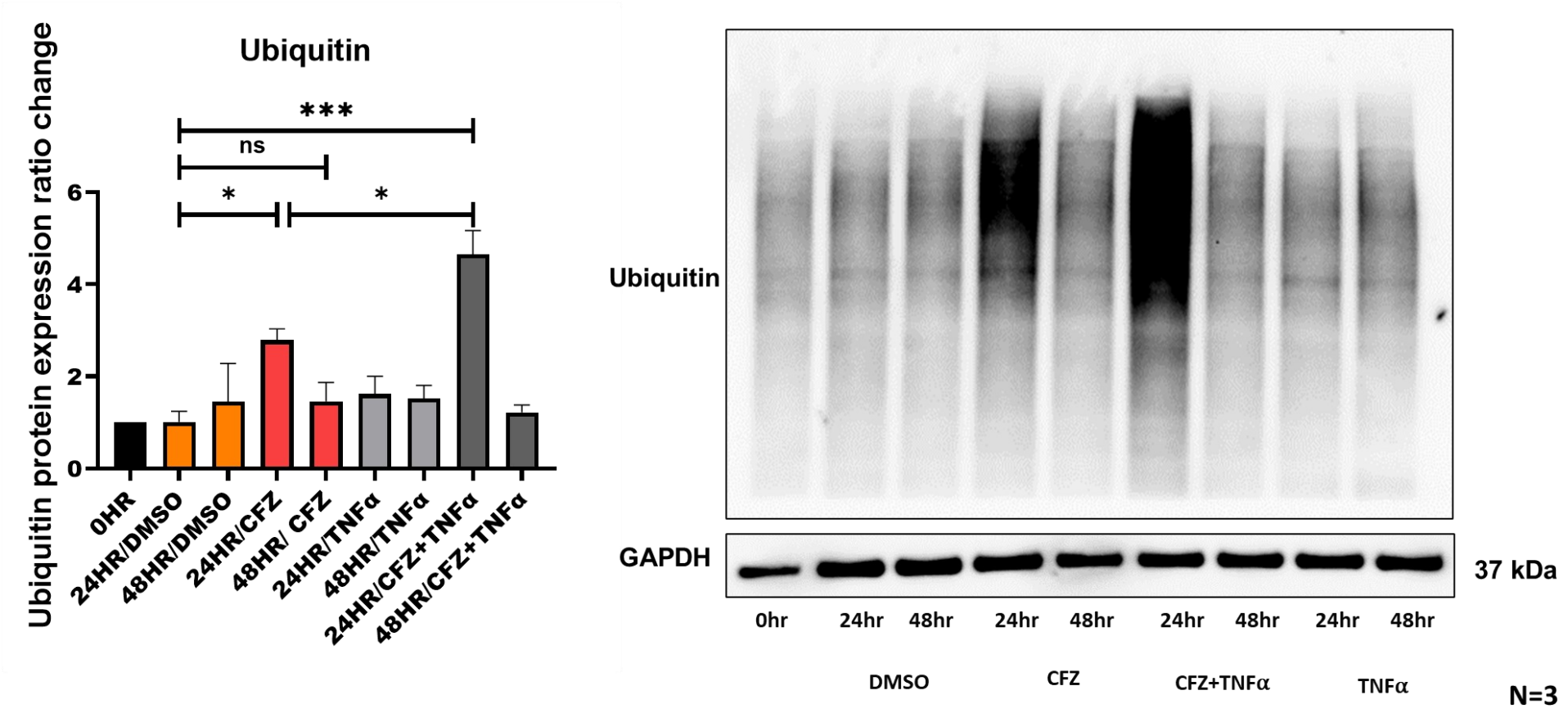


Figure 3.2.6: Prolonged TNFα stimulation of HUVECs did not enhance CFZ proteasome inhibition. HUVECs were treated with 750nM of CFZ and DMSO for 1 hour, followed by washing the cells with PBS and replacing them in a fresh EBM-2 medium. Some cells were stimulated 24/48 hr with 20 ng/ml of TNFα after 1hr treatment with 750nM CFZ. Cells were harvested to extract protein at 0hr, 24hr, and 48 hr. Western blot was used to determine the extent of ubiquitination. Western blot analysis of ubiquitin-protein level expression and density quantification of Western blot. DMSO, Dimethyl sulfoxide; CFZ, Carfilzomib; TNFα, Tumour Necrosis Factor α. Three technical repeats were performed in one experiment, and the quantification of data was normalised to GAPDH levels and presented as the mean ± SEM. The data represents the average of three independent experiments. All treated cells' expression trends of ubiquitin were compared using one-way ANOVA. Significance: *P < 0.05, **P < 0.01, ***P < 0.001

In keeping with my previous findings, the qPCR and Western blot analysis revealed that there was no upregulation of BiP at either gene or protein level at 24 hours recovery of CFZ treatment or after 24 hours stimulation with TNFα alone or in combination with CFZ treatment (Figure 3.2.7 A, B). Similarly, there was no induction of ER stress in the endothelium even with the prolonged 48-hour exposure of HUVECs with TNFα after 1 hour of treatment with CFZ. This was demonstrated by a similar BIP mRNA expression and protein expression in cells treated for 48hr with /CFZ+TNFα compared to both untreated and DMSO controls (Figure 3.2.7 A, B). Taken together, this indicates that the combination of TNFα and CFZ showed significant ubiquitination induction but did not induce ER stress in HUVECs.

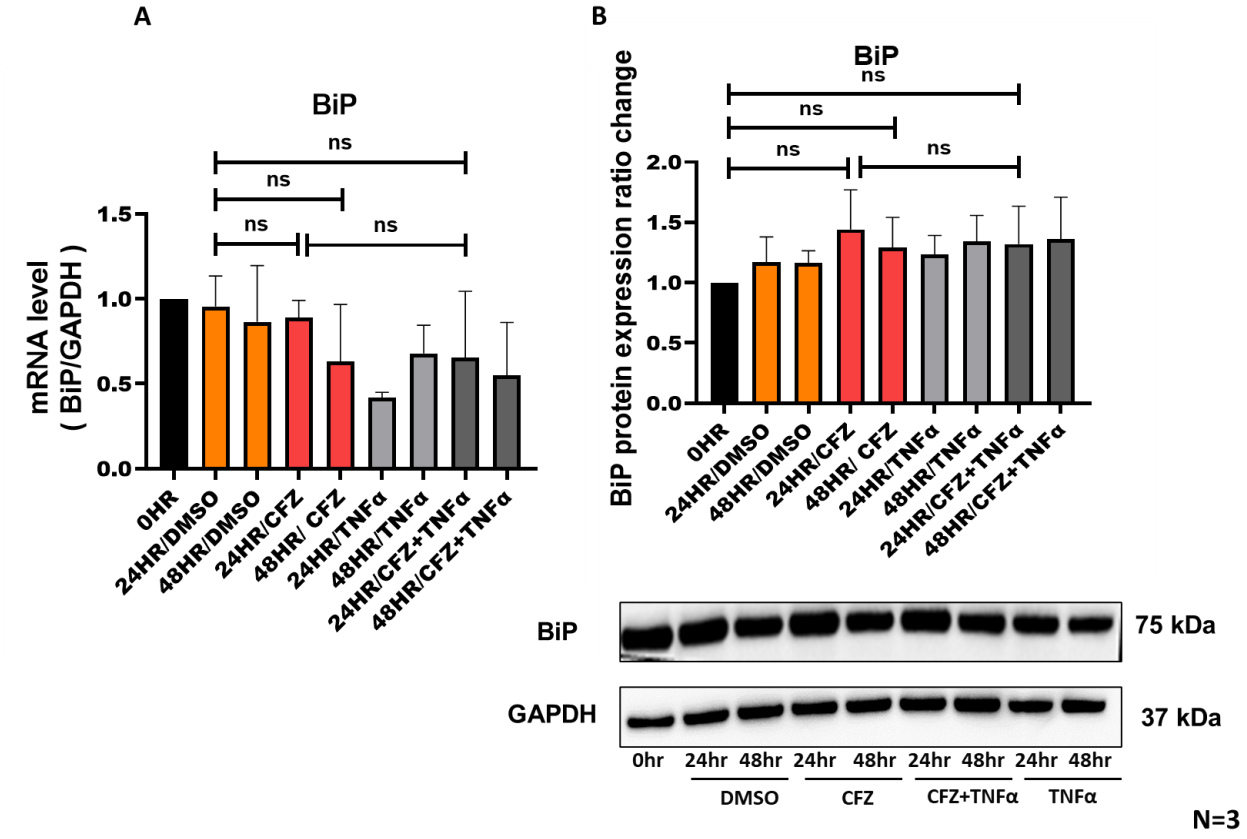


Figure 3.2.7: Prolonged TNFα stimulation did not induce ER stress in HUVECs. HUVECs were treated with 750nM of CFZ and DMSO for 1 hour, followed by washing the cells with PBS and replacing them in a fresh EBM-2 medium. Some cells were stimulated 24/48 hr with 20 ng/ml of TNFα after 1hr treatment with 750nM CFZ. qPCR analysis of BiP-protein level expression. DMSO, Dimethyl sulfoxide; CFZ, Carfilzomib; TNFα, Tumour Necrosis Factor α. Three technical repeats were performed in one experiment, and the quantification of data was normalised to GAPDH levels and presented as the mean ± SEM. The data represents the average of three independent experiments. The expression trends of BiP of all treated cells were compared using one-way ANOVA. Significance: *P < 0.05, **P < 0.01, ***P < 0.001.

3.2.2.3 CFZ induces structural rearrangement of the endothelium

The above data shows no evidence supporting the hypothesis that CFZ could induce ER stress in the endothelium, even when combined with TNFα and/ or IL-1β. However, we observed an apparent morphological alteration in the CFZ treated cells among all conducted experiments. Therefore, I hypothesised that this alteration of endothelial cell morphology could activate the endothelium by affecting the HUVEC cytoskeletal architecture. To investigate this hypothesis, I treated the cells with DMSO, or 750nM CFZ alone for 1 hour or combined them with 20ng/ml of TNFα for 24 hours. Subsequently, I stained the cells with F-actin phalloidin-iFluor 594 stains (Methods 2.6.2) to identify potential structural changes of the endothelium cytoskeleton.

In control HUVECs, I observed that mature stress fibres were assembled in parallel groups alongside the basal surface of the cells (Figure 3.2.8). It is well established that TNF-α affects EC morphology; the cells become more elongated, more prominent with a significant reorganisation of F-actin that aligns alongside the cell's central axis. (369) All of these morphological events commonly correlated to enhanced cell stiffness and contractility. (369) In agreement, my findings show that stimulation of HUVECs with TNF-α triggered considerable shifts in the F-actin arrangement of ECs. The F-actin of most cells was assembled in parallel to the central (long) axis of cells after a 24-hour stimulation with TNF-α (Figure 3.2.8), indicating an alteration of the cytoskeleton structure of cells. The CFZ treatment of the cells showed a similar morphological effect to that seen in the TNFα stimulated cells; however, this was to a lesser extent (Figure 3.2.8). Taken together, the alteration of the endothelium morphology induced by CFZ treatment could be an indicator of the inflammatory process or an adaption process to enhance the endothelium functional ability and stiffness.

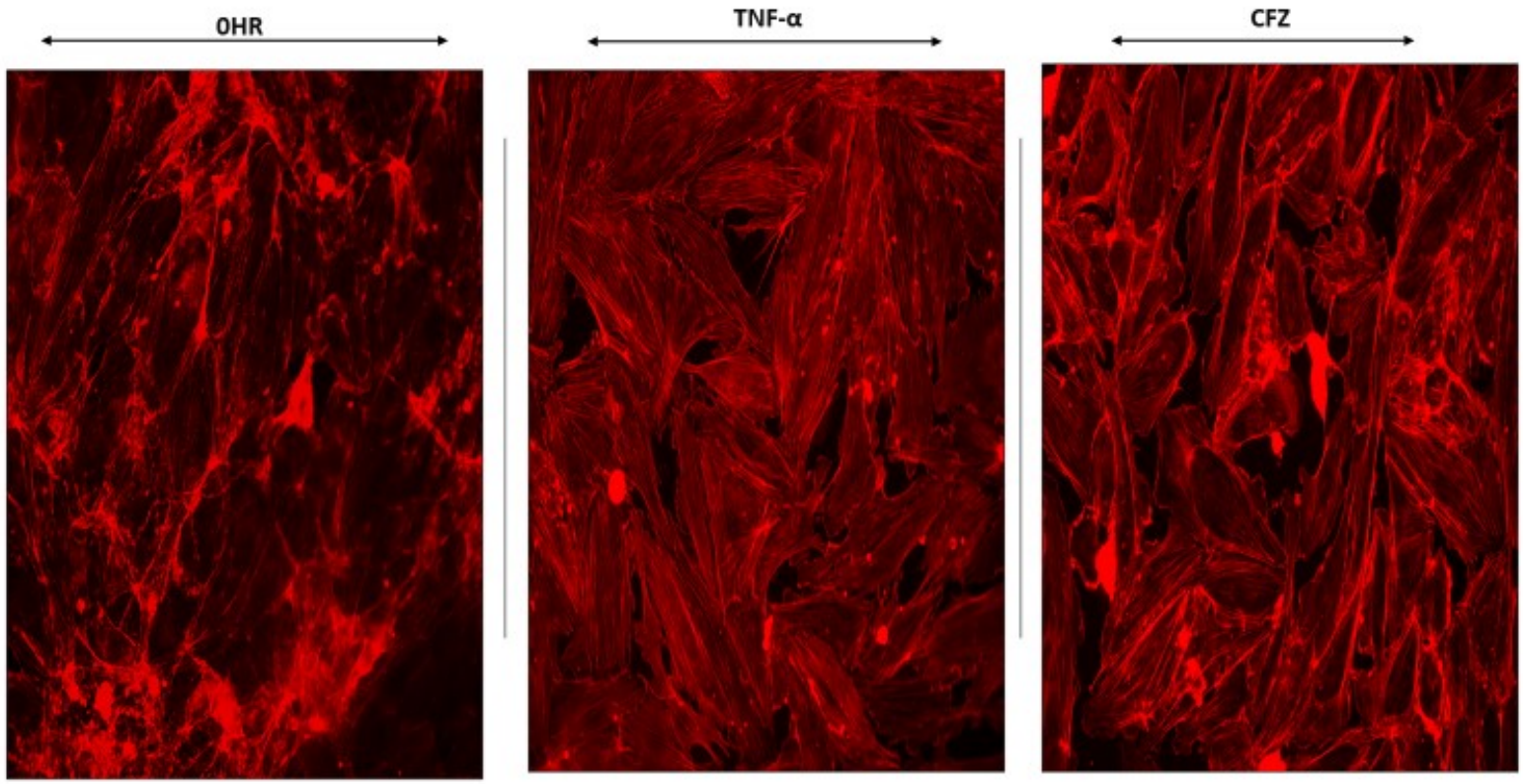


Figure 3.2.8: CFZ induces morphological alteration and F-actin rearrangement in the endothelium. HUVECs were treated with 750nM of CFZ and DMSO for 1 hour, followed by washing the cells with PBS and replacing them in a fresh EBM-2 medium. Some cells were stimulated with 20 ng/ml of TNFα after CFZ treatment for 24 hours. Cells were stained with phalloidin-iFluor 594 to visualise the actin filament arrangement within the endothelium. Cells were visualised and pictured using an EVOS M5000 microscope (20 x objective).

3.2.2.4 CFZ treatment did not induce endothelial ICAM-1 expression

Intercellular adhesion molecule (ICAM-1) is a cell surface glycoprotein that binds to CD11/CD18 integrins of targeted cells. (370) It is continuously expressed in low concentration in the membrane of both leukocyte and endothelial cells. (371) However, when endothelial cells undergo pro-inflammatory and cytokine stimulation, this protein expression is significantly upregulated and interacts with Lymphocyte function-associated antigen 1 (LFA-1) found on the leukocyte surface. (371) This interaction allows leukocyte attachment and transmigration to the endothelium, thus initiating the pro-inflammatory response. (372)

In order to further investigate the effect of CFZ on HUVECs, I performed a flow cytometry study to investigate the effect of CFZ treatment on the expression of ICAM-1 protein on the surface of the endothelial cells. Cells were treated and prepared as described (Methods 2.7.1). In agreement with previously published data, the treatment of HUVECs with TNFα resulted in increased surface ICAM-1 expression. (373) In contrast, CFZ did not induce ICAM-1 expression (Figure 3.2.9 A). Interestingly, when the cells were treated with CFZ and then subsequently with TNFα, the TNFα-induced ICAM-1 expression was significantly reduced, indicating that CFZ may have a protective effect on the endothelium (Figure 3.2.9, A).

Similarly, findings were observed for the release of soluble ICAM-1(sICAM-1), which matched the flow cytometry findings (Figure 3.2.9, B), indicating that CFZ had a protective effect in the endothelium against the pro-inflammatory impact of TNFα.

Supporting the previous investigation tools, the Western blot analysis revealed that CFZ suppressed the well-known TNFα ability to induce ICAM-1 expression on the endothelium. This was demonstrated by a significant reduction of ICAM-1 expression when CFZ treatment combined with TNFα stimulation was compared with the TNFα stimulation alone (Figure 3.2.9, C). Western blot data also revealed no induction of ICAM-1 expression in CFZ treated HUVECs compared to the controls (Figure 3.2.9, C). However, the Western blot analysis was conducted using the data of two biological repeats only; thus, further repetition should be performed before establishing a conclusion from the assay.

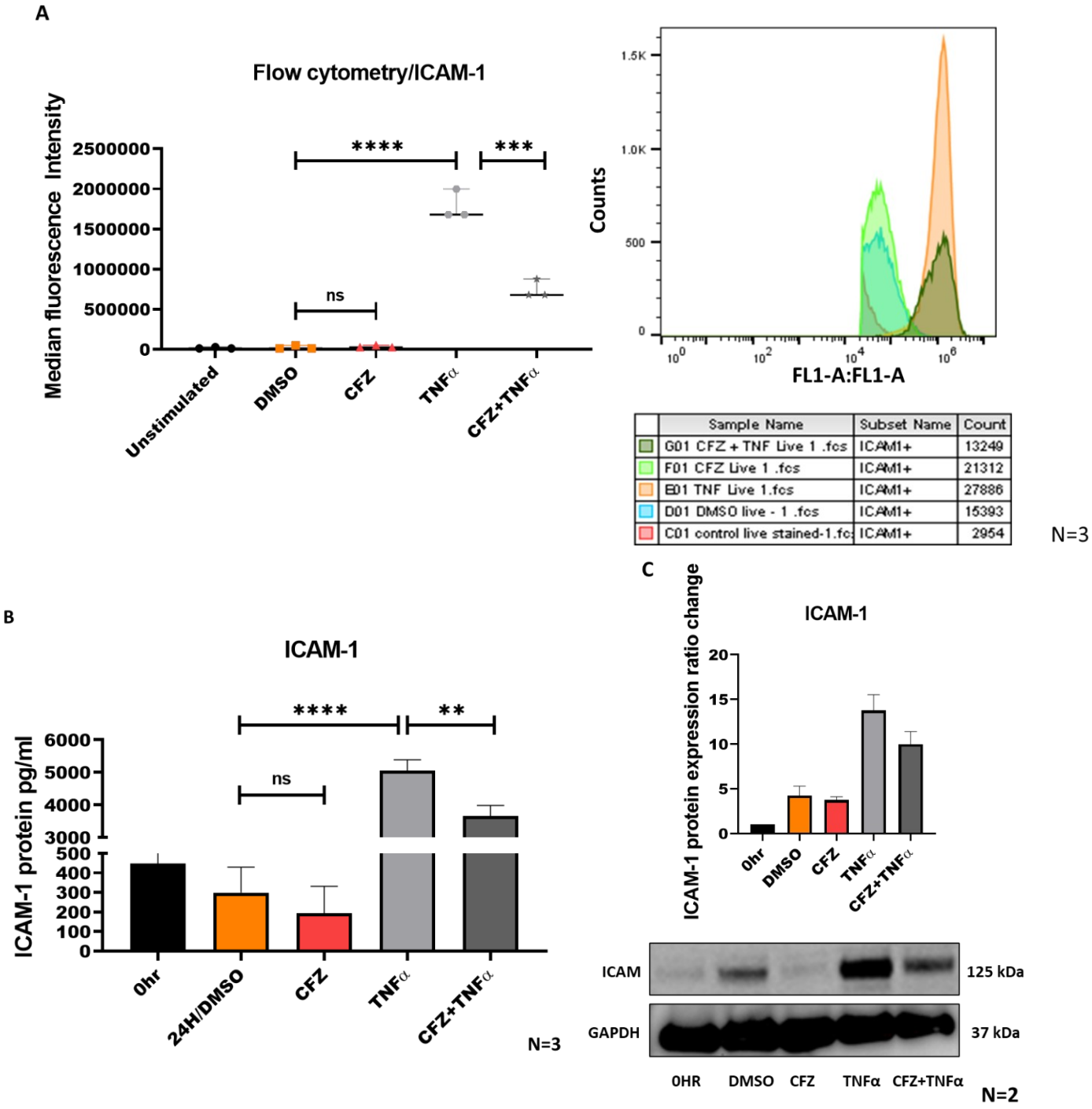


Figure 3.2.9: CFZ did not induce endothelial cell ICAM-1 expression from HUVECs. HUVECs were treated with 750nM of CFZ and DMSO for 1 hour, followed by washing the cells with PBS and replacing them in a fresh EBM-2 medium. Some cells were stimulated with 20 ng/ml of TNFα after 1hr 750nM CFZ treatment A) Flow cytometry analysis for ICAM-1 expression. B) ELISA analysis for soluble ICAM-1 expression in the collected medium. C) Western blot analysis for ICAM-1 expression DMSO, Dimethyl sulfoxide; CFZ, Carfilzomib; TNFα, Tumour Necrosis Factor α. Three technical repeats were performed in one experiment, and the quantification of data was normalised to GAPDH levels and presented as the mean ± SEM. The data represents the average of three independent experiments. The expression trends of ICAM-1 of all treated cells were compared using one-way ANOVA. Significance: *P < 0.05, **P < 0.01, ***P < 0.001.

3.2.2.5 CFZ induced an anti-thrombotic and cytoprotective effect on the endothelium

As CFZ did not demonstrate an ability to induce ER stress in the confluence HUVECs, I suggested that CFZ mediated pro-thrombotic and pro-inflammatory effects on the endothelium might provide an alternative to addressing the hypothesis CFZ effect on the endothelium. For this aim, I examined some of the well-known pro-thrombotic and pro-inflammatory markers after 1hr of 750nM CFZ and 20ng/ml TNFα for 4hr/24hr treatment individually/combination. Shorter stimulation with TNFα (4hr) was newly examined in this experimental setting to identify any potential earlier CFZ and TNFα combined induction of either a pro-thrombotic or pro-inflammatory effect in the endothelium.

There was no noticeable change after 4hr of TNFα stimulation or CFZ treatment and 4hr recovery of mRNA levels for some of the well-known anti-thrombotic marker genes, thrombomodulin (TM), endothelial nitric oxide synthase (eNOS), and Kruppel Like Factor 4(KLF-4). Even though CFZ treated cells slightly reduced these genes compared to the vehicle-DMSO control, it was not statistically significant (Figure 3.2.10). These data indicate that CFZ did not induce these markers during the early recovery period of the cells.

In contrast to the findings at 4h, the qPCR analysis at 24hr showed significant induction of mRNA for TM and KLF-4 among all CFZ treated cells (Figure 10). Similarly, the Western blot analysis showed there was a significant upregulation of eNOS, p-eNOS, and TM proteins among the same groups of cells (Figure 11). These data suggest that CFZ is directly involved in the induction of thrombo-protective activity in HUVECs.

In the same trend of thrombo-protective derived activity by CFZ, the qPCR and Western blot studies showed that CFZ reduced the extent of TNFα mediated TF expression after 4hr and 24h TNFα stimulation. This was illustrated by a significant reduction in TF mRNA in CFZ+TNFα treated cells compared to CFZ treated cells alone at both 4hr and 24 hr TNFα stimulation (Figure 3.2.12 A). This was confirmed by protein expression, where there was a significant reduction in TF expression after CFZ treatment indicating a potential protective effect of CFZ against the TNFα mediated

expression of TF from HUVECs at the same indicated time points. (Figure 3.2.12 B) Taken together, these data indicate that CFZ has a potential anti-thrombotic effect on HUVECs.

VWF and angiopoietin-2 (Ang-2) are major endothelium-derived pro-thrombotic and pro-inflammatory proteins, respectively. There was a comparable secretion of VWF and Ang-2 in CFZ treated cells compared to those untreated and the DMSO control, indicating the absence of pro-thrombotic and pro-inflammatory activation in these groups of cells (Figure 3.2.13). Interestingly, while TNFα treatment of HUVECs induced VWF and Ang-2 expression, CFZ significantly reduced both marker's release levels when combined with the cytokine (Figure 3.2.13). These findings suggest that instead of CFZ rendering the cells pro-thrombotic/pro-inflammatory active, it showed a cytoprotective effect in confluence HUVECs.

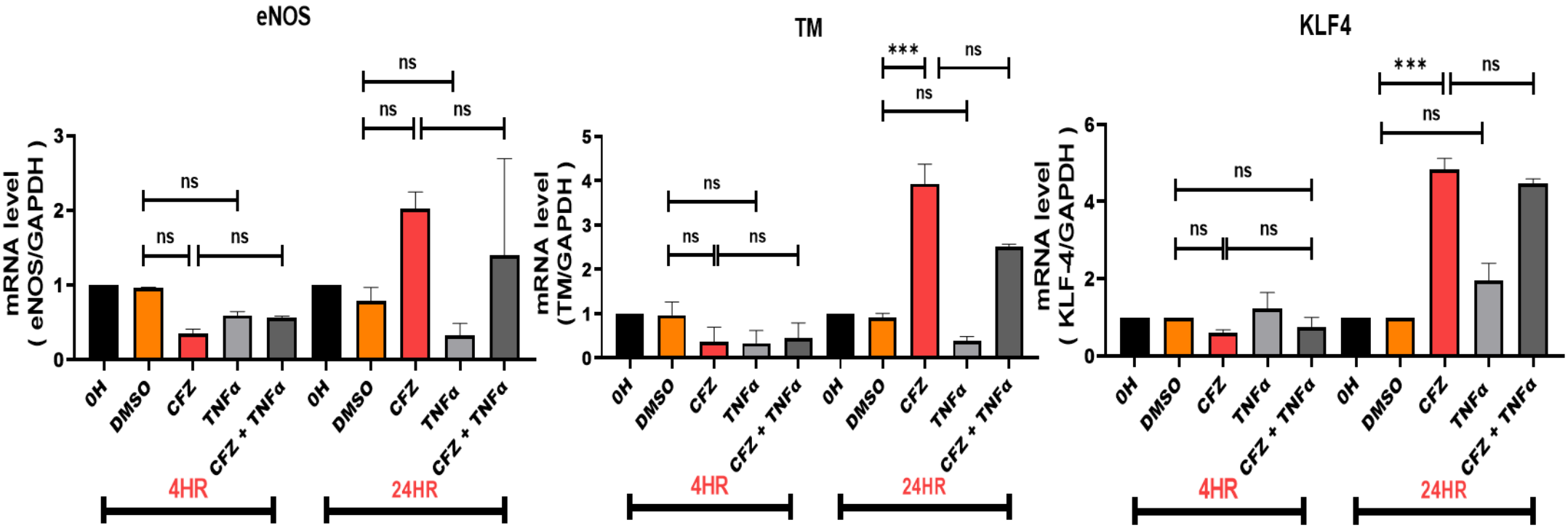


Figure 3.2.10: CFZ induced the genes of some of the anti-thrombotic markers in HUVECS. HUVECs were treated with 750nM of CFZ and DMSO for 1 hour, followed by washing the cells with PBS and replacing them in a fresh EBM-2 medium. Some cells were stimulated with 20 ng/ml of TNFα after 1hr 750nM CFZ treatment. qPCR analysis of eNOS, TM, and KLF-4. DMSO, Dimethyl sulfoxide; CFZ, Carfilzomib; TNFα, Tumour Necrosis Factor α; TM, thrombomodulin, KLF-4, Kruppel Like Factor 4. Three technical repeats were performed in one experiment, and the quantification of data was normalised to GAPDH levels and presented as the mean ± SEM. The data represents the average of three independent experiments. The expression trends of all these genes of all treated cells were compared using one-way ANOVA. Significance: *P < 0.05, **P < 0.01, ***P < 0.001.

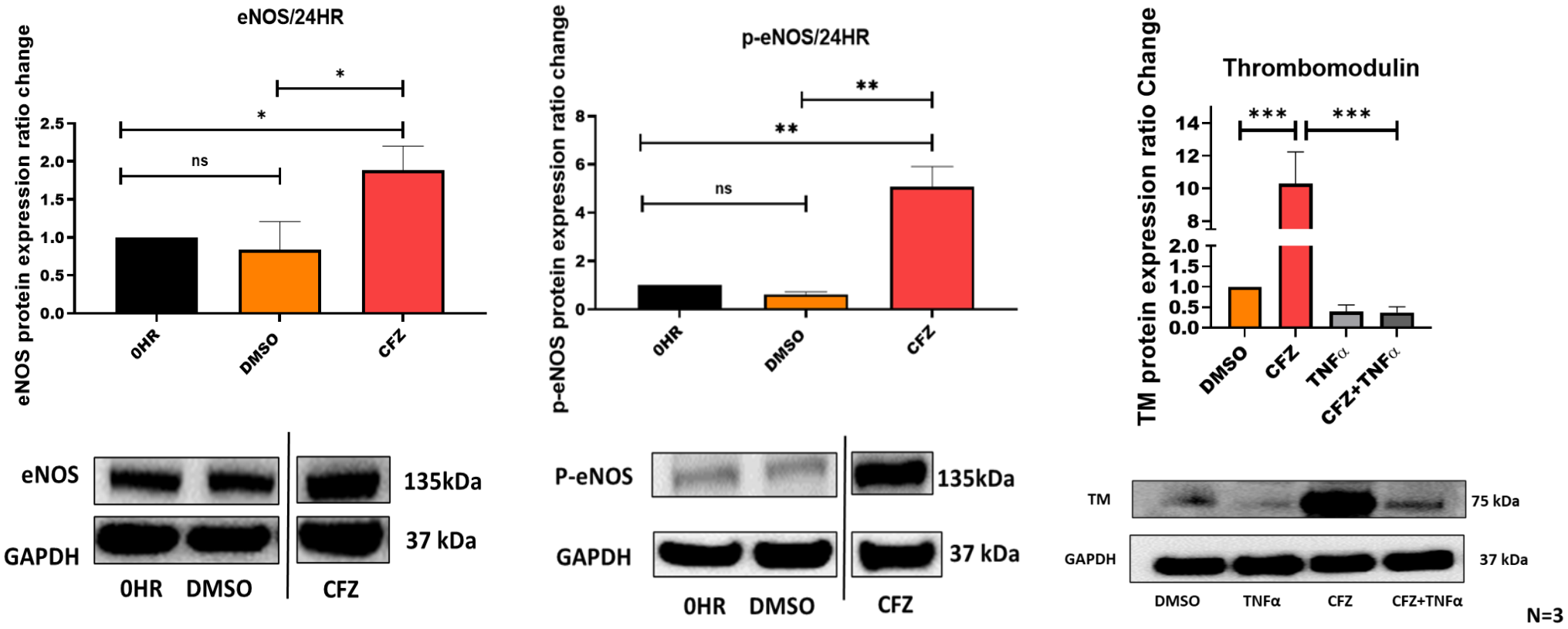


Figure 3.2.11: CFZ induced the proteins of some of the anti-thrombotic markers in HUVECs. HUVECs were treated with 750nM of CFZ and DMSO for 1 hour, followed by washing the cells with PBS and replacing them in a fresh EBM-2 medium. Some cells were stimulated with 20 ng/ml of TNFα after 1hr 750nM CFZ treatment. Western blot analysis of eNOS, p-eNOS, and TM. DMSO, Dimethyl sulfoxide; CFZ, Carfilzomib; TNFα, Tumour Necrosis Factor α; TM, thrombomodulin. Three technical repeats were performed in one experiment, and the quantification of data was normalised to GAPDH levels and presented as the mean ± SEM. The data represents the average of three independent experiments. The expression trends of all these proteins of all treated cells were compared using one-way ANOVA. Significant: *P < 0.05, **P < 0.01, ***P < 0.001.

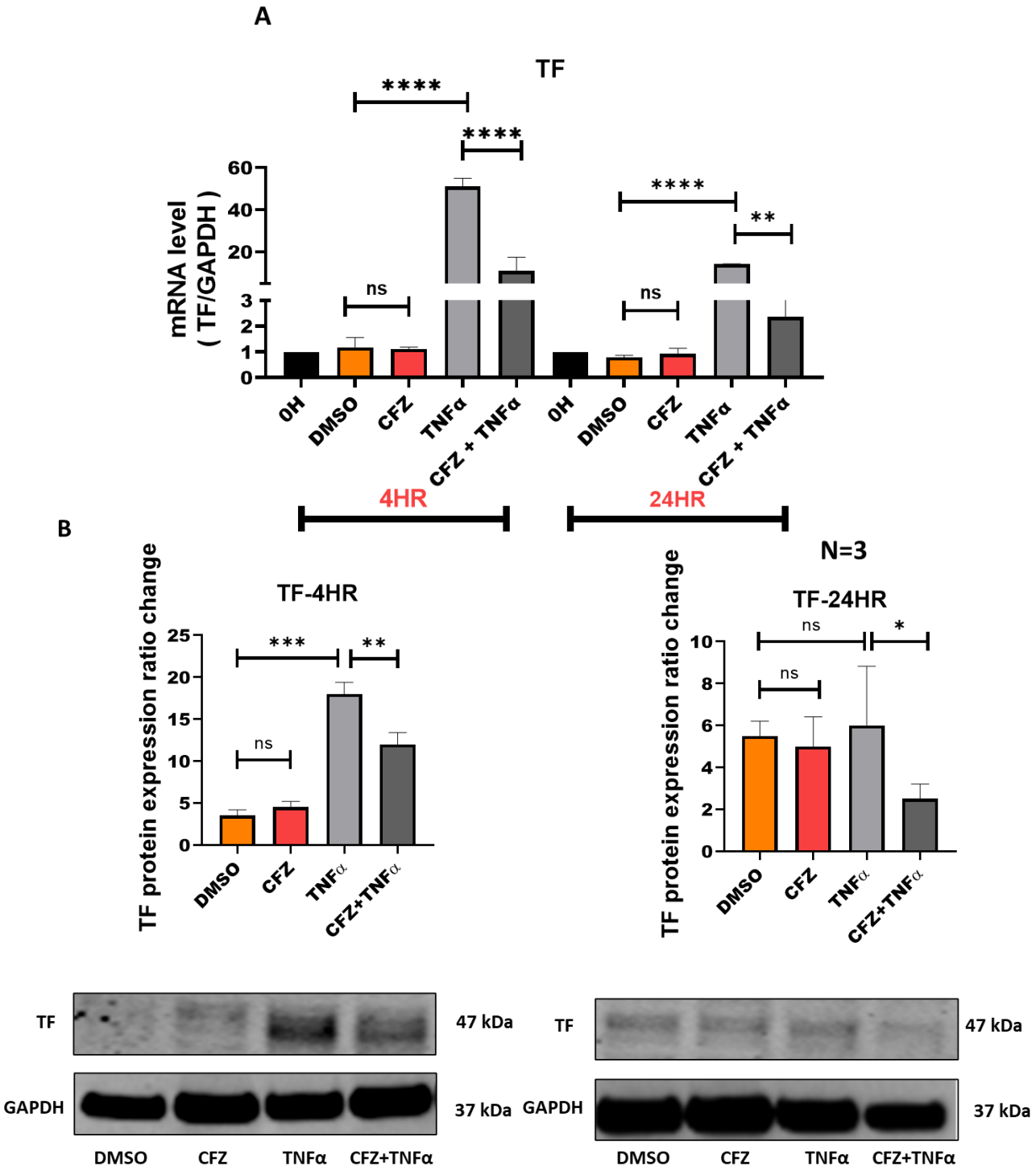


Figure 3.2.12: CFZ reduced TNFα mediated TF expression in HUVECS. HUVECs were treated with 750nM of CFZ and DMSO for 1 hour, followed by washing the cells with PBS and replacing them in a fresh EBM-2 medium. Some cells were stimulated with 20 ng/ml of TNFα after 1hr 750nM CFZ treatment. A) qPCR analysis of TF mRNA level. B) Western blot analysis of TF protein expression. Dimethyl sulfoxide; CFZ, Carfilzomib; TNFα, Tumour Necrosis Factor α; TF, tissue factor. Three technical repeats were performed in one experiment, and the quantification of data was normalised to GAPDH levels and presented as the mean ± SEM. The data represents the average of three independent experiments. The expression trends of TF of all treated cells were compared using one-way ANOVA. Significant: *P < 0.05, **P < 0.01, ***P < 0.001.

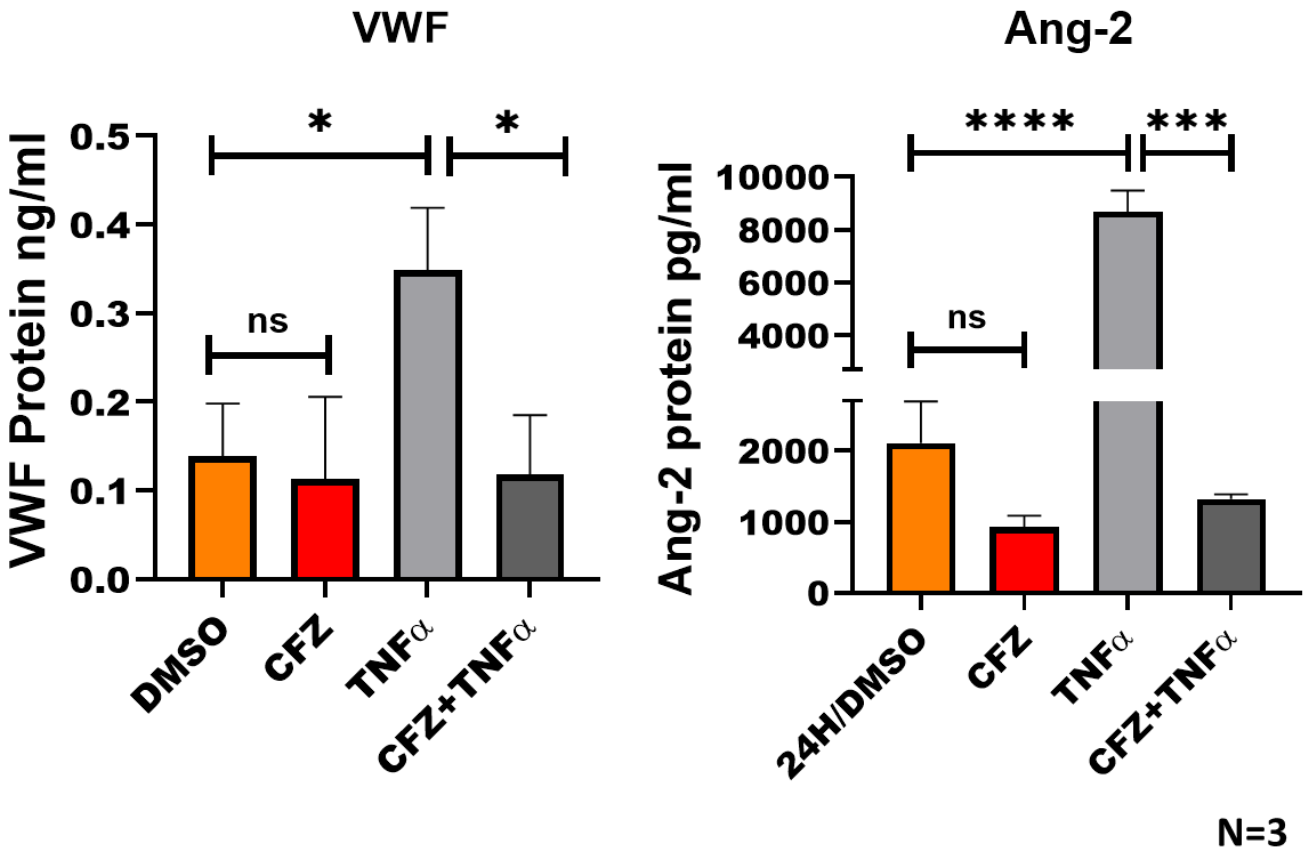


Figure 3.2.13: CFZ reduced TNFα mediated VWF and Ang-2 expression in HUVECS. HUVECs were treated with 750nM of CFZ and DMSO for 1 hour, followed by washing the cells with PBS and replacing them in a fresh EBM-2 medium. Some cells were stimulated with 20 ng/ml of TNFα after 1hr 750nM CFZ treatment. ELISA analysis of soluble VWF and Ang-2 in the culture medium. Dimethyl sulfoxide; CFZ, Carfilzomib; TNFα, Tumour Necrosis Factor α; Ang-2, Angiopiotien-2. Three technical repeats were performed in one experiment, and the quantification of data was normalised to GAPDH levels and presented as the mean ± SEM. The data represents the average of three independent experiments. The expression trends of VWF and Ang-2 of all treated cells were compared using one-way ANOVA. Significant: *P < 0.05, **P < 0.01, ***P < 0.001.

3.2.3 Discussion

The previous chapter demonstrated that CFZ did not induce ER stress in the endothelium, even with the maximum clinically relevant or accumulative dosage of CFZ. It is well-established that MM patients have an upregulation of some pro-inflammatory cytokines, including TNFα and Il-1β. (16) To mimic the clinical exposer of the endothelium in MM patients to these cytokines and CFZ treatment, cells were treated with 750nM of CFZ, and then stimulated with 20 ng/ml of either TNFα and/or Il-1β for 24 hours or 48 hours, as described (Methods 2.2.3). This could prime the endothelium to be activated, hence causing ER stress.

Interestingly, the data obtained showed no significant induction of ER stress, though TNFα enhanced the extent of the ubiquitination caused by CFZ in the endothelium at 24 hours. However, consistent with my earlier findings, the ubiquitination in these cells returned to the baseline after 48 hours, indicating ECs recovery. Furthermore, the expression of all ER stress markers investigated was almost comparable between CFZ treated cells alone or cells treated with CFZ combined with cytokines compared to the untreated and DMSO controls.

It is widely accepted that ER stress activation leads to the initiation of inflammation in the endothelium (374); however, this was not the case, as CFZ failed to induce ER stress in HUVECs. This led me to accept the null hypothesis about the potential induction of ER stress in the endothelium if cells were stimulated after CFZ treatment with cytokines. Thus, under my experimental settings, according to my data, the pro-inflammatory environment of MM patients does not provide a suitable explanation for the ER stress activation that CFZ could cause in the endothelium. This could be because cytokine stimulation of the endothelium does not directly affect the endothelium's proteasome function and does not induce ER stress. Alternatively, this could be because of the endothelium's mechanisms to avoid the induction of ER stress, as described earlier in the discussion of the first chapter (Discussion 3.1.3). Nevertheless, there was a consistent morphological change among all CFZ treated ECs, similarly to those observed in the first chapter. All CFZ treated cells showed consistent elongation and a similar spindle appearance of ECs. The new observations reported in this chapter indicated that the effect of TNFα on EC morphology displayed similar morphological manifestations that were observed in the CFZ treated cells,

indicating a potential activation of the endothelium in both groups. Therefore, F-actin staining of HUVECs cell membranes was conducted to evaluate the effects of CFZ on the HUVECs cytoskeletal architecture. My data showed that TNFα stimulated ECs showed a structural rearrangement of ECs, including remarkable reorganisation of the F-actin cytoskeleton along the central axis of the cells, cell elongation and stress fibre reorganisation. This was observed similarly, but to a lesser extent, in the CFZ treated ECs, and could be linked to the initiation of the inflammatory response by the endothelium in both groups of cells. (336) However, in the untreated control cells, mature stress fibres were created, organised in parallel groups alongside the basal surface of the cells. The organisation of cytoskeletal fibres is vital for functional EC signal transduction-associated proteins, permeability regulation, shear stress response, and gene expression. (375) In agreement with my findings, other groups have reported that TNFα can induce alterations in the morphology of confluence endothelial cells where they become more elongated and enlarged. It also alters EC cytoskeletal dynamics, biomechanics, cellular volume, and endothelium migration. (376) According to Dick *et al*. HUVECs stimulated with TNFα showed a remarkable rearrangement of F-actin filaments and ligands within the EC cytoskeleton. (377) Similarly, a study investigating the effect of BTZ in HUVECs demonstrated that it substantially expanded the cell membrane and permeability of HUVECs via vascular endothelial growth factor receptor (VEGFR)-independent mechanism. The standard cobblestone-like morphology of HUVECs was shifted to be elongated and with a spindle-like shape when HUVECs were treated with BTZ, similar to my observations with CFZ. (376) The authors reported that this alteration in cell morphology was due to the disruption of VE-cadherin adherent junctions and a rearrangement of actin filaments within the EC cytoskeleton, which was influential in expanding vasculature permeability. (376) In addition, Mariana *et al*. demonstrated the ability of BTZ to alter the cytoskeletal formation and the morphology of HUVECs, inducing F-actin re-distribution within the endothelial cells. (378) This was linked to the expression of urokinase plasminogen activator (u-PA) and its receptor (uPAR), a modulation of matrix metalloproteinases (MMPs) and the suppression of plasmin activity in the endothelium. All these effects suggest a functional link between EC morphology and endothelium function during an inflammatory response, which helps maintain the rigidity and stiffness of the cell.(379, 380) However, unfortunately, there are limited

studies exploring the CFZ effect on endothelium morphology to compare my findings. Therefore, since both CFZ and BTZ shared the exact mechanism of action and expressed a similar morphological alteration of the endothelium, I proposed that CFZ could induce HUVEC cytoskeleton reorganisation in a similar mechanism to BTZ. However, it should be noted that my F-actin staining of CFZ-treated HUVEC's was accomplished with fixed cells; hence the data corresponds to one snapshot in time. It would be noteworthy to perform an experiment using live cells under shear stress to realise the true complexity of the system, as recommended by Doggett and Breslin. (375)

The null hypothesis indicated that CFZ induced significant ER stress in the endothelial cells, which was not rejected according to my earlier data. Therefore**, it was hypothesised that CFZ might render the cells more pro-inflammatory or thrombotic, which was next investigated in this chapter.** Subsequent to the F-actin analysis, endothelial ICAM-1 expression analysis was conducted using flow cytometry, ELISA and Western blot. ICAM-1 is considered a significant endothelial cell activation marker that mediates the early inflammation process through its interaction with several leukocyte ligands allowing them to adhere to the site of inflammation.
TNF-α is a member of a group of cytokines that induce ICAM-1 expression in vascular ECs, thus enabling leukocyte adhesion and transmigration into the interstitial space. (381) Remarkably, while treatment of HUVECs with TNFα resulted in a significant increase in EC surface ICAM-1 expression, which agreed with the literature (382, 383), CFZ did not induce ICAM-1 expression. Moreover, CFZ showed a significant capacity to attenuate the pro-inflammatory effect of TNFα to induce ICAM-1, indicating a possible cytoprotective effect of CFZ on the endothelium. In agreement with my findings, BTZ has also been reported to reduce the expression of some inflammatory mediators, including ICAM-1, in a rat model of ischemia-reperfusion injury in a dose-dependent manner. (292) This suppression was achieved by inhibiting the NOX4-dependent IKKβ/NF-κB inflammatory pathway. (384) Chen *et al*. reported that pre-treatment with a high dose of BTZ considerably diminished the inflammatory response, including reducing ICAM-1 expression in endotoxin-induced uveitis (EIU). (385) Considering all these facts, CFZ could suppress ICAM-1 expression in a similar pattern to BTZ. In general, it was clear from the ICAM-1 results that CFZ did not induce

inflammation in the endothelium; interestingly, moreover, it showed a potential to conduct an anti-inflammatory effect.

To investigate the potential ability of CFZ to induce pro-thrombotic activation in the endothelium, some well-known pro-inflammatory markers were examined using several techniques. Surprisingly, CFZ appeared to exert a potential thrombo-protective effect on the endothelium. qPCR data corresponded with published articles, demonstrating that TNFα and Il-1β cytokines increase the gene expression of procoagulant factors.(16, 386, 387) Tissue factor (TF) is a major initiator of the coagulation cascade by binding to factor VIIa to convert factor X to factor Xa. TF is expressed mainly from the damaged endothelium to initiate the coagulation process. (388) There was significant upregulation of TF gene and protein expression in TNFα-stimulated cells at 4 and 24 hours compared to CFZ and CFZ+TNFα-treated cells, suggesting that CFZ stimulated cells to have a diminished coagulation potential. In contrast, TNFα decreased some well-known anticoagulants' gene and protein expression, primarily TM, consistent with several studies. (387, 389) On the other hand, CFZ enhanced the genes and protein expression of TM, eNOS, and KLF-4, which are key anti-thrombotic regulators. Although some controversy exists regarding the overall protective effect of increased eNOS expression(390), a significant number of studies (144, 391) indicate that eNOS plays a critical role in maintaining a healthy endothelium. Wang *et al*. reported that stimulation of the endothelium with TNFα caused upregulation of TF, while this influence was abrogated by overexpression of eNOS via gene transfection, indicating that increased expression of eNOS reduces TF, thus implying an anti-thrombotic effect. (392) It was also reported that BTZ increased nitric oxide production, eNOS and phosphorylated eNOS and that all were involved in the cytoprotective effect of BTZ on the endothelium. (393) Several other studies have reported that BTZ encourages eNOS expression and reduces secondary thrombotic complications and inflammatory responses. (394) An evaluation of eNOS expression from ECs isolated from brain tissue after treatment with BTZ on a rat model of embolic stroke showed a significant upregulation of this protein and blocked NF-κB activation. (394) Taken together, these data suggest that BTZ induces eNOS-dependent vascular protection and diminishes NF-κB dependent vascular disturbance to provide cytoprotective mechanisms. The BTZ-eNOS findings indicate that a CFZ cytoprotective effect could also occur in an eNOS dependent manner since I found

that CFZ mediated significant induction of protein expression and phosphorylation of eNOS.

Thrombomodulin is a crucial anticoagulant protein present on the endothelial cell surface that combines with thrombin to enhance the activation of protein C by thrombin. (290) It is widely accepted that Kruppel-like factors (KLF) 2 & 4 upregulate thrombomodulin expression in endothelial cells. (290) Interestingly, my data showed that CFZ upregulated the expression of KLF4, providing a possible mechanism behind the increased thrombomodulin expression. Also, heat shock factor 1 (HSF1) has been shown to upregulate thrombomodulin at a transcriptional level. (24) Interestingly, BTZ has been shown to enhance HSF1 expression, which may promote, among other effects, thrombomodulin expression. (25) Indeed, in multiple myeloma cells, expression of HSF1 confers resistance to BTZ and studies have suggested inhibiting HSF1 to sensitise cells to BTZ. (25) Future work is required to see if this is similar for CFZ. Additionally, proteasome inhibition is thought to inhibit activation of NF-kB (26), suggesting a role for the NF-kB pathway, and proteasome inhibition by the general proteasome inhibitor MG132 has resulted in the upregulation of eNOS in aortic endothelial cells. (27) It was reported that diminished production of both TM and eNOS was associated with systemic microvasculitis. (389) While CFZ is significantly more potent and demonstrates irreversible binding to the proteasome, my data are in keeping with this notion, but future work will need to determine how proteasome inhibition leads to upregulated eNOS expression.

The anti-thrombotic trend of CFZ treated cells data were consistent with the outcome of my extracellular VWF-expression ELISA study. VWF is an adhesive glycoprotein of a multidomain structure that binds to platelet glycoprotein, ultimately stimulating platelets and introducing platelet aggregation. (395) My data showed that TNFα increased the concentration of VWF, which was consistent with the well-established TNFα pro-thrombotic effect (396), while CFZ reduced its release from HUVECs. Interestingly, the drug showed a remarkable resistance to the pro-thrombotic activity of TNFα, where there was a significant reduction of the EC's VWF release in the CFZ+TNFα cells compared to TNFα stimulated alone. Several studies have reported a regulatory correlation between nitric oxide and VWF release from the endothelium. According to Nakayama *et al*. a lack of eNOS resulted in the release of endothelium VWF, suggesting that NO could at least partially regulate the VWF release from the endothelium. (397) In addition, the exocytosis of Weibel-Palade bodies (WPBs) that

contains VWF and P-selectin from the endothelium is additionally well-known to be stimulated in the absence of nitric oxide. (398) By linking these facts to my findings that CFZ significantly induced the upregulation of eNOS and p-eNOS protein expression from HUVECs, I proposed that an eNOS dependent mechanism could suppress the VWF release from CFZ treated cells. However, the mechanism behind this effect is not yet completely understood, which could be further investigated in future research.

Angiopoietin-2 (Ang2) is a ligand of the Tie2 receptor, which is implicated in controlling inflammation and vascular integrity. (399) In agreement with my observation of the anti-inflammatory effect of CFZ, there was no induction of Ang-2 release from the CFZ treated ECs. More importantly, CFZ showed a significant reduction of the well-known pro-inflammatory TNFα effect that triggered the endothelium to release Ang-2 (400), thus indicating the anti-inflammatory effect of CFZ. It has been revealed that an over-expression of Ang-2 was found in stressed endothelium and the process of atherosclerosis. (401) Diminished levels of eNOS were shown to be correlated with the amplified level of Ang-2. (402) It is well established that Ang-2 reduces the phosphorylation of eNOS via the AT1R Nox/ROS/PP2A pathway (403) and Tie2-Akt-eNOS pathway regulating Ang-2 activity. (404) BTZ was shown to hold an anti-angiogenic agent to a remarkable extent. According to Anargyrou *et al*. there was a significant reduction of the Ang-2 patient's serum level after treating them with BTZ. (405) *In vivo* preclinical experiments on rats have also demonstrated that BTZ has an anti-angiogenic effect by reducing the expression of Ang-2. (406) However, the mechanism behind it is still not fully understood, but the involvement of the NF-kB pathway was proposed to be involved in this effect. (406) Therefore, taken together, I proposed that CFZ could recruit NO-dependent mechanism treated ECs to suppress the release of Ang-2 from the ECs.

In conclusion, two primary outcomes were observed in this chapter: 1) stimulation of HUVECs with cytokines was not adequate to promote CFZ to induce ER stress in HUVECs. 2) Observations indicated the anti-thrombotic and cytoprotective effect of CFZ on the endothelium in a similar manner to that reported for BTZ.

3.3 CFZ enhances anti-thrombotic activity in HUVECs

3.3.1 Introduction

The process that leads to bleeding cessation from the damaged blood vessel is known as haemostasis. (160) It is a multiple interlinked events procedure that aims to form a "plug" covering the injured vessel, thus controlling the bleeding. (160) Four main stages are involved in this mechanism: contraction of the blood vessels, generation of a non-permanent "platelet plug" ,stimulation of the coagulation cascade, and lastly, construction of the final clot "fibrin plug". (407) This clot covers the damaged area, regulates and inhibits advanced bleeding while tissue restoration course occurs. (408) When the injury begins to resolve, the plug gradually remodels, dissolving with the reestablishment of normal tissue at the location of the damage. (408)

The cytoprotective effect of the first-generation proteasome inhibitor BTZ has been widely studied in the last decade. Even though there are some reported findings of the cardiac toxicity of the drug, many studies have indicated the anti-thrombotic and cytoprotective effects of the drug in the endothelium. (290) Nayak *et al*. have reported that BTZ showed a significant anti-thrombotic effect in the mouse vascular compartment, which was dependent on the expression of KLF-2. (290) Another *in vivo* study revealed that systemic administration of BTZ enhanced endothelium thrombomodulin expression, which was dependent on the KLF-2 and KLF-4 pathways. (306) These reports of the cytoprotective effect of BTZ are similar to the cytoprotective effect of CFZ on the endothelium observed in my previous second result chapter. I found that CFZ increased the expression of some of the well-known anti-thrombotic markers (eNOS, KLF4 and thrombomodulin), indicating a thrombo-protective effect on the endothelium. Moreover, I found that it attenuates the pro-inflammatory effect of TNFα on the endothelium by reducing the TNFα-driven expression of some of the pro-inflammatory and pro-thrombotic markers (VWF, ICAM-1 and TF).

Therefore, **in this result chapter, I hypothesised and investigated at a functional level** the hypothesis that CFZ could enhance the anti-thrombotic and anti-inflammatory activity of the endothelium.

3.3.2 Results

3.3.2.1 CFZ reduces TNF-mediated fibrin clot formation in HUVECs

In the previous chapter, I found that CFZ apparently exerted a protective effect on HUVECs. In this chapter, several functional studies were conducted to investigate further the potential CFZ cytoprotective effect on the endothelium at the functional level. Initially, turbidity assays were conducted to assess the effect of CFZ on fibrin clot formation on the endothelium. The turbidity assay is a commonly used method to measure fibrin clot formation *in vitro.* In this assay, as fibrinogen is converted to fibrin, a “turbidity” curve is generated by plotting absorbance at 405nm against time. From the curve, three main parameters can be obtained; 1) Lag-time – which represents the time for the fibrin protofibrils to grow to allow lateral aggregation. 2) The slope – which represents the rate of aggregation. 3) Time to maximal absorbance – this is often dependent on fibrinogen concentration and various features of the clot structure. In this study, HUVECS were treated with CFZ, stimulated with TNFα for 4 or 24 hours, and then incubated with re-calcified plasma and absorbance measured at 405nm as detailed in Methods 2.9.1.

As expected, after 4 hours of incubation with TNFα, the shape of the turbidity curve was altered compared to the DMSO and CFZ treated cells (Figure 3.3.1A), and TNFα simulated cells demonstrated a significantly shorter lag-time compared to DMSO and CFZ treated cells; 1.3 mins compared to ~5.5mins (Figure 3.3.1B). This is consistent with TNFα inducing tissue factor expression in HUVECS that can drive fibrin formation and demonstrates that CFZ alone does not affect either tissue factor expression of clot formation. Interestingly, however, cells pre-treated with CFZ before TNFα demonstrated a significantly increased lag-time compared to TNFα treated cells, indicating a reduced rate of fibrin formation and suggesting that CZF could attenuate the effects of TNFα (Figure 3.3.1B).

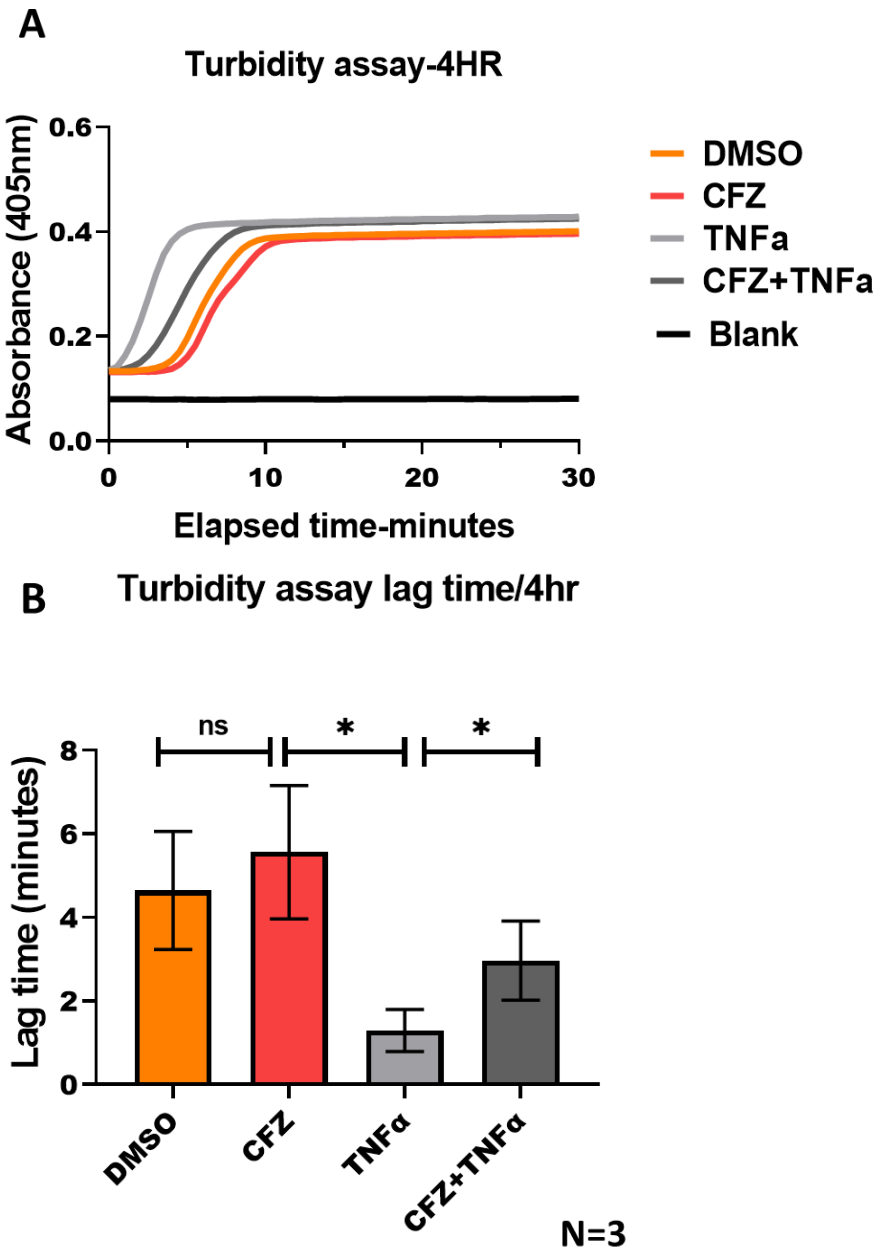


Figure 3.3.1: CFZ attenuated TNFα-induced fibrin formation in HUVECs at 4h. HUVECs were treated with 750nM of CFZ and DMSO for 1 hour, followed by washing the cells with PBS and replacing them in a fresh EBM-2 medium. Some cells were stimulated with 20 ng/ml of TNFα after CFZ treatment for 4 hr. Cells were incubated with the reaction mixture containing plasma 5mM CaCl2 and 50mM HEPES/NaCl buffer; the 48-well plate was read at 405nm for 30-minutes/30-second measurement interval**.** (A) The absorbance curve of a single representative experiment. (B) the lag time bar chart for DMSO, CFZ, TNFα, and CFZ+TNFα treated cells combined data from three separate experiments. DMSO; Dimethyl sulfoxide, CFZ; Carfilzomib, TNFα, Tumor Necrosis Factor α. Three technical repeats were performed in one experiment, and the data were presented as the mean ± SEM. The data represented the average of three independent experiments. The expression trends of all treated cells were compared using one-way ANOVA. Significance: *P < 0.05, **P < 0.01, ***P < 0.001

In common with my previous findings, the 24hr study group showed a similar trend of turbidity curve of TNFα stimulated cells, compared to the DMSO and CFZ treated cells (Figure 3.3.2A). In agreement, TNFα simulated cells established a significantly shorter lag-time compared to DMSO and CFZ treated cells; 1.5 mins compared to ~9.7 mins (Figure 3.3.2B) and shorter time to maximal absorbance; 3 mins compared to 10.2 mins (Figure 3.3.3C). This indicates that CFZ alone has no effect on clot formation in HUVECs, while TNFα render the cells more pro-thrombotic and drives fibrin formation, which is consistent with the induced tissue factor expression. Even though this time cells that were pre-treated with CFZ before TNFα showed a similar turbidity curve compared to TNFα treated cells (Figure 3.3.2A), there was a slight non-significant increase in the lag-time ~2.3 mins compared to 1.5 mins, and in time to maximal absorbance, 3.8 mins compared to 3 mins indicating a slighter reduced rate of fibrin formation and suggesting that CZF could attenuate the effects of TNFα, but with a greater extent at 4hr time point (Figure 3.3.2B).

Overall, these findings are consistent with the earlier tissue factor mRNA findings (Result 3.2.2.5), where there was a greater expression of tissue factor at 4hr in TNFα and CFZ+ TNFα stimulated cells compared to 24 hr stimulation, which indicates that an earlier pro-thrombotic response of HUVECs to TNFα stimulation and earlier attenuating effect of TNFα mediated by CFZ in HUVECs.

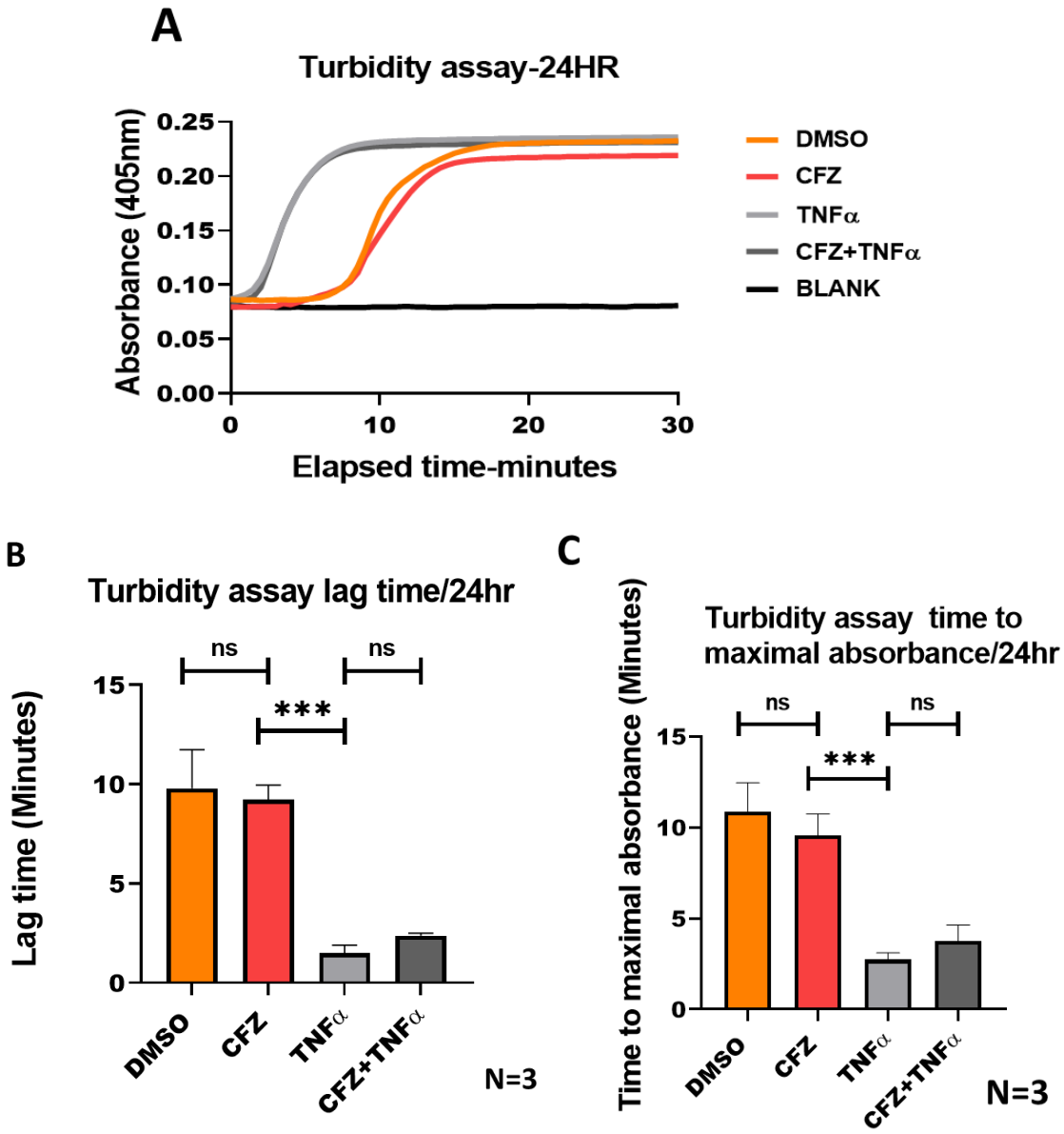


Figure 3.3.2: CFZ did not induce fibrin formation in HUVECs at 24h. HUVECs were treated with 750nM of CFZ and DMSO for 1 hour, followed by washing the cells with PBS and replacing them in a fresh EBM-2 medium. Some cells were stimulated with 20 ng/ml of TNFα after CFZ treatment for 24 hr. Cells were incubated with the reaction mixture containing plasma (5mM) CaCl2 and 50mM HEPES/NaCl buffer, same here. The 48-well plate was read at 405nm for 30-minutes/30-second measurement interval**.** (A) The absorbance curve of a single representative experiment. (B) The lag time bar chart for DMSO, CFZ, TNFα, and CFZ+TNFα treated cells combined data from three separate experiments. (C) The time to maximal absorbance of the same group of cells. DMSO; Dimethyl sulfoxide, CFZ; Carfilzomib, TNFα, Tumor Necrosis Factor α. Three technical repeats were performed in one experiment, and the data were presented as the mean ± SEM. The data represented the average of three independent experiments. The expression trends of all treated cells were compared using one-way ANOVA. Significance: *P < 0.05, **P < 0.01, ***P < 0.001.

3.3.2.2 CFZ reduces TNFα-induced Factor Xa formation on HUVECs

To confirm the observations that CFZ could attenuate TNFα induced fibrin clot formation in the turbidity assay, a Factor Xa generation assay using a purified system was conducted. In this system, cells are incubated with purified FVIIa and Factor X with the tissue factor supplied by the HUVECs. Therefore, if the cells express more TF on their surface, this will allow for more FVIIa binding, which will enhance the amount of FXa generation. The generation of Xa can then be monitored by the cleavage of a fluorogenic factor Xa specific peptide substrate.
The cells were treated with 750nM of CFZ for 1hr, some cells were stimulated for 4hr or 24hr with TNFα, and the experiment was conducted as described in (Methods 2.9.3). Like the turbidity assay principle, there is a positive correlation between the absorbance and the end-product amount of FXa.

Both DMSO and CFZ treated cells did not support the generation of FXa; consistent with DMSO and CFZ not inducing TF expression in HUVECS (Figure 3.3.3 A, B, C, D). Interestingly, at both 4h and 24h, cells treated with CFZ and TNFα generated significantly less FXa when compared to cells treated with TNF alone (Figure 3.3.3 A, B, C, D). This is in keeping with CFZ reducing the extent of TNFα induced tissue factor expression, with this being more effective at the 4h time point than at the 24h time-point.

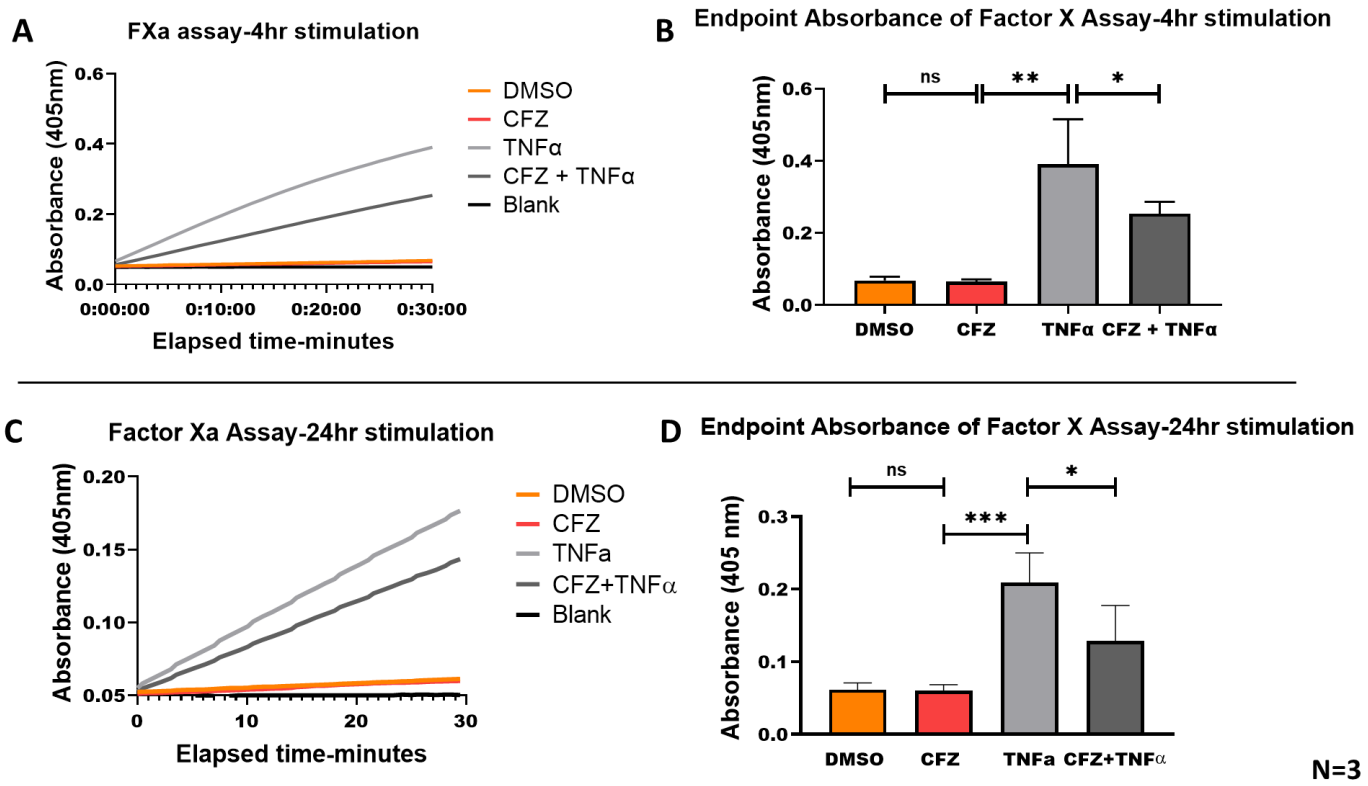


Figure 3.3.3: CFZ reduces TNFα-induced Factor X formation in HUVECs. HUVECs were treated with 750nM of CFZ and DMSO for 1 hour, followed by washing the cells with PBS and replacing them in a fresh EBM-2 medium. Some cells were stimulated with 20 ng/ml of TNFα after CFZ treatment for 4hr and 24 hr. Cells were incubated with the reaction mixture containing plasma VIIa (FVIIa) (2.5nM), factor X (175nM) and 50mM HEPES/NaCl buffer. The 48-well plate was read at 405nm for 30 minutes/30-second measurement intervals. (A) The absorbance curve of a single representative experiment at 4hr. (B) The endo point absorbance bar chart for DMSO, CFZ, TNFα, and CFZ+TNFα treated cells at 4hr combined data from 3 separate experiments. (C) The absorbance curve of a single representative experiment at 24hr. (D) The endo point absorbance bar chart for DMSO, CFZ, TNFα, and CFZ+TNFα treated cells at 24hr combined data from three separate experiments. DMSO; Dimethyl sulfoxide, CFZ; Carfilzomib, TNFα, Tumor Necrotic Factor. Three technical repeats were performed in one experiment, and the data were presented as the mean ± SEM. The data represented the average of three independent experiments. The expression trends of all treated cells were compared using one-way ANOVA. Significance: *P < 0.05, **P < 0.01, ***P < 0.001

3.3.2.3 CFZ enhanced the APC generation in HUVECs

To further investigate the protective effect of CFZ on the endothelium, the ability of HUVECs to generate activated protein C was investigated. The activated form of protein C is a significant anticoagulant sourced from the zymogen protein C that is activated once it interacts with the thrombomodulin-thrombin complex. The data in the previous chapter indicated that CFZ could induce thrombomodulin expression and thus could lead to enhanced APC production. To investigate this, an APC generation assay was performed, cells were incubated with protein C and thrombin; thus, the more the cells are expressed thrombomodulin on the surface, the more thrombomodulin-thrombin complex forms, thus more generation of APC. The generation of APC can then be monitored by the cleavage of a fluorogenic factor APC specific peptide substrate (Methods 2.9.4). Similar to the principle of turbidity assay, there is a direct positive correlation between the absorbance and the amount of APC generated during the assay. This is an indirect measurement of the amount of thrombomodulin expressed by the endothelial cells.

As expected, CFZ treated cells showed the highest absorbance curve (Figure 3.3.4 A), indicating that this group of cells generated the maximum amount of APC. This was further illustrated by the expression of the highest endpoint absorbance and the area under the curve values 0.24 and 8.6, respectively (Figure 3.3.4 B, C). This is consistent with CFZ inducing thrombomodulin expression in HUVECs. In keeping with the TNFα attenuating effect of CFZ, cells that were pre-treated with CFZ before TNFα demonstrated a slight increase of the absorbance curve (Figure 3.3.4 A) and a significant increase in the area under the curve compared to TNFα stimulated cells; 6 compared to 4.2 (Figure 3.3.4C). This indicates that CFZ counter the thrombomodulin suppression effect mediated by TNFα in the endothelium.

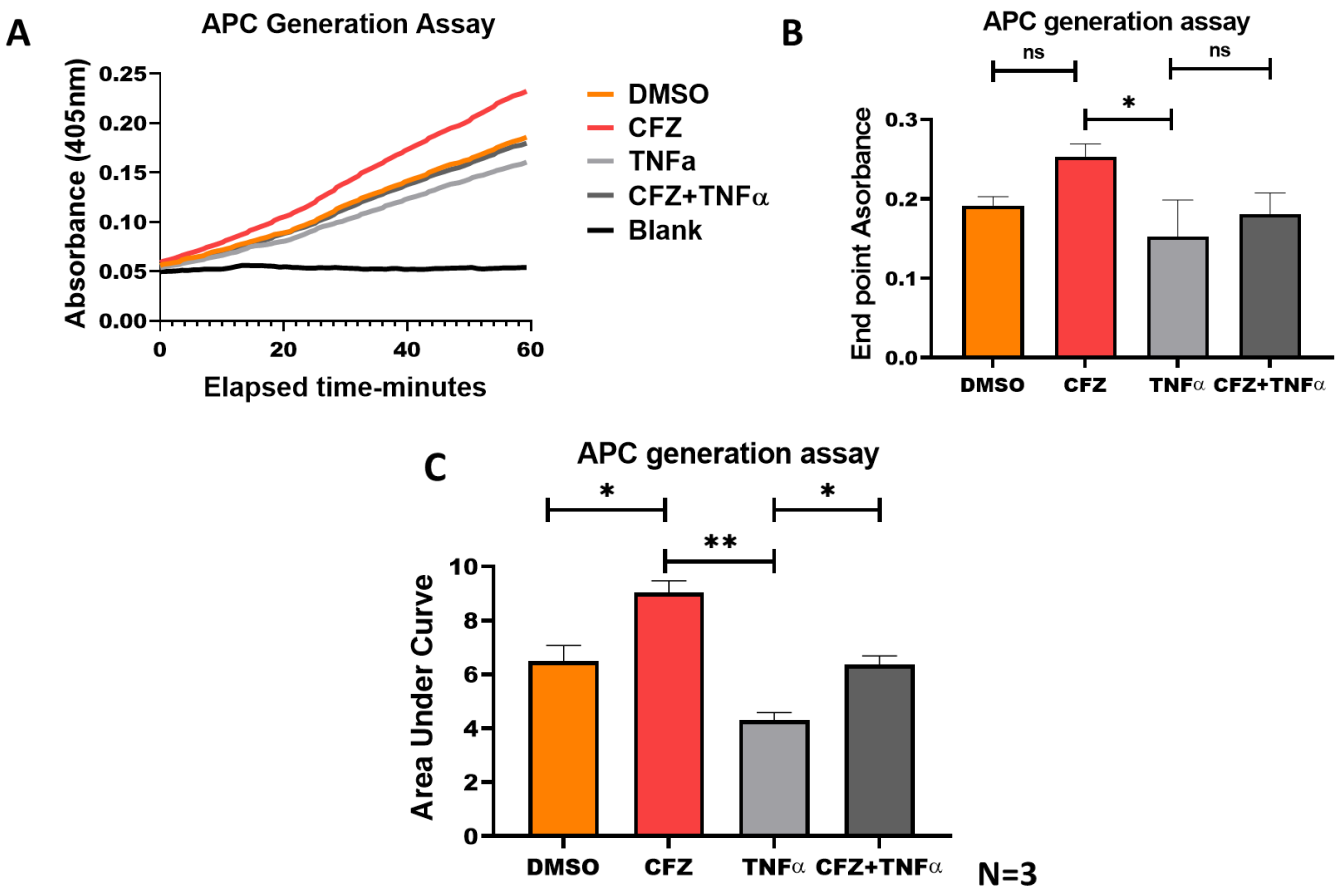


Figure 3.3.4: CFZ induces APC generation in HUVECs. HUVECs were treated with 750nM of CFZ and DMSO for 1 hour, followed by washing the cells with PBS and replacing them in a fresh EBM-2 medium. Some cells were stimulated with 20 ng/ml of TNFα after CFZ treatment for 24 hr. Cells were incubated with the reaction mixture containing plasma, thrombin, and 50mM HEPES/NaCl buffer. The plate was read at 405nm for 60-minutes/47-second measurement intervals**.** (A) The absorbance curve of a single representative experiment at 24hr. (B, C), the endpoint absorbance, and the area under the curve for DMSO, CFZ, TNFα, and CFZ+TNFα treated cells of combined data from three separate experiments, respectively. DMSO; Dimethyl sulfoxide, CFZ; Carfilzomib, TNFα, Tumour Necrosis Factor α. Three technical repeats were performed in one experiment, and the data were presented as the mean ± SEM. The data represented the average of three independent experiments. The expression trends of all treated cells were compared using one-way ANOVA. Significance: *P < 0.05, **P < 0.01, ***P < 0.001

3.3.2.4 CFZ reduced TNFα-mediation of VWF release from HUVECs

As well as cytoprotective effecting TF and TM expression, it was demonstrated in the previous chapter that CFZ also influenced the release of VWF from HUVECs. To further investigate this, HUVECS treated with CFZ and/or TNFα were fixed and stained with anti-VWF-FITC antibodies after 4 or 24h treatment with TNFα to directly visualise VWF released from the endothelium (Methods 2.6.1). In agreement with my VWF-ELISA findings (3.2.2.5), CFZ treated cells showed a similar VWF release pattern as the DMSO control cells at both 4hr and 24 hr recovery, with the immunofluorescent staining mainly located to the cell: detecting stored VWF in WPBs and the ER (Figure 3.3.6, 7). In contrast, cells treated with TNFα had a visibly different staining pattern, with patchier extracellular VWF staining; this was most pronounced at 24h with clear areas of extracellular VWF and the presence of VWF strings that had formed over the cells (Figure 3.3.8, 9). Consistent with its anti-thrombotic effect, TNFα treated cells that had been prior incubated with CFZ demonstrated visibly less extracellular VWF staining and no formation of VWF strings (Figure 3.3.8, 9).

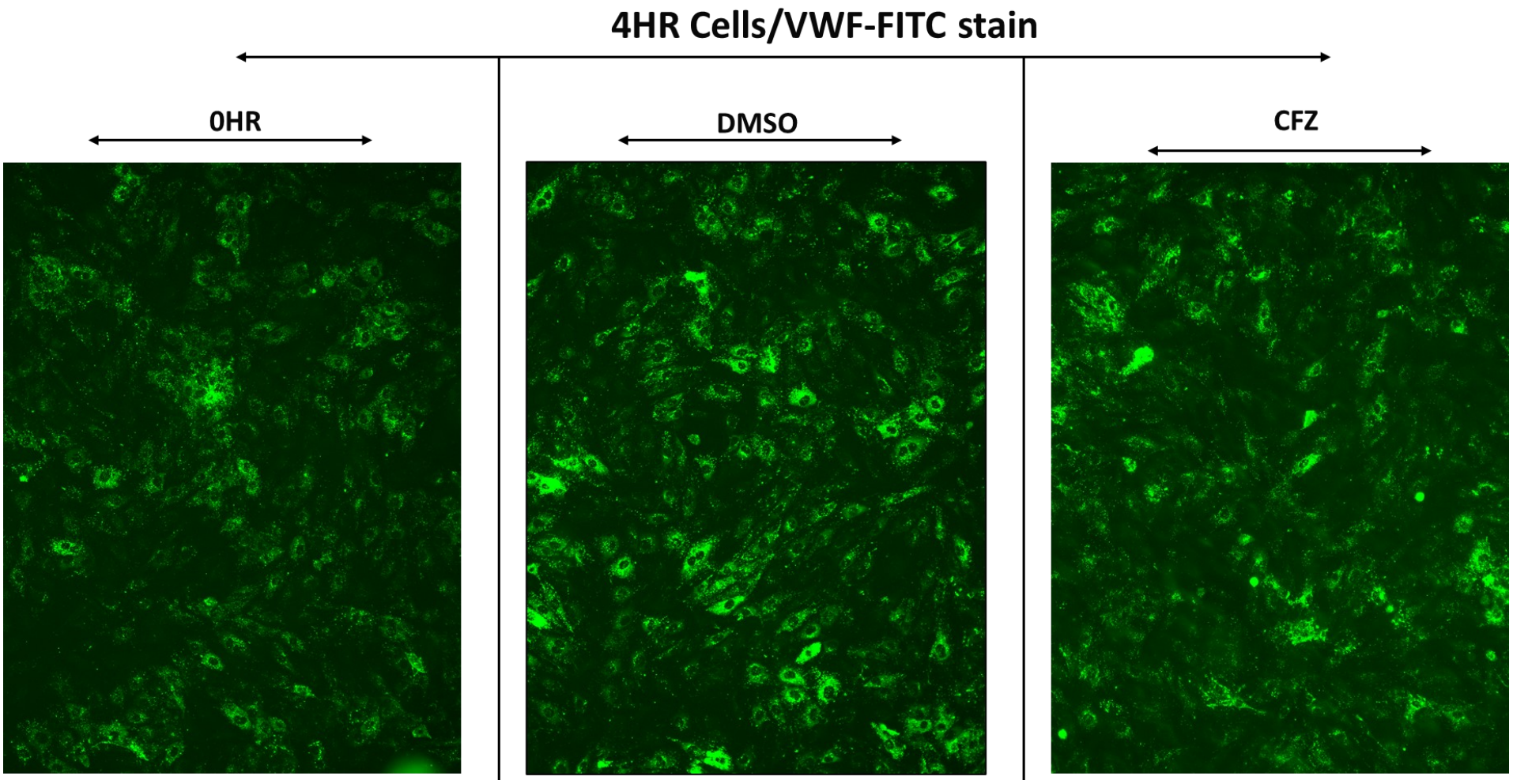


Figure 3.3.6: CFZ did not induce VWF release from HUVECs at 4hr recovery. HUVECs were treated with 750nM of CFZ and DMSO for 1hr, followed by 24 hr recovery. The cells were permeabilized with 1x triton and stained with anti-VWF-FITC antibodies. The fluorescence intensity for the stained cells was visualised using a fluorescence microscope (10X objective). DMSO, Dimethyl sulfoxide; CFZ, carfilzomib.

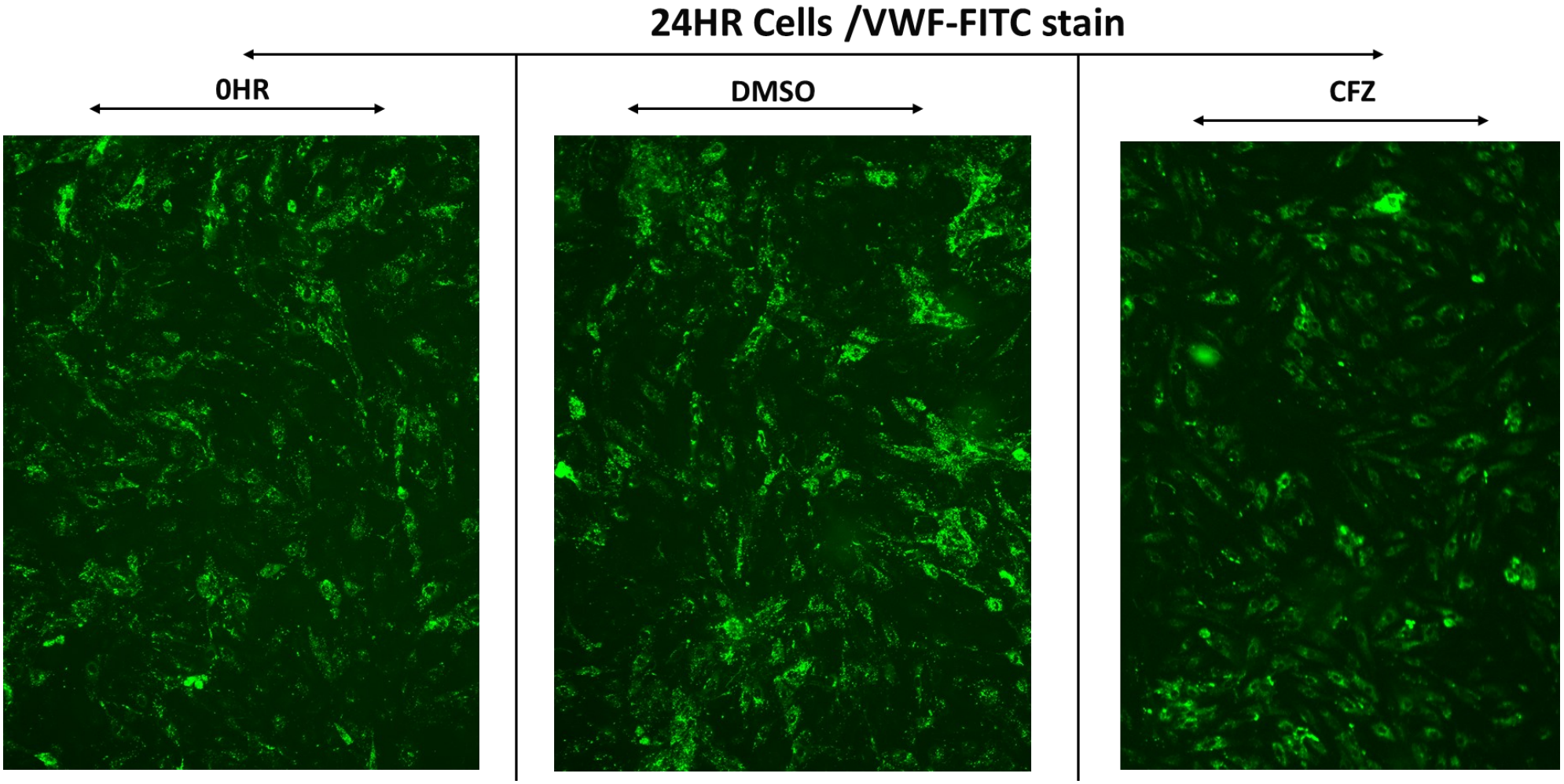


Figure 3.3.7: CFZ did not induce VWF release from HUVECs at 24hr recovery. HUVECs were treated with 750nM of CFZ and DMSO for 1hr, followed by 24 hr recovery. The cells were permeabilized with 1x triton and stained with VWF-FITC stain. The fluorescence intensity for the stained cells was visualised using a fluorescence microscope (10X objective). DMSO, Dimethyl sulfoxide; CFZ, carfilzomib.

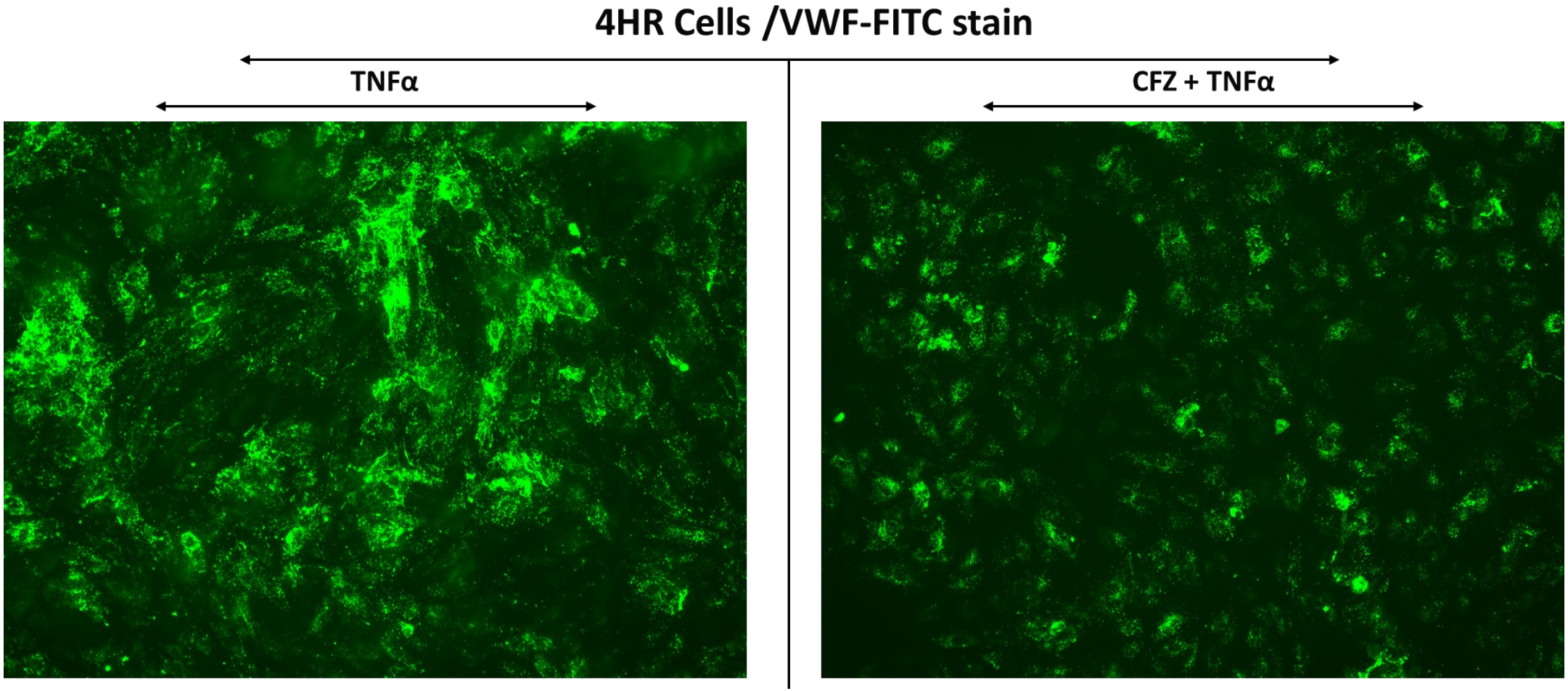


Figure 3.3.8: CFZ reduced TNFα-mediated VWF release from HUVECs at 4hr stimulation. HUVECs were treated with 750nM of CFZ and DMSO for 1 hour, followed by washing the cells with PBS and replacing them in a fresh EBM-2 medium. Some cells were stimulated with 20 ng/ml of TNFα alone or after CFZ treatment for 4 hr. The cells were permeabilized with 1x triton and stained with VWF-FITC stain. The fluorescence intensity for the stained cells was visualised using a fluorescence microscope (10X objective). DMSO, Dimethyl sulfoxide; CFZ, carfilzomib.

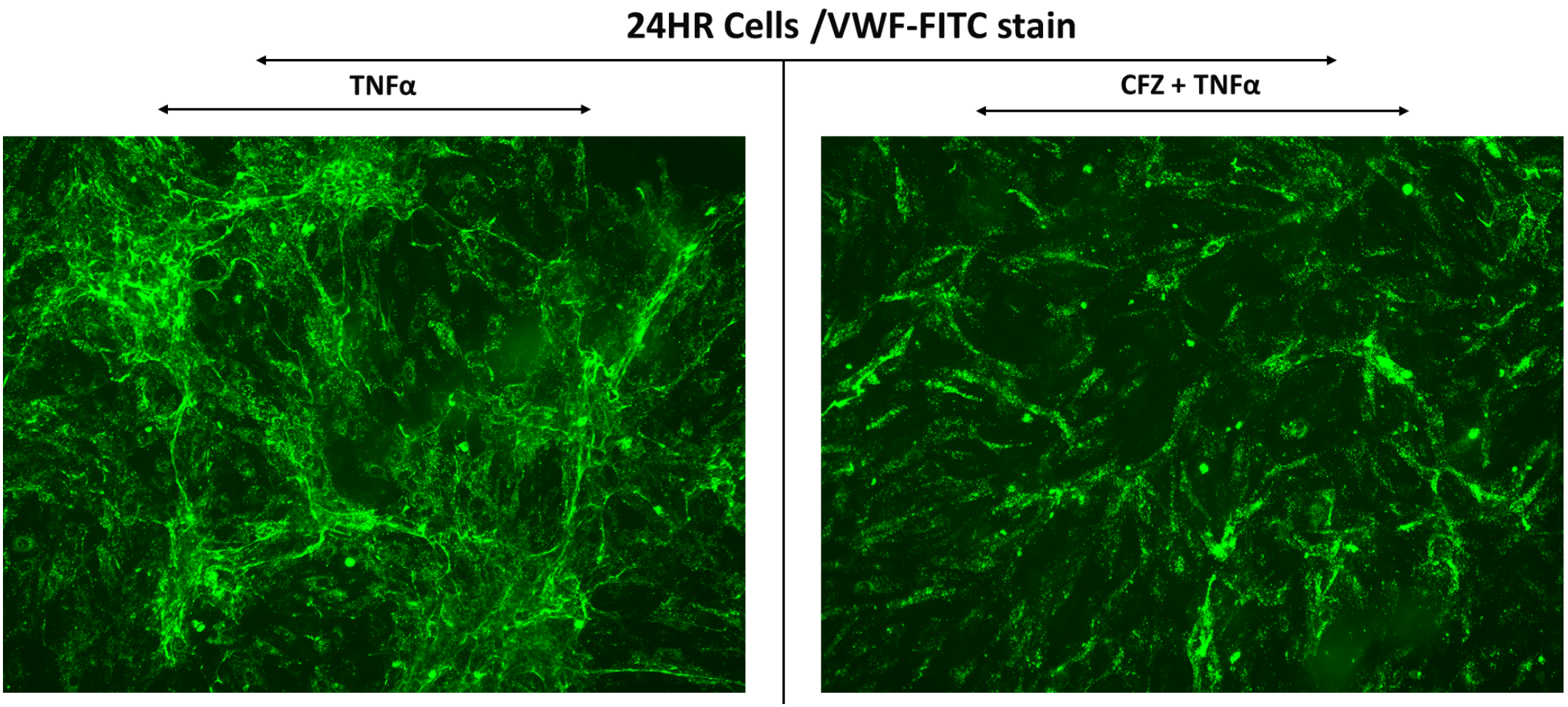


Figure 3.3.9: CFZ reduced TNFα-mediated VWF release from HUVECs at 24hr stimulation. HUVECs were treated with 750nM of CFZ and DMSO for 1 hour, followed by washing the cells with PBS and replacing them in a fresh EBM-2 medium. Some cells were stimulated with 20 ng/ml of TNFα alone or after CFZ treatment for 24 hr. The cells were permeabilized with 1x triton and stained with VWF-FITC stain. The fluorescence intensity for the stained cells was visualised using a fluorescence microscope (10X objective). DMSO, Dimethyl sulfoxide; CFZ, carfilzomib.

3.3.2.5 CFZ reduced TNFα-induced string formation on HUVECs

In addition, a platelet capture flow assay was performed to examine the VWF immuno staining findings in a more physiologically relevant environment. As a result of endothelial damage or activation, the VWF content of the endothelial cells is released, allowing the interaction with the platelet, thus initiating primary haemostasis. This assay measures the formation of platelet-binding VWF-strings on endothelial cells. The cells were treated with 750nM of CFZ for 1hr, and some cells were stimulated for 4hr or 24hr stimulation only with TNFα. The experiment was conducted as described in (Methods 2.9.5). In keeping with my observations, when platelets were perfused over HUVECS pre-treated with TNFα, platelet strings were recorded in the flow direction due to VWF release and subsequent VWF mediated platelet capture (Figure 3.3.10A, B).

There was almost an absence of strings formed in both DMSO and CFZ treated cells, indicating an absence of the pro-thrombotic activation of the endothelium by either of these treatments alone (Figure 3.3.10A, B). Interestingly, cells treated with both CFZ and TNFα formed significantly fewer VWF/platelet strings than those treated with TNFα only. (25 and 12 strings, respectively) (Figure 3.3.10A, B). These observations agreed with the anti-thrombotic effect of CFZ observations found earlier.

All these outcomes suggest that CFZ is not only not damaging the endothelium; moreover, it supports and maintains the endothelium's physiological haemostasis.

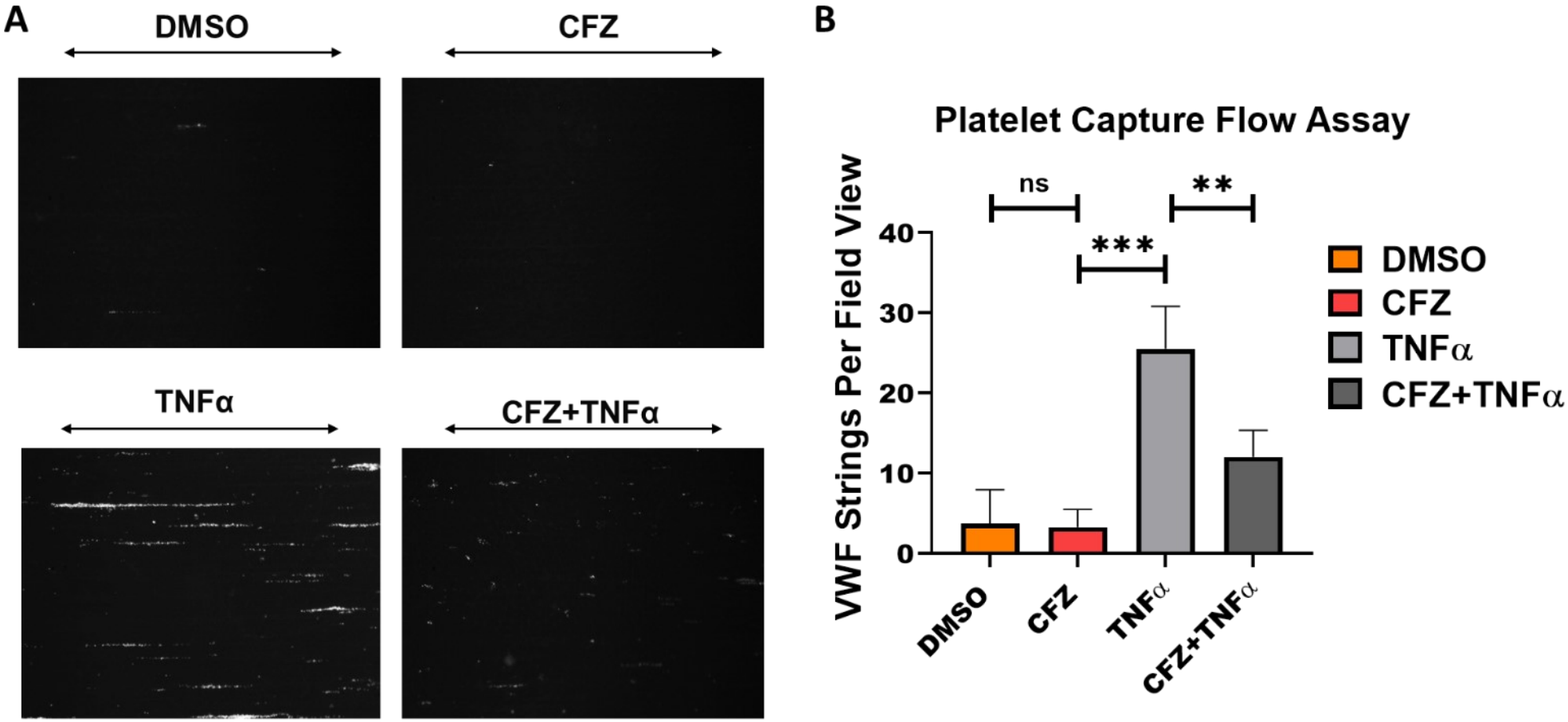


Figure 3.3.10: CFZ reduced the platelet capture mediated by TNFα in HUVECs. HUVECs were treated with 750nM of CFZ and DMSO for 1 hour, followed by washing the cells with PBS and replacing them in a fresh EBM-2 medium. Some cells were stimulated with 20 ng/ml of TNFα alone or after CFZ treatment for 24 hr. A) VWF string visualisation using the fluorescent microscope (10X objective). B) the quantification of VWF strings per field view. DMSO; Dimethyl sulfoxide, CFZ; Carfilzomib, TNFα, Tumor Necrosis Factor α. Three technical repeats were performed in one experiment, and the data were presented as the mean ± SEM. The data represented the average of three independent experiments. The expression trends of all treated cells were compared using one-way ANOVA. Significance: *P < 0.05, **P < 0.01, ***P < 0.001.

3.3.2.6 CFZ reduced TNFα-mediated leukocyte adhesion to HUVECs

A leukocyte adhesion assay was conducted to investigate my ICAM-1 expression findings in a more physiologically relevant environment as described in (Methods 2.9.6). The leukocyte interfaces with vascular endothelium during inflammatory responses and establishes a strong attachment with endothelial cells via several adhesion molecules, such as ICAM-1, measured in this assay. In agreement with my ICAM-1 study, when leukocytes were perfused over HUVECs pre-treated with TNFα, there was a progressive increase in leukocyte attachment to the endothelium over the five minutes recorded in the assay (Figure 3.3.11A, B). This indicates a pro-inflammatory activation of HUVECs in response to TNFα. In contrast, there was almost a complete absence of leukocyte adhesion to the endothelial cells in DMSO and CFZ treated cells (Figure 3.3.11A, B). This indicates that there was no inflammatory activation of HUVECs caused by CFZ. In agreement with CFZ cytoprotective effect, CFZ attenuated the well-established pro-inflammatory action of TNFα. (409) This was revealed by its ability to significantly reduce leukocyte adherence to the endothelial cells after TNFα treatment (Figure 3.3.11A, B) among all the time points observed in the assay. However, this assay was only conducted once; therefore, another biological repeat is required before deriving a conclusion about the significance of this experiment.

In general, all the data observed in this chapter indicate that CFZ provides anti-thrombotic and anti-proinflammatory effects on the endothelium.

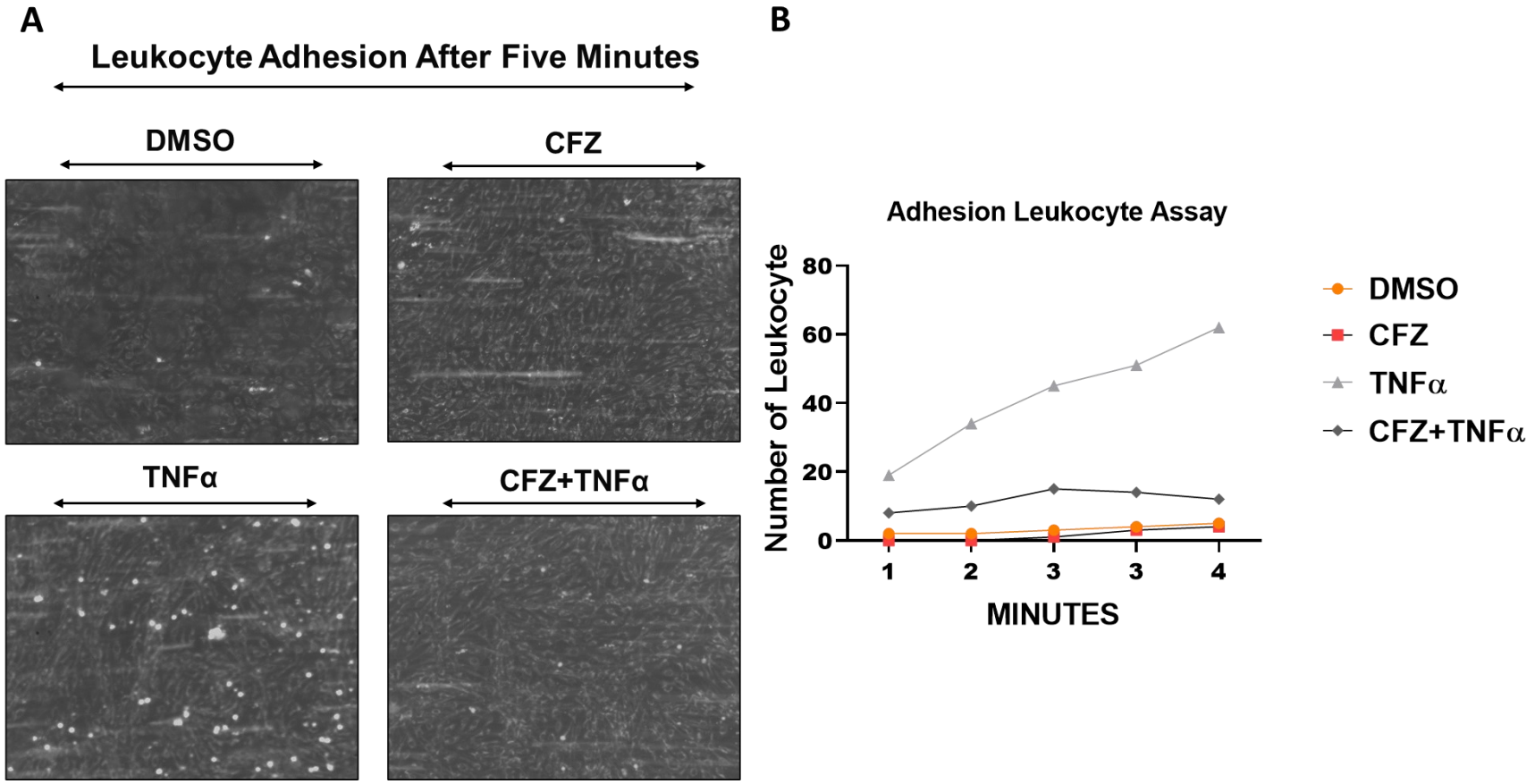


Figure 3.3.11: CFZ did not induce the inflammation of HUVECs. HUVECs were treated with 750nM of CFZ and DMSO for 1 hour, followed by washing the cells with PBS and replacing them in a fresh EBM-2 medium. Some cells were stimulated with 20 ng/ml of TNFα alone or after CFZ treatment for 24 hr. A) Leukocyte adhesion visualisation using the fluorescent microscope (10X objective). B) The quantification of adhered leukocytes to the endothelial cells. DMSO; Dimethyl sulfoxide, CFZ; Carfilzomib, TNFα, Tumor Necrosis Factor. Three technical repeats were performed in one experiment. The data represented one biological repeat experiment.

3.3.3 Discussion

My previous chapter showed that CFZ induced gene and protein expression of some of the well-known anti-thrombotic markers; thrombomodulin and eNOS. In addition, CFZ was able to significantly suppress the ability of TNFα to mediate the expression of some of the well-known pro-thrombotic markers; TF and VWF and the pro-inflammatory marker, ICAM-1, implying that CFZ has a potential cytoprotective effect on the endothelium. This chapter examined these findings further in more physiologically relevant conditions, employing some functional studies.

Tissue factor (TF) expression is a potent activator of the coagulation cascade. While evidence for endothelial TF expression *in vivo* is controversial, it is widely accepted that endothelial cells expression little or no TF in resting conditions. (410) However, at least *in vitro,* it is known that TNFα can induce its expression in HUVECs and other endothelial cells. (411) In keeping with this, the data from this and the previous chapter clearly confirms this and demonstrates that TNFα treated HUVECs can support fibrin clot formation and FXa generation. Considerably, while CFZ treatment alone did not affect TF expression, CFZ was able to attenuate the effects of TNFα at a functional level significantly. Stimulation of TF gene expression in the human endothelium exposed to TNF-α is regulated at the transcriptional level. (412) It is widely accepted that TNFα triggers TF gene transcription via functional interactions between c-Rel–p65 and Fos-Jun heterodimers. (413) In response to the endothelial activation by TNFα, this family complex dissociates from inhibitor proteins, including IκBα allowing transcriptional induction of TF expression. (414) Inhibition of the NF-κB pathway triggered by TNFα has shown intensive suppression of the endothelial pro-thrombotic response, including suppression of TF expression. (415) A potential inhibitory interaction between CFZ and the NF-κB pathway could at least involve the observed CFZ cytoprotective effect on the TF expression. (416)

Nitric oxide (NO) is created by normally operative endothelial cells as an effect of the act of the endothelial isoform of NO synthase (eNOS), which has been revealed to affect a diversity of endothelial responses including the prevention of vascular thrombosis. (417) Tissue-type plasminogen activator (t-PA) plays a central role in

blood fibrinolytic activity. (418) Upon stimulation, the endothelium releases t-PA rapidly, which, therefore, plays a crucial role in dissolving fibrin during the initial fibrin formation event, thus preventing thrombosis. (419) The interaction between NO and t-PA has been studied extensively in the last decade. It is well-established that NO inhibits the plasminogen activator inhibitor-1 (PAI-1), a major physiological inhibitor of plasminogen activator (t-PA), via cyclic guanosine monophosphate (aGMP)-dependent mechanism. (420) This was further illustrated in the clinical setting by Chiara and his colleagues, where they found a correlation between the availability of tonic and stimulated NO in essential hypertension and the endothelium release of t-PA. (421) In a similar manner, several reports have proved a direct negative correlation between eNOS expression and TF expression from the endothelium. (422) In agreement with my results, Yang *et al*. reported that eNOS overexpression and phosphorylation decreased TNFα mediated expression of TF. (423) Most recently, data about the thrombotic complications of COVID-19 have indicated a beneficial involvement of NO in suppressing the endothelial cell release of TF by involving the suppression of the NF-κB pathway. (424) Taken together, there is clear evidence about the regulatory involvement of endothelial e-NOS and the expression of TF. Since I observed that CFZ had significantly induced eNOS protein and phosphorylation of e-NOS in HUVECs, I proposed that NO may diminish thrombotic tendency by overwhelming TF-dependent coagulation and enhancing the expression of t-PA in the endothelium. This effect could be due to the suppression of the NF-κB pathway and (PAI-1) through CFZ induced NO overexpression dependent mechanism which could be an interesting target for future research focuses.

Thrombomodulin (TM) is a crucial anticoagulant protein present on the endothelial cell surface that complexes with thrombin to enhance activation of protein C by thrombin. (425) In keeping with my thrombomodulin expression findings, I found that CFZ induced APC generation in HUVECs, and with a lower extent counter the well-known suppression impact of TNFα on thrombomodulin expression, implying a potential thrombomodulin dependent antithrombotic CFZ effect. A recent study demonstrated that thrombomodulin expression was essential for maintaining endothelial quiescence (426), with thrombomodulin deficient endothelial cells being more sensitive to TNFα and demonstrating the increased release of VWF, which in turn resulted in increased

leukocyte and platelet recruitment. (426) The increased thrombomodulin expression caused by CFZ may have the opposite effect on its knockdown and confer protection to the endothelium. Suppression of thrombomodulin expression by TNFα has been described to arise through several mechanisms. (427) Among them, NF-κB stimulation has been linked to defects in the thrombomodulin pathway and restrains APC creation, demonstrating a joint inhibitory interaction between the thrombomodulin and NF-κB pathways. (428) Equally, it is well-known that APC generation from the endothelium attenuates thrombin formation, inhibits NF-κB activation, reduces the inflammatory cytokine release, enhances fibrinolysis, and maintains endothelial integrity. (429) As I demonstrated earlier, CFZ induced NO and TM expression in HUVECs. It is well-known that nitric oxide-dependent mechanisms partially control the expression of TM. (430) Similar to my CFZ findings, the BTZ cytoprotective effect showed a nitric oxide-dependent mechanism involving the inhibition of the NF-κB pathway. (431) Therefore, by taking a broader view of all my data and considering previously published data, I could hypothesise that NO is potentially regulating the CFZ antithrombotic effects through the involvement of the NF-κB pathway, which would be of great interest to explore in detail in future work.

VWF and ICAM-1 expression from the endothelium are early signs of pro-thrombotic and pro-inflammatory activation of the endothelium, respectively. (432) Lastly, in this chapter, I found that in common with the soluble VWF and ICAM-1 findings, CFZ treated cells showed almost an absence of platelet capture and leukocyte adhering to the endothelium, implying that CFZ did not trigger pro-thrombotic or pro-inflammatory activities. Interestingly, CFZ caused a significant reduction of both platelets captured to the VWF strings and leukocytes adhered to HUVECs mediated by TNFα. This was visually further illustrated by a remarkable reduction of the VWF-immuno staining fluorescence intensity when CFZ was combined with TNFα in HUVECs compared to TNFα alone treated cells, all implying anti-thrombotic and anti-inflammatory effects of CFZ. To my knowledge, this is the first known report of a proteasome inhibitor affecting the stimulated release of VWF from endothelial cells. As discussed earlier, it is well-known that NO expression by endothelial cells has a significant role in controlling the pro-inflammatory and pro-thrombotic activation of the endothelium. (433) NO has been shown to regulate the release of both ICAM-1 and VWF from the endothelium. (434)

According to Secco *et al*. NO inhibits neutrophil migration to the endothelium by suppressing the expression of ICAM-1. (435) Ritter *et al*. claimed that NO suppression from HUVECs was significantly correlated with increased VWF release. (436) Several mechanisms were proposed to describe these effects; among them, the endothelium expression of NO suppresses the NF-κB-dependent pathways pro-thrombotic and pro-inflammatory activation. (437) According to Tham *et al*. NF-κB activation mediated induction of pro-inflammatory and pro-thrombotic genes, such as VWF and ICAM-1. (438) Taken together, a potential suppression of the NF-κB pathway dependent on the over expression of NO-mediated by CFZ could be the central regulator of CFZ cytoprotective effect in HUVECs.

In summary, in this chapter, I confirmed at the functional level the observed CFZ cytoprotective effect in HUVECs at the cellular level.

3.4 Nitric oxide is an important regulator of the endothelium and for CFZ cytoprotective effect in the endothelium

3.4.1 Introduction

The eukaryotic central degradation system for intracellular proteins is the ubiquitin-proteasome system. (439) This system is central to cellular mechanisms to maintain normal homeostasis. (440) The 26S proteasome is the most abundant human proteasome. (441) It is mainly composed of two subunits, the 19S regulatory cap where protein reorganisation occurs and the 20S core unit where protein degradation occurs. (442) Protein maturation and folding activities are favourably maintained and controlled in the eukaryotic cell. Only correctly assembled proteins can transport to the Golgi apparatus, while those that misfold are directed to ER-associated degradation (ERAD) or autophagy. (29) The accumulation of misfolded/unfolded proteins in the ER stimulates pathways that coordinate adaptive cellular reactions. (443) This collective cellular response is known as the unfolded protein response (UPR), which aims to maintain normal cellular homeostasis. (443) Mainly, the UPR improves ERAD of misfolded proteins, diminishes global protein synthesis and raises the ER protein-folding capacity. (49) However, if this mechanism fails to restore ordinary ER homeostasis, the UPR initiates apoptosis, signalling the death of the defective cell. (444) Three transmembrane ER-resident proteins are responsible for this mechanism: IRE1α, ATF6 and PERK. (444) The luminal domain of the individual sensor tends to react to the unfolded/misfolded protein in the ER. (346) These sensors are controlled and inactivated through binding with the major ER-resident chaperone protein, BiP. (346) This protein has been recognised as an essential component of ER translocation, protein folding and ERAD. (445) BiP is significantly responsible for preserving the penetrability barrier of the ER membrane and maintaining newly synthesised proteins in a form that is competent for oligomerisation and folding. (446) It also has a vital role in defective protein translocation across the ER membrane to the proteasome. (447) When there is an accumulation of misfolded proteins in the cytosol, BiP disconnects from the ER sensors and binds to the accumulated misfolded proteins in the ER cytosol, leading to the activation of the ER-stress transducer

pathway. (448) In addition, BiP overproduction reflects an active ER stress environment. (449)

The vascular endothelium is a monolayer sheet of cells between the smooth muscle vascular cells and the vessel lumen. (358) Nitric oxide (NO) is the principal endothelium-derived substance manufactured in the vasculature whose synthesis is dependent on the endothelial form of the nitric oxide synthase enzyme, eNOS. (450) It has a broad range of biological properties and multi-branch functions, such as the regulation of local cell growth, vasodilation, oxidative stress, inflammation and modulation of vascular tone; thus, collectively, it maintains a healthy vascular system with other substances. (110) An emergent list of disorders such as diabetes mellitus, hypertension, hypercholesterolemia, and heart failure are associated with reduced NO production due to diminished synthesis or excessive oxidative degradation. (144) The reduced formation of NO in these medical disorders triggers severe complications in endothelial equilibrium. (144) Additionally, reduced nitric oxide bioactivity may accelerate vascular inflammation that could cause foam cell formation and oxidation of lipoproteins, which is the foundation of the atherosclerotic plaque. (451) NO also has a significant role in leukocyte adhesion to the endothelial surface by regulating endothelium adhesion molecules, such as ICAM-1 and P-selectin. (452) The involvement of NO in the regulation of vascular haemostasis has been widely investigated. (453) It effectively inhibits platelet adhesion and aggregation to the endothelium under physiological conditions. (452) In addition, it has shown a potent ability to prevent platelet granule exocytosis, thus inhibiting platelet aggregation and activation. (398)

In the previous chapters, I demonstrated that CFZ did not affect the ER stress status of HUVECs; instead, it showed a cytoprotective effect. Therefore, in this chapter, **I investigated the hypothesis that this activity was dependent on the CFZ-mediated induction of BIP and/or NO** so that either BiP or NO knockdown in the endothelium could eliminate the observed cytoprotective effect of CFZ due to their vital roles in ER stress and haemostasis, respectively.

3.4.2 Results

3.4.2.1 BiP knockdown did not induce ER stress or pro-thrombotic activation in HUVECs

According to data obtained in the previous chapters, clear evidence was found to support the conclusion that CFZ did not induce ER stress but rather induced a cytoprotective effect in HUVECs. Since BiP plays a significant role in the cell's response to ER stress, it was hypothesized that knocking down BiP expression would prevent CFZ from exerting its cytoprotective effects and eliminate the ability of the endothelium to escape from ER stress activation that CFZ could cause. A siRNA sequence directed against BiP was initially titrated to obtain the concentration giving optimal knockdown of protein expression (Methods 2.8). All the concentrations of siRNA tested (5, 10, 15 and 20nM) significantly reduced BiP protein expression as determined by Western blot, with almost complete knockdown achieved with 20nM siRNA (Figure 3.4.1).

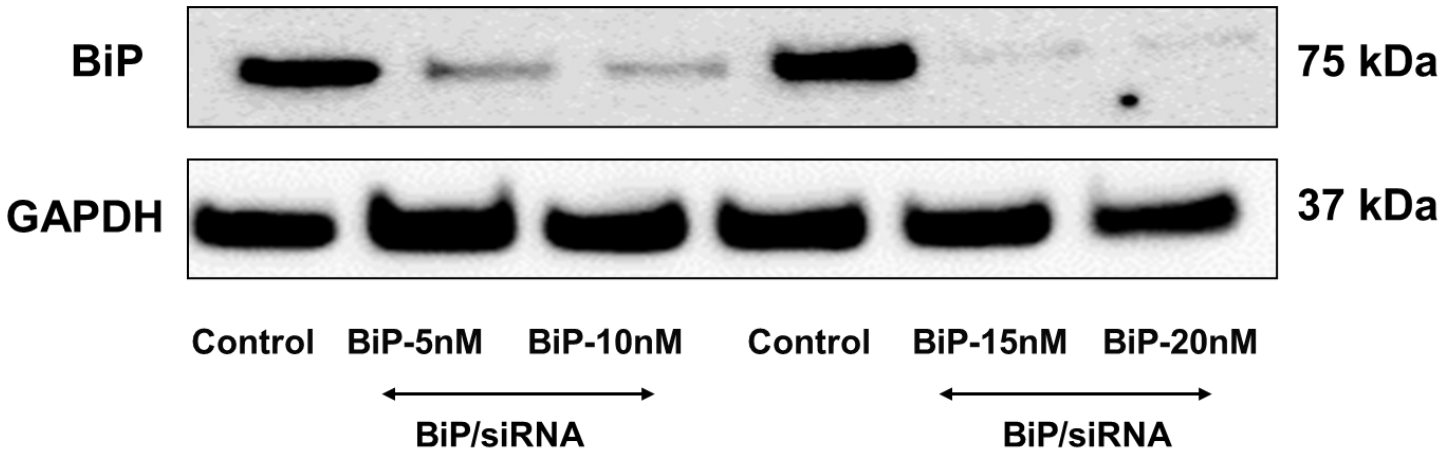


Figure 3.4.1: Optimisation of BiP knockdown in HUVECs. HUVECs were treated with 5nM, 10nM, 15nM and 20nM of BiP/siRNA for 24 hours, then washed with PBS and replaced with a fresh EBM-2 medium. Cells were harvested to extract protein at 24 hours; Western blot was used to determine the extent of BiP protein expression at 24hr.

I then investigated the impact of BiP silencing on the response of HUVECs to CFZ treatment. The cells were transfected first with 20nM of BiP siRNA for 24 hours; then, the cells were supplemented with fresh EBM-2 medium and treated with 750nM of CFZ for 1 hour (Methods 2.8). In agreement with the previous finding, there was a consistent alteration of HUVEC morphology after CFZ treatment in control siRNA transfected cells. Interestingly, the morphological appearance of DMSO and CFZ-treated control siRNA transfected cells was similar to that of the corresponding BiP siRNA transfected cells, implying that BiP silencing did not enhance the CFZ effect on HUVEC morphology (Figure 3.4.2).

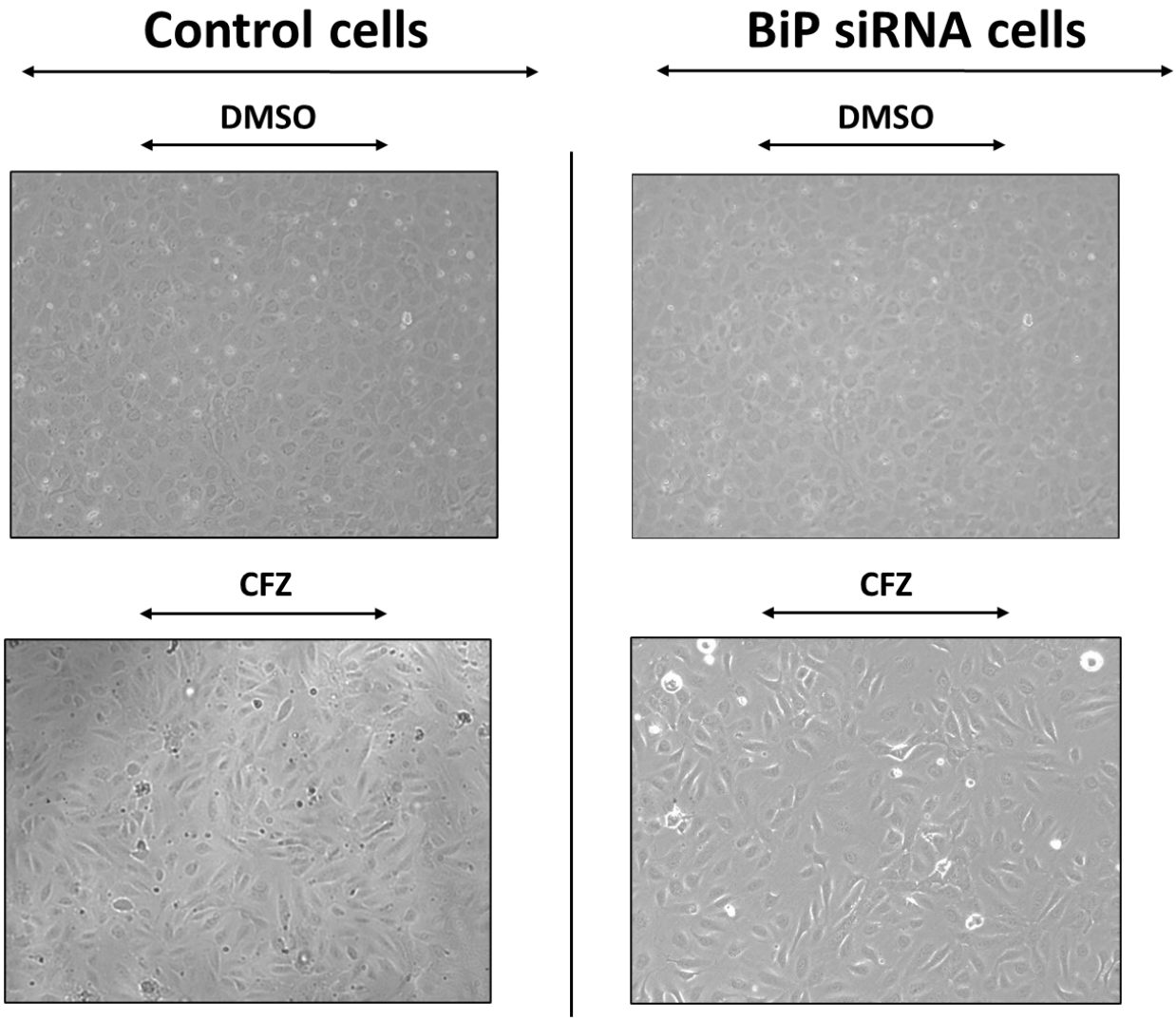


Figure 3.4.2: BiP knockdown did not enhance CFZ morphological change in HUVECs. HUVECs were treated with 20nM of control/BiP-siRNA for 24 hours, followed by washing the cells with PBS and resuspending them in a fresh EBM-2 medium. The cells were treated with 750nM of CFZ, DMSO for 1hr followed by 24hr recovery. The Morphological observation using a light microscope (10X objective).

Afterwards, it was investigated if endothelial BiP silencing could induce ER stress in HUVECs. First, transfected cell pellets were collected after a 24-hour recovery period to study the relative alteration in BiP protein expression via Western blot analysis to confirm that BiP knockdown was achieved in this experiment. As shown in Figure 3.4.3A, BiP expression significantly reduced in all BiP siRNA transfected cells compared to their corresponding controls. Similar to my previous findings, there was no induction of BiP in CFZ treated cells compared to the untreated and the vector-DMSO controls, implying the absence of ER stress (Figure 3.4.3A).

Since BiP was silenced in this experiment, other ER stress markers (P58 and IRE1α) were selected to assess the ER stress state in the BiP knockdown cells. Interestingly, the Western blot analysis revealed no change in either of these markers in BiP knockdown-CFZ treated cells compared to the control siRNA transfected CFZ treated cells (Figure 3.4.3B), implying that BiP silencing in HUVECs did not contribute to enhancing ER stress activation in HUVECs.

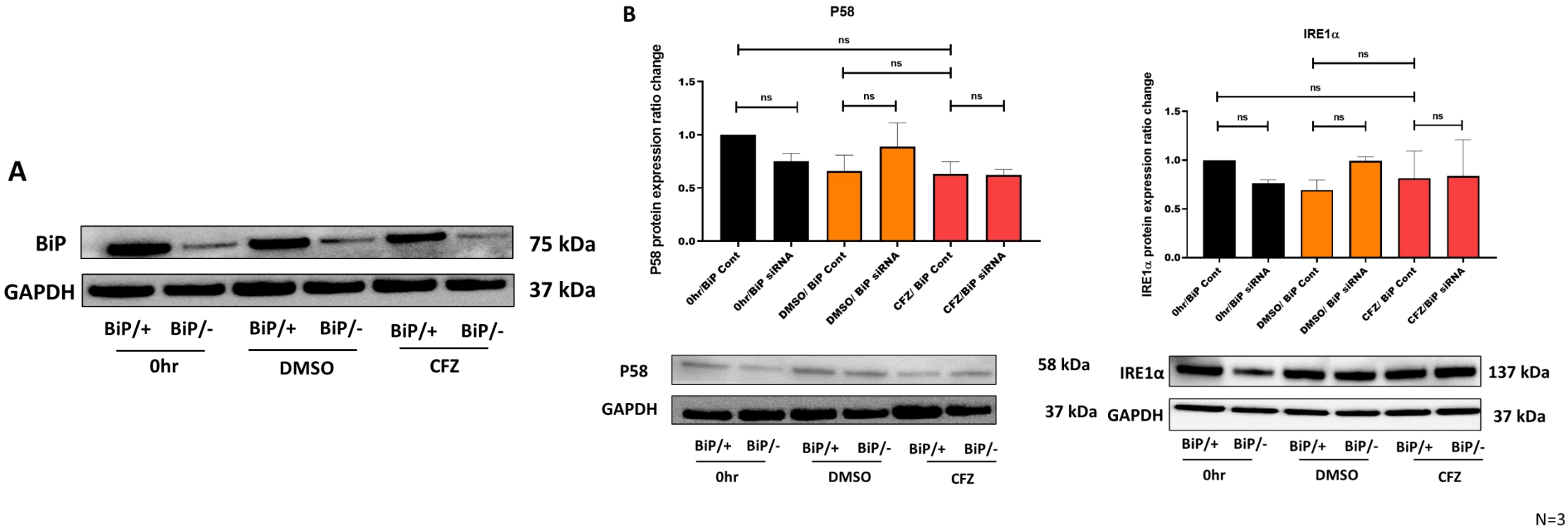


Figure 3.4.3: BiP knockdown did not induce ER stress in HUVECs. HUVECs were treated with 20nM of control/BiP-siRNA for 24 hours, followed by washing the cells with PBS and replacing them with a fresh EBM-2 medium; The cells were treated with 750nM of CFZ, DMSO for 1hr followed by 24hr recovery. A) Western blot analysis of BiP. B) Western blot analysis and density quantification of P58 and IRE1α protein expression. DMSO, Dimethyl sulfoxide; CFZ, carfilzomib. Three technical repeats were performed in one experiment, and the quantification of data was normalised to GAPDH levels and presented as the mean ± SEM. The data represented the average of three independent experiments. The expression trends of proteins between CFZ and DMSO cells are compared using one-way ANOVA. Significant: *P < 0.05; **P < 0.01; ***P < 0.001; ****P < 0.0001.

Alternatively, I hypothesised that BiP silencing in HUVECs might induce a pro-thrombotic effect in HUVECs. For this purpose, I prepared the cells as described earlier and stained the cells with anti-VWF-FITC antibodies (Methods 2.6.1) to evaluate the release of VWF from HUVECS. Interestingly, BiP knockdown did not induce VWF release or observable string formation under any conditions, indicating that silencing BiP expression in HUVECs does not induce VWF release or cause CFZ treatment to induce VWF release. (Figure 3.4.4). Together these data suggest that BiP is not the critical regulator of the CFZ cytoprotective effect in HUVECs.

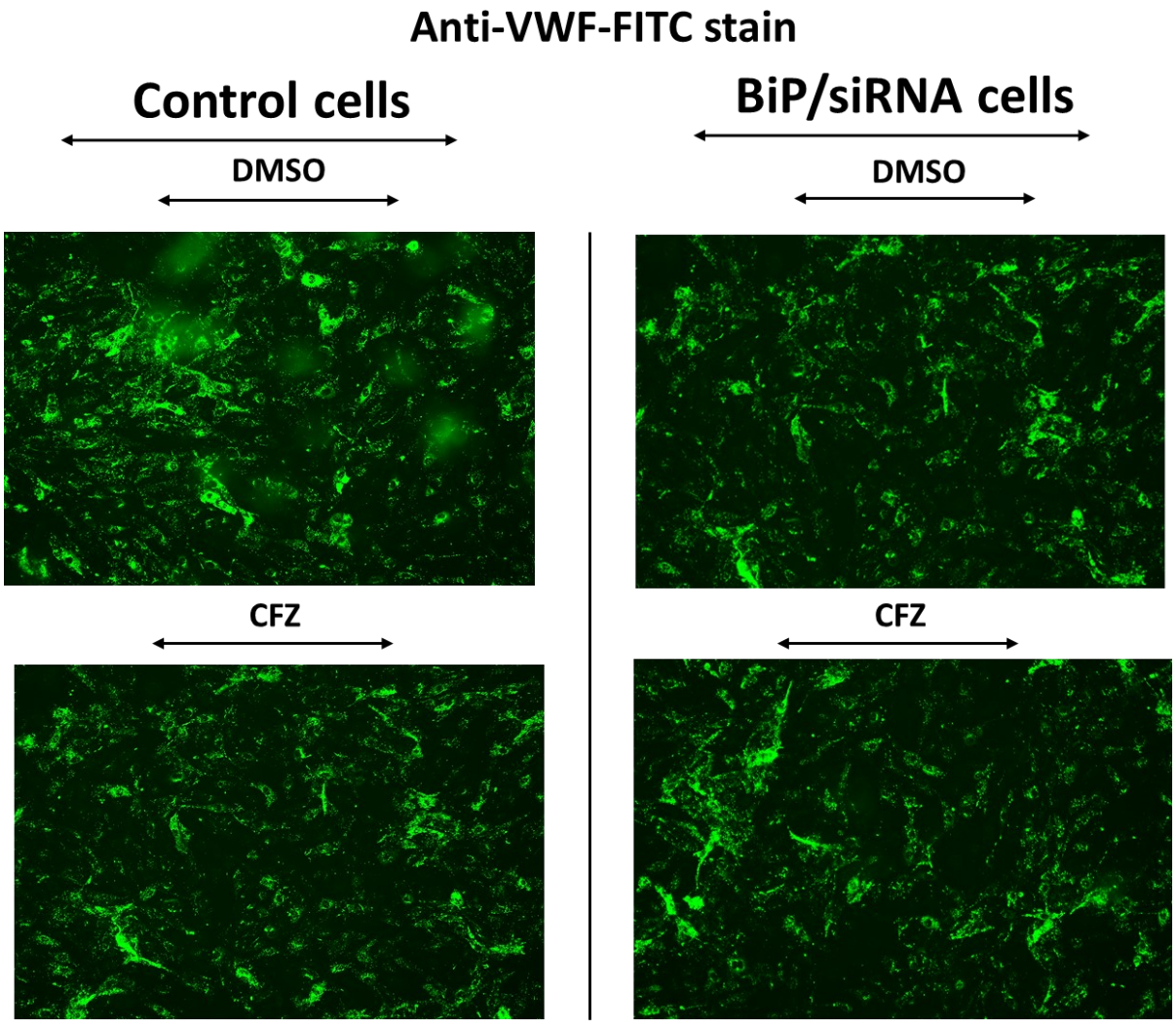


Figure 3.4.4: BiP knockdown did not induce VWF release from HUVECs. HUVECs were treated with 20nM of control/BiP-siRNA for 24 hours, followed by washing the cells with PBS and replacing them with a fresh EBM-2 medium. The cells were treated with 750nM of CFZ, DMSO for 1hr followed by 24hr recovery; then, the cells were permeabilized with 1x triton and stained with anti-VWF-FITC stain. DMSO, Dimethyl sulfoxide; CFZ, carfilzomib. The fluorescence intensity for the stained cells was visualised using a fluorescence microscope (10X objective).

3.4.2.2 eNOS knockdown induced ER stress in HUVECs

Since BiP knockdown did not alter the response of the endothelium to CFZ, it was next hypothesized that eNOS could play a crucial role in mediating the response of HUVECs to CFZ. eNOS is the endothelial isoform enzyme responsible for producing endothelium nitric oxide. Nitric oxide is the primary endothelial cell-derived substance and modulates broad endothelium functions. (454) It is well established that nitric oxide is involved in regulating endothelial haemostasis and has a part in regulating the endothelium inflammatory response. (454) Similar to BiP, to investigate the potential role of eNOS as a regulator of the observed CFZ cytoprotective effects in HUVECs, eNOS expression was knocked down using siRNA (Methods 2.8). Initially, the optimal concentration of eNOS siRNA was determined. Almost complete knockdown or eNOS and virtually no p-eNOS was seen with 20nM siRNA at 24 and 48 hours (Figure 3.4.5).

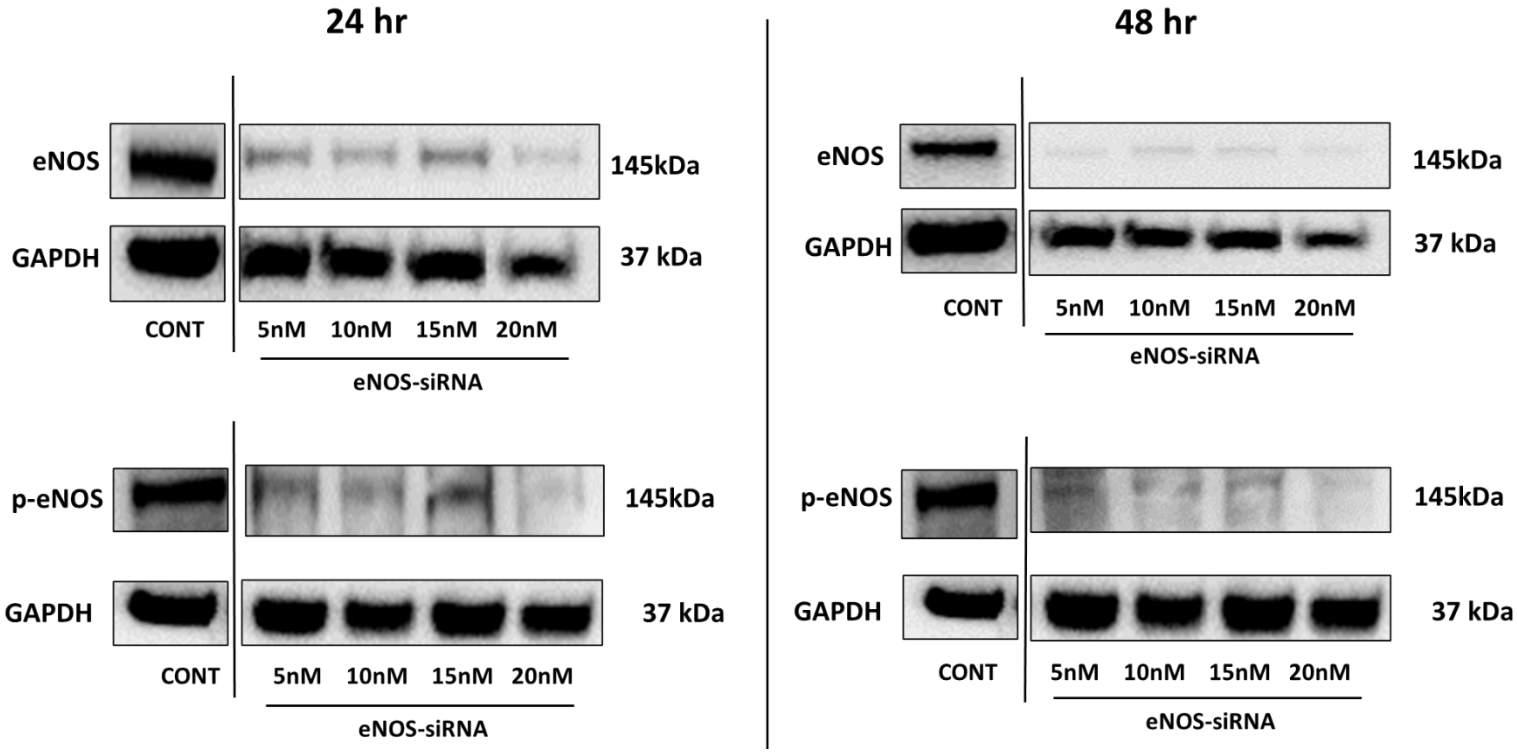


Figure 3.4.5: Optimisation of eNOS knockdown in HUVECs. HUVECs were treated with 5nM, 10nM, 15nM and 20nM of control/eNOS siRNA for 24 and 48 hours, then washed with PBS and replaced with a fresh EBM-2 medium. Cells were harvested to extract protein at 24 and 48 hours; Western blot was used to determine the extent of eNOS and p-eNOS protein expression.

Next, the impact of eNOS silencing on the response of HUVECs to CFZ was investigated. The cells were transfected with 20nM control siRNA or 20nM of eNOS-specific siRNA for 24 hours; then, media was changed for fresh EBM-2 medium and treated with 750nM of CFZ for 1 hour (Methods 2.8). After 24 hours recovery, transfected cells were imaged to evaluate any morphological modifications that the silencing of eNOS from HUVECs could cause; second, the cells were harvested, and the pellets were collected to confirm the silencing of eNOS in HUVECs using Western blot and to study relative alterations in BiP expression using qPCR. Each eNOS transfection was compared to the control transfected cells.

As shown in Figure 3.4.6, the morphological appearance of DMSO and CFZ-treated control transfected cells was similar to their corresponding eNOS-specific siRNA transfected cells, implying that eNOS silencing did not induce any effects on HUVEC morphology and that lack of eNOS did not influence CFZ-mediated changes in morphology.

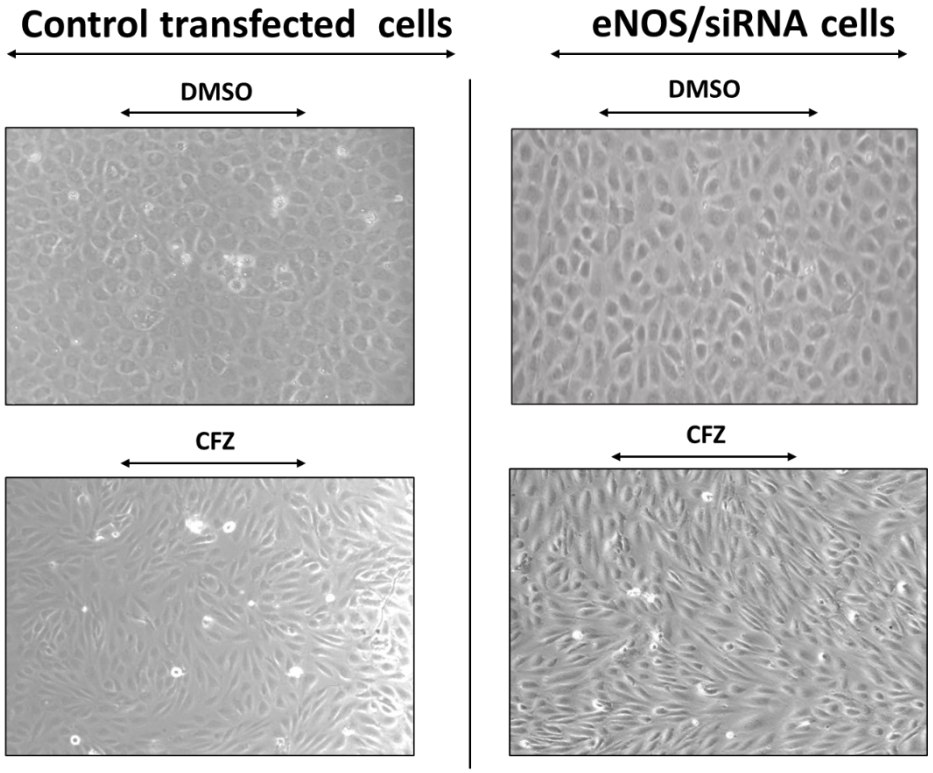


Figure 3.4.6: eNOS knockdown did not enhance CFZ morphological change in HUVECs. HUVECs were treated with 20nM of control or eNOS/siRNA for 24 hours, followed by washing the cells with PBS and replacing them with a fresh EBM-2 medium. The cells were treated with 750nM of CFZ, DMSO for 1hr followed by 24hr recovery. The Morphological observation using a light microscope (10X objective).

As shown in Figure 3.4.7A, there was an almost complete reduction of eNOS expression in all eNOS siRNA transfected cells compared to their corresponding controls, and there was visual induction of eNOS expression in control transfected CFZ treated cells compared to the untreated/DMSO controls, which was consistent with my earlier findings. Moreover, in agreement with my previous findings, there was no induction of BiP mRNA expression in control siRNA transfected CFZ treated cells at 24h (Figure 3.4.7B). Interestingly, however, there was a significant upregulation of BiP mRNA expression among all eNOS knockdown cells compared to their corresponding controls (Figure 3.4.7B), indicating a direct correlation between eNOS silencing in HUVECs the expression of BiP. However, treatment with CFZ did not alter the level of BIP further.

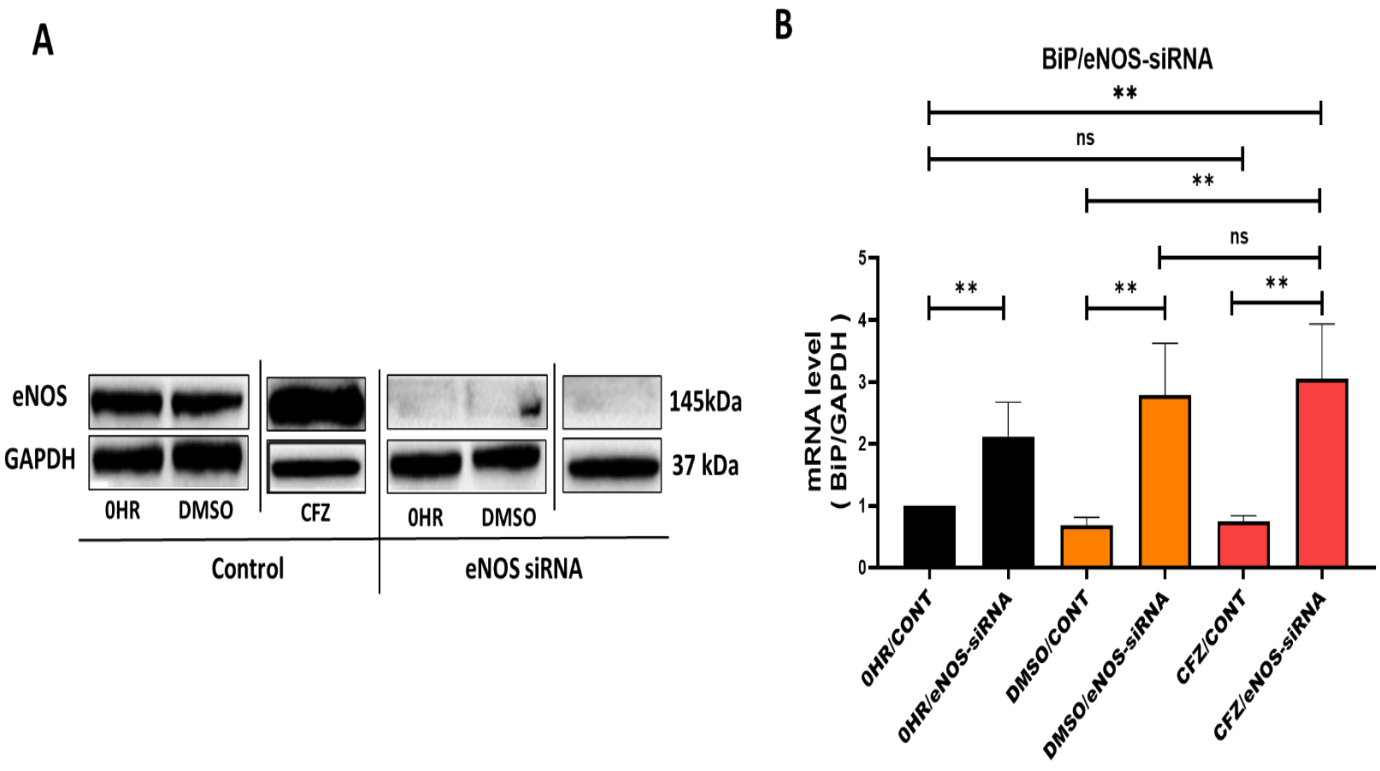


Figure 3.4.7: eNOS knockdown induced ER stress in HUVECs. HUVECs were treated with 20nM of control/eNOS siRNA for 24 hours, followed by washing the cells with PBS and replacing them with a fresh EBM-2 medium. The cells were treated with 750nM of CFZ, DMSO for 1hr followed by 24hr recovery. A) Western blot analysis of eNOS protein expression. B) qPCR analysis of BiP mRNA level expression. DMSO, Dimethyl sulfoxide; CFZ, carfilzomib. Three technical repeats were performed in one experiment, and the quantification of data was normalised to GAPDH levels and presented as the mean ± SEM. The data represented the average of three independent experiments. The expression trends of proteins between CFZ and DMSO cells are compared using one-way ANOVA. Significance: *P < 0.05; **P < 0.01; ***P < 0.001; ****P < 0.0001.

3.4.2.3 eNOS knockdown induced thrombotic and inflammatory responses in HUVECs

Since eNOS silencing induced ER stress activation in HUVECs, it was next investigated if eNOS silencing could induce a pro-thrombotic and pro-inflammatory response in HUVECS and how CFZ treatment would affect this. For this purpose, some well-known coagulation and inflammatory endothelial-derived regulators were investigated. Consistent with published data, Western blot analysis revealed significant ICAM-1 protein expression induction in all eNOS knockdown cells compared to their corresponding controls (Figure 3.4.8A). (23) But the level of ICAM-1 expression was not affected by CFZ, suggesting that this is dependent on the loss of eNOS expression rather than the effects of CFZ. eNOS knockdown cells also released more soluble ICAM-1 compared to the corresponding controls. Interestingly, while the CFZ treatment of control cells did not induce the release of soluble ICAM-1, there was a small but statistically significant increase in soluble ICAM-1 released from eNOS knockdown cells following CFZ treatment compared to the controls (Figure 3.4.8B). Together this data may putatively indicate that while CFZ did not alter membrane-bound ICAM-1, it may enhance cleavage of ICAM-1 from the endothelium; however, since this was observed in eNOS silenced cells and effects of CFZ are apparently constrained by eNOS activity in HUVECs.

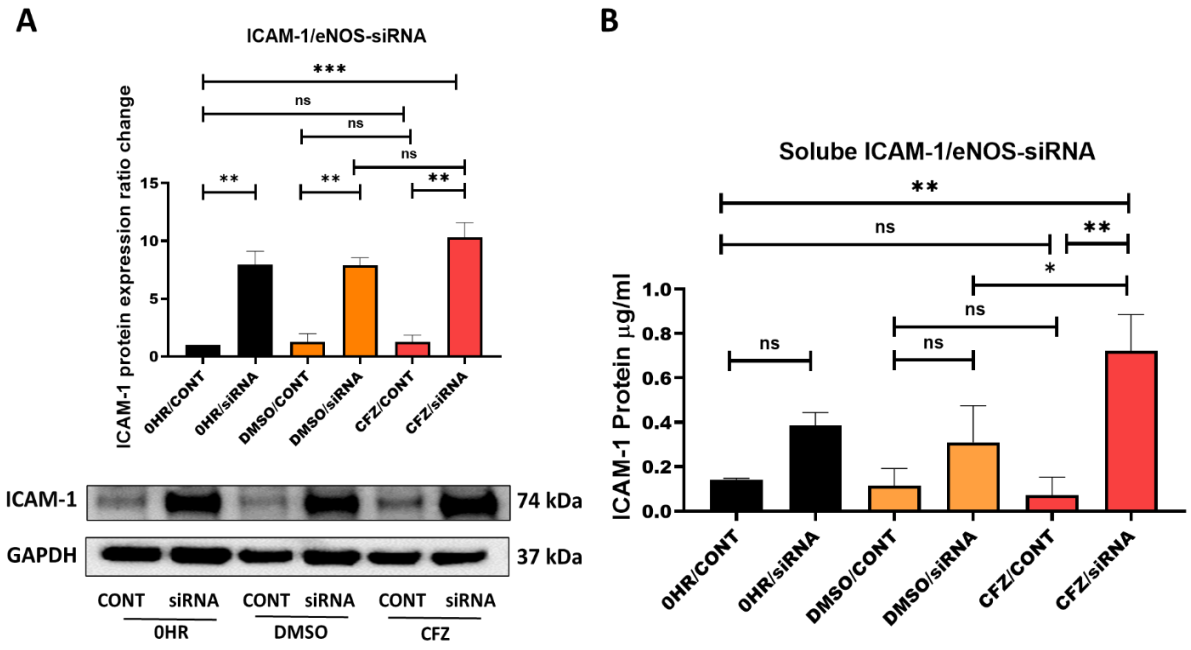


Figure 3.4.8: eNOS knockdown induced soluble ICAM-1 expression by HUVECs. HUVECs were treated with 20nM of control/eNOS siRNA for 24 hours, followed by washing the cells with PBS and replacing them with a fresh EBM-2 medium. The cells were treated with 750nM of CFZ, DMSO for 1hr followed by 24hr recovery. A) Western blot analysis of ICAM-1 protein level expression. B) Soluble ICAM-1 protein level expression. DMSO, Dimethyl sulfoxide; CFZ, carfilzomib. Three technical repeats were performed in one experiment, and the quantification of data was normalised to GAPDH levels and presented as the mean ± SEM. The data represented the average of three independent experiments. The expression trends of ICAM-1 between CFZ and DMSO cells are compared using one-way ANOVA. Significance: *P < 0.05; **P < 0.01; ***P < 0.001; ****P < 0.0001.

Next, I examined the expression of tissue factor (TF). In agreement with my previous findings, control cells treated with CFZ did not show any upregulation of TF gene expression; however, eNOS knockdown caused significant upregulation of TF under all conditions, indicating that eNOS may regulate TF expression (Figure 3.4.9A). Interestingly, in eNOS knockdown cells, CFZ slightly but significantly increased TF gene expression compared to DMSO treated eNOS knockdown cells (Figure 3.4.9A). Thus, similar to the soluble ICAM-1 findings, eNOS expression could at least partially regulate the anti-thrombotic and anti-inflammatory activity mediated by CFZ treatment in HUVECs. Interestingly, it was also observed that CFZ induced the expression of Tissue Plasmin Activator (t-PA) in HUVECS. T-PA is a central endothelial-derived anti-thrombotic regulator that converts plasminogen into plasmin, thus mediating the lysis of fibrin clots. While eNOS silencing did not alter the expression of t-PA in control cells (i.e., time zero or DMSO treated), there was a significant reduction in t-PA mRNA when

eNOS knockdown cells were incubated with CFZ compared to non-knock down cells treated with CFZ, implying a potential direct correlation between eNOS expression and CFZ mediated t-PA expression in HUVECs (Figure 3.4.9B). Finally, the expression of thrombomodulin (TM) was examined. Consistent with my previous data, CFZ caused a significant increase in TM expression at the gene and a remarkable observable increase at the protein level. However, eNOS knockdown did not affect TM either in the absence or presence of CFZ (Figure 3.4.9 C, D).

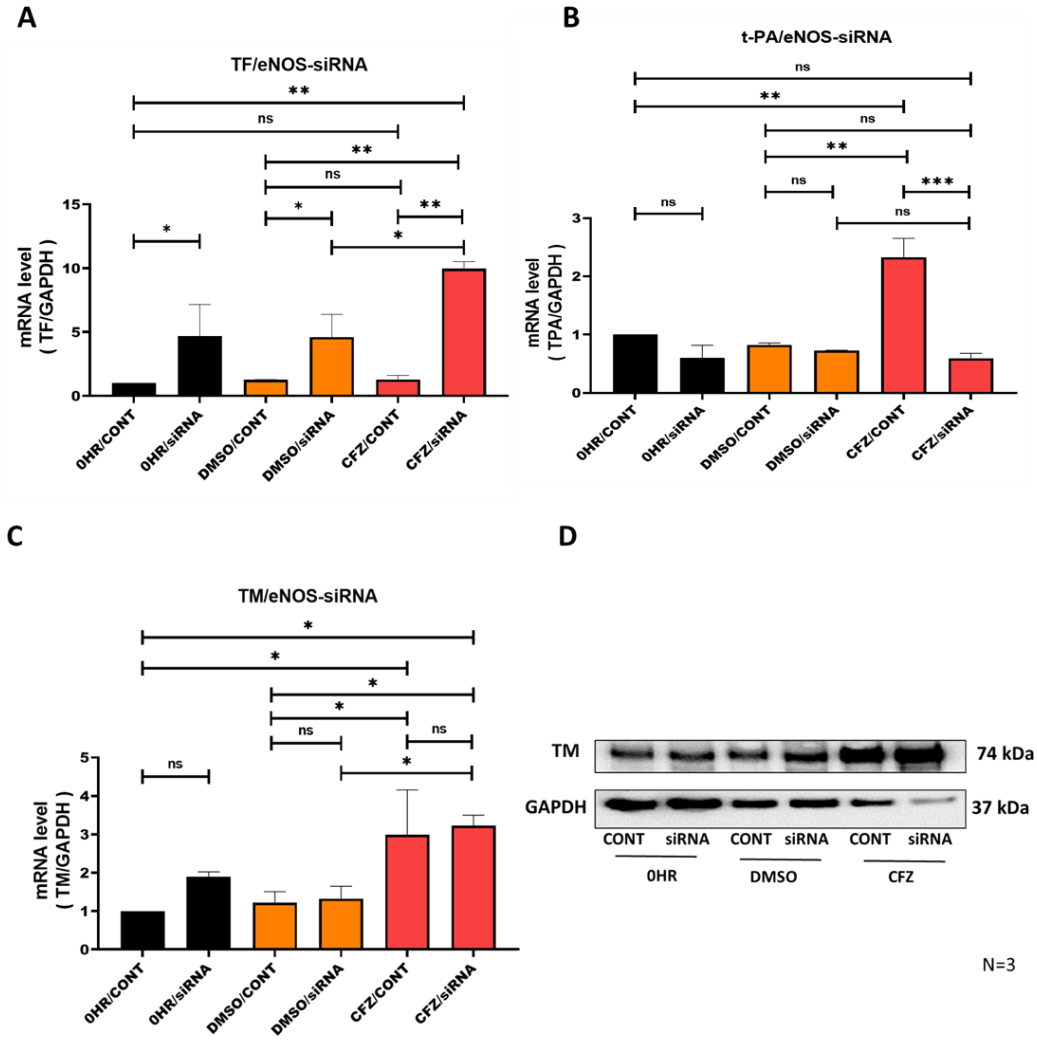


Figure 3.4.9: eNOS knockdown induced TF, reduced CFZ mediated t-PA and did not alter TM expression in HUVECs. HUVECs were treated with 20nM of control/eNOS siRNA for 24 hours, followed by washing the cells with PBS and replacing them with a fresh EBM-2 medium. The cells were treated with 750nM of CFZ, DMSO for 1hr followed by 24hr recovery. A) qPCR analysis of TF mRNA level expression B) qPCR analysis of t-PA mRNA level expression. C) qPCR analysis of TM level expression. D) Western blot analysis of TM level expression. DMSO, Dimethyl sulfoxide; CFZ, carfilzomib TF, tissue factor; t-PA, tissue plasmin activator; TM, thrombomodulin. Three technical repeats were performed in one experiment, and the quantification of data was normalised to GAPDH levels and presented as the mean ± SEM. The data represented the average of three independent experiments. The expression trends of mRNA and proteins between CFZ and DMSO cells are compared using one-way ANOVA. Significance: *P < 0.05; **P < 0.01; ***P < 0.001; ****P < 0.0001

3.4.2.4 eNOS knockdown induced fibrin formation in HUVECs

My previous results showed that eNOS knockdown induced TF expression in HUVECs. Therefore, turbidity assays were conducted to assess the correlation between the observed induced expression of TF in eNOS knocked down cells and fibrin clot formation. The cells were stimulated with 20 ng/ml of TNFα after a 1-hour treatment with 750 nM CFZ, and the cellular eNOS siRNA transfection was conducted, as indicated earlier.

Consistent with my previous findings, the control siRNA transfected CFZ treated cells showed the lowest absorbance, the highest lag time and t-Max values (15.5 minutes and 18.3 minutes, respectively) (Figure 3.4.10 A, C, D), implying that these cells form the least fibrin clot among all other conditions. Interestingly, however, this protective effect was abrogated due to eNOS silencing in HUVECs. This was demonstrated by a remarkable increase of the absorbance and the significant reduction in a lag time and in t-Max of the eNOS siRNA CFZ and CFZ+TNFα treated cells only compared to their corresponding control transfected cells (Figure 3.4.10 B, C, D), implying that these cells formed more thrombin clot. These data indicate a potential contribution of eNOS knockdown and the elimination of the CFZ thrombo-protective effect in HUVECs.

Similarly, cells that were pre-treated with CFZ before TNFα demonstrated a significantly increased lag-time compared to TNFα treated cells, indicating a reduced rate of fibrin formation, and suggesting that CZF could attenuate the effects of TNFα in control transfected cells. However, this protective feature of CFZ was eliminated as a consequence of eNOS silencing since I observed a significant reduction in both lag time and t-Max in the eNOS siRNA CFZ+TNFα treated cells compared to control transfected CFZ+TNFα treated cells (Figure 3.4.10 A, B, C, D). This was further illustrated when I recorded the absence of the CFZ-mediated TNFα fibrin formation attenuating effect in HUVECs when eNOS was knockdown. This was demonstrated by lower absorbance and a significant increase of lag time in CFZ+TNFα treated cells compared to the TNFα alone stimulated cells in the transfected control cells, while this was not observed when eNOS was knocked down from HUVECs. These observations suggest that a potential direct correlation between eNOS expression in the endothelium and the observed CFZ mediated thrombo-protective effect.

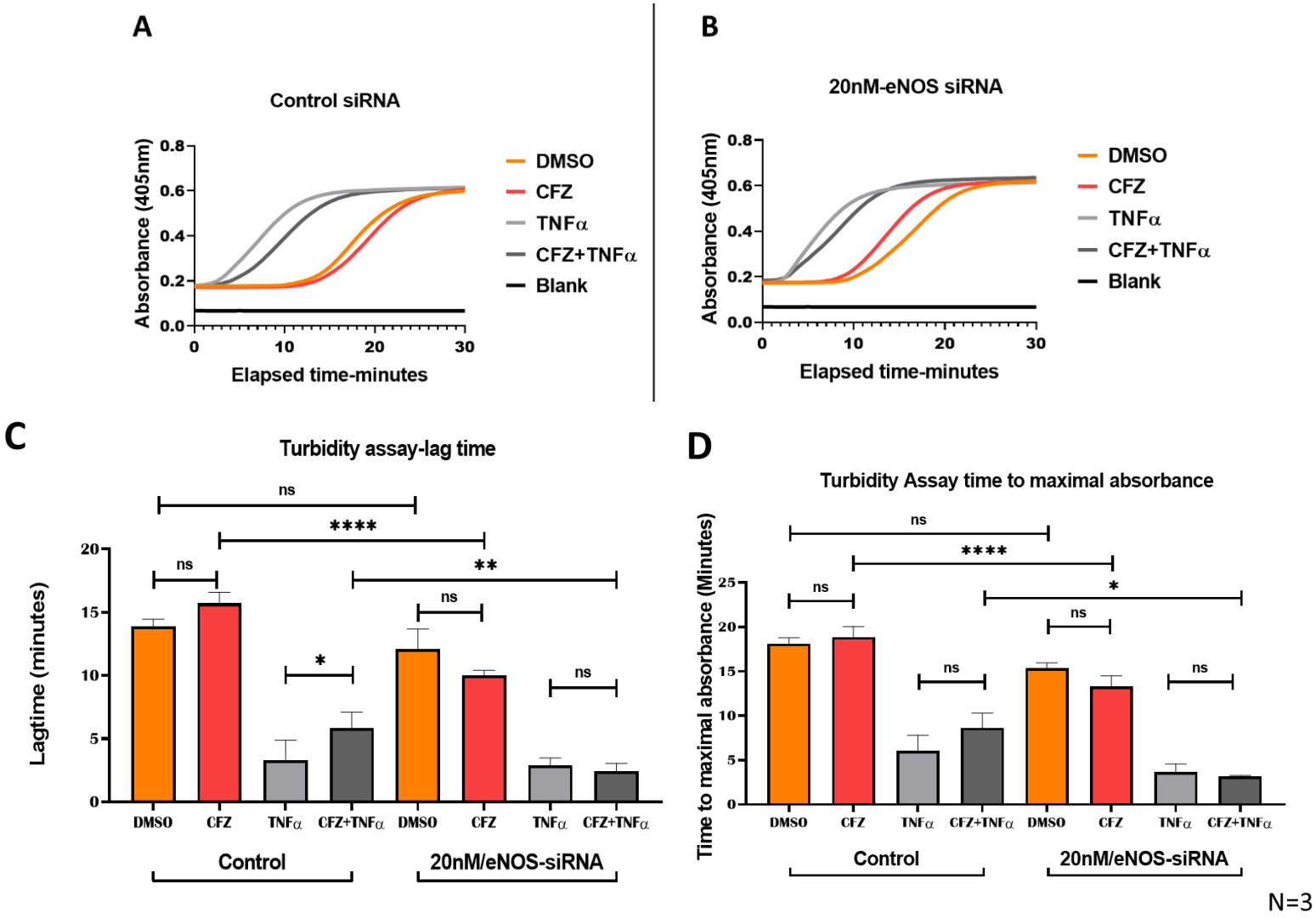


Figure 3.4.10: eNOS knockdown induced fibrin formation in HUVECs at 48 hr. HUVECs were treated with 20nM of control/eNOS siRNA, followed by washing the cells with PBS and replacing them with a fresh EBM-2 medium. Some cells were stimulated with 20ng of TNFα after 1 hour with CFZ treatment. The cells were incubated with the reaction mixture containing plasma (5mM) $CaCl_2$ and 50mM HEPES /NaCl buffer. The 48-well plate was read at 405nm for 30-minutes/30-second measurement intervals. A) The absorbance curve of control cells. B) The absorbance curve of eNOS siRNA cells. C) the lag time graphic par chart for DMSO, CFZ, TNFα and CFZ+TNFα 24 hours control and eNOS/siRNA transfected cells. D) the time to maximal absorbance of the same group of cells. DMSO, Dimethyl sulfoxide; CFZ, Carfilzomib; TNFα, Tumour Necrotic Factor. Three technical repeats were performed in one experiment, and the data were presented as the mean ± SEM. The data represented the average of three independent experiments. The expression trends of all treated cells are compared using one-way ANOVA. Significant: *P < 0.05, **P < 0.01, ***P < 0.001

3.4.2.5 eNOS knockdown induced VWF release from HUVECs

Since I observed that knocking down eNOS from HUVECs eliminated CFZ mediated cytoprotective effect, I hypothesised that it could affect the VWF release from HUVECs in a similar manner. For this purpose, anti-VWF-FITC immuno staining was conducted (Methods 2.6.1). The cells were first transfected with control siRNA or 20nM of eNOS siRNA for 24 hours; then, the cells were replaced with a fresh EBM-2 medium and treated with 750 nM CFZ for 1 hour (Methods 2.8). After 24 hours of recovery, transfected cells were stained with anti-VWF-FITC to visualise the extent of VWF expression in HUVECs (Methods 2.6.1). There was a comparable expression of VWF in control siRNA transfected CFZ treated cells compared to the transfected control DMSO cells (Figure 3.4.11). This implies that CFZ did not induce VWF release from HUVECs; thus, there was no pro-thrombotic activity in HUVECs. On the other hand, silencing of eNOS from HUVECs led to a great release and observable string formation of VWF in eNOS siRNA CFZ transfected cells compared to eNOS siRNA DMSO control cells (Figure 3.4.11). This suggests a direct correlation between nitric oxide expression in HUVECs and the CFZ inhibition effect of VWF release from HUVECs.

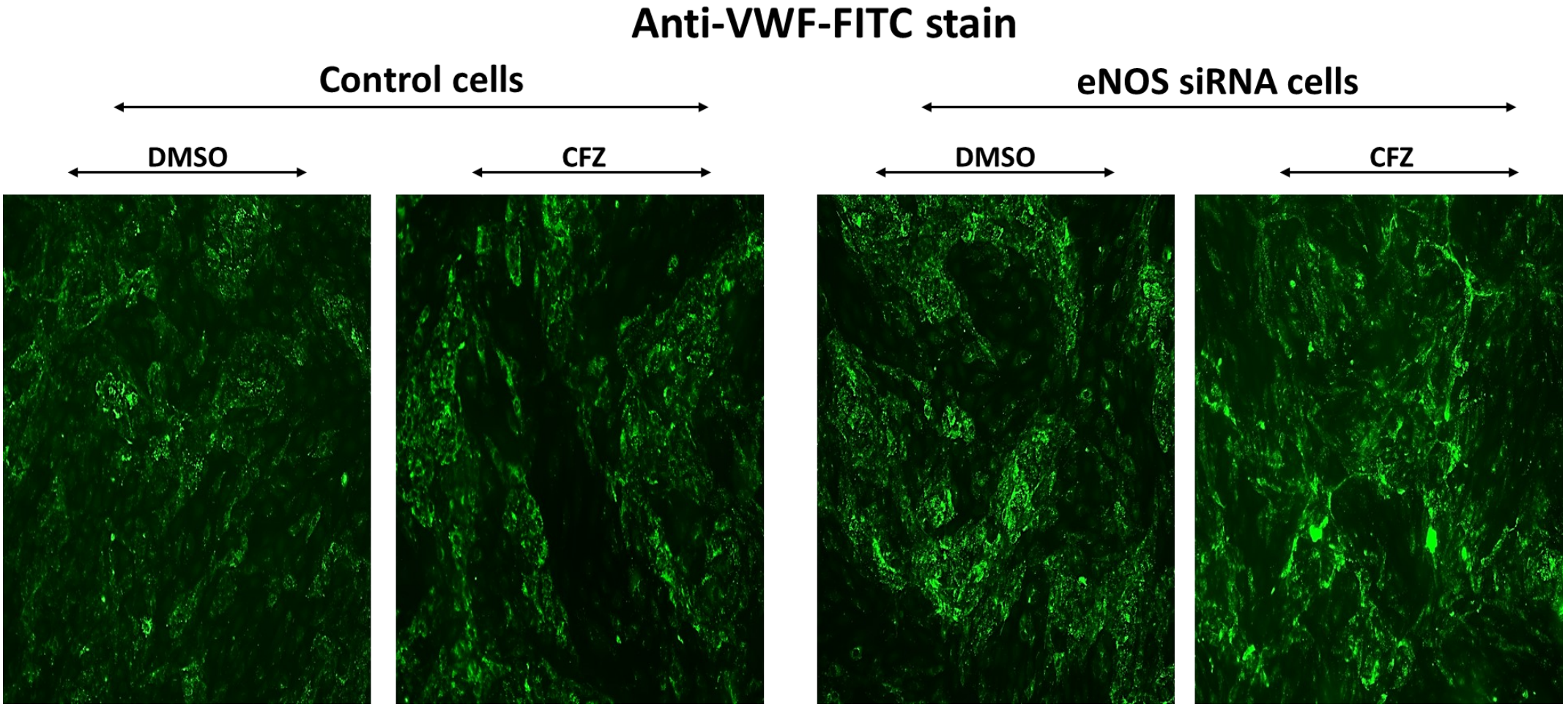


Figure 3.4.11: eNOS knockdown induced VWF release from CFZ treated HUVECs. HUVECs were treated with 20nM of control/eNOS siRNA for 24, followed by washing the cells with PBS and replacing them with a fresh EBM-2 medium. The cells were treated for 1-hour with 750nM CFZ or DMSO. The cells were permeabilized with 1x triton and stained with anti-VWF-FITC and visualised through a fluorescent microscope (10X objective).

3.4.3 Discussion

According to the data obtained from previous chapters, there was a lack of evidence to support the hypothesis that CFZ induces ER stress in HUVECs in a similar manner to the effect of CFZ on MM cells. Indeed, CFZ showed a cytoprotective, anti-thrombotic and anti-inflammatory effect in HUVECs, which was proved earlier at the cellular and functional level. This chapter aimed to identify the potential key regulator of these CFZ effects on the endothelium.

Initially, I hypothesised that silencing BiP from HUVECs would trigger CFZ-mediated activation of ER stress and consequently pro-thrombotic activation in HUVECs. There were two main reasons why BiP was selected from all other ER stress markers to be studied as a critical regulator: 1) I observed that BiP overexpression was consistently upregulated among all experiments when ER stress was activated with tunicamycin or with sub-confluence cells, while other markers did not maintain the same expression suggesting that BiP could be the key regulator of the ER stress response in HUVECs. 2) According to the well-known significance of BiP in the regulation of ER stress responses in the literature, which has identified an over-expression of BiP as the definition of ER stress (330, 455, 456); thus, I hypothesised that depletion of BiP could induce ER stress and consequently pro-thrombotic activation in HUVECs.

According to Vitale *et al*. inadequate BiP availability was a definitive reason for proteostatic ER stress and UPR activation in Hela cells. (330) Moreover, Kawaguchi and his colleagues reported that BiP knockdown in mice led to significant induction of ER stress and cell death in mice. (457) However, this was not consistent with my findings; I found that silencing BiP expression in HUVECs did not induce ER stress or enhance the ability of CFZ to induce ER stress in HUVECs. This could be because the endothelial cells can recruit another mechanism to control healthy protein manufacturing and degradation when ERAD is impaired, such as autophagy. (458) Alternatively, the load vs capacity mechanism, where cells reduce the load of protein production, thus, restoring cellular homeostasis, could be another mechanism used by HUVECs in this manner. (333) Another explanation may be that the ubiquitination proteasome system can regulate protein turnover when BiP is impaired. (459) Indeed, this agrees with my previous observations, where I found a consistent significant upregulation of ubiquitin expression at 24 hours recovery after 1 hour of CFZ

treatment. This implies that the ubiquitin system could partially prevent ER stress activation in HUVECs when BiP is knocked down. Other ER chaperone proteins, such as calreticulin, can contribute to ER stress regulation once there is a reduction in BiP expression. (460, 461) This could be another mechanism involved to avoid ER stress activation in HUVECs when BiP expression is reduced. Thus, collectively all these facts could explain the absence of ER stress activation I found when BiP production was impaired in HUVECs.

It is well-established that there is a direct correlation between ER stress and endothelial dysfunction. (462) Osman *et al*. proposed a direct interplay between the activation of ER stress and the release of endothelial pro-inflammatory and pro-thrombotic particles. (374) Another study suggested that ER stress activation in endothelial cells was directly correlated with pro-thrombotic activation, including the release of VWF from the affected endothelium. (107) However, all these facts were reported during active ER stress in the endothelium, which was not found in my study when BiP was knocked down. Therefore, this could explain the absence of negative consequences in the normal cellular coagulator balance and the alteration of the VWF release profile upon the silencing of BiP from HUVECs where there was no induction of ER stress. Generally, according to my data, I can conclude that BiP knockdown was insufficient to induce ER stress in HUVECs or render the cell to induce VWF secretion.

Since BiP knockdown did not explain the apparent cytoprotective effect of CFZ, therefore, I hypothesised that eNOS could potentially be an alternative regulator of the CFZ cytoprotective effect in HUVECs. Two main reasons were behind my selection of eNOS for this purpose: 1) It is well established that BTZ cytoprotective effect is partially dependent on the nitric oxide pathway. (290) 2) I observed that CFZ significantly induced the expression of eNOS and phosphorylation of eNOS in HUVECs; thus, I proposed that similar to BTZ, CFZ could induce cytoprotective effect employing eNOS dependent mechanism. eNOS is constitutively expressed in endothelial cells in response to the mechanical, humoral, or pharmacological stimulus. (463) eNOS action is controlled primarily by multisite phosphorylation and protein-protein interactions. (463) There is a direct positive correlation between the extent of eNOS phosphorylation and its activity. (464) Tyrosine phosphorylation of eNOS controls myocardial survival once an ischaemic insult happens. (465) Li and his colleagues

reported that reduced eNOS phosphorylation is a means of vascular dysfunction in diabetic vascular mice. (466) According to Mal *et al*. eNOS expression and eNOS phosphorylation are a determinant of cardioprotective effects. (467) Taken all these facts, the significant induction of both eNOS expression and eNOS phosphorylation mediated by CFZ encouraged me to hypothesise that CFZ could potentially deliver the observed endothelial cytoprotective effect in a similar manner.

Interestingly, upregulation of BiP upon eNOS knockdown indicated a potential inverse correlation between NO production and ER stress. The correlation between ER stress and the disruption of the nitric oxide pathway has previously been documented in preeclampsia (PE). (468) The expression of ER stress-related markers in preeclampsia, including BiP, was higher when eNOS expression was depleted, suggesting a correlation between the induction of ER stress and diminished production of eNOS in the endothelium. (22) In agreement, several pieces of literature have reported a correlation between NO dysregulation and the induction of ER stress. Gotoh *et al*. described that endothelial NO balance disruption was associated with the induction of ER stress in the endothelium. (469) Heng *et al.* reported induction of BiP protein expression when endothelial NO expression was reduced (470). Moreover, a direct correlation was reported between the reduction of eNOS expression and phosphorylation and the activation of ER stress in endothelial cells. (471) Taken together, there is a direct correlation between the reduction of NO in the endothelium and ER stress activation, which could explain my findings in this regard. Furthermore, to my knowledge, this is the first report of eNOS silencing in HUVECs causing an upregulation of BiP expression.

After I established the correlation between eNOS dysregulation and the activation of ER stress in HUVECs, I latterly investigated if a similar modification in coagulation and the inflammatory balance would occur. Interestingly, I found a direct negative correlation between eNOS and ICAM-1 expression in the endothelium. Indeed, this was agreed with several literatures. Jana *et al*. revealed a lower expression of ICAM-1 when there was an induction of eNOS in the aorta of C3H mice. (472) Another author reported a direct inverse correlation between eNOS and ICAM-1 expression in HUVECs under oxidative conditions. (473) In agreement, it has been reported that a reduced level of eNOS increases the adhesiveness of constitutive endothelial

membrane ICAM-1 via the Src family of protein tyrosine kinases Src-mediated phosphorylation. (474) Moreover, I observed an upregulation of TF, a major endothelial pro-thrombotic marker, upon eNOS knockdown in all eNOS siRNA transfected groups compared to their corresponding controls and, more importantly, between DMSO and CFZ eNOS knocked down cells. This implies a direct link between eNOS expression and the regulation of ICAM-1 and TF expression; it also indicates that silencing eNOS from the endothelium eliminates CFZ thrombo-protective effect and renders the cells to become more pro-thrombotic. This was further reflected in alteration of the lag-time in these cells leading to faster clot formation, probably due to enhanced TF expression, as shown in the turbidity study. These findings provided evidence of the potential correlation between eNOS expression and the induction of TF expression, thus activating the pro-thrombotic situation in HUVECs. In agreement with my findings, Wang *et al*. demonstrated a correlation between elevated tissue factor expression and lack of eNOS. (475) Similarly, data from Yang *et al*. found that increased creation of endothelium-derived nitric oxide decreased cytokine and the endotoxin-induced expression of tissue factor, thus, the pro-thrombotic phenotype of endothelial cells. (423) In keeping with this, eNOS knockdown enhanced soluble ICAM-1 release in CFZ treated cells. Similarly, the anti-thrombotic effect of CFZ was eliminated as a result of eNOS knockdown from HUVECs, where there was a significant release and formation of VWF strings. It is known that reduced eNOS expression results in VWF release from endothelial cells, and recent data suggest that TNFα reduces eNOS expression, resulting in exocytosis of VWF from Weibel-Palade bodies. (476) Kang *et al*. demonstrated that eNOS dysregulation promoted VWF secretion in Fabry disease. (477) Moreover, it has been reported that there was an induction of endothelial VWF and soluble ICAM-1 secretion due to eNOS deficiency. (397) Qaian *et al*. proved a significant attenuation of endothelial VWF secretion when nitric oxide was overexpressed. (478) Taken together, treatment of cells with siRNA against eNOS attenuated the 'CFZ effect', suggesting that enhanced eNOS expression is at least partly responsible for the apparent protective effect of CFZ.

I also observed a significant reduction of the CFZ-mediated t-PA mRNA expression upon eNOS knockdown, indicating a potential correlation between NO production and t-PA expression. However, this was not similarly observed with CFZ-mediated TM

mRNA expression, where both eNOS knockdown and the control group showed a similar expression of thrombomodulin. In agreement with my findings, Mark *et al*. reported an alteration of t-PA activity after endothelial nitric oxide dysregulation via controlling the exocytosis of t-PA stored in Weibel-Palade body granules. (479) Moreover, Goglia and his colleagues reported a direct correlation between induced eNOS expression and eNOS-Ser(1177)-phosphorylation and the induction of t-PA activity. (480) However, the TM expression was not altered in the eNOS knocked down CFZ treated cells, which could be independent of eNOS expression in the endothelium. Even though there is a broad agreement about the role of eNOS in regulating TM expression (481), on the other hand, it has been reported that KLF-4 upregulates thrombomodulin expression in endothelial cells. (306) Interestingly, in the last data (Result 3.2.2.5), I found that CFZ induced the expression of KLF-4, which delivered a probable mechanism behind increased thrombomodulin expression, though in the presence of eNOS knockdown. In agreement with my findings, Nayak *et al*. reported that the BTZ-TM overexpression effect was dependent on the overexpression of KLF-2 and KLF-4 pathways. (290) Similarly, endothelial expression of KLF-4 has been seen to enhance the anti-thrombotic effect via the regulation of TM endothelial expression. (482, 483) Considering these facts, the endothelial cells privilege to maintain thrombomodulin expression is not completely dependent on the expression of eNOS. Generally, according to my outcomes, there is clear evidence indicating a correlation between eNOS dysregulation and an alteration of the endothelial coagulation balance. Overall, the work in this chapter has shown that the activities of CFZ in HUVECs fall into two groups; those that are dependent on eNOS (suppression of TF, induction of BiP, soluble ICAM-1, t-PA and fibrin formation) , and those that do NOT require eNOS (TM induction and surface ICAM-1 formation).

In summary, the data presented in this chapter implicates eNOS expression in HUVECs as a potentially important determinant of the CFZ cytoprotective effect in HUVECs. While the variation of BiP expression in HUVECs was not altered by this cytoprotective effect.

4. Summary, General Discussion, and Conclusion

4.1 Summary

Multiple Myeloma (MM) is a neoplastic disorder characterized by transformed cancerous plasma cell growth in the bone marrow and raised monoclonal paraprotein amounts. (11) It is a genetically complex disease generally affecting people later in life, with the most significant incidence between 65 and 70 years. (13) Cellular homeostasis is preserved by the capacity to remove irreversibly abnormal proteins with toxic impacts via an adaptable and efficient mechanism known as endoplasmic reticulum-associated degradation (ERAD), mainly via the 26S proteasome. (484) The treatment options for MM increase with the development of drugs such as proteasome inhibitors (PIs), with greatly enhanced clinical outcomes. (485) The new proteasome inhibitor of interest, CFZ, binds irreversibly to the β5 subunit of the 20S immunoproteasome, thus inhibiting ERAD function and ultimately leading to MM cell death. (486) CFZ shows enhanced efficacy and has been demonstrated effective against bortezomib-resistant MM cell lines. (90) However, various clinical trials have linked CFZ with an increased risk of cardiotoxicity and adverse vascular effects. (487) Even though significant research has been conducted in this area, there is almost an absence of research on the effects of CFZ on the endothelium.

The endothelium is a single sheet of squamous endothelial cells (ECs) covering the internal surface of blood and lymphatic vessels. (488) ECs are established to be regulators of haemostasis, vascular tone, immunity, permeability, angiogenesis, and coagulation. (108) Due to the exceptional features of endothelial cells, studying the effects of CFZ on the endothelium is a logical step in CFZ research. Therefore, I initially hypothesised that CFZ could mediate ER stress damage on the endothelium, causing enhanced vasospasms, vascular tone, vasoconstriction, diminished reaction to vasodilators such as nitric oxide (NO), and induce the pro-thrombotic and pro-inflammatory activation of the endothelium, which all could be the determinant of CFZ associated cardiovascular complications.

In my PhD project, I aimed to study the effect of CFZ on the endothelium enquiring about the potential induction of ER stress in endothelial cells (HUVECs). Significantly, CFZ induced ubiquitin expression indicating inhibition of the proteasome, although this effect was only transient, with ubiquitin levels restored to baseline after 48 hours. Interestingly, no ER stress induction was observed despite this apparent proteasomal inhibition, even when higher or multiple drug doses were used. The drug dose and exposure time were designed to closely mimic the plasma half-life and concentration achieved in vivo. Interestingly, other studies examining proteasome inhibitors have used longer incubation times and high concentrations of the inhibitor(s) being studied. However, these do not adequately represent the *in vivo* setting and are likely to produce results that may not reflect the physiological setting.

Thus, while it is possible that supra-clinical doses and exposure times may have resulted in ER stress induction, these experiments were not deemed relevant to perform. It was, however, noted that CFZ did induce ER stress in sub-confluence (~80%) HUVECS, with significant induction of BiP expression. While the natural state of the endothelium is a continuous monolayer of cells, a number of physiological and pathological states exist where the endothelium may be actively proliferating, such as wound healing and angiogenesis. Why CFZ is able to induce ER stress in sub-confluence HUVECs, but not confluence, HUVECs is not clear. However, it has been previously reported that broad-spectrum proteasome inhibitors such as MG132 also demonstrate similar contextual dependent effects on HUVECs. (489) As discussed (Discussion 3.1.3), the energy demands and protein synthesis status of proliferating endothelial cells are likely to be higher than resting cells and make them more susceptible to proteasome inhibition. Interestingly, inhibition of angiogenesis has been proposed to be an effective treatment for various carcinomas; therefore, further work to test CFZ as an anti-angiogenesis agent may be of interest. Moreover, various studies have demonstrated that tumour endothelial cells have a different phenotype than their non-malignant counterparts; thus, it would be interesting to determine if tumour ECs are more susceptible to CFZ. (490, 491)

While the initial data obtained indicated that CFZ could not induce ER stress in HUVECS, it was seen that CFZ induced a clear morphological change in the cell structure. Microscopic observations showed CFZ treated cells to be more elongated and stretched, changes that are often associated with activation of the endothelium.

The F-actin staining of HUVECs revealed that both TNFα and CFZ induced rearrangement of F-actin stress fibres along the cell's central axis, implying activation or a functional response in HUVECs; however, with a lower extent of CFZ. (27) As discussed in (Discussion 3.2.3) the organisation of the cytoskeleton of the endothelial cell is an integral part of the response and functionality of the cell. (492) The junctions between endothelial cells maintain endothelial integrity and regulate vascular development and homeostasis. (493) In general, cell-cell junctions are shown as linear morphologies connecting adjacent cells and contacting cortical F-actin. (494) Nevertheless, the endothelium is characterized by morphologically heterogeneous and very dynamic cell-cell junctions. (495) Similar to my findings, Jaime and his colleagues reported that in response to TNFα, highly dynamic discontinuous adherents junctions (AJs) in endothelial cells form when cell-cell junctions connect to the ends of stress fibres rather than to the cortex's F-actin. (380) Another author proposed that TNFα mediated microtubule rearrangement (via p38 mitogen-activated protein kinase activation) could describe the mechanism of action rearrangement in activated HUVECs. (496)

A similar elongated appearance has been observed by others in MG132 proteasome inhibitor-treated HUVECs, where the cells became elongated and stretched due to the disturbance of VE-cadherin adherent junctions and a rearrangement of actin filaments within the EC cytoskeleton, suggesting increased vascular permeability and endothelium activation in a similar manner to what I have described in CFZ-treated cells. (376) Even though these morphological alterations are known to be linked to the inflammatory response in the endothelium, equally, they describe a functional physiological response of the endothelial cells. (497) Taken together, CFZ mediated EC morphological alterations could indicate a potential alteration of endothelium physiology or an adaptable and functional response to maintain normal endothelium function.

In the absence of ER stress induction, it was next hypothesized that CFZ might induce pro-inflammatory and pro-thrombotic triggering in HUVECs and induce ER stress if the cells were exposed to relevant cytokines. Indeed, MM patients often present with elevated pro-inflammatory cytokine levels that could act with CFZ to cause phenotypical changes to the endothelium. However, in stark contrast to this hypothesis, even after both CFZ and cytokine treatment, no induction of ER stress

was observed. Instead, CFZ demonstrated an apparent cytoprotective effect on the endothelium and was able to inhibit, to varying degrees, the pro-inflammatory and pro-thrombotic effects of TNFα (Summarised in Table 4.1).

HUVECs stimulated with			
Gene/protein	**CFZ**	**TNFα**	**CFZ+TNFα**
TF	No change	Increase	Decrease
ICAM-1	No change	Increase	Decrease
eNOS	Increase	Decrease	Increase
TM	Increase	Decrease	Increase
KLF-4	Increase	Decrease	Increase
VWF	No change	Increase	Decrease
Ang-2	No change	Increase	Decrease

Table 4.1: Summary of CFZ effect on some of the pro-thrombotic and pro-inflammatory markers

In agreement with these findings, the functional analysis demonstrated that CFZ had a clear thrombo-protective effect on HUVECs. Thus, while TNFα induced TF expression and subsequent fibrin formation, CFZ was able to suppress this by reducing TF expression and subsequent Factor Xa generation. Moreover, CFZ mediated TM-upregulation was consistent with the maximum amount of APC generated. Equally, CFZ dramatically inhibited TNFα induced leukocyte adhesion to HUVECs and prevented platelet capture to VWF strings by inhibiting the release of VWF from WPBs. Collectively all these functional studies supported the initial CFZ cryoprotective findings observed at the cellular level; thus, apparently, CFZ had a cryoprotective effect in HUVECs.

TF is present in the subendothelial tissue and is considered a principle pro-thrombotic inducer of the pro-coagulation activation through its binding with the naïve FVII. (22) TNFα induces TF expression in the endothelium through various mechanisms, including the interaction between TNFα and the endothelial thromboxane receptor (TP) receptor (411) and functional interactions between c-Rel–p65 subunits of nuclear

factor kappa B and Fos-Jun heterodimers, genes known as cellular immediate-early genes, which they form the AP1 transcription factor that eventually triggers the transcription of TF, suggesting that these transcription factors play a regulatory role in TF transcription. (498) Indeed, studies on the regulation of TF gene expression in human endothelial cells have consistently shown that TNFα increases the rate of TF gene transcription, indicating that transcription can be a modulator of TF expression. (412) Thus, potential inhibitory interactions of CFZ with those signalling pathways in addition to those discussed earlier (Discussion 3.2.3, 3.3.3) could at least be involved in the regulation of the CFZ suppression effect of TNFα mediated TF expression in HUVECs.

ICAM-1 is considered a significant endothelial cell activation marker that regulates the early inflammation process by its interaction with several leukocyte ligands allowing these cells adherence to the site of the inflammation. (370) TNFα induces soluble ICAM-1 release from the endothelium via the stimulation of tyrosine kinases. (499) The NADPH Oxidase 4 (NOX4)-dependent IKKβ/ NF-κB pathway was also found to be involved in the regulation of TNFα -induced ICAM-1 expression and subsequent monocyte adhesion to endothelial cells. (500) Freitas and his group described BTZ as an NF-κB pathway modulator through its inhibitory effect on IKKβ subunits; thus, a potential drug candidate for the control of inflammatory diseases. (501) Similarly, Yang *et al*. reported that using MG-132 had improved the inhibition of the IKKβ/NF-κB signalling pathway in squamous cell carcinoma. (502) Collectively, these agents seem to have a potent inhibitory effect on the inflammatory arm of NF-κB. Thus, a similar approach of CFZ, in addition to those discussed earlier (Discussion 3.2.3, 3.3.3), could be proposed to describe the significant suppression of TNFα mediated ICAM-1 and Ang-2 expression in HUVECs. A future investigation of this mechanism as a potential CFZ regulator of pro-inflammatory suppression would be of great interest to establish further approach to study the potential utilisation of CFZ as immunomodulator in clinical practice.

Several potential mechanisms used by other proteosome inhibitors have been shown by other workers to affect eNOS. Nitric oxide (NO) is the most significant endothelium-derived substance that regulates a wide range of endothelium functions, including regulating the vascular haemostasis balance. (503) eNOS, the enzyme responsible

for NO generation in endothelial cells, is regulated by several means, including post-translational modification, phosphorylation, interactions with proteins such as Hsp90 and caveolin, as well as transcriptional regulation. (504-506) Inhibition of the proteasome is suspected to be involved in regulating eNOS expression and activity, but there are surprisingly few data available on this topic. Similar to my findings, Stangle *et al*. found that low-doses of the MG-132 proteasome inhibitor improved eNOS expression, activity and enhanced endothelial function in bovine pulmonary artery endothelial cells (CPAE cells); besides, it improved endothelial-dependent vasorelaxation in rat aortic rings. (390) He suggested that the increase in eNOS protein levels is due to *de novo* protein synthesis instead of the proposed accumulation of eNOS following proteasome inhibition. (390) Another study has suggested that increased eNOS mRNA levels after MG-132 treatment of HUVECs could result from extended mRNA stability and/or *de novo* transcription. (507) Zhang and his colleagues observed nuclear translocation of the transcription factors specificity protein 1 (Sp1) and JunD, a member of the transcription factor activator protein (AP)-1 family, after inhibition of the proteasome, which could clarify the cellular mechanism behind MG-132 induced eNOS expression and phosphorylation in HUVECs. (508) Interactions between eNOS and regulatory and structural proteins provide another mechanism for controlling NO synthesis in HUVECs. (509) eNOS activity is controlled by its localization in caveolae in collaboration with numerous proteins. (510) Under the condition of proteasome inhibition, a binding of heat shock protein 90 (Hsp90) to eNOS increases calmodulin affinity and reduces its binding to caveolin-1, enhancing eNOS expression, phosphorylation and activity. (511) Additionally, Hsp90 recruits the Ak strain transforming (Akt) protein (serine/threonine kinase) to the Hsp90/eNOS complex. Akt is responsible for phosphorylating eNOS, increasing NO amount produced. Taken together, these mechanisms, besides those described earlier (Discussion 3.2.3, 3.3.3), could explain the potential cellular mechanisms recruited by CFZ to induce eNOS expression in HUVECs.

Thrombomodulin is an endothelial cell surface integral membrane protein which performs an essential role in the anti-coagulant system by acting as a cofactor in the thrombin-induced activation of protein C. (512) As discussed earlier (Discussion 3.2.3, 3.3.3), BTZ mediated eNOS-dependent thrombo-protective effect was linked to increased expression of KLF-2,4 in HUVECs. I found CFZ induced the expression of

both eNOS and KLF-4; thus, this could be one of the potential pathways that regulate CFZ induced TM expression in HUVECs.

A study indicated that NF-κB inhibition effectively prevented cytokine-induced TM down-regulation *in vitro* and animal models through a noncanonical binding site or a classic consensus sequence. (513) The author suggested that NF-κB inhibits TM expression via interfering between E26 transformation-specific or E-twenty-six (ETS) transcription factors binding to the TM promoter or inhibiting TM transcriptional activity. (513) Another study has revealed that by competing for limited pools of transcription coactivator p300/CBP, cytokine-induced NF-κB activation indirectly inhibits TM expression. (514)

The suppressive effect of NO on the NF-κB pro-thrombotic pathway is also widely investigated. NO suppresses NF-kB activity by stabilizing and increasing the activity of the NF-κB inhibitor, IκB-α, by preventing its degradation from NF-κB, and by increasing the expression of IκB-α mRNA without affecting that of NF-κB subunits, p65 or p50 (437) NO has also been shown to inhibit NF-κB DNA binding by S-nitrosylating the cys62 residue in the p50 subunit. (515) S-nitrosylation of transcription factors by NO does not affect c-jun DNA binding, thus indicating that NO-mediated S-nitrosylation of transcription factors affects gene transcription selectively. (516)

Thus, it could be speculated that a potential interaction between CFZ-mediated eNOS expression and the inhibitory effect of NF-κB could be partially involved in regulating induced TM expression mediated by CFZ in HUVECs. Collectively, all these mechanisms, in addition to those described earlier (Discussion 3.2.3, 3.3.3), could be involved in the regulatory role of CFZ in the TM expression in HUVECs.

VWF is a significant component synthesised and stored in the endothelium that majorly initiates platelet adhesion upon vascular damage (252). Several experimental and clinical reports indicate that elevated VWF levels reflect injury to the endothelium, activation, and endothelial dysfunction(252). My data showed that TNF-α stimulates the endothelium to release VWF, which is consistent with the well-known fact about the pro-thrombotic effect of TNFα on the endothelium. (252) TNFα stimulates the release of ultra-large and hyperreactive VWF (ULVWF) from the activated endothelium and inhibits ULVWF cleavage by ADAMTS13; thus, it leads to the build-up of hyperreactive ULVWF on the surface of endothelial cells and in the plasma. (517) Consequently, this stimulates platelet aggregation and adhesion on the vascular

endothelium. (517) The classical NFκB pathway is stimulated by TNFα, via toll-like receptors (TLR-2 and TLR-4), or NEMO (NFκB essential modulator) in the presence of heterodimer IκB kinase-α/β (IKKα/IKKβ) complex, which eventually induces VWF release from the endothelium. (518) The inhibitory effect of NO on VWF and Ang-2 release from the endothelium has been intensively investigated. It has been reported that NO-mediated overexpression of the annexin A2 (AnxA2)-S100A10 complex meaningfully diminishes acute Weibel-Palade bodies (WPB), storage of VWF and Ang-2 in the endothelium (476). Similar to my findings, Caputa *et al*. reported that MG132 strongly suppressed the VWF release from the endothelium, which depended on eNOS overexpression. (519) In agreement, Kenji and his group reported that MG132 significantly suppressed the release of VWF and ICAM-1 via the suppression of the NFκB pathway and histone deacetylase 3 (HDAC3) in HUVECs. (520) Moreover, *in vitro* study revealed that MG132 significantly suppressed the secretion of both ICAM-1 and VWF in the brain endothelial via the suppression of MAP kinases and (NF)-κB p65. Thus, besides those described earlier (Discussion 3.2.3, 3.3.3), all these mechanisms could be a potential target of the CFZ inhibitory effect on VWF in HUVECs. Taken together, CFZ exhibits cytoprotective effects by controlling to varying degrees the expression of some of the well-known pro-thrombotic and pro-inflammatory mediators (Figure 4.1).

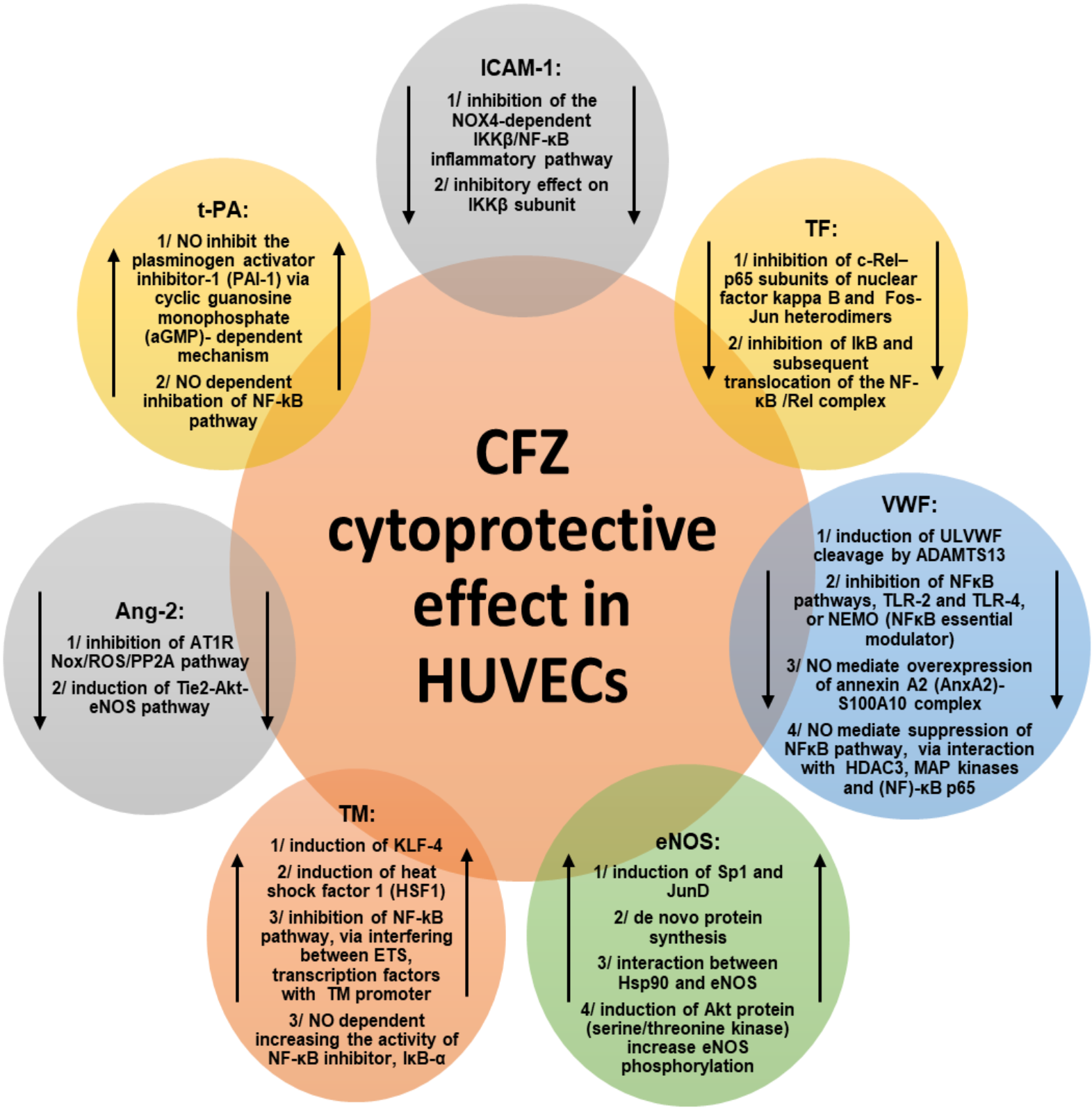


Figure 4.1: Diagram of potential pathways involved in CFZ cytoprotective effect in HUVECs.

These findings raised the question about the potential regulator of CFZ cryoprotective effect in HUVECs. As I discussed earlier, I hypothesised that either BiP or eNOS could be the potential regulator of this phenomenon (Discussion 3.4.3). Therefore, I initially proposed that silencing BiP from HUVECs could eliminate the cellular protection mechanisms, thus inducing ER stress activation and, consequently, the pro-thrombotic activation in HUVECs. To study this, BiP siRNA was used to knock down BiP protein expression in HUVECs. Interestingly, even though BiP is well-established to play a crucial role in regulating ER stress (446), I found that BiP knockdown from HUVECs was not sufficient to induce CFZ to mediate ER stress. Similarly, as expected, there was no induction of VWF expression profile and fluorescence intensity caused by BiP silencing from HUVECs. These data suggested that BiP was not the potential key regulator of the CFZ cytoprotective effect, at least under my experimental conditions.

As discussed earlier (Discussion 3.4.3), several mechanisms were proposed to explain the absence of ER stress activation upon BiP knockdown from HUVECs. The autophagy, load vs capacity, and the ubiquitination proteasome system all can regulate protein turnover when BiP is impaired from HUVECs. In agreement, Cheng *et al*. reported that MG123 induced autophagy in HUVECs when BiP-proteasome function was impaired via the human, murine double minute 2 (HDM2)-dependent mechanism degradation of cytoplasmic p53 at 26S proteasome, thus restoring normal protein turn over. (458) Similarly, *in vitro* study revealed that inhibition of endothelial cells by MG123 rapidly increased the concentration of microtubule-associated proteins 1A/1B light chain 3B (LC3B), a central cellular regulator of autophagosome biogenesis and autophagy substrate selection; thus, inducing the autophagy and reduced the accumulation of polyubiquitinated proteins. (521) The load vs capacity is an adaptive cellular response aimed to reduce protein generation via the suppression of transitional and transcriptional processes; thus, decrees the dependence of proteasome degradation. Holger *et al*. claimed that this mechanism is a potential cellular mechanism utilised by the affected cells when proteasome function is impaired. (522) Similarly, Giada and his colleague reported that adverse load vs capacity mechanisms render the multiple myeloma cells more vulnerable to the action of proteasome inhibitors, suggesting the crucial role of this mechanism when there is inhibition of proteasome function. (523) Collectively, all these mechanisms were

proposed to be supplementary mechanisms recruited by HUVECs to avoid a potential activation of ER stress due to BiP knockdown.

Finally, an eNOS selective siRNA was used to silence the expression of this protein from HUVECs. Interestingly, I found that knocking down eNOS from HUVECs correlated with the induction of ER stress separately from the CFZ effect. As discussed earlier (Discussion 3.4.3), the correlation between the absence of endothelial cell eNOS expression and the induction of ER stress is widely accepted. Lenna *et al*. reported a significant induction of BiP, a significant ER stress regulator, up on suppressing eNOS expression in endothelial cells. (524) Similarly, Basha and his group established the correlation between impaired endothelial eNOS expression and the induction of ER stress. (525) *In vitro* study revealed that the induction of ER stress in HUVECs by oxidized low-density lipoprotein (ox-LDL) was essentially correlated with significant suppression of eNOS expression, activity and increased dephosphorylation of eNOS at Ser1179, implying a direct correlation between ER stress and alteration of eNOS expression. However, the mechanism behind it is still poorly understood. Guha *et al*. proposed activating the mammalian target of rapamycin complex 1 (mTORC1) through the eNOS-RagC pathway induces ER stress induction in eNOS silenced HUVECs. (526) Another study indicated that the PI3K-Akt-eNOS signalling pathway is the mechanism behind ER stress induced by eNOS suppression in endothelial cells. (527) Taken together, besides those described earlier (Discussion 3.4.3), these mechanisms could at least explain the potential cellular ground of the induced ER stress upon eNOS silencing from HUVECs.

I then asked if a similar effect could be caused regarding the pro-thrombotic and the pro-inflammatory response. As expected, silencing of eNOS from HUVECs induced the cells to activate pro-thrombotic and pro-inflammatory responses. This was verified by the significant induction of TF mRNA in all eNOS siRNA transfected cells, which was also mirrored with the fibrin clot formation findings. Similar to this effect, I found that silencing of eNOS caused the cells to become more prone to pro-inflammatory activation, where all eNOS siRNA transfected cells expressed significant ICAM-1 compared to their corresponding controls. These findings indicate the importance of eNOS in regulating the haemostasis and inflammatory balance separate from the CFZ effect in HUVECs. However, I also found a significant difference in TF and soluble

ICAM-1 expression between CFZ-eNOS siRNA transfected cells and its corresponding vehicle-DMSO eNOS siRNA transfected cells. Besides, I found that silencing eNOS from HUVECs reduced the expression of the primary endothelial-derived fibrinolysis regulator, t-PA, mediated by CFZ in HUVECs. However, there was no effect observed regarding CFZ mediated TM expression when eNOS was knocked down from HUVECs, where there was a continuous induction of TM in both control and eNOS siRNA transfected cells.

In agreement on eNOS knockdown, more fibrin formation was observed in CFZ pre-treated TNFα stimulated cells than its corresponding control, implying loss of CFZ thrombo-protective effect of CFZ. Similarly, I found a remarkable release of VWF and observable VWF string formation up on eNOS knockdown in HUVECs. In summary, my data indicated that eNOS expression in HUVECs is a potentially important regulator of CFZ cytoprotective effect in HUVECs under my experimental setting.

As discussed earlier (Discussion 3.4.3), the correlation between eNOS and ICAM-1, TF expression in HUVECs is widely investigated. Liu and his group documented the negative correlation between eNOS expression and eNOS phosphorylation with ICAM-1 expression in HUVECs, dependent on PI3K/Akt signalling activation. (528) In agreement, Olena and his group found that a transient reduction of eNOS expression in human aortic endothelial cells was associated with significant induction of ICAM-1 expression. More importantly, in an animal study, they found that administration of donor nitric oxide inhibited ICAM-1 expression mediated by fructose, whereas the blocking of nitric oxide synthase enhanced it. (529) In a similar manner, decreased expression of eNOS caused by C-reactive protein in human aortic endothelial cells (HAECs) was associated with significantly increased expression of endothelial cell TF expression, suggesting a direct correlation between eNOS and TF expression. (530) Another study revealed that increased NFκB and mitogen-activated protein kinase activities caused by eNOS reduction was associated with amplified TF expression. (531) An increased phosphorylation of NFκB and extracellular signal-regulated kinases 1 and 2 (ERK1/2) was linked to the induction of TF expression. (532) In agreement, an animal study revealed that preventing endothelial eNOS expression accelerated TF expression via an NF-κB pathway-dependent mechanism. (533) NF-κB binds to distinct regions of the TF and ICAM-1 promoters, including interaction with a proximal enhancer (-111 to +14 bp) containing three overlapping Egr-l/Spl binding

sites. (533) Thus, a potential direct interaction between CFZ and NF-κB mediated TF, VWF and ICAM-1 promoter may be involved in regulating CFZ cytoprotective effect in HUVECs. As I mentioned earlier (Discussion 3.4.3), the involvement of eNOS in the regulation of endothelium TM expression is well-established. However, other cellular regulatory elements were discovered recently. Among them the expression of KLF-4 has showed a crucial role in the regulation of TM expression, where an increased expression of KLF-4 was linked to enhanced endothelium TM expression. Since I observed CFZ induced KLF-4 expression in HUVECs I proposed that a potential direct correlation between CFZ mediated KLF-4 expression and TM expression independent from eNOS expression in HUVECs. Collectively, it seems that eNOS expression in HUVECs was a potential regulator of the CFZ mediated cytoprotective effect, apart from TM expression which was independently regulated from eNOS expression in HUVECs.

In summary, the data generated by this study revealed that CFZ did not induce ER stress, pro-thrombotic, or pro-inflammatory activation in HUVECs. Moreover, some evidence showed a cryoprotective effect of CFZ in HUVECs. Lastly, I demonstrated the potential involvement of eNOS expression in HUVECs in regulating the CFZ cytoprotective effect.

4.2 General discussion

Even though CFZ is claimed to be one of the most cardiotoxic drugs used in multiple myeloma, it is difficult to evaluate the actual incidence of drug-induced cardiovascular diseases(10). This is because most present data about drug-induced cardiovascular disorders were obtained in clinical trials, from which patients with acute cardiovascular comorbidities were omitted. However, in real-life clinical practice, different parameters could involve assessing the risk of the development of CAVEs in MM patients. MM patients are typically older people with a median age of > 66 years at the time of diagnosis, so that most of them are considered a high-risk group and present several comorbidities of cardiovascular disease at the time of diagnosis. (534) Arrhythmias, sinus node dysfunction and bradyarrhythmia are common cardiac abnormalities observed in MM patients, where arterial fibrillation is the most common arrhythmia

among these patients. (535) Rosenthal *et al*. demonstrated that amplified levels of B-type natriuretic peptide (BNP) and N-terminal pro-B-type natriuretic peptide (NT-proBNP), an indicator of heart failure, were correlated with endothelial dysfunction in MM patients. (487) Among 22,076 patients newly diagnosed with MM, 63% of these patients have reported a variety of cardiac comorbidities, including arrhythmias (14%), congestive heart failure (8%), and ischemic heart disease (14%). (536) In general, there is a clear association between MM and a wide range of endothelial dysfunction, implying the association of MM and various cardiovascular disorders. Moreover, MM patients are exposed to numerous chemotherapies, including autologous stem cell transplantation related medications and immunomodulatory drugs. Additional comorbidities such as cardiac amyloidosis, anaemia, and renal dysfunction, could be additional risk factors of MM associated cardiac abnormalities. (537) Cardiomyopathy is often reported in MM patients, with 12%-30% due to amyloidosis and deposition of protein chains in the myocardium. (538) A joint analysis of phase-four clinical studies in patients with progressive MM demonstrated that 73.6% and 70% of patients had a history of CAVEs and baseline cardiac risks, respectively. (539) In agreement, a retrospective observational cohort study among 31,193 MM patients showed that 66% of them had a history of severe cardiac abnormalities, including cardiac heart failure, arrhythmias, and ischemic heart disease. (538) Taken together, the comorbidities of MM should be considered in the assessing of CFZ associated CAVEs (Figure 4.2).

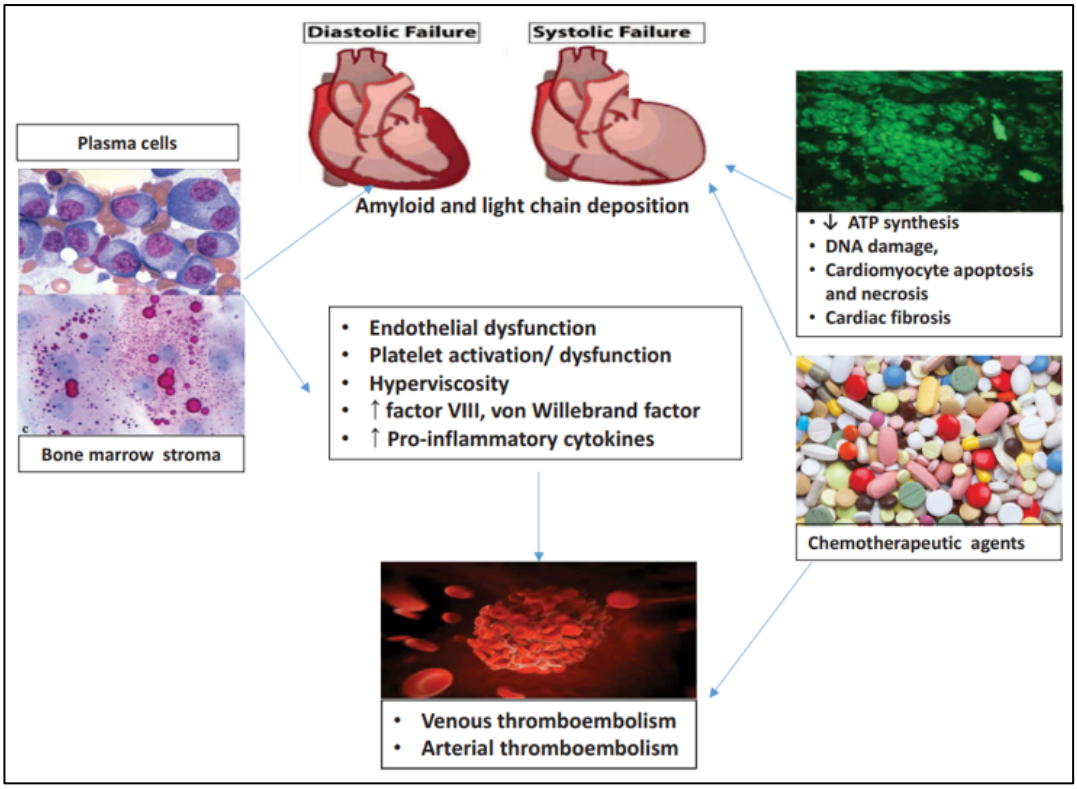


Figure 4.2: MM potential mechanisms to induce cardiovascular complications. This figure was taken from (Stroka, Cellular and molecular bioengineering, 2011). (535)

Emerging evidence has demonstrated the crucial role of circulating endothelial progenitor cells (EPCs) in the neovascularization of injured blood vessels (540). Consequently, EPCs dysfunction is correlated with atherosclerosis, thrombotic complications, and other cardiovascular diseases (541), while a reduced number of these cells is an independent predictor of mortality and morbidity of cardiovascular disorders (541). It has been demonstrated that the proteasome inhibitor MG132 suppress the function, number, proliferation, migration capacity and increases apoptosis of EPCs by a mechanism that involves nitric oxide synthase inhibition. (542) Additionally, proteasome inhibition in proliferating endothelial cells significantly induced the apoptosis of these cells by the involvement of caspase cascade activation. (542) Therefore, CFZ could also similarly impact the EPCs and inhibit endothelium regeneration, which could be another possible mechanism of CFZ associated CAVEs.

Cardiomyocyte survival mainly depends on the ubiquitin-proteasome system (UPS) that primarily regulates protein synthesis, folding and turnover (6). In common with MM cells, proteasome activity and protein turnover are higher in the heart tissue compared

with other tissues, and the potential inhibition of proteasome activity in cardiac myocyte by CFZ could lead to intracellular accumulation of abnormal proteins that can combine into aggresomes, aggregates and oligomers, all of which are toxic to cellular function and hence promote cellular apoptosis. (543) Indeed, this has been demonstrated where the activation of caspase 3/7-mediated apoptosis via the activation of the NF-κB pathway mediated by BTZ was proposed as one of the mechanisms involved in BTZ myocardium toxicity. (71) An *In vivo* study investigated the effect of CFZ on heart (myocardial) tissue, and peripheral blood mononuclear cells (PBMC) revealed that CFZ reduces mouse left ventricular function by enhancing protein phosphatase-2 (PP2A) action and inhibiting activated protein kinase subunit α (AMPKα) regulatory axes. (95) All of these could explain the mechanistic basis for the cardiac toxicity resulting from CFZ.

Lastly, varying treatment parameters, such as dose and infusion duration-dependent variables, could be involved as factors of CFZ correlated CVAEs. This was demonstrated in clinical practice by Bringhen and his colleagues, where they found that amplified grades of CAVEs have been correlated to increased dosage of CFZ. (544) Similarly, a systemic review and meta-analysis concluded that using a higher dosage of CFZ was associated with a significant increase of CFZ associated cardiovascular adverse events. (94) The direct comparisons between two different clinically relevant dosages of CFZ, less than 45 mg/m2 and higher than 45 mg/$m^{2,}$ were associated with a 6.4% 11.9% rate of CAVEs, respectively (P = .02). (94) Similarly, an *in vivo* study by Brioli *et al*. claimed a progressively increased incident of CAVEs correlated with the increased concentration of CFZ in MM patients. (545) Similarly, the drug infusion rate was also reported as another variable determining the incidence of CAVEs associated with CFZ. A systemic review and meta-analysis study indicated that a longer infusion duration (30 minutes) exhibited a trend toward a greater ratio of CVAEs (11.0%) compared to shorter infusion duration (≤10 minutes), where this correlated with a lower trend of CAVEs (6.7%). (94) In agreement, Kyriakos and his colleagues reported that CFZ administration in a 30-minute IV infusion rate was commonly well-tolerated, remarkably active, and had lower toxicity in patients with MM compared to longer infusion time. (314) Thus, treatment dependent variables could be a highly suitable candidate to be involved in the regulation and assessment

of CFZ associated CAVEs. In summary, all these described variables could be attributed to the development of CFZ associated cardiovascular complications.

It is ordinary to report any emerging adverse events mediated by any newly released drug, particularly in cancer therapy. There was a raised report about the cardiovascular adverse events associated with CFZ. (546) However, as I stated earlier, there was an extreme deficiency of *in vitro* study to examine the cellular mechanisms behind these events. Indeed, this was a significant challenge for me since comparing my findings with other studies was not approachable. Therefore, I found the most logical approach was to compare my findings with those published about the first-generation proteasome inhibitor, BTZ, since they share the same principle and mode of effect. Similar to my findings, there was an extreme reporting of the significant toxicity of BTZ at the beginning of the drug approval and administration process as a treatment of MM. (547) For example, Diwadkar *et al.* claimed that there is growing evidence that BTZ can lead to cardiac adverse events, including atrioventricular block and left ventricular dysfunction. (548) In agreement, Abdullah and his colleagues reported that BTZ was associated with the development of acute congestive heart failure in some MM patients. (549) However, recent data suggested that BTZ provides a cytoprotective effect and is clinically beneficial in different medical conditions. In this manner, Christopher *et al*. reported that BTZ showed significant effectiveness in treating severe refractory thrombotic thrombocytopenic purpura (TTP) cases involving excluding the autoreactive plasma cells generating anti-ADAMTS13 antibodies. (550) In agreement, BTZ showed remarkable advantages in the treatment of autoimmune diseases and graft versus host disease (GVHD) in animal models by altering immune responses through inhibition of dendritic cells (DCs) maturation. (551) These suggestions were supported by Xuebin and his group, where they found that BTZ has a potential role in the treatment of Immune thrombocytopenia via the involvement in the correction of abnormal T cell immunity response. (552) In an animal model study, they found that BTZ is an efficient inhibitor of neuroblastoma angiogenesis and cell growth and interestingly recommended establishing a clinical study of BTZ in paediatric neuroblastoma. (553) Similarly, Angela and her colleagues proved the synergised effect of BTZ combined with TNFα in pre-clinical models of human bladder cancer via the induction of apoptosis and the inhibition of angiogenesis. (554) Regarding the cellular level, BTZ was reported to mediate several

features of the cytoprotective effect in different experimental conditions. Among them, it has been documented that BTZ induced the expression of heat shock protein A1B/B1, which has a significant role in the folding of newly translated proteins in the cytosol, stabilises existing cytosol proteins against aggregation, intensify the antioxidant protection of cells and regulation of the ubiquitin-proteasome pathway, thus providing a cytoprotective effect in the cells. Indeed, the latter observation is highly correlated to my study findings, where I found that CFZ induced the ubiquitination response but not ER stress, suggesting the potential involvement of these heat shock proteins in the regulation of the ubiquitination expression found in my experiment, thus involved in the regulation of CFZ cytoprotective effect. Moreover, an *in vivo* study found that administration of BTZ twice weekly for five weeks to obese mice enhanced insulin resistance, JNK inhibition in skeletal muscle, reduced ER stress marker levels, and increased AMPK phosphorylation, thus delivering a significant cytoprotective effect. (555) Considering all these described facts about BTZ and linking it with my novel finding of CFZ cytoprotective effect, it would be remarkable to examine CFZ cytoprotective effect *in vivo* studies and perhaps in clinical practice in the long-term future.

4.2.1 Limitations of this work

Several limitations were encountered in this study; initially, all the experiments were conducted using one cell line of human endothelial cells, the human umbilical vein endothelial cells (HUVECs). Due to the apparent extent of heterogeneity among endothelial cells from various tissues, choosing the proper type of cells are vital for a productive experimental setting. HUVECs may not be illustrative of the real *in vivo* situations as they originate from immune-privileged fetal tissue and might vary considerably from adult vascular endothelium. (79) Thus, outcomes achieved from these cells should be treated with caution due to the cautious relevance in adults. (79) Therefore, whilst HUVECs deliver a great initial model, adult endothelial cells, such as cells from large vessels (the aorta or saphenous vein), may be the ideal option for a clearer understanding of the tissue-specific dynamics. (556) These primary adult cells present a new point of view on the human endothelium, as they intimately characterise their natural environment. (556) Nevertheless, the restricted accessibility of human endothelial tissue represents the main restriction. However, a considerable number of

scientists recognise HUVECs as the backbone of vascular endothelium research, as they are relatively easy to culture, highly proliferative, readily available, and capable of migrating and invading new tissues. (557) This implies that either HUVECs or adult endothelial cells could be appropriate in the field of cardiovascular research.

Another limitation observed in this study was that all the experiments were conducted under static conditions, which does not truly represent the natural shear stress in physiological conditions. Ala *et al*. described laminar shear stress as the most physiologically relevant environment in vascular endothelium studies. (558) This experimental setting is believed to inhibit both endothelial cell apoptosis and proliferation. (559) Some researchers had observed an alteration of the haemostasis response in endothelial cells when cultured under static conditions, which was not reflected in the controlled balanced haemostasis regulation found under shear stress. (560) Collectively, culturing the cells under shear stress provides a more accurate reflection about the interaction inside the human vascular system, thus delivering a robust conclusion.

In clinical practice, CFZ is given after the exposure of MM to other chemotherapy and immunomodulatory drugs. (561) Thus, CFZ may not induce ER stress or cytotoxic effects on HUVECs as a mono drug but may have a potential synergistic effect if combined with other MM therapies, such as dexamethasone or BTZ. This was demonstrated in clinical practice by Zou and his colleagues, where they reported that CFZ combined with dexamethasone showed a significant cytotoxic effect against MM compared to CFZ treatment alone. (562) In agreement, a head-to-head comparison of CFZ with CFZ plus dexamethasone showed a more effective outcome and cytotoxic profile with the latter group against MM cells. (563) Taken together, it seems that the combination of CFZ and other anti-MM regimens could enhance the drug's cytotoxicity. Mimicking endothelium exposure to CFZ and other drugs in real life was not approached in my experimental settings.

4.2.2 Future studies

The work presented in this thesis uncovered some novel findings of the CFZ effect on the endothelium under static conditions. Since my experiments were conducted with a single endothelium cell line, it would be interesting to establish if other cardiovascular adult-derived endothelial beds, such as arterial, vein, or pulmonary endothelial cells,

would mimic the adult endothelial CFZ response profile. Studying the CFZ effect in cardiomyocytes could also address the potential CFZ impact on the cardiovascular system since they are known to have more protein demand and turnover. Therefore, these cells would depend more on the ubiquitination system, which is vulnerable to the CFZ potential cytotoxic effect. I also recommend investigating the effect of CFZ on endothelial progenitor cells isolated from the peripheral circulation of MM patients due to their significant involvement in vascular repair and regeneration. Studies with these cells could answer their potential involvement in the development of CFZ associated cardiovascular adverse events.

Another thing to consider is that in my experimental setting, the cells have been stimulated with the cytokines after exposure to CFZ, which would not mimic the prior exposure of MM patient's endothelium to inflammatory cytokines before the administration of CFZ treatment. Thus, it will be interesting to study if a prior stimulation of the endothelium with inflammatory cytokines could enhance CFZ cytotoxicity effect. Since this study was conducted under static conditions only, it would be of great interest to study the potential effect of CFZ under shear stress conditions, where it will provide a more physiologically relevant answer about the CFZ effect on the endothelium. Regarding mimicking the clinical treatment approach of using different drugs in treating multiple myeloma, it could be interesting to combine CFZ with other MM treatments to identify any potential synergistic effects on the endothelium. Since I compared all my outcomes to the first-generation proteasome inhibitor, BTZ, it would be more efficient to conduct another head-to-head comparison study between CFZ and BTZ to directly compare these drugs' effect on the endothelium.

The last part of my study indicated that eNOS expression in the endothelium was a potentially important regulator of the CFZ cytoprotective effect on HUVECs; therefore, conducting further experiments to dissect the potential cellular mechanism seems to be crucial if a future utilisation of the CFZ cytoprotective effect is aimed to be applied in clinical practice.

Lastly, since my assays have been performed *in vitro*, it would be noteworthy to conduct similar experiments *in vivo* with an animal model such as the 5TMM immunocompetent mouse model (5T Radl), frequently used to mimic MM conditions. (543) These further investigations, alongside those defined throughout this study, would supply an extensive assessment of the effects of CFZ on the endothelium.

4.3 Conclusion

The global incidence of MM is continuously growing, and MM disease progression and drug resistance have become an extreme challenge for the physician in clinical practice. (564) However, the continuous focusing of research in this field has revealed a new potent, effective drug, the second-generation proteasome inhibitor CFZ. This drug showed a significant improvement and effectiveness in treating multiple myeloma, especially in those cases where other anti-MM drugs failed. (565) However, this advantageous outcome was not a perfect approach, and significant cardiovascular severe adverse events were associated with the usage of the drug in MM patients. (563) Therefore, this study aimed to investigate the effect of CFZ on the endothelium.

The findings of this study are summarised as follows:

1) CFZ temporarily inhibited proteasome function and modified the morphology of confluence HUVECs but did induce ER stress in these cells even when stimulated after CFZ treatment with well-known pro-inflammatory cytokines, TNFα and IL-1β.
2) CFZ induced ER stress but not apoptosis in sub-confluence HUVECs
3) CFZ did not induce apoptosis, pro-thrombotic or pro-inflammatory activation in confluence HUVECs
4) At the cellular level, CFZ induced the amplification of some of the anti-thrombotic regulators, eNOS, P-eNOS, TM, TPA and KLF-4 and attenuated the expression of TNFα mediated TF, sICAM-1 and VWF expression in HUVECs
5) At a functional level, CFZ did not induce fibrin clot formation or FXa generation but enhanced the expression of the endothelial-derived anti-coagulant protein APC. In agreement with cellular level findings, CFZ showed remarkable cytoprotective features by suppressing fibrin formation, FXa generation and VWF release mediated by TNFα in HUVECs
6) BiP was not required for the effects of CFZ on ER stress or CFZs cytoprotective effects.
7) eNOS was identified as a suitable candidate involved in maintaining non-active ER stress states and is required to regulate some CFZ cytoprotective effects in HUVECs (TF, ICAM-1, VWF, t-PA) but not TM expression.

References

1. Redic K. Carfilzomib: a novel agent for multiple myeloma. Journal of Pharmacy and Pharmacology. 2013;65(8):1095-106.
2. Hungria VTdM, Crusoé EdQ, Bittencourt RI, Maiolino A, Magalhães RJP, Nascimento Jd, et al. New proteasome inhibitors in the treatment of multiple myeloma. Hematology, transfusion and cell therapy. 2019;41:76-83.
3. Demo SD, Kirk CJ, Aujay MA, Buchholz TJ, Dajee M, Ho MN, et al. Antitumor activity of PR-171, a novel irreversible inhibitor of the proteasome. Cancer research. 2007;67(13):6383-91.
4. Altruamedia. Multiple Myeloma 2017 [Available from: https://diseasesandconditions.net/multiple-myeloma/.
5. UK CR. Myeloma statistics2021 [Available from: https://www.cancerresearchuk.org/health-professional/cancer-statistics/statistics-by-cancer-type/myeloma#heading-Two.
6. Grandin EW, Ky B, Cornell RF, Carver J, Lenihan DJ. Patterns of cardiac toxicity associated with irreversible proteasome inhibition in the treatment of multiple myeloma. Journal of cardiac failure. 2015;21(2):138-44.
7. Ruschak AM, Slassi M, Kay LE, Schimmer AD. Novel proteasome inhibitors to overcome bortezomib resistance. Journal of the National Cancer Institute. 2011;103(13):1007-17.
8. Andreu-Vieyra C, Berenson JR. Carfilzomib in multiple myeloma. Expert opinion on biological therapy. 2014;14(11):1685-99.
9. Kyle RA, editor Multiple myeloma: review of 869 cases. Mayo Clinic Proceedings; 1975.
10. Auner HW, Cenci S. Recent advances and future directions in targeting the secretory apparatus in multiple myeloma. British journal of haematology. 2015;168(1):14-25.
11. Barlogie B, Shaughnessy J, Tricot G, Jacobson J, Zangari M, Anaissie E, et al. Treatment of multiple myeloma. Blood. 2004;103(1):20-32.
12. Alexanian R, Dimopoulos M. The treatment of multiple myeloma. New England Journal of Medicine. 1994;330(7):484-9.
13. Greipp PR, Miguel JS, Durie BG, Crowley JJ, Barlogie B, Bladé J, et al. International staging system for multiple myeloma. Journal of clinical oncology. 2005;23(15):3412-20.
14. Kyle RA, Gertz MA, Witzig TE, Lust JA, Lacy MQ, Dispenzieri A, et al., editors. Review of 1027 patients with newly diagnosed multiple myeloma. Mayo Clinic Proceedings; 2003: Elsevier.
15. Hideshima T, Bergsagel PL, Kuehl WM, Anderson KC. Advances in biology of multiple myeloma: clinical applications. Blood. 2004;104(3):607-18.
16. Musolino C, Allegra A, Innao V, Allegra AG, Pioggia G, Gangemi S. Inflammatory and anti-inflammatory equilibrium, proliferative and antiproliferative balance: The role of cytokines in multiple myeloma. Mediators of inflammation. 2017;2017.
17. Cao Y, Luetkens T, Kobold S, Hildebrandt Y, Gordic M, Lajmi N, et al. The cytokine/chemokine pattern in the bone marrow environment of multiple myeloma patients. Experimental hematology. 2010;38(10):860-7.
18. Dewald JH, Colomb F, Bobowski-Gerard M, Groux-Degroote S, Delannoy P. Role of cytokine-induced glycosylation changes in regulating cell interactions and cell signaling in inflammatory diseases and cancer. Cells. 2016;5(4):43.
19. Prabhala RH, Neri P, Bae JE, Tassone P, Shammas MA, Allam CK, et al. Dysfunctional T regulatory cells in multiple myeloma. Blood. 2006;107(1):301-4.
20. Rajkumar SV, Kyle RA, editors. Multiple myeloma: diagnosis and treatment. Mayo Clinic Proceedings; 2005: Elsevier.
21. Mitsiades CS, Mitsiades N, Munshi NC, Anderson KC. Focus on multiple myeloma. Cancer cell. 2004;6(5):439-44.
22. Anderson KC. Progress and paradigms in multiple myeloma. AACR; 2016.

23. Kuehl WM, Bergsagel PL. Multiple myeloma: evolving genetic events and host interactions. Nature Reviews Cancer. 2002;2(3):175-87.
24. Kumar SK, Rajkumar SV, Dispenzieri A, Lacy MQ, Hayman SR, Buadi FK, et al. Improved survival in multiple myeloma and the impact of novel therapies. Blood, The Journal of the American Society of Hematology. 2008;111(5):2516-20.
25. Group IMW. Criteria for the classification of monoclonal gammopathies, multiple myeloma and related disorders: a report of the International Myeloma Working Group. British journal of haematology. 2003;121(5):749-57.
26. Fonseca R, Bergsagel P, Drach J, Shaughnessy J, Gutierrez N, Stewart A, et al. International Myeloma Working Group molecular classification of multiple myeloma: spotlight review. Leukemia. 2009;23(12):2210-21.
27. Nandi D, Tahiliani P, Kumar A, Chandu D. The ubiquitin-proteasome system. Journal of biosciences. 2006;31(1):137-55.
28. Muratani M, Tansey WP. How the ubiquitin–proteasome system controls transcription. Nature reviews Molecular cell biology. 2003;4(3):192-201.
29. Heinemeyer W, Ramos P, Dohmen R. Ubiquitin-proteasome system. Cellular and Molecular Life Sciences CMLS. 2004;61(13):1562-78.
30. Schweitzer A, Aufderheide A, Rudack T, Beck F, Pfeifer G, Plitzko JM, et al. Structure of the human 26S proteasome at a resolution of 3.9 Å. Proceedings of the National Academy of Sciences. 2016;113(28):7816-21.
31. Kwon YT, Ciechanover A. The ubiquitin code in the ubiquitin-proteasome system and autophagy. Trends in biochemical sciences. 2017;42(11):873-86.
32. Wang J, Maldonado MA. The ubiquitin-proteasome system and its role in inflammatory and autoimmune diseases. Cell Mol Immunol. 2006;3(4):255-61.
33. Löw P. The role of ubiquitin–proteasome system in ageing. General and comparative endocrinology. 2011;172(1):39-43.
34. Deshaies RJ. Proteotoxic crisis, the ubiquitin-proteasome system, and cancer therapy. BMC biology. 2014;12(1):1-14.
35. Leestemaker Y, Ovaa H. Tools to investigate the ubiquitin proteasome system. Drug Discovery Today: Technologies. 2017;26:25-31.
36. Wojcik C, Di Napoli M. Ubiquitin-proteasome system and proteasome inhibition: new strategies in stroke therapy. Stroke. 2004;35(6):1506-18.
37. Vincenz L, Jäger R, O'Dwyer M, Samali A. Endoplasmic reticulum stress and the unfolded protein response: targeting the Achilles heel of multiple myeloma. Molecular cancer therapeutics. 2013;12(6):831-43.
38. Obeng EA, Carlson LM, Gutman DM, Harrington Jr WJ, Lee KP, Boise LH. Proteasome inhibitors induce a terminal unfolded protein response in multiple myeloma cells. Blood. 2006;107(12):4907-16.
39. Manni S, Brancalion A, Tubi LQ, Colpo A, Pavan L, Cabrelle A, et al. Protein kinase CK2 protects multiple myeloma cells from ER stress–induced apoptosis and from the cytotoxic effect of hsp90 inhibition through regulation of the unfolded protein response. Clinical cancer research. 2012;18(7):1888-900.
40. Lee A-H, Iwakoshi NN, Anderson KC, Glimcher LH. Proteasome inhibitors disrupt the unfolded protein response in myeloma cells. Proceedings of the National Academy of Sciences. 2003;100(17):9946-51.
41. Cao SS, Kaufman RJ. Unfolded protein response. Current biology. 2012;22(16):R622-R6.
42. Patterson J, Palombella VJ, Fritz C, Normant E. IPI-504, a novel and soluble HSP-90 inhibitor, blocks the unfolded protein response in multiple myeloma cells. Cancer chemotherapy and pharmacology. 2008;61(6):923-32.
43. Nikesitch N, Tao C, Lai K, Killingsworth M, Bae S, Wang M, et al. Predicting the response of multiple myeloma to the proteasome inhibitor Bortezomib by evaluation of the unfolded protein response. Blood cancer journal. 2016;6(6):e432-e.
44. Davenport EL, Morgan GJ, Davies FE. Untangling the unfolded protein response. Cell Cycle. 2008;7(7):865-9.

45. Ling SC, Lau EK, Al-Shabeeb A, Nikolic A, Catalano A, Iland H, et al. Response of myeloma to the proteasome inhibitor bortezomib is correlated with the unfolded protein response regulator XBP-1. Haematologica. 2012;97(1):64.
46. Li X, Zhang K, Li Z. Unfolded protein response in cancer: the physician's perspective. Journal of hematology & oncology. 2011;4(1):1-10.
47. Lerner AG, Upton J-P, Praveen P, Ghosh R, Nakagawa Y, Igbaria A, et al. IRE1α induces thioredoxin-interacting protein to activate the NLRP3 inflammasome and promote programmed cell death under irremediable ER stress. Cell metabolism. 2012;16(2):250-64.
48. Hetz C, Chevet E, Harding HP. Targeting the unfolded protein response in disease. Nature reviews Drug discovery. 2013;12(9):703-19.
49. Ron D, Walter P. Signal integration in the endoplasmic reticulum unfolded protein response. Nature reviews Molecular cell biology. 2007;8(7):519-29.
50. Grootjans J, Kaser A, Kaufman RJ, Blumberg RS. The unfolded protein response in immunity and inflammation. Nature Reviews Immunology. 2016;16(8):469-84.
51. Gargalovic PS, Gharavi NM, Clark MJ, Pagnon J, Yang W-P, He A, et al. The unfolded protein response is an important regulator of inflammatory genes in endothelial cells. Arteriosclerosis, thrombosis, and vascular biology. 2006;26(11):2490-6.
52. Kitamura M. Control of NF-κB and inflammation by the unfolded protein response. International reviews of immunology. 2011;30(1):4-15.
53. Kawanami D, Matoba K, Okada R, Tsukamoto M, Kinoshita J, Ishizawa S, et al. Fasudil inhibits ER stress-induced VCAM-1 expression by modulating unfolded protein response in endothelial cells. Biochemical and biophysical research communications. 2013;435(2):171-5.
54. Ren J, Bi Y, Sowers JR, Hetz C, Zhang Y. Endoplasmic reticulum stress and unfolded protein response in cardiovascular diseases. Nature Reviews Cardiology. 2021;18(7):499-521.
55. Beriault DR, Werstuck GH. The role of glucosamine-induced ER stress in diabetic atherogenesis. Experimental diabetes research. 2012;2012.
56. Yoshida H, Oku M, Suzuki M, Mori K. pXBP1 (U) encoded in XBP1 pre-mRNA negatively regulates unfolded protein response activator pXBP1 (S) in mammalian ER stress response. The Journal of cell biology. 2006;172(4):565-75.
57. Gandolfi S, Laubach JP, Hideshima T, Chauhan D, Anderson KC, Richardson PG. The proteasome and proteasome inhibitors in multiple myeloma. Cancer and Metastasis Reviews. 2017;36(4):561-84.
58. Manasanch EE, Orlowski RZ. Proteasome inhibitors in cancer therapy. Nature reviews Clinical oncology. 2017;14(7):417-33.
59. Orlowski RZ, Kuhn DJ. Proteasome inhibitors in cancer therapy: lessons from the first decade. Clinical cancer research. 2008;14(6):1649-57.
60. Voorhees PM, Orlowski RZ. The proteasome and proteasome inhibitors in cancer therapy. Annu Rev Pharmacol Toxicol. 2006;46:189-213.
61. Testa U. Proteasome inhibitors in cancer therapy. Current drug targets. 2009;10(10):968-81.
62. Kaplan GS, Torcun CC, Grune T, Ozer NK, Karademir B. Proteasome inhibitors in cancer therapy: Treatment regimen and peripheral neuropathy as a side effect. Free Radical Biology and Medicine. 2017;103:1-13.
63. Moreau P, Richardson PG, Cavo M, Orlowski RZ, San Miguel JF, Palumbo A, et al. Proteasome inhibitors in multiple myeloma: 10 years later. Blood, The Journal of the American Society of Hematology. 2012;120(5):947-59.
64. Chauhan D, Ajita D, Singh D, Anderson K. Proteasome Inhibitors as Therapy in Multiple Myeloma. Myeloma Therapy. 2008:421-32.
65. Field-Smith A, Morgan GJ, Davies FE. Bortezomib (Velcade™) in the treatment of multiple myeloma. Therapeutics and clinical risk management. 2006;2(3):271.
66. Mateos M-V, Richardson PG, Schlag R, Khuageva NK, Dimopoulos MA, Shpilberg O, et al. Bortezomib plus melphalan and prednisone compared with melphalan and prednisone in previously untreated multiple myeloma: updated follow-up and impact of subsequent therapy in the phase III VISTA trial. Journal of Clinical Oncology. 2010;28(13):2259-66.

67. Sung B, Kunnumakkara AB, Sethi G, Anand P, Guha S, Aggarwal BB. Curcumin circumvents chemoresistance in vitro and potentiates the effect of thalidomide and bortezomib against human multiple myeloma in nude mice model. Molecular cancer therapeutics. 2009;8(4):959-70.
68. Delforge M, Terpos E, Richardson PG, Shpilberg O, Khuageva NK, Schlag R, et al. Fewer bone disease events, improvement in bone remodeling, and evidence of bone healing with bortezomib plus melphalan–prednisone vs. melphalan–prednisone in the phase III VISTA trial in multiple myeloma. European journal of haematology. 2011;86(5):372-84.
69. Scott K, Hayden PJ, Will A, Wheatley K, Coyne I. Bortezomib for the treatment of multiple myeloma. Cochrane Database of Systematic Reviews. 2016(4).
70. Xiao Y, Yin J, Wei J, Shang Z. Incidence and risk of cardiotoxicity associated with bortezomib in the treatment of cancer: a systematic review and meta-analysis. PLoS One. 2014;9(1):e87671.
71. Pancheri E, Guglielmi V, Wilczynski GM, Malatesta M, Tonin P, Tomelleri G, et al. Non-hematologic toxicity of bortezomib in multiple myeloma: The neuromuscular and cardiovascular adverse effects. Cancers. 2020;12(9):2540.
72. C Potts B, X Albitar M, C Anderson K, Baritaki S, Berkers C, Bonavida B, et al. Marizomib, a proteasome inhibitor for all seasons: preclinical profile and a framework for clinical trials. Current cancer drug targets. 2011;11(3):254-84.
73. Corrales-Medina FF, Manton CA, Orlowski RZ, Chandra J. Efficacy of panobinostat and marizomib in acute myeloid leukemia and bortezomib-resistant models. Leukemia research. 2015;39(3):371-9.
74. Kortuem KM, Stewart AK. Carfilzomib. Blood, The Journal of the American Society of Hematology. 2013;121(6):893-7.
75. Moore S, Atwal S, Sachchithanantham S, Streetly M, Khan I, Percy L, et al. Weekly intravenous bortezomib is effective and well tolerated in relapsed/refractory myeloma. European journal of haematology. 2013;90(5):420-5.
76. Stewart AK, Rajkumar SV, Dimopoulos MA, Masszi T, Špička I, Oriol A, et al. Carfilzomib, lenalidomide, and dexamethasone for relapsed multiple myeloma. New England Journal of Medicine. 2015;372(2):142-52.
77. Dimopoulos MA, Moreau P, Palumbo A, Joshua D, Pour L, Hájek R, et al. Carfilzomib and dexamethasone versus bortezomib and dexamethasone for patients with relapsed or refractory multiple myeloma (ENDEAVOR): a randomised, phase 3, open-label, multicentre study. The Lancet Oncology. 2016;17(1):27-38.
78. McCormack PL. Carfilzomib. Drugs. 2012;72(15):2023-32.
79. Onat D, Brillon D, Colombo PC, Schmidt AM. Human vascular endothelial cells: a model system for studying vascular inflammation in diabetes and atherosclerosis. Current diabetes reports. 2011;11(3):193-202.
80. Ziogas DC, Terpos E, Kastritis E, Dimopoulos MA. An overview of the role of carfilzomib in the treatment of multiple myeloma. Expert opinion on pharmacotherapy. 2017;18(17):1883-97.
81. Usmani SZ, Quach H, Mateos M-V, Landgren O, Leleu X, Siegel DS, et al. Carfilzomib, dexamethasone, and daratumumab versus carfilzomib and dexamethasone for the treatment of patients with relapsed or refractory multiple myeloma (RRMM): primary analysis results from the randomized, open-label, phase 3 study Candor (NCT03158688). Blood. 2019;134:LBA-6.
82. Mark TM, Yadlapati S, Neglyad L, Bourke J, Jayabalan D, Rossi AC, et al. High-dose carfilzomib and dexamethasone as first-line treatment in symptomatic multiple myeloma. American Society of Hematology Washington, DC; 2015.
83. Besse A, Besse L, Kraus M, Mendez-Lopez M, Bader J, Xin B-T, et al. Proteasome inhibition in multiple myeloma: head-to-head comparison of currently available proteasome inhibitors. Cell chemical biology. 2019;26(3):340-51. e3.
84. van de Donk NW. Carfilzomib versus bortezomib: no longer an ENDEAVOR. The Lancet Oncology. 2017;18(10):1288-90.

85. Yong KL, Hinsley S, Auner HW, Bygrave C, Kaiser MF, Ramasamy K, et al. Carfilzomib or bortezomib in combination with cyclophosphamide and dexamethasone followed by carfilzomib maintenance for patients with multiple myeloma after one prior therapy: results from a multi-centre, phase II, randomized, controlled trial (MUKfive). Haematologica. 2021.
86. Kumar SK, Jacobus SJ, Cohen AD, Weiss M, Callander N, Singh AK, et al. Carfilzomib or bortezomib in combination with lenalidomide and dexamethasone for patients with newly diagnosed multiple myeloma without intention for immediate autologous stem-cell transplantation (ENDURANCE): a multicentre, open-label, phase 3, randomised, controlled trial. The Lancet Oncology. 2020;21(10):1317-30.
87. Hideshima T, Mazitschek R, Santo L, Mimura N, Gorgun G, Richardson PG, et al. Induction of differential apoptotic pathways in multiple myeloma cells by class-selective histone deacetylase inhibitors. Leukemia. 2014;28(2):457-60.
88. Walter P, Ron D. The unfolded protein response: from stress pathway to homeostatic regulation. science. 2011;334(6059):1081-6.
89. Hetz C, Chevet E, Oakes SA. Proteostasis control by the unfolded protein response. Nature cell biology. 2015;17(7):829.
90. Khan ML, Stewart AK. Carfilzomib: a novel second-generation proteasome inhibitor. Future oncology. 2011;7(5):607-12.
91. Cornell RF, Ky B, Weiss BM, Dahm CN, Gupta DK, Du L, et al. Prospective study of cardiac events during proteasome inhibitor therapy for relapsed multiple myeloma. Journal of Clinical Oncology. 2019;37(22):1946-55.
92. Bruno G, Bringhen S, Maffei I, Iannaccone A, Crea T, Ravera A, et al. Cardiovascular organ damage and blood pressure levels predict adverse events in multiple myeloma patients undergoing carfilzomib therapy. Cancers. 2019;11(5):622.
93. Bringhen S, Milan A, Ferri C, Wäsch R, Gay F, Larocca A, et al. Cardiovascular adverse events in modern myeloma therapy–Incidence and risks. A review from the European Myeloma Network (EMN) and Italian Society of Arterial Hypertension (SIIA). haematologica. 2018;103(9):1422.
94. Waxman AJ, Clasen S, Hwang W-T, Garfall A, Vogl DT, Carver J, et al. Carfilzomib-associated cardiovascular adverse events: a systematic review and meta-analysis. JAMA oncology. 2018;4(3):e174519-e.
95. Efentakis P, Kremastiotis G, Varela A, Nikolaou P-E, Papanagnou E-D, Davos CH, et al. Molecular mechanisms of carfilzomib-induced cardiotoxicity in mice and the emerging cardioprotective role of metformin. Blood, The Journal of the American Society of Hematology. 2019;133(7):710-23.
96. Siegel D, Martin T, Nooka A, Harvey RD, Vij R, Niesvizky R, et al. Integrated safety profile of single-agent carfilzomib: experience from 526 patients enrolled in 4 phase II clinical studies. Haematologica. 2013;98(11):1753.
97. Dimopoulos MA, Roussou M, Gavriatopoulou M, Psimenou E, Ziogas D, Eleutherakis-Papaiakovou E, et al. Cardiac and renal complications of carfilzomib in patients with multiple myeloma. Blood advances. 2017;1(7):449-54.
98. Bringhen S, D'Agostino M, De Paoli L, Montefusco V, Liberati A, Galieni P, et al. Phase 1/2 study of weekly carfilzomib, cyclophosphamide, dexamethasone in newly diagnosed transplant-ineligible myeloma. Leukemia. 2018;32(4):979-85.
99. Kistler KD, Rajangam K, Faich G, Lanes S. Cardiac event rates in patients with newly diagnosed and relapsed multiple myeloma in US clinical practice. American Society of Hematology; 2012.
100. Lenna S, Han R, Trojanowska M. Endoplasmic reticulum stress and endothelial dysfunction. IUBMB life. 2014;66(8):530-7.
101. Verfaillie T, Garg AD, Agostinis P. Targeting ER stress induced apoptosis and inflammation in cancer. Cancer letters. 2013;332(2):249-64.
102. Choi S-K, Lim M, Byeon S-H, Lee Y-H. Inhibition of endoplasmic reticulum stress improves coronary artery function in the spontaneously hypertensive rats. Scientific reports. 2016;6:31925.

103. Shen M, Wang L, Yang G, Gao L, Wang B, Guo X, et al. Baicalin protects the cardiomyocytes from ER stress-induced apoptosis: inhibition of CHOP through induction of endothelial nitric oxide synthase. PLoS One. 2014;9(2):e88389.
104. Suganya N, Bhakkiyalakshmi E, Suriyanarayanan S, Paulmurugan R, Ramkumar K. Quercetin ameliorates tunicamycin-induced endoplasmic reticulum stress in endothelial cells. Cell proliferation. 2014;47(3):231-40.
105. Taniyama Y, Griendling KK. Reactive oxygen species in the vasculature: molecular and cellular mechanisms. Hypertension. 2003;42(6):1075-81.
106. Vane JR, Änggård EE, Botting RM. Regulatory functions of the vascular endothelium. New England Journal of Medicine. 1990;323(1):27-36.
107. Maamoun H, Abdelsalam SS, Zeidan A, Korashy HM, Agouni A. Endoplasmic reticulum stress: A critical molecular driver of endothelial dysfunction and cardiovascular disturbances associated with diabetes. International journal of molecular sciences. 2019;20(7):1658.
108. Rajendran P, Rengarajan T, Thangavel J, Nishigaki Y, Sakthisekaran D, Sethi G, et al. The vascular endothelium and human diseases. International journal of biological sciences. 2013;9(10):1057.
109. Sandoo A, Van Zanten JJV, Metsios GS, Carroll D, Kitas GD. The endothelium and its role in regulating vascular tone. The open cardiovascular medicine journal. 2010;4:302.
110. Moncada S, Higgs E. Nitric oxide and the vascular endothelium. The vascular endothelium I. 2006:213-54.
111. Flavahan NA. Balancing prostanoid activity in the human vascular system. Trends in pharmacological sciences. 2007;28(3):106-10.
112. FitzGerald GA. Mechanisms of platelet activation: thromboxane A2 as an amplifying signal for other agonists. The American journal of cardiology. 1991;68(7):B11-B5.
113. Nicosia S, Oliva D, Noe M, Corsini A, Folco G, Fumagalli R. PGI2 receptors in vasculature and platelets: 5Z-carbacyclin discriminates between them. Advances in prostaglandin, thromboxane, and leukotriene research. 1987;17:474-8.
114. Chow KB, Jones RL, Wise H. Protein kinase A-dependent coupling of mouse prostacyclin receptors to Gi is cell-type dependent. European journal of pharmacology. 2003;474(1):7-13.
115. Beverelli F, Bea M, Puybasset L, Giudicelli J, Berdeaux A. Chronic inhibition of NO synthase enhances the production of prostacyclin in coronary arteries through upregulation of the cyclooxygenase type 1 isoform. Fundamental & clinical pharmacology. 1997;11(3):252-9.
116. Thomas DW, Mannon RB, Mannon PJ, Latour A, Oliver JA, Hoffman M, et al. Coagulation defects and altered hemodynamic responses in mice lacking receptors for thromboxane A2. The Journal of clinical investigation. 1998;102(11):1994-2001.
117. Alexander R, Griendling K. Signal transduction in vascular smooth muscle. Journal of hypertension Supplement: official journal of the International Society of Hypertension. 1996;14(5):S51-4.
118. Alonso D, Radomski MW. The nitric oxide-endothelin-1 connection. The Role of Nitric Oxide in Heart Failure. 2004:149-57.
119. De Nucci G, Thomas R, D'Orleans-Juste P, Antunes E, Walder C, Warner TD, et al. Pressor effects of circulating endothelin are limited by its removal in the pulmonary circulation and by the release of prostacyclin and endothelium-derived relaxing factor. Proceedings of the National Academy of Sciences. 1988;85(24):9797-800.
120. Cardillo C, Kilcoyne CM, Cannon III RO, Panza JA. Interactions between nitric oxide and endothelin in the regulation of vascular tone of human resistance vessels in vivo. Hypertension. 2000;35(6):1237-41.
121. Böhm F, Ahlborg G, Johansson B-L, Hansson L-O, Pernow J. Combined endothelin receptor blockade evokes enhanced vasodilatation in patients with atherosclerosis. Arteriosclerosis, thrombosis, and vascular biology. 2002;22(4):674-9.
122. Pernow J, Gonon A, Gourine A. The role of the endothelium for reperfusion injury. European heart journal supplements. 2001;3(suppl_C):C22-C7.

123. Maguire JJ, YU JC-M, Davenport AP. ETA receptor antagonists inhibit intimal smooth muscle cell proliferation in human vessels. Portland Press Ltd.; 2002.
124. Kowala MC, Rose PM, Stein PD, Goller N, Recce R, Beyer S, et al. Selective blockade of the endothelin subtype A receptor decreases early atherosclerosis in hamsters fed cholesterol. The American journal of pathology. 1995;146(4):819.
125. Feletou M, Vanhoutte PM. Endothelium-dependent hyperpolarization of canine coronary smooth muscle. British journal of pharmacology. 1988;93(3):515-24.
126. Cohen RA, Vanhoutte PM. Endothelium-dependent hyperpolarization: beyond nitric oxide and cyclic GMP. Circulation. 1995;92(11):3337-49.
127. Scotland RS, Madhani M, Chauhan S, Moncada S, Andresen J, Nilsson H, et al. Investigation of vascular responses in endothelial nitric oxide synthase/cyclooxygenase-1 double-knockout mice: key role for endothelium-derived hyperpolarizing factor in the regulation of blood pressure in vivo. Circulation. 2005;111(6):796-803.
128. Edwards G, Weston AH. Potassium and potassium clouds in endothelium-dependent hyperpolarizations. Pharmacological research. 2004;49(6):535-41.
129. Bucci M, Gratton J-P, Rudic RD, Acevedo L, Roviezzo F, Cirino G, et al. In vivo delivery of the caveolin-1 scaffolding domain inhibits nitric oxide synthesis and reduces inflammation. Nature medicine. 2000;6(12):1362-7.
130. Bae SW, Kim HS, Cha YN, Park YS, Jo SA, Jo I. Rapid increase in endothelial nitric oxide production by bradykinin is mediated by protein kinase A signaling pathway. Biochemical and biophysical research communications. 2003;306(4):981-7.
131. Moncada S, Higgs E. The discovery of nitric oxide and its role in vascular biology. British journal of pharmacology. 2006;147(S1):S193-S201.
132. Schilling WP, Cabello OA, Rajan L. Depletion of the inositol 1, 4, 5-trisphosphate-sensitive intracellular Ca2+ store in vascular endothelial cells activates the agonist-sensitive Ca2+-influx pathway. Biochemical Journal. 1992;284(2):521-30.
133. Fleming I, Busse R. Signal transduction of eNOS activation. Cardiovascular research. 1999;43(3):532-41.
134. Michel T, Feron O. Nitric oxide synthases: which, where, how, and why? The Journal of clinical investigation. 1997;100(9):2146-52.
135. Li C, Ruan L, Sood SG, Papapetropoulos A, Fulton D, Venema RC. Role of eNOS phosphorylation at Ser-116 in regulation of eNOS activity in endothelial cells. Vascular pharmacology. 2007;47(5-6):257-64.
136. Fleming I. Molecular mechanisms underlying the activation of eNOS. Pflügers Archiv-European Journal of Physiology. 2010;459(6):793-806.
137. Ignarro LJ, Harbison RG, Wood KS, Kadowitz PJ. Activation of purified soluble guanylate cyclase by endothelium-derived relaxing factor from intrapulmonary artery and vein: stimulation by acetylcholine, bradykinin and arachidonic acid. Journal of Pharmacology and Experimental Therapeutics. 1986;237(3):893-900.
138. Collins P, Griffith T, Henderson A, Lewis M. Endothelium-derived relaxing factor alters calcium fluxes in rabbit aorta: a cyclic guanosine monophosphate-mediated effect. The Journal of physiology. 1986;381(1):427-37.
139. Kubes P, Suzuki M, Granger D. Nitric oxide: an endogenous modulator of leukocyte adhesion. Proceedings of the National Academy of Sciences. 1991;88(11):4651-5.
140. Schalkwijk CG, Stehouwer CD. Vascular complications in diabetes mellitus: the role of endothelial dysfunction. Clinical science. 2005;109(2):143-59.
141. Nong Z, Hoylaerts M, Van Pelt N, Collen Ds, Janssens S. Nitric oxide inhalation inhibits platelet aggregation and platelet-mediated pulmonary thrombosis in rats. Circulation research. 1997;81(5):865-9.
142. Davenpeck KL, Gauthier TW, Lefer AM. Inhibition of endothelial-derived nitric oxide promotes P-selectin expression and actions in the rat microcirculation. Gastroenterology. 1994;107(4):1050-8.
143. Lefer DJ, Jones SP, Girod WG, Baines A, Grisham MB, Cockrell AS, et al. Leukocyte-endothelial cell interactions in nitric oxide synthase-deficient mice. American Journal of Physiology-Heart and Circulatory Physiology. 1999;276(6):H1943-H50.

144. Tousoulis D, Kampoli A-M, Tentolouris Nikolaos Papageorgiou C, Stefanadis C. The role of nitric oxide on endothelial function. Current vascular pharmacology. 2012;10(1):4-18.
145. Jin F, Cheng D, Tao J-Y, Zhang S-L, Pang R, Guo Y-J, et al. Anti-inflammatory and anti-oxidative effects of corilagin in a rat model of acute cholestasis. BMC gastroenterology. 2013;13(1):1-10.
146. Murphy ME, Sies H. Reversible conversion of nitroxyl anion to nitric oxide by superoxide dismutase. Proceedings of the National Academy of Sciences. 1991;88(23):10860-4.
147. Solomon H, Man J, Jackson G. Erectile dysfunction and the cardiovascular patient: endothelial dysfunction is the common denominator. Heart. 2003;89(3):251-3.
148. Poredos P. Endothelial dysfunction and cardiovascular disease. Pathophysiology of haemostasis and thrombosis. 2002;32(5-6):274-7.
149. Gurav AN. The implication of periodontitis in vascular endothelial dysfunction. European journal of clinical investigation. 2014;44(10):1000-9.
150. Clapp BR, Hingorani AD, Kharbanda RK, Mohamed-Ali V, Stephens JW, Vallance P, et al. Inflammation-induced endothelial dysfunction involves reduced nitric oxide bioavailability and increased oxidant stress. Cardiovascular research. 2004;64(1):172-8.
151. Sáenz-Medina J, Martinez M, Rosado S, Durán M, Prieto D, Carballido J. Urolithiasis Develops Endothelial Dysfunction as a Clinical Feature. Antioxidants. 2021;10(5):722.
152. Cannon III RO. Role of nitric oxide in cardiovascular disease: focus on the endothelium. Clinical chemistry. 1998;44(8):1809-19.
153. Mudau M, Genis A, Lochner A, Strijdom H. Endothelial dysfunction: the early predictor of atherosclerosis. Cardiovascular journal of Africa. 2012;23(4):222-31.
154. Gale AJ. Continuing education course# 2: current understanding of hemostasis. Toxicologic pathology. 2011;39(1):273-80.
155. Kaushansky K, editor Thrombopoiesis. Seminars in hematology; 2015: Elsevier.
156. Kaushansky K. The molecular mechanisms that control thrombopoiesis. The Journal of clinical investigation. 2005;115(12):3339-47.
157. Kaushansky K. Historical review: megakaryopoiesis and thrombopoiesis. Blood, The Journal of the American Society of Hematology. 2008;111(3):981-6.
158. Arnout J, Hoylaerts M, Lijnen H. Haemostasis. The Vascular Endothelium II. 2006:1-41.
159. Clemetson KJ. Platelets and primary haemostasis. Thrombosis research. 2012;129(3):220-4.
160. Versteeg HH, Heemskerk JW, Levi M, Reitsma PH. New fundamentals in hemostasis. Physiological reviews. 2013;93(1):327-58.
161. Berndt MC, Metharom P, Andrews RK. Primary haemostasis: newer insights. Haemophilia. 2014;20:15-22.
162. Eugster M, Reinhart WH. The influence of the haematocrit on primary haemostasis in vitro. Thrombosis and haemostasis. 2005;94(12):1213-8.
163. Clemetson KJ. Primary haemostasis: sticky fingers cement the relationship. Current biology. 1999;9(3):R110-R2.
164. Quach ME, Li R. Structure-function of platelet glycoprotein Ib-IX. Journal of Thrombosis and Haemostasis. 2020;18(12):3131-41.
165. Reininger A. Primary haemostasis and its assessment by laboratory tests. Hämostaseologie. 2006;26(01):42-7.
166. Scharf RE. Platelet signaling in primary haemostasis and arterial thrombus formation: Part 2. Hämostaseologie. 2018;38(04):211-22.
167. Dahlbäck B. Blood coagulation. The Lancet. 2000;355(9215):1627-32.
168. Palta S, Saroa R, Palta A. Overview of the coagulation system. Indian journal of anaesthesia. 2014;58(5):515.
169. Blair P, Flaumenhaft R. Platelet α-granules: basic biology and clinical correlates. Blood reviews. 2009;23(4):177-89.
170. McNicol A, Israels SJ. Platelet dense granules: structure, function and implications for haemostasis. Thrombosis research. 1999;95(1):1-18.

171. Chen Y, Yuan Y, Li W. Sorting machineries: how platelet-dense granules differ from α-granules. Bioscience reports. 2018;38(5):BSR20180458.
172. Gunay-Aygun M, Huizing M, Gahl WA, editors. Molecular defects that affect platelet dense granules. Seminars in thrombosis and hemostasis; 2004: Published in 2004 by Thieme Medical Publishers, Inc., 333 Seventh Avenue ….
173. Lee YH, Kim HS, Pai J-K, Ryu SH, Suh P-G. Activation of phospholipase D induced by platelet-derived growth factor is dependent upon the level of phospholipase C-gamma 1. Journal of Biological Chemistry. 1994;269(43):26842-7.
174. Rucker D, Dhamoon AS. Physiology, thromboxane A2. StatPearls [Internet]. 2020.
175. Reddy EC, Rand ML. Procoagulant phosphatidylserine-exposing platelets in vitro and in vivo. Frontiers in cardiovascular medicine. 2020;7:15.
176. Ma R, Xie R, Yu C, Si Y, Wu X, Zhao L, et al. Phosphatidylserine-mediated platelet clearance by endothelium decreases platelet aggregates and procoagulant activity in sepsis. Scientific reports. 2017;7(1):1-14.
177. Lentz BR. Exposure of platelet membrane phosphatidylserine regulates blood coagulation. Progress in lipid research. 2003;42(5):423-38.
178. Kailashiya J. Platelet-derived microparticles analysis: Techniques, challenges and recommendations. Analytical biochemistry. 2018;546:78-85.
179. Xu XR, Carrim N, Neves MAD, McKeown T, Stratton TW, Coelho RMP, et al. Platelets and platelet adhesion molecules: novel mechanisms of thrombosis and anti-thrombotic therapies. Thrombosis journal. 2016;14(1):37-46.
180. Coughlin SR. Protease-activated receptors and platelet function. Thrombosis and haemostasis. 1999;82(08):353-6.
181. Wrighton KH. The'ins' and'outs' of integrin signalling. Nature reviews Molecular cell biology. 2013;14(12):753-.
182. Ye F, Kim C, Ginsberg MH. Molecular mechanism of inside-out integrin regulation. Journal of Thrombosis and Haemostasis. 2011;9:20-5.
183. Vilahur G, Gutiérrez M, Arzanauskaite M, Mendieta G, Ben-Aicha S, Badimon L. Intracellular platelet signalling as a target for drug development. Vascular pharmacology. 2018;111:22-5.
184. Sangkuhl K, Shuldiner AR, Klein TE, Altman RB. Platelet aggregation pathway. Pharmacogenetics and genomics. 2011;21(8):516.
185. Monagle P, Barnes C, Ignjatovic V, Furmedge J, Newall F, Chan A, et al. Developmental haemostasis. Thrombosis and haemostasis. 2006;95(02):362-72.
186. Austin SK. Haemostasis. Medicine. 2017;45(4):204-8.
187. Monagle P, Massicotte P, editors. Developmental haemostasis: secondary haemostasis. Seminars in Fetal and Neonatal Medicine; 2011: Elsevier.
188. Mischke R. Overview of haemostasis. BSAVA Manual of Canine and Feline Haematology and Transfusion Medicine: BSAVA Library; 2012. p. 182-8.
189. Butenas S, Mann K. Blood coagulation. Biochemistry (Moscow). 2002;67(1):3-12.
190. McVey JH. Tissue factor pathway. Best Practice & Research Clinical Haematology. 1999;12(3):361-72.
191. Lwaleed BA, Bass PS. Tissue factor pathway inhibitor: structure, biology and involvement in disease. The Journal of Pathology: A Journal of the Pathological Society of Great Britain and Ireland. 2006;208(3):327-39.
192. Wolberg AS. Thrombin generation and fibrin clot structure. Blood reviews. 2007;21(3):131-42.
193. Price G, Thompson S, Kam P. Tissue factor and tissue factor pathway inhibitor. Anaesthesia. 2004;59(5):483-92.
194. Mackman N, Tilley RE, Key NS. Role of the extrinsic pathway of blood coagulation in hemostasis and thrombosis. Arteriosclerosis, thrombosis, and vascular biology. 2007;27(8):1687-93.
195. Mann KG, Ziedens K. Overview of hemostasis. Textbook of Hemophilia USA, Blackwell Publishing. 2005:1-4.

196. Horne M. Overview of hemostasis and thrombosis; current status of antithrombotic therapies. Thrombosis research. 2005;117(1):15-7.
197. Castellone D. Overview of hemostasis and platelet physiology. Hematology in practice Philadelphia: FA Davis Company. 2007:229-44.
198. Weitz JI. Overview of hemostasis and thrombosis. Hematology: Basic Principles and Practice 6th ed Philadelphia, PA: Saunders/Elsevier. 2013:1774-83.
199. Björk I, Olson ST. Antithrombin. Chemistry and biology of serpins. 1997:17-33.
200. Broze Jr GJ, Girard TJ. Tissue factor pathway inhibitor: structure-function. Frontiers in bioscience: a journal and virtual library. 2012;17:262.
201. Griffin J, Fernandez J, Gale A, Mosnier L. Activated protein C. Journal of Thrombosis and Haemostasis. 2007;5:73-80.
202. Dirkmann D, Görlinger K, Gisbertz C, Dusse F, Peters J. Factor XIII and tranexamic acid but not recombinant Factor VIIa attenuate tissue plasminogen activator–induced hyperfibrinolysis in human whole blood. Anesthesia & Analgesia. 2012;114(6):1182-8.
203. Gailani D, Renné T. Intrinsic pathway of coagulation and arterial thrombosis. Arteriosclerosis, thrombosis, and vascular biology. 2007;27(12):2507-13.
204. Gailani D, Renne T. The intrinsic pathway of coagulation: a target for treating thromboembolic disease? Journal of Thrombosis and Haemostasis. 2007;5(6):1106-12.
205. Green D. Coagulation cascade. Hemodialysis International. 2006;10(S2):S2-S4.
206. Mast AE. Tissue factor pathway inhibitor: multiple anticoagulant activities for a single protein. Arteriosclerosis, thrombosis, and vascular biology. 2016;36(1):9-14.
207. Villiers E, Ristić J. BSAVA manual of canine and feline clinical pathology: British Small Animal Veterinary Association; 2016.
208. Esmon CT. Role of coagulation inhibitors in inflammation. Thrombosis and haemostasis. 2001;86(07):51-6.
209. Demir C, Dilek I. Natural coagulation inhibitors and active protein c resistance in preeclampsia. Clinics. 2010;65:1119-22.
210. Esmon CT. The protein C pathway. Chest. 2003;124(3):26S-32S.
211. Dahlbäck B. Progress in the understanding of the protein C anticoagulant pathway. International journal of hematology. 2004;79(2):109-16.
212. Dahlbäck B, Villoutreix BO. The anticoagulant protein C pathway. FEBS letters. 2005;579(15):3310-6.
213. Mosnier LO, Zlokovic BV, Griffin JH. The cytoprotective protein C pathway. Blood. 2007;109(8):3161-72.
214. Esmon CT. The endothelial cell protein C receptor. Thrombosis and haemostasis. 2000;83(05):639-43.
215. Mazurkiewicz-Pisarek A, Płucienniczak G, Ciach T, Płucienniczak A. The factor VIII protein and its function. Acta Biochimica Polonica. 2016;63(1):11-6.
216. Thompson AR, editor Structure and function of the factor VIII gene and protein. Seminars in thrombosis and hemostasis; 2003: Copyright© 2003 by Thieme Medical Publishers, Inc., 333 Seventh Avenue, New ….
217. Szabó G, Veres G, Radovits T, Haider H, Krieger N, Bährle S, et al. Effects of novel synthetic serine protease inhibitors on postoperative blood loss, coagulation parameters, and vascular relaxation after cardiac surgery. The Journal of thoracic and cardiovascular surgery. 2010;139(1):181-8.
218. Quinsey NS, Greedy AL, Bottomley SP, Whisstock JC, Pike RN. Antithrombin: in control of coagulation. The international journal of biochemistry & cell biology. 2004;36(3):386-9.
219. Bilgen D, Sönmez H, Ekmekçi H, Ulutin T, Öztürk Z, Kökoğlu E, et al. The relationship of TFPI, Lp (a), and oxidized LDL antibody levels in patients with coronary artery disease. Clinical biochemistry. 2005;38(1):92-6.
220. Girard TJ, Tuley E, Broze Jr GJ. TFPIβ is the GPI-anchored TFPI isoform on human endothelial cells and placental microsomes. Blood, The Journal of the American Society of Hematology. 2012;119(5):1256-62.

221. Girard TJ, Warren LA, Novotny WF, Likert KM, Brown SG, Miletich JP, et al. Functional significance of the Kunitz-type inhibitory domains of lipoprotein-associated coagulation inhibitor. Nature. 1989;338(6215):518-20.
222. Hackeng TM, Seré KM, Tans G, Rosing J. Protein S stimulates inhibition of the tissue factor pathway by tissue factor pathway inhibitor. Proceedings of the National Academy of Sciences. 2006;103(9):3106-11.
223. Peraramelli S, Rosing J, Hackeng TM. TFPI-dependent activities of protein S. Thrombosis research. 2012;129:S23-S6.
224. Demers C, Ginsberg JS, Hirsh J, Henderson P, Blajchman MA. Thrombosis in antithrombin-III-deficient persons: report of a large kindred and literature review. Annals of internal medicine. 1992;116(9):754-61.
225. Ishiguro K, Kojima T, Kadomatsu K, Nakayama Y, Takagi A, Suzuki M, et al. Complete antithrombin deficiency in mice results in embryonic lethality. The Journal of clinical investigation. 2000;106(7):873-8.
226. Rau J, Beaulieu L, Huntington J, CHURCH FC. Serpins in thrombosis, hemostasis and fibrinolysis. Journal of thrombosis and haemostasis. 2007;5:102-15.
227. Lawrence DA, Ginsburg D, Day DE, Berkenpas MB, Verhamme IM, Kvassman J-O, et al. Serpin-Protease Complexes Are Trapped as Stable Acyl-Enzyme Intermediates (∗). Journal of Biological Chemistry. 1995;270(43):25309-12.
228. Huntington J. Serpin structure, function and dysfunction. Journal of thrombosis and haemostasis. 2011;9:26-34.
229. Olson ST, Swanson R, Raub-Segall E, Bedsted T, Sadri M, Petitou M, et al. Accelerating ability of synthetic oligosaccharides on antithrombin inhibition of proteinases of the clotting and fibrinolytic systems Comparison with heparin and low-molecular-weight heparin. Thrombosis and haemostasis. 2004;92(11):929-39.
230. Chapin JC, Hajjar KA. Fibrinolysis and the control of blood coagulation. Blood reviews. 2015;29(1):17-24.
231. Schafer AI. Overview of Hemostasis and Fibrinolysis. New Therapeutic Agents in Thrombosis and Thrombolysis: CRC Press; 2016. p. 23-30.
232. Gersh K, Edmondson K, Weisel J. Flow rate and fibrin fiber alignment. Journal of thrombosis and haemostasis: JTH. 2010;8(12):2826.
233. Undas A, Ariëns RA. Fibrin clot structure and function: a role in the pathophysiology of arterial and venous thromboembolic diseases. Arteriosclerosis, thrombosis, and vascular biology. 2011;31(12):e88-e99.
234. Nayyar N, Mannasian H, Yang L, Liu H. The Coagulation System and Blood Clot Stability. Essentials of Blood Product Management in Anesthesia Practice. 2021:29-35.
235. Ye Y, Vattai A, Zhang X, Zhu J, Thaler CJ, Mahner S, et al. Role of plasminogen activator inhibitor type 1 in pathologies of female reproductive diseases. International journal of molecular sciences. 2017;18(8):1651.
236. Declerck P. Thrombin activatable fibrinolysis inhibitor. Hämostaseologie. 2011;31(03):165-73.
237. Cesarman-Maus G, Hajjar KA. Molecular mechanisms of fibrinolysis. British journal of haematology. 2005;129(3):307-21.
238. Plow EF, Collen D. The presence and release of alpha 2-antiplasmin from human platelets. 1981.
239. Doolittle RF. Searching for differences between fibrinogen and fibrin that affect the initiation of fibrinolysis. Cardiovascular & Hematological Agents in Medicinal Chemistry (Formerly Current Medicinal Chemistry-Cardiovascular & Hematological Agents). 2008;6(3):181-9.
240. Bai H, Baik N, Kiosses WB, Krajewski S, Miles LA, Parmer RJ. The novel plasminogen receptor, plasminogen receptorKT (Plg-RKT), regulates catecholamine release. Journal of Biological Chemistry. 2011;286(38):33125-33.
241. Rescher U, Gerke V. S100A10/p11: family, friends and functions. Pflügers Archiv-European Journal of Physiology. 2008;455(4):575-82.

242. Hajjar K, Hamel N. Identification and characterization of human endothelial cell membrane binding sites for tissue plasminogen activator and urokinase. Journal of Biological Chemistry. 1990;265(5):2908-16.
243. Waisman DM. Annexin II tetramer: structure and function. Signal Transduction Mechanisms. 1995:301-22.
244. Bailey K, Bettelheim F, Lorand L, Middlebrook W. Action of thrombin in the clotting of fibrinogen. Nature. 1951;167(4241):233-4.
245. Pandi L, Kollman JM, Lopez-Lira F, Burrows JM, Riley M, Doolittle RF. Two families of synthetic peptides that enhance fibrin turbidity and delay fibrinolysis by different mechanisms. Biochemistry. 2009;48(30):7201-8.
246. Ittyerah TR, Weidner N, Wochner RD, Sherman LA. Effect of fibrin degradation products and thrombin on fibrinogen synthesis. British journal of haematology. 1979;43(4):661-8.
247. Kanji R, Gue YX, Memtsas V, Gorog DA. Fibrinolysis in Platelet Thrombi. International Journal of Molecular Sciences. 2021;22(10):5135.
248. Peyvandi F, Garagiola I, Baronciani L. Role of von Willebrand factor in the haemostasis. Blood Transfusion. 2011;9(Suppl 2):s3.
249. Bryckaert M, Rosa J-P, Denis CV, Lenting PJ. Of von Willebrand factor and platelets. Cellular and Molecular Life Sciences. 2015;72(2):307-26.
250. Reininger A. Function of von Willebrand factor in haemostasis and thrombosis. Haemophilia. 2008;14:11-26.
251. CAEN JP, Levy-Toledano S. Interaction between platelets and von Willebrand factor provides a new scheme for primary haemostasis. Nature New Biology. 1973;244(135):159-60.
252. Lip GY, Blann A. von Willebrand factor: a marker of endothelial dysfunction in vascular disorders? Cardiovascular research. 1997;34(2):255-65.
253. Rumley A, Lowe G, Sweetnam P, Yarnell J, Ford R. Factor VIII, von Willebrand factor and the risk of major ischaemic heart disease in the Caerphilly Heart Study. British journal of haematology. 1999;105(1):110-6.
254. Whincup P, Danesh J, Walker M, Lennon L, Thomson A, Appleby P, et al. von Willebrand factor and coronary heart disease. Prospective study and meta-analysis. European heart journal. 2002;23(22):1764-70.
255. Horvath B, Hegedus D, Szapary L, Marton Z, Alexy T, Koltai K, et al. Measurement of von Willebrand factor as the marker of endothelial dysfunction in vascular diseases. Experimental & Clinical Cardiology. 2004;9(1):31.
256. Blann AD. Assessment of endothelial dysfunction: focus on atherothrombotic disease. Pathophysiology of haemostasis and thrombosis. 2003;33(5-6):256-61.
257. Montalescot G, Bal-dit-Sollier C, Chibedi D, Collet J-P, Soulat T, Dalby M, et al. Comparison of effects on markers of blood cell activation of enoxaparin, dalteparin, and unfractionated heparin in patients with unstable angina pectoris or non–ST-segment elevation acute myocardial infarction (the ARMADA study). The American journal of cardiology. 2003;91(8):925-30.
258. Bøtker HE, Ingerslev J. Plasma concentrations of von Willebrand factor in patients with angina pectoris secondary to coronary atherosclerosis or cardiac syndrome X. Thrombosis research. 2000;97(6):519-23.
259. Sonneveld MA, de Maat MP, Leebeek FW. Von Willebrand factor and ADAMTS13 in arterial thrombosis: a systematic review and meta-analysis. Blood reviews. 2014;28(4):167-78.
260. Jansson J-H, Nilsson T, Johnson Ov. von Willebrand factor in plasma: a novel risk factor for recurrent myocardial infarction and death. Heart. 1991;66(5):351-5.
261. Westein E, van der Meer AD, Kuijpers MJ, Frimat J-P, van den Berg A, Heemskerk JW. Atherosclerotic geometries exacerbate pathological thrombus formation poststenosis in a von Willebrand factor-dependent manner. Proceedings of the National Academy of Sciences. 2013;110(4):1357-62.

262. Lufkin EG, Fass DN, O'fallon WM, Bowie E. Increased von Willebrand factor in diabetes mellitus. Metabolism. 1979;28(1):63-6.
263. Mossard J, Wiesel M, Cazenave J, Grunebaum L, Drawin T, Kieny J, et al. Relation of an increase of von Willebrand factor in the blood, acute myocardial infarction, unstable angina and coronary thrombosis. Archives des maladies du coeur et des vaisseaux. 1989;82(11):1813-8.
264. Morange P, Simon C, Alessi M, Luc G, Arveiler D, Ferrieres J, et al. Endothelial cell markers and the risk of coronary heart disease: the Prospective Epidemiological Study of Myocardial Infarction (PRIME) study. Circulation. 2004;109(11):1343-8.
265. Montalescot G, Philippe Fo, Ankri A, Vicaut E, Bearez E, Poulard JE, et al. Early increase of von Willebrand factor predicts adverse outcome in unstable coronary artery disease: beneficial effects of enoxaparin. Circulation. 1998;98(4):294-9.
266. Gragnano F, Sperlongano S, Golia E, Natale F, Bianchi R, Crisci M, et al. The role of von Willebrand factor in vascular inflammation: from pathogenesis to targeted therapy. Mediators of inflammation. 2017;2017.
267. KAHALEH MB, OSBORN I, LeROY EC. Increased factor VIII/von Willebrand factor antigen and von Willebrand factor activity in scleroderma and in Raynaud's phenomenon. Annals of internal medicine. 1981;94(4_Part_1):482-4.
268. Scheja A, Åkesson A, Geborek P, Wildt M, Wollheim CB, Wollheim FA, et al. Von Willebrand factor propeptide as a marker of disease activity in systemic sclerosis (scleroderma). Arthritis Research & Therapy. 2001;3(3):1-6.
269. Jonsson SW, Backman C, Johnson O, Karp K, Lundström E, Sundqvist K-G, et al. Increased prevalence of atherosclerosis in patients with medium term rheumatoid arthritis. The Journal of rheumatology. 2001;28(12):2597-602.
270. Dankbar B, Padró T, Leo R, Feldmann B, Kropff M, Mesters RM, et al. Vascular endothelial growth factor and interleukin-6 in paracrine tumor-stromal cell interactions in multiple myeloma. Blood, The Journal of the American Society of Hematology. 2000;95(8):2630-6.
271. Mannucci PM. Treatment of von Willebrand's disease. New England Journal of Medicine. 2004;351(7):683-94.
272. Zimmerman TS, Ratnoff OD, Powell AE. Immunologic differentiation of classic hemophilia (factor VIII deficiency) and von Willebrand's disease: with observations on combined deficiencies of antihemophilic factor and proaccelerin (factor V) and on an acquired circulating anticoagulant against antihemophilic factor. The Journal of clinical investigation. 1971;50(1):244-54.
273. Wagner DD. Cell biology of von Willebrand factor. Annual review of cell biology. 1990;6(1):217-42.
274. van der Kwast TH, Stel HV, Cristen E, Bertina RM, Veerman EC. Localization of factor VIII-procoagulant antigen: an immunohistological survey of the human body using monoclonal antibodies. 1986.
275. Tsai H-M, Nagel RL, Hatcher VB, Sussman II. Multimeric composition of endothelial cell-derived von Willebrand factor. 1989.
276. Mayadas TN, Wagner DD. von Willebrand Factor Biosynthesis and Processing a. Annals of the New York Academy of Sciences. 1991;614(1):153-66.
277. Cramer EM, Breton-Gorius J, Beesley JE, Martin JF. Ultrastructural demonstration of tubular inclusions coinciding with von Willebrand factor in pig megakaryocytes. 1988.
278. Wencel-Drake JD, Painter RG, Zimmerman TS, Ginsberg MH. Ultrastructural localization of human platelet thrombospondin, fibrinogen, fibronectin, and von Willebrand factor in frozen thin section. 1985.
279. Koutts J, Walsh P, Plow E, Fenton Jn, Bouma B, Zimmerman T. Active release of human platelet factor VIII-related antigen by adenosine diphosphate, collagen, and thrombin. The Journal of clinical investigation. 1978;62(6):1255-63.
280. Nesheim M, Pittman D, Giles A, Fass D, Wang J, Slonosky D, et al. The effect of plasma von Willebrand factor on the binding of human factor VIII to thrombin-activated human platelets. Journal of Biological Chemistry. 1991;266(27):17815-20.

281. Ribes JA, Francis CW. Multimer size dependence of von Willebrand factor binding to crosslinked or noncrosslinked fibrin. 1990.
282. Loscalzo J, Inbal A, Handin R. von Willebrand protein facilitates platelet incorporation in polymerizing fibrin. The Journal of clinical investigation. 1986;78(4):1112-9.
283. Hantgan RR, Hindriks G, Taylor RG, Sixma JJ, de Groot PG. Glycoprotein Ib, von Willebrand factor, and glycoprotein IIb: IIIa are all involved in platelet adhesion to fibrin in flowing whole blood. 1990.
284. Hill-Eubanks DC, Lollar P. von Willebrand factor is a cofactor for thrombin-catalyzed cleavage of the factor VIII light chain. Journal of Biological Chemistry. 1990;265(29):17854-8.
285. Koppelman SJ, van Hoeij M, Vink T, Lankhof H, Schiphorst ME, Damas C, et al. Requirements of von Willebrand factor to protect factor VIII from inactivation by activated protein C. 1996.
286. Nesbitt WS, Kulkarni S, Giuliano S, Goncalves I, Dopheide SM, Yap CL, et al. Distinct glycoprotein Ib/V/IX and integrin αIIbβ3-dependent calcium signals cooperatively regulate platelet adhesion under flow. Journal of Biological Chemistry. 2002;277(4):2965-72.
287. Scharf RE. Platelet signaling in primary haemostasis and arterial thrombus formation: Part 1. Hämostaseologie. 2018;38(04):203-10.
288. Leebeek FW, Kruip MJ, Sonneveld P. Risk and management of thrombosis in multiple myeloma. Thrombosis research. 2012;129:S88-S92.
289. Zangari M, Fink L, Zhan F, Tricot G. Low venous thromboembolic risk with bortezomib in multiple myeloma and potential protective effect with thalidomide/lenalidomide-based therapy: review of data from phase 3 trials and studies of novel combination regimens. Clinical Lymphoma Myeloma and Leukemia. 2011;11(2):228-36.
290. Nayak L, Shi H, Atkins GB, Lin Z, Schmaier AH, Jain MK. The thromboprotective effect of bortezomib is dependent on the transcription factor Kruppel-like factor 2 (KLF2). Blood, The Journal of the American Society of Hematology. 2014;123(24):3828-31.
291. Can I, Büyük B, Can S, Karakaş B, Bozkurt M, Karameşe S, et al. The protective effect of the proteasome inhibitor bortezomib on the uterus of ovariectomized rats. Clinical and experimental obstetrics & gynecology. 2021;43(5):737-41.
292. Chen F-T, Yang C-M, Yang C-H. The protective effects of the proteasome inhibitor bortezomib (velcade) on ischemia-reperfusion injury in the rat retina. PloS one. 2013;8(5):e64262.
293. Mele A, Prete E, De Risi C, Citiso S, Greco G, Falcone AP, et al. Carfilzomib, lenalidomide, and dexamethasone in relapsed/refractory multiple myeloma patients: the real-life experience of Rete Ematologica Pugliese (REP). Annals of Hematology. 2021;100(2):429-36.
294. Latif A, Kapoor V, Lateef N, Ahsan MJ, Usman RM, Malik SU, et al. Incidence and Management of Carfilzomib-induced Cardiovascular Toxicity; A Systematic Review and Meta-analysis. Cardiovascular & Haematological Disorders-Drug Targets (Formerly Current Drug Targets-Cardiovascular & Hematological Disorders). 2021;21(1):30-45.
295. Fotiou D, Roussou M, Gakiopoulou C, Psimenou E, Gavriatopoulou M, Migkou M, et al. Carfilzomib-associated renal toxicity is common and unpredictable: a comprehensive analysis of 114 multiple myeloma patients. Blood cancer journal. 2020;10(11):1-5.
296. Kastritis E, Laina A, Georgiopoulos G, Gavriatopoulou M, Papanagnou E-D, Eleutherakis-Papaiakovou E, et al. Carfilzomib-induced endothelial dysfunction, recovery of proteasome activity, and prediction of cardiovascular complications: a prospective study. Leukemia. 2021;35(5):1418-27.
297. Groen K, Van De Donk N, Stege C, Zweegman S, Nijhof I. Carfilzomib for relapsed and refractory multiple myeloma. Cancer management and research. 2019;11:2663.
298. Yu JB, Jiang H, Zhan RY. Aberrant Notch signaling in glioblastoma stem cells contributes to tumor recurrence and invasion. Molecular medicine reports. 2016;14(2):1263-8.
299. Bian M, He J, Jin H, Lian N, Shao J, Guo Q, et al. Oroxylin A induces apoptosis of activated hepatic stellate cells through endoplasmic reticulum stress. Apoptosis. 2019;24(11):905-20.

300. Lee DY, Lee K-S, Lee HJ, Kim DH, Noh YH, Yu K, et al. Activation of PERK signaling attenuates Aβ-mediated ER stress. PloS one. 2010;5(5):e10489.
301. Underhill MF, Marchant RJ, Carden MJ, James DC, Smales CM. On the effect of transient expression of mutated eIF2α and eIF4E eukaryotic translation initiation factors on reporter gene expression in mammalian cells upon cold-shock. Molecular biotechnology. 2006;34(2):141-9.
302. Yi Y, Zhao F, Wang N, Liu H, Yu L, Wang A, et al. Endoplasmic reticulum stress is involved in the T-2 toxin-induced apoptosis in goat endometrium epithelial cells. Journal of Applied Toxicology. 2018;38(12):1492-501.
303. Nedungadi D, Binoy A, Pandurangan N, Pal S, Nair BG, Mishra N. 6-Shogaol induces caspase-independent paraptosis in cancer cells via proteasomal inhibition. Experimental cell research. 2018;364(2):243-51.
304. Fung TS, Liao Y, Liu DX. The endoplasmic reticulum stress sensor IRE1α protects cells from apoptosis induced by the coronavirus infectious bronchitis virus. Journal of virology. 2014;88(21):12752-64.
305. Rong Y, Hu F, Huang R, Mackman N, Horowitz JM, Jensen RL, et al. Early growth response gene-1 regulates hypoxia-induced expression of tissue factor in glioblastoma multiforme through hypoxia-inducible factor-1–independent mechanisms. Cancer research. 2006;66(14):7067-74.
306. Hiroi T, Deming CB, Zhao H, Hansen BS, Arkenbout EK, Myers TJ, et al. Proteasome inhibitors enhance endothelial thrombomodulin expression via induction of Kruppel-like transcription factors. Arteriosclerosis, thrombosis, and vascular biology. 2009;29(10):1587-93.
307. Starke RD, Ferraro F, Paschalaki KE, Dryden NH, McKinnon TA, Sutton RE, et al. Endothelial von Willebrand factor regulates angiogenesis. Blood, The Journal of the American Society of Hematology. 2011;117(3):1071-80.
308. Diamond MP, El-Hammady E, Wang R, Kruger M, Saed G. Regulation of expression of tissue plasminogen activator and plasminogen activator inhibitor-1 by dichloroacetic acid in human fibroblasts from normal peritoneum and adhesions. American journal of obstetrics and gynecology. 2004;190(4):926-33.
309. Ducros E, Mirshahi S, Bermot C, Mirshahi M. Analysis of Endothelial Protein C Receptor Functionality on Living Cells'. The open biochemistry journal. 2009;3:49.
310. Yamashita T, Sekiguchi A, Iwasaki Y-k, Sagara K, Hatano S, Iinuma H, et al. Thrombomodulin and tissue factor pathway inhibitor in endocardium of rapidly paced rat atria. Circulation. 2003;108(20):2450-2.
311. Kojda G, Cheng YC, Burchfield J, Harrison DG. Dysfunctional regulation of endothelial nitric oxide synthase (eNOS) expression in response to exercise in mice lacking one eNOS gene. Circulation. 2001;103(23):2839-44.
312. Zeng Y, Conner J, Ozias-Akins P. Identification of ovule transcripts from the Apospory-Specific Genomic Region (ASGR)-carrier chromosome. BMC genomics. 2011;12(1):1-15.
313. Kim S, Woo C-H. Laminar flow inhibits ER stress-induced endothelial apoptosis through PI3K/Akt-dependent signaling pathway. Molecules and cells. 2018;41(11):964.
314. Papadopoulos KP, Siegel DS, Vesole DH, Lee P, Rosen ST, Zojwalla N, et al. Phase I study of 30-minute infusion of carfilzomib as single agent or in combination with low-dose dexamethasone in patients with relapsed and/or refractory multiple myeloma. Journal of Clinical Oncology. 2015;33(7):732-9.
315. Chen Cy, Malchus NS, Hehn B, Stelzer W, Avci D, Langosch D, et al. Signal peptide peptidase functions in ERAD to cleave the unfolded protein response regulator XBP 1u. The EMBO journal. 2014;33(21):2492-506.
316. Iwawaki T, Hosoda A, Okuda T, Kamigori Y, Nomura-Furuwatari C, Kimata Y, et al. Translational control by the ER transmembrane kinase/ribonuclease IRE1 under ER stress. Nature cell biology. 2001;3(2):158-64.
317. Parzych K, Saavedra-García P, Valbuena GN, Al-Sadah HA, Robinson ME, Penfold L, et al. The coordinated action of VCP/p97 and GCN2 regulates cancer cell metabolism and proteostasis during nutrient limitation. Oncogene. 2019;38(17):3216-31.

318. Harvey RD. Incidence and management of adverse events in patients with relapsed and/or refractory multiple myeloma receiving single-agent carfilzomib. Clinical pharmacology: advances and applications. 2014;6:87.
319. Shah C, Bishnoi R, Wang Y, Zou F, Bejjanki H, Master S, et al. Efficacy and safety of carfilzomib in relapsed and/or refractory multiple myeloma: Systematic review and meta-analysis of 14 trials. Oncotarget. 2018;9(34):23704.
320. Xie Y, Liu J, Jiang H, Wang J, Li X, Wang J, et al. Proteasome inhibitor induced SIRT1 deacetylates GLI2 to enhance hedgehog signaling activity and drug resistance in multiple myeloma. Oncogene. 2020;39(4):922-34.
321. Shaughnessy Jr JD, Qu P, Usmani S, Heuck CJ, Zhang Q, Zhou Y, et al. Pharmacogenomics of bortezomib test-dosing identifies hyperexpression of proteasome genes, especially PSMD4, as novel high-risk feature in myeloma treated with Total Therapy 3. Blood, The Journal of the American Society of Hematology. 2011;118(13):3512-24.
322. Raasi S, Wolf DH, editors. Ubiquitin receptors and ERAD: a network of pathways to the proteasome. Seminars in cell & developmental biology; 2007: Elsevier.
323. Yoshida H, Oku M, Suzuki M, Mori K. pXBP1 (U) encoded in XBP1 pre-mRNA negatively regulates unfolded protein response activator pXBP1 (S) in mammalian ER stress response. J Cell Biol. 2006;172(4):565-75.
324. Chen Cy, Malchus NS, Hehn B, Stelzer W, Avci D, Langosch D, et al. Signal peptide peptidase functions in ERAD to cleave the unfolded protein response regulator XBP1u. The EMBO journal. 2014;33(21):2492-506.
325. Iwawaki T, Hosoda A, Okuda T, Kamigori Y, Nomura-Furuwatari C, Kimata Y, et al. Translational control by the ER transmembrane kinase/ribonuclease IRE1 under ER stress. Nature cell biology. 2001;3(2):158.
326. Belloni D, Veschini L, Foglieni C, Dell'Antonio G, Caligaris-Cappio F, Ferrarini M, et al. Bortezomib induces autophagic death in proliferating human endothelial cells. Experimental cell research. 2010;316(6):1010-8.
327. Wang Z, Yang J, Kirk C, Fang Y, Alsina M, Badros A, et al. Clinical pharmacokinetics, metabolism, and drug-drug interaction of carfilzomib. Drug Metabolism and Disposition. 2013;41(1):230-7.
328. Tsai YC, Weissman AM. Ubiquitylation in ERAD: reversing to go forward? PLoS biology. 2011;9(3):e1001038.
329. Yang H, Xue Y, Kuang S, Zhang M, Chen J, Liu L, et al. Involvement of Orai1 in tunicamycin-induced endothelial dysfunction. The Korean Journal of Physiology & Pharmacology. 2019;23(2):95-102.
330. Vitale M, Bakunts A, Orsi A, Lari F, Tade L, Danieli A, et al. Inadequate BiP availability defines endoplasmic reticulum stress. Elife. 2019;8:e41168.
331. Muchtar E, Gertz MA, Magen H. A practical review on carfilzomib in multiple myeloma. European journal of haematology. 2016;96(6):564-77.
332. Fortun J, Dunn WA, Joy S, Li J, Notterpek L. Emerging role for autophagy in the removal of aggresomes in Schwann cells. Journal of Neuroscience. 2003;23(33):10672-80.
333. Hanna J, Finley D. A proteasome for all occasions. FEBS letters. 2007;581(15):2854-61.
334. Neumüller J, Neumüller-Guber S-E, Lipovac M, Mosgoeller W, Vetterlein M, Pavelka M, et al. Immunological and ultrastructural characterization of endothelial cell cultures differentiated from human cord blood derived endothelial progenitor cells. Histochemistry and cell biology. 2006;126(6):649-64.
335. Stroka KM, Aranda-Espinoza H. Effects of morphology vs. cell–cell interactions on endothelial cell stiffness. Cellular and molecular bioengineering. 2011;4(1):9-27.
336. McKenzie JA, Ridley AJ. Roles of Rho/ROCK and MLCK in TNF-α-induced changes in endothelial morphology and permeability. Journal of cellular physiology. 2007;213(1):221-8.
337. Stroka KM, Vaitkus JA, Aranda-Espinoza H. Endothelial cells undergo morphological, biomechanical, and dynamic changes in response to tumor necrosis factor-α. European Biophysics Journal. 2012;41(11):939-47.

338. Carlsson SI, Bertilaccio MT, Ballabio E, Maier JA. Endothelial stress by gravitational unloading: effects on cell growth and cytoskeletal organization. Biochimica et Biophysica Acta (BBA)-Molecular Cell Research. 2003;1642(3):173-9.
339. Ferrara N. Vascular endothelial growth factor and the regulation of angiogenesis. Recent progress in hormone research. 2000;55:15-35; discussion
340. Melincovici CS, Boşca AB, Şuşman S, Mărginean M, Mihu C, Istrate M, et al. Vascular endothelial growth factor (VEGF)-key factor in normal and pathological angiogenesis. Rom J Morphol Embryol. 2018;59(2):455-67.
341. Marcelo KL, Goldie LC, Hirschi KK. Regulation of endothelial cell differentiation and specification. Circulation research. 2013;112(9):1272-87.
342. Kelly MA, Hirschi KK. Signaling hierarchy regulating human endothelial cell development. Arteriosclerosis, thrombosis, and vascular biology. 2009;29(5):718-24.
343. Roccaro AM, Hideshima T, Raje N, Kumar S, Ishitsuka K, Yasui H, et al. Bortezomib mediates antiangiogenesis in multiple myeloma via direct and indirect effects on endothelial cells. Cancer research. 2006;66(1):184-91.
344. Kocherova I, Bryja A, Mozdziak P, Angelova Volponi A, Dyszkiewicz-Konwińska M, Piotrowska-Kempisty H, et al. Human umbilical vein endothelial cells (HUVECs) co-culture with osteogenic cells: from molecular communication to engineering prevascularised bone grafts. Journal of clinical medicine. 2019;8(10):1602.
345. Feneberg W, Aepfelbacher M, Sackmann E. Microviscoelasticity of the apical cell surface of human umbilical vein endothelial cells (HUVEC) within confluent monolayers. Biophysical journal. 2004;87(2):1338-50.
346. Liu CY, Kaufman RJ. The unfolded protein response. Journal of cell science. 2003;116(10):1861-2.
347. Chakrabarti A, Chen AW, Varner JD. A review of the mammalian unfolded protein response. Biotechnology and bioengineering. 2011;108(12):2777-93.
348. Mishima Y, Santo L, Eda H, Cirstea D, Nemani N, Yee AJ, et al. Ricolinostat (ACY-1215) induced inhibition of aggresome formation accelerates carfilzomib-induced multiple myeloma cell death. British journal of haematology. 2015;169(3):423-34.
349. Efentakis P, Psarakou G, Varela A, Papanagnou ED, Chatzistefanou M, Nikolaou P-E, et al. Elucidating Carfilzomib's Induced Cardiotoxicity in an In Vivo Model of Aging: Prophylactic Potential of Metformin. International Journal of Molecular Sciences. 2021;22(20):10956.
350. Kyle RA. Treatment of multiple myeloma: a small step forward? : Mass Medical Soc; 1984.
351. Coussens LM, Werb Z. Inflammation and cancer. Nature. 2002;420(6917):860-7.
352. Lee JW, Chung HY, Ehrlich LA, Jelinek DF, Callander NS, Roodman GD, et al. IL-3 expression by myeloma cells increases both osteoclast formation and growth of myeloma cells. Blood. 2004;103(6):2308-15.
353. Jasrotia S, Kumar L, Gupta R. Serum Cytokine Levels in Patients of Multiple Myeloma at Diagnosis and at Relapse. Clinical Lymphoma, Myeloma and Leukemia. 2015;15:e252.
354. Mehtap O, Atesoglu E, Tarkun P, Hacihanefioglu A, Dolasik I, Musul M. IL-21 and other serum proinflammatory cytokine levels in patients with multiple myeloma at diagnosis. Journal of Postgraduate Medicine. 2014;60(2):141.
355. Gimbrone Jr M. Vascular endothelium nature's blood container. Vascular endothelium in hemostasis and thrombosis. 1986:1-13.
356. Wolinsky H. A proposal linking clearance of circulating lipoproteins to tissue metabolic activity as a basis for understanding atherogenesis. Circulation research. 1980;47(3):301-11.
357. Garland CJ, Hiley CR, Dora KA. EDHF: spreading the influence of the endothelium. British journal of pharmacology. 2011;164(3):839-52.
358. Pries A, Kuebler W. Normal endothelium. The Vascular Endothelium I. 2006:1-40.
359. Galley HF, Webster NR. Physiology of the endothelium. British journal of anaesthesia. 2004;93(1):105-13.
360. Herrmann J, Lerman A. The endothelium: dysfunction and beyond. Journal of Nuclear Cardiology. 2001;8(2):197-206.

361. Ramasamy I. Inherited bleeding disorders: disorders of platelet adhesion and aggregation. Critical reviews in oncology/hematology. 2004;49(1):1-35.
362. Hadi HA, Carr CS, Al Suwaidi J. Endothelial dysfunction: cardiovascular risk factors, therapy, and outcome. Vascular health and risk management. 2005;1(3):183.
363. Zangari M, Saghafifar F, Mehta P, Barlogie B, Fink L, Tricot G, editors. The blood coagulation mechanism in multiple myeloma. Seminars in thrombosis and hemostasis; 2003: Copyright© 2003 by Thieme Medical Publishers, Inc., 333 Seventh Avenue, New ….
364. Zangari M, Anaissie E, Barlogie B, Badros A, Desikan R, Gopal AV, et al. Increased risk of deep-vein thrombosis in patients with multiple myeloma receiving thalidomide and chemotherapy. Blood, The Journal of the American Society of Hematology. 2001;98(5):1614-5.
365. Carr Jr ME, Zekert SL. Abnormal clot retraction, altered fibrin structure, and normal platelet function in multiple myeloma. American Journal of Physiology-Heart and Circulatory Physiology. 1994;266(3):H1195-H201.
366. Gabriel D, Smith L, Folds JD, Davis L, Cancelosi S. The influence of immunoglobulin (IgG) on the assembly of fibrin gels. The Journal of laboratory and clinical medicine. 1983;101(4):545-52.
367. Danhof S, Schreder M, Rasche L, Strifler S, Einsele H, Knop S. 'Real-life'experience of preapproval carfilzomib-based therapy in myeloma–analysis of cardiac toxicity and predisposing factors. European journal of haematology. 2016;97(1):25-32.
368. Bosseboeuf A, Allain-Maillet S, Mennesson N, Tallet A, Rossi C, Garderet L, et al. Pro-inflammatory state in monoclonal gammopathy of undetermined significance and in multiple myeloma is characterized by low sialylation of pathogen-specific and other monoclonal immunoglobulins. Frontiers in immunology. 2017;8:1347.
369. Stroka KM, Aranda-Espinoza H. Endothelial cell substrate stiffness influences neutrophil transmigration via myosin light chain kinase-dependent cell contraction. Blood, The Journal of the American Society of Hematology. 2011;118(6):1632-40.
370. Lawson C, Wolf S. ICAM-1 signaling in endothelial cells. Pharmacological Reports. 2009;61(1):22-32.
371. Yang L, Froio RM, Sciuto TE, Dvorak AM, Alon R, Luscinskas FW. ICAM-1 regulates neutrophil adhesion and transcellular migration of TNF-α-activated vascular endothelium under flow. Blood. 2005;106(2):584-92.
372. Kevil CG, Orr AW, Langston W, Mickett K, Murphy-Ullrich J, Patel RP, et al. Intercellular adhesion molecule-1 (ICAM-1) regulates endothelial cell motility through a nitric oxide-dependent pathway. Journal of Biological Chemistry. 2004;279(18):19230-8.
373. Landsberger M, Wolff B, Jantzen F, Rosenstengel C, Vogelgesang D, Staudt A, et al. Cerivastatin reduces cytokine-induced surface expression of ICAM-1 via increased shedding in human endothelial cells. Atherosclerosis. 2007;190(1):43-52.
374. Osman A, Benameur T, Korashy HM, Zeidan A, Agouni A. Interplay between endoplasmic reticulum stress and large extracellular vesicles (microparticles) in endothelial cell dysfunction. Biomedicines. 2020;8(10):409.
375. Doggett TM, Breslin JW. Study of the actin cytoskeleton in live endothelial cells expressing GFP-actin. Journal of visualized experiments: JoVE. 2011(57).
376. Kim C, Kasuya J, Jeon J, Chung S, Kamm RD. A quantitative microfluidic angiogenesis screen for studying anti-angiogenic therapeutic drugs. Lab on a chip. 2015;15(1):301-10.
377. Dick M, Jonak P, Leask RL. Statin therapy influences endothelial cell morphology and F-actin cytoskeleton structure when exposed to static and laminar shear stress conditions. Life sciences. 2013;92(14-16):859-65.
378. Schmidt MCB, Morais KL, Almeida MESd, Iqbal A, Goldfeder MB, Chudzinski-Tavassi AM. Amblyomin-X, a recombinant Kunitz-type inhibitor, regulates cell adhesion and migration of human tumor cells. Cell adhesion & migration. 2020;14(1):129-38.
379. Cook-Mills JM, Deem TL. Active participation of endothelial cells in inflammation. Journal of leukocyte biology. 2005;77(4):487-95.

380. Millán J, Cain RJ, Reglero-Real N, Bigarella C, Marcos-Ramiro B, Fernández-Martín L, et al. Adherens junctions connect stress fibres between adjacent endothelial cells. BMC biology. 2010;8(1):1-13.
381. Hangai M, Yoshimura N, Honda Y. Increased cytokine gene expression in rat retina following transient ischemia. Ophthalmic research. 1996;28(4):248-54.
382. Liu C-W, Sung H-C, Lin S-R, Wu C-W, Lee C-W, Lee I-T, et al. Resveratrol attenuates ICAM-1 expression and monocyte adhesiveness to TNF-α-treated endothelial cells: evidence for an anti-inflammatory cascade mediated by the miR-221/222/AMPK/p38/NF-κB pathway. Scientific reports. 2017;7(1):1-14.
383. Bernot D, Peiretti F, Canault M, Juhan-Vague I, Nalbone G. Upregulation of TNF-α-induced ICAM-1 surface expression by adenylate cyclase-dependent pathway in human endothelial cells. Journal of cellular physiology. 2005;202(2):434-41.
384. Sun M-H, Pang J-HS, Chen S-L, Han W-H, Ho T-C, Chen K-J, et al. Retinal protection from acute glaucoma-induced ischemia-reperfusion injury through pharmacologic induction of heme oxygenase-1. Investigative Ophthalmology & Visual Science. 2010;51(9):4798-808.
385. Chen F-T, Liu Y-C, Yang C-M, Yang C-H. Anti-inflammatory effect of the proteasome inhibitor bortezomib on endotoxin-induced uveitis in rats. Investigative ophthalmology & visual science. 2012;53(7):3682-94.
386. van der Poll T. Coagulation and inflammation. Journal of endotoxin research. 2001;7(4):301-4.
387. Grignani G, Maiolo A. Cytokines and hemostasis. Haematologica. 2000;85(9):967-72.
388. Witkowski M, Landmesser U, Rauch U. Tissue factor as a link between inflammation and coagulation. Trends in cardiovascular medicine. 2016;26(4):297-303.
389. Shen Gl, Lv H, Bi HY, Zhang W, Yao S, Yuan Y. Reduction expression of thrombomodulin and endothelial cell nitric oxide synthase in dermatomyositis. Neuropathology. 2007;27(4):309-13.
390. Stangl V, Lorenz M, Meiners S, Ludwig A, Bartsch C, Moobed M, et al. Long-term up-regulation of eNOS and improvement of endothelial function by inhibition of the ubiquitin–proteasome pathway. The FASEB journal. 2004;18(2):272-9.
391. Heiss C, Rodriguez-Mateos A, Kelm M. Central role of eNOS in the maintenance of endothelial homeostasis. Antioxidants & redox signaling. 2015;22(14):1230-42.
392. Wang F, Li G, Guan X, Han Z, Yu X, You Q. Overexpression of eNOS decrease tissue factor (TF) level in CD34+ cells exhibit increased antithrombogenic property in small caliber vascular graft. The Journal of cardiovascular surgery. 2015;60(1):136-43.
393. Kim S-Y, Lee J-H, Huh JW, Kim HJ, Park MK, Ro JY, et al. Bortezomib alleviates experimental pulmonary arterial hypertension. American journal of respiratory cell and molecular biology. 2012;47(5):698-708.
394. Zhang L, Zhang ZG, Liu X, Hozeska A, Stagliano N, Riordan W, et al. Treatment of embolic stroke in rats with bortezomib and recombinant human tissue plasminogen activator. Thrombosis and haemostasis. 2006;95(01):166-73.
395. Löf A, Müller JP, Brehm MA. A biophysical view on von Willebrand factor activation. Journal of cellular physiology. 2018;233(2):799-810.
396. Joseph L, Fink L, Hauer-Jensen M. Cytokines in coagulation and thrombosis: a preclinical and clinical review. Blood coagulation & fibrinolysis. 2002;13(2):105-16.
397. Nakayama T, Sato W, Yoshimura A, Zhang L, Kosugi T, Campbell-Thompson M, et al. Endothelial von Willebrand factor release due to eNOS deficiency predisposes to thrombotic microangiopathy in mouse aging kidney. The American journal of pathology. 2010;176(5):2198-208.
398. Matsushita K, Morrell CN, Cambien B, Yang S-X, Yamakuchi M, Bao C, et al. Nitric oxide regulates exocytosis by S-nitrosylation of N-ethylmaleimide-sensitive factor. Cell. 2003;115(2):139-50.
399. Ju R, Zhuang ZW, Zhang J, Lanahan AA, Kyriakides T, Sessa WC, et al. Angiopoietin-2 secretion by endothelial cell exosomes: regulation by the phosphatidylinositol 3-kinase (PI3K)/Akt/endothelial nitric oxide synthase (eNOS) and syndecan-4/syntenin pathways. Journal of Biological Chemistry. 2014;289(1):510-9.

400. Le CT, Laidlaw G, Morehouse CA, Naiman B, Brohawn P, Mustelin T, et al. Synergistic actions of blocking angiopoietin-2 and tumor necrosis factor-α in suppressing remodeling of blood vessels and lymphatics in airway inflammation. The American journal of pathology. 2015;185(11):2949-68.
401. Daly C, Pasnikowski E, Burova E, Wong V, Aldrich TH, Griffiths J, et al. Angiopoietin-2 functions as an autocrine protective factor in stressed endothelial cells. Proceedings of the National Academy of Sciences. 2006;103(42):15491-6.
402. Ahmed A, Fujisawa T, Niu X-L, Ahmad S, Al-Ani B, Chudasama K, et al. Angiopoietin-2 confers Atheroprotection in apoE−/− mice by inhibiting LDL oxidation via nitric oxide. Circulation research. 2009;104(12):1333-6.
403. Ding J, Yu M, Jiang J, Luo Y, Zhang Q, Wang S, et al. Angiotensin II Decreases Endothelial Nitric Oxide Synthase Phosphorylation via AT1R Nox/ROS/PP2A Pathway. Frontiers in Physiology. 2020;11:1245.
404. Xu J, Lan D, Li T, Yang G, Liu L. Angiopoietins regulate vascular reactivity after haemorrhagic shock in rats through the Tie2-nitric oxide pathway. Cardiovascular research. 2012;96(2):308-19.
405. Anargyrou K, Terpos E, Vassilakopoulos TP, Pouli A, Sachanas S, Tzenou T, et al. Normalization of the serum angiopoietin-1 to angiopoietin-2 ratio reflects response in refractory/resistant multiple myeloma patients treated with bortezomib. haematologica. 2008;93(3):451-4.
406. Politou M, Naresh K, Terpos E, Crawley D, Lampert I, Apperley JF, et al. Anti-angiogenic effect of bortezomib in patients with multiple myeloma. Acta haematologica. 2005;114(3):170-3.
407. Hoffman M, Monroe III DM. A cell-based model of hemostasis. Thrombosis and haemostasis. 2001;85(06):958-65.
408. Smith SA, Travers RJ, Morrissey JH. How it all starts: Initiation of the clotting cascade. Critical reviews in biochemistry and molecular biology. 2015;50(4):326-36.
409. Makó V, Czúcz J, Weiszhár Z, Herczenik E, Matkó J, Prohászka Z, et al. Proinflammatory activation pattern of human umbilical vein endothelial cells induced by IL-1β, TNF-α, and LPS. Cytometry Part A. 2010;77(10):962-70.
410. Østerud B, Bjørklid E, editors. Sources of tissue factor. Seminars in thrombosis and hemostasis; 2006: Copyright© 2006 by Thieme Medical Publishers, Inc., 333 Seventh Avenue, New ….
411. Del Turco S, Basta G, Lazzerini G, Chancharme L, Lerond L, De Caterina R. Involvement of the TP receptor in TNF-α-induced endothelial tissue factor expression. Vascular pharmacology. 2014;62(2):49-56.
412. Fei H, Berliner JA, Parhami F, Drake TA. Regulation of endothelial cell tissue factor expression by minimally oxidized LDL and lipopolysaccharide. Arteriosclerosis and thrombosis: a journal of vascular biology. 1993;13(11):1711-7.
413. Parry GC, Mackman N. Transcriptional regulation of tissue factor expression in human endothelial cells. Arteriosclerosis, thrombosis, and vascular biology. 1995;15(5):612-21.
414. Zelová H, Hošek J. TNF-α signalling and inflammation: interactions between old acquaintances. Inflammation Research. 2013;62(7):641-51.
415. Nam N-H. Naturally occurring NF-κB inhibitors. Mini reviews in medicinal chemistry. 2006;6(8):945-51.
416. Gilmore T, Herscovitch M. Inhibitors of NF-κ B signaling: 785 and counting. Oncogene. 2006;25(51):6887-99.
417. Davis KL, Martin E, Turko IV, Murad F. Novel effects of nitric oxide. Annual review of pharmacology and toxicology. 2001;41(1):203-36.
418. Suzuki Y, Nagai N, Umemura K, Collen D, Lijnen H. Stromelysin-1 (MMP-3) is critical for intracranial bleeding after t-PA treatment of stroke in mice. Journal of Thrombosis and Haemostasis. 2007;5(8):1732-9.
419. Kooistra T, Schrauwen Y, Arts J, Emeis J. Regulation of endothelial cell t-PA synthesis and release. International journal of hematology. 1994;59(4):233-55.

420. Bouchie JL, Hansen H, Feener EP. Natriuretic factors and nitric oxide suppress plasminogen activator inhibitor-1 expression in vascular smooth muscle cells: role of cGMP in the regulation of the plasminogen system. Arteriosclerosis, thrombosis, and vascular biology. 1998;18(11):1771-9.
421. Giannarelli C, De Negri F, Virdis A, Ghiadoni L, Cipriano A, Magagna A, et al. Nitric oxide modulates tissue plasminogen activator release in normotensive subjects and hypertensive patients. Hypertension. 2007;49(4):878-84.
422. Viswambharan H, Ming X-F, Zhu S, Hubsch A, Lerch P, Vergères G, et al. Reconstituted high-density lipoprotein inhibits thrombin-induced endothelial tissue factor expression through inhibition of RhoA and stimulation of phosphatidylinositol 3-kinase but not Akt/endothelial nitric oxide synthase. Circulation research. 2004;94(7):918-25.
423. Yang Y, Loscalzo J. Regulation of tissue factor expression in human microvascular endothelial cells by nitric oxide. Circulation. 2000;101(18):2144-8.
424. Okamoto H, Ichikawa N. The pivotal role of the angiotensin-II–NF-κB axis in the development of COVID-19 pathophysiology. Hypertension Research. 2021;44(1):126-8.
425. ÖHLIN AK, Larsson K, Hansson M. Soluble thrombomodulin activity and soluble thrombomodulin antigen in plasma. Journal of Thrombosis and Haemostasis. 2005;3(5):976-82.
426. Giri H, Panicker SR, Cai X, Biswas I, Weiler H, Rezaie AR. Thrombomodulin is essential for maintaining quiescence in vascular endothelial cells. Proceedings of the National Academy of Sciences. 2021;118(11).
427. Lentz SR, Tsiang M, Sadler JE. Regulation of thrombomodulin by tumor necrosis factor-alpha: comparison of transcriptional and posttranscriptional mechanisms. 1991.
428. Song D, Ye X, Xu H, Liu SF. Activation of endothelial intrinsic NF-κB pathway impairs protein C anticoagulation mechanism and promotes coagulation in endotoxemic mice. Blood, The Journal of the American Society of Hematology. 2009;114(12):2521-9.
429. White B, Schmidt M, Murphy C, Livingstone W, O'toole D, Lawler M, et al. Activated protein C inhibits lipopolysaccharide-induced nuclear translocation of nuclear factor κB (NF-κB) and tumour necrosis factor α (TNF-α) production in the THP-1 monocytic cell line. British journal of haematology. 2000;110(1):130-4.
430. Shi J, Wang J, Zheng H, Ling W, Joseph J, Li D, et al. Statins increase thrombomodulin expression and function in human endothelial cells by a nitric oxide-dependent mechanism and counteract tumor necrosis factor alpha-induced thrombomodulin downregulation. Blood coagulation & fibrinolysis. 2003;14(6):575-85.
431. Fahy BN, Schlieman MG, Mortenson MM, Virudachalam S, Bold RJ. Targeting BCL-2 overexpression in various human malignancies through NF-κB inhibition by the proteasome inhibitor bortezomib. Cancer chemotherapy and pharmacology. 2005;56(1):46-54.
432. Rohlena J, Volger OL, van Buul JD, Hekking LH, van Gils JM, Bonta PI, et al. Endothelial CD81 is a marker of early human atherosclerotic plaques and facilitates monocyte adhesion. Cardiovascular research. 2009;81(1):187-96.
433. Napoli C, Ignarro LJ. Nitric oxide and pathogenic mechanisms involved in the development of vascular diseases. Archives of pharmacal research. 2009;32(8):1103-8.
434. Pino P, Vouldoukis I, Dugas N, Conti M, Nitcheu J, Traore B, et al. Induction of the CD23/nitric oxide pathway in endothelial cells downregulates ICAM-1 expression and decreases cytoadherence of Plasmodium falciparum-infected erythrocytes. Cellular microbiology. 2004;6(9):839-48.
435. Dal Secco D, Moreira AP, Freitas A, Silva JS, Rossi MA, Ferreira SH, et al. Nitric oxide inhibits neutrophil migration by a mechanism dependent on ICAM-1: role of soluble guanylate cyclase. Nitric oxide. 2006;15(1):77-86.
436. Gkaliagkousi E, Ritter J, Ferro A. Platelet-derived nitric oxide signaling and regulation. Circulation research. 2007;101(7):654-62.
437. Colasanti M, Persichini T. Nitric oxide: an inhibitor of NF-κB/Rel system in glial cells. Brain research bulletin. 2000;52(3):155-61.

438. Tham DM, Martin-McNulty B, Wang Y-X, Wilson DW, Vergona R, Sullivan ME, et al. Angiotensin II is associated with activation of NF-κB-mediated genes and downregulation of PPARs. Physiological genomics. 2002;11(1):21-30.
439. Gong B, Radulovic M, Figueiredo-Pereira ME, Cardozo C. The ubiquitin-proteasome system: potential therapeutic targets for Alzheimer's disease and spinal cord injury. Frontiers in molecular neuroscience. 2016;9:4.
440. Shabek N, Herman-Bachinsky Y, Ciechanover A. Ubiquitin degradation with its substrate, or as a monomer in a ubiquitination-independent mode, provides clues to proteasome regulation. Proceedings of the National Academy of Sciences. 2009;106(29):11907-12.
441. Shang F, Taylor A. Ubiquitin–proteasome pathway and cellular responses to oxidative stress. Free Radical Biology and Medicine. 2011;51(1):5-16.
442. Riederer BM, Leuba G, Vernay A, Riederer IM. The role of the ubiquitin proteasome system in Alzheimer's disease. Experimental Biology and Medicine. 2011;236(3):268-76.
443. Schröder M, Kaufman RJ. The mammalian unfolded protein response. Annu Rev Biochem. 2005;74:739-89.
444. Schröder M, Kaufman RJ. ER stress and the unfolded protein response. Mutation Research/Fundamental and Molecular Mechanisms of Mutagenesis. 2005;569(1-2):29-63.
445. Hetz C, Papa FR. The unfolded protein response and cell fate control. Molecular cell. 2018;69(2):169-81.
446. Bertolotti A, Zhang Y, Hendershot LM, Harding HP, Ron D. Dynamic interaction of BiP and ER stress transducers in the unfolded-protein response. Nature cell biology. 2000;2(6):326-32.
447. Lewy TG, Grabowski JM, Bloom ME. Focus: Infectious Diseases: BiP: Master Regulator of the Unfolded Protein Response and Crucial Factor in Flavivirus Biology. The Yale journal of biology and medicine. 2017;90(2):291.
448. Pincus D, Chevalier MW, Aragón T, Van Anken E, Vidal SE, El-Samad H, et al. BiP binding to the ER-stress sensor Ire1 tunes the homeostatic behavior of the unfolded protein response. PLoS biology. 2010;8(7):e1000415.
449. Ham H, Woolery AR, Tracy C, Stenesen D, Krämer H, Orth K. Unfolded protein response-regulated Drosophila Fic (dFic) protein reversibly AMPylates BiP chaperone during endoplasmic reticulum homeostasis. Journal of Biological Chemistry. 2014;289(52):36059-69.
450. Bruckdorfer R. The basics about nitric oxide. Molecular aspects of medicine. 2005;26(1-2):3-31.
451. Naseem KM. The role of nitric oxide in cardiovascular diseases. Molecular aspects of medicine. 2005;26(1-2):33-65.
452. Sharma J, Al-Omran A, Parvathy S. Role of nitric oxide in inflammatory diseases. Inflammopharmacology. 2007;15(6):252-9.
453. Abakumov M, Golikov P. Nitric oxide and blood coagulation system in clinical practice. Vestnik Rossiiskoi akademii meditsinskikh nauk. 2005(10):53-6.
454. Govers R, Rabelink TJ. Cellular regulation of endothelial nitric oxide synthase. American Journal of Physiology-Renal Physiology. 2001;280(2):F193-F206.
455. Lee AS. The ER chaperone and signaling regulator GRP78/BiP as a monitor of endoplasmic reticulum stress. Methods. 2005;35(4):373-81.
456. Kimata Y, Oikawa D, Shimizu Y, Ishiwata-Kimata Y, Kohno K. A role for BiP as an adjustor for the endoplasmic reticulum stress-sensing protein Ire1. The Journal of cell biology. 2004;167(3):445-56.
457. Kawaguchi Y, Hagiwara D, Miyata T, Hodai Y, Kurimoto J, Takagi H, et al. Endoplasmic reticulum chaperone BiP/GRP78 knockdown leads to autophagy and cell death of arginine vasopressin neurons in mice. Scientific reports. 2020;10(1):1-13.
458. Li C-F, Pan Y-K, Gao Y, Shi F, Wang Y-C, Sun X-Q. Autophagy protects HUVECs against ER stress-mediated apoptosis under simulated microgravity. Apoptosis. 2019;24(9):812-25.

459. Speese SD, Trotta N, Rodesch CK, Aravamudan B, Broadie K. The ubiquitin proteasome system acutely regulates presynaptic protein turnover and synaptic efficacy. Current biology. 2003;13(11):899-910.
460. Luo B, Lee AS. The critical roles of endoplasmic reticulum chaperones and unfolded protein response in tumorigenesis and anticancer therapies. Oncogene. 2013;32(7):805-18.
461. Yang Y, Ma F, Liu Z, Su Q, Liu Y, Liu Z, et al. The ER-localized Ca2+-binding protein calreticulin couples ER stress to autophagy by associating with microtubule-associated protein 1A/1B light chain 3. Journal of Biological Chemistry. 2019;294(3):772-82.
462. Cimellaro A, Perticone M, Fiorentino T, Sciacqua A, Hribal M. Role of endoplasmic reticulum stress in endothelial dysfunction. Nutrition, Metabolism and Cardiovascular Diseases. 2016;26(10):863-71.
463. Kolluru GK, Siamwala JH, Chatterjee S. eNOS phosphorylation in health and disease. Biochimie. 2010;92(9):1186-98.
464. Dimmeler S, Fleming I, Fisslthaler B, Hermann C, Busse R, Zeiher AM. Activation of nitric oxide synthase in endothelial cells by Akt-dependent phosphorylation. Nature. 1999;399(6736):601-5.
465. Bibli S-I, Zhou Z, Zukunft S, Fisslthaler B, Andreadou I, Szabo C, et al. Tyrosine phosphorylation of eNOS regulates myocardial survival after an ischaemic insult: role of PYK2. Cardiovascular research. 2017;113(8):926-37.
466. Li Q, Atochin D, Kashiwagi S, Earle J, Wang A, Mandeville E, et al. Deficient eNOS phosphorylation is a mechanism for diabetic vascular dysfunction contributing to increased stroke size. Stroke. 2013;44(11):3183-8.
467. Kukreja RC, Xi L. eNOS phosphorylation: a pivotal molecular switch in vasodilation and cardioprotection? Journal of molecular and cellular cardiology. 2007;42(2):280.
468. Du L, He F, Kuang L, Tang W, Li Y, Chen D. eNOS/iNOS and endoplasmic reticulum stress-induced apoptosis in the placentas of patients with preeclampsia. Journal of human hypertension. 2017;31(1):49-55.
469. Gotoh T, Mori M. Nitric oxide and endoplasmic reticulum stress. Arteriosclerosis, thrombosis, and vascular biology. 2006;26(7):1439-46.
470. Hu HJ, Jiang ZS, Qiu J, Zhou SH, Liu QM. Protective effects of hydrogen sulfide against angiotensin II-induced endoplasmic reticulum stress in HUVECs. Molecular medicine reports. 2017;15(4):2213-22.
471. Galán M, Kassan M, Kadowitz PJ, Trebak M, Belmadani S, Matrougui K. Mechanism of endoplasmic reticulum stress-induced vascular endothelial dysfunction. Biochimica et biophysica acta (BBA)-molecular cell research. 2014;1843(6):1063-75.
472. Rathouska J, Nemeckova I, Zemankova L, Strasky Z, Jezkova K, Varejckova M, et al. Cell adhesion molecules and eNOS expression in aorta of normocholesterolemic mice with different predispositions to atherosclerosis. Heart and vessels. 2015;30(2):241-8.
473. SHI L-h, MA J, ZHANG L-p. Effect of ginkgo flavone glycosides on the production of NO, eNOS and ICAM-1 in cultured human umbilical vein endothelial cells under oxidative damage. China Practical Medicine. 2008;2008:22.
474. Gao F, Lucke-Wold BP, Li X, Logsdon AF, Xu L-C, Xu S, et al. Reduction of endothelial nitric oxide increases the adhesiveness of constitutive endothelial membrane ICAM-1 through Src-mediated phosphorylation. Frontiers in physiology. 2018;8:1124.
475. Li F, WANG CH, WANG JG, Thai T, Boysen G, Xu L, et al. Elevated tissue factor expression contributes to exacerbated diabetic nephropathy in mice lacking eNOS fed a high fat diet. Journal of Thrombosis and Haemostasis. 2010;8(10):2122-32.
476. Holthenrich A, Gerke V. Regulation of von-willebrand factor secretion from endothelial cells by the annexin A2-S100A10 complex. International journal of molecular sciences. 2018;19(6):1752.
477. Kang JJ, Kaissarian NM, Desch KC, Kelly RJ, Shu L, Bodary PF, et al. α-galactosidase A deficiency promotes von Willebrand factor secretion in models of Fabry disease. Kidney international. 2019;95(1):149-59.
478. Qian J, Zhang Q, Fulton D. Control of VWF secretion in human endothelial cells by local production of NO. Wiley Online Library; 2008.

479. Iafrati MD, Vitseva O, Tanriverdi K, Blair P, Rex S, Chakrabarti S, et al. Compensatory mechanisms influence hemostasis in setting of eNOS deficiency. American Journal of Physiology-Heart and Circulatory Physiology. 2005;288(4):H1627-H32.
480. Goglia L, Tosi V, Sanchez A, Flamini M, Fu X-D, Zullino S, et al. Endothelial regulation of eNOS, PAI-1 and t-PA by testosterone and dihydrotestosterone in vitro and in vivo. Molecular human reproduction. 2010;16(10):761-9.
481. Rossi J, Rouleau L, Tardif J-C, Leask RL. Effect of simvastatin on Kruppel-like factor2, endothelial nitric oxide synthase and thrombomodulin expression in endothelial cells under shear stress. Life sciences. 2010;87(3-4):92-9.
482. Zhou G, Hamik A, Nayak L, Tian H, Shi H, Lu Y, et al. Endothelial Kruppel-like factor 4 protects against atherothrombosis in mice. The Journal of clinical investigation. 2012;122(12):4727-31.
483. Hamik A, Lin Z, Kumar A, Balcells M, Sinha S, Katz J, et al. Kruppel-like factor 4 regulates endothelial inflammation. Journal of Biological Chemistry. 2007;282(18):13769-79.
484. Römisch K. Endoplasmic reticulum–associated degradation. Annu Rev Cell Dev Biol. 2005;21:435-56.
485. Schäfer J, Burhenne J, Weiss J, Theile D. Elucidating the beneficial effects of melphalan, adriamycin, and corticoids in combination with bortezomib against multiple myeloma in vitro. Naunyn-Schmiedeberg's archives of pharmacology. 2019;392(4):461-6.
486. Chen-Scarabelli C, Corsetti G, Pasini E, Dioguardi FS, Sahni G, Narula J, et al. Spasmogenic effects of the proteasome inhibitor carfilzomib on coronary resistance, vascular tone and reactivity. EBioMedicine. 2017;21:206-12.
487. Rosenthal A, Luthi J, Belohlavek M, Kortüm K, Mookadam F, Mayo A, et al. Carfilzomib and the cardiorenal system in myeloma: an endothelial effect? Blood cancer journal. 2016;6(1):e384-e.
488. Boulanger CM. Endothelium. Arteriosclerosis, thrombosis, and vascular biology. 2016;36(4):e26-e31.
489. Matsuo Y, Sawai H, Ochi N, Yasuda A, Sakamoto M, Takahashi H, et al. Proteasome inhibitor MG132 inhibits angiogenesis in pancreatic cancer by blocking NF-κB activity. Digestive diseases and sciences. 2010;55(4):1167-76.
490. Maishi N, Hida K. Tumor endothelial cells accelerate tumor metastasis. Cancer science. 2017;108(10):1921-6.
491. Lambrechts D, Wauters E, Boeckx B, Aibar S, Nittner D, Burton O, et al. Phenotype molding of stromal cells in the lung tumor microenvironment. Nature medicine. 2018;24(8):1277-89.
492. Yeung T, Georges PC, Flanagan LA, Marg B, Ortiz M, Funaki M, et al. Effects of substrate stiffness on cell morphology, cytoskeletal structure, and adhesion. Cell motility and the cytoskeleton. 2005;60(1):24-34.
493. Vandenbroucke E, Mehta D, Minshall R, Malik AB. Regulation of endothelial junctional permeability. Annals of the new York Academy of Sciences. 2008;1123(1):134-45.
494. Dejana E, Orsenigo F, Molendini C, Baluk P, McDonald DM. Organization and signaling of endothelial cell-to-cell junctions in various regions of the blood and lymphatic vascular trees. Cell and tissue research. 2009;335(1):17-25.
495. Hirase T, Node K. Endothelial dysfunction as a cellular mechanism for vascular failure. American Journal of Physiology-Heart and Circulatory Physiology. 2012;302(3):H499-H505.
496. Petrache I, Birukova A, Ramirez SI, Garcia JG, Verin AD. The role of the microtubules in tumor necrosis factor-α–induced endothelial cell permeability. American journal of respiratory cell and molecular biology. 2003;28(5):574-81.
497. Michiels C. Endothelial cell functions. Journal of cellular physiology. 2003;196(3):430-43.
498. Solovey A, Kollander R, Chang Milbauer L, Abdulla F, Chen Y, Kelm Jr RJ, et al. Endothelial nitric oxide synthase and nitric oxide regulate endothelial tissue factor expression in vivo in the sickle transgenic mouse. American journal of hematology. 2010;85(1):41-5.

499. Burke-Gaffney A, Hellewell PG. Tumour necrosis factor-α-induced ICAM-1 expression in human vascular endothelial and lung epithelial cells: modulation by tyrosine kinase inhibitors. British journal of pharmacology. 1996;119(6):1149-58.
500. Zhao W, Feng H, Guo S, Han Y, Chen X. Danshenol A inhibits TNF-α-induced expression of intercellular adhesion molecule-1 (ICAM-1) mediated by NOX4 in endothelial cells. Scientific Reports. 2017;7(1):1-13.
501. Freitas RH, Fraga CA. NF-κB-IKKβ pathway as a target for drug development: Realities, challenges and perspectives. Current drug targets. 2018;19(16):1933-42.
502. Yang Z, Liao J, Cullen KJ, Dan H. Inhibition of IKKβ/NF-κB signaling pathway to improve Dasatinib efficacy in suppression of cisplatin-resistant head and neck squamous cell carcinoma. Cell death discovery. 2020;6(1):1-9.
503. Hermann M, Flammer A, Lüscher TF. Nitric oxide in hypertension. The Journal of Clinical Hypertension. 2006;8:17-29.
504. Alp NJ, Channon KM. Regulation of endothelial nitric oxide synthase by tetrahydrobiopterin in vascular disease. Arteriosclerosis, thrombosis, and vascular biology. 2004;24(3):413-20.
505. Boo YC, Kim HJ, Song H, Fulton D, Sessa W, Jo H. Coordinated regulation of endothelial nitric oxide synthase activity by phosphorylation and subcellular localization. Free Radical Biology and Medicine. 2006;41(1):144-53.
506. Forstermann U, Munzel T. Endothelial nitric oxide synthase in vascular disease: from marvel to menace. Circulation. 2006;113(13):1708-14.
507. Li H, Wallerath T, Förstermann U. Physiological mechanisms regulating the expression of endothelial-type NO synthase. Nitric oxide. 2002;7(2):132-47.
508. Zhang R, Min W, Sessa WC. Functional Analysis of the Human Endothelial Nitric Oxide Synthase Promoter: SP1 AND GATA FACTORS ARE NECESSARY FOR BASAL TRANSCRIPTION IN ENDOTHELIAL CELLS (∗). Journal of Biological Chemistry. 1995;270(25):15320-6.
509. H Heiss E, M Dirsch V. Regulation of eNOS enzyme activity by posttranslational modification. Current pharmaceutical design. 2014;20(22):3503-13.
510. Gratton J-P, Fontana J, O'Connor DS, García-Cardeña G, McCabe TJ, Sessa WC. Reconstitution of an endothelial nitric-oxide synthase (eNOS), hsp90, and caveolin-1 complex in vitro: evidence that hsp90 facilitates calmodulin stimulated displacement of eNOS from caveolin-1. Journal of Biological Chemistry. 2000;275(29):22268-72.
511. Fontana J, Fulton D, Chen Y, Fairchild TA, McCabe TJ, Fujita N, et al. Domain mapping studies reveal that the M domain of hsp90 serves as a molecular scaffold to regulate Akt-dependent phosphorylation of endothelial nitric oxide synthase and NO release. Circulation research. 2002;90(8):866-73.
512. Fink LM, Eidt JF, Johnson K, Cook J, Cook C, Morser J, et al. Thrombomodulin activity and localization. International Journal of Developmental Biology. 2003;37(1):221-6.
513. Sohn RH, Deming CB, Johns DC, Champion HC, Bian C, Gardner K, et al. Regulation of endothelial thrombomodulin expression by inflammatory cytokines is mediated by activation of nuclear factor-kappa B. Blood. 2005;105(10):3910-7.
514. Yan SB, Helterbrand JD, Hartman DL, Wright TJ, Bernard GR. Low levels of protein C are associated with poor outcome in severe sepsis. Chest. 2001;120(3):915-22.
515. Delatorre A, Schroeder RA, Kuo PC. Alteration of NF-κB p50 DNA binding kinetics by S-nitrosylation. Biochemical and biophysical research communications. 1997;238(3):703-6.
516. Schroeder RA, Bartlett ST, Kuo PC. Differential effects of nitric oxide–mediated S-nitrosylation on p50 and c-Jun DNA binding. Surgery. 1998;124(2):137-42.
517. Bernardo A, Ball C, Nolasco L, Moake JF, Dong J-f. Effects of inflammatory cytokines on the release and cleavage of the endothelial cell–derived ultralarge von Willebrand factor multimers under flow. Blood. 2004;104(1):100-6.
518. van Hinsbergh VW, editor Endothelium—role in regulation of coagulation and inflammation. Seminars in immunopathology; 2012: Springer.

519. Gupta N, Li W, Willard B, Silverstein RL, McIntyre TM. Proteasome proteolysis supports stimulated platelet function and thrombosis. Arteriosclerosis, thrombosis, and vascular biology. 2014;34(1):160-8.
520. Inoue K, Kobayashi M, Yano K, Miura M, Izumi A, Mataki C, et al. Histone deacetylase inhibitor reduces monocyte adhesion to endothelium through the suppression of vascular cell adhesion molecule-1 expression. Arteriosclerosis, thrombosis, and vascular biology. 2006;26(12):2652-9.
521. Zhang W, Xu W, Chen W, Zhou Q. Interplay of autophagy inducer rapamycin and proteasome inhibitor mg132 in reduction of foam cell formation and inflammatory cytokine expression. Cell transplantation. 2018;27(8):1235-48.
522. Auner HW, Yong KL. More convenient proteasome inhibition for improved outcomes. The Lancet Oncology. 2018;19(7):856-8.
523. Bianchi G, Oliva L, Cascio P, Pengo N, Fontana F, Cerruti F, et al. The proteasome load versus capacity balance determines apoptotic sensitivity of multiple myeloma cells to proteasome inhibition. Blood, The Journal of the American Society of Hematology. 2009;113(13):3040-9.
524. Lenna S, Townsend DM, Tan FK, Kapanadze B, Markiewicz M, Trojanowska M, et al. HLA-B35 upregulates endothelin-1 and downregulates endothelial nitric oxide synthase via endoplasmic reticulum stress response in endothelial cells. The Journal of Immunology. 2010;184(9):4654-61.
525. Basha B, Samuel SM, Triggle CR, Ding H. Endothelial dysfunction in diabetes mellitus: possible involvement of endoplasmic reticulum stress? Experimental diabetes research. 2012;2012.
526. Zhou J, Abid MDN, Xiong Y, Chen Q, Chen J. ox-LDL downregulates eNOS activity via LOX-1-mediated endoplasmic reticulum stress. International journal of molecular medicine. 2013;32(6):1442-50.
527. Wu J, Xu X, Li Y, Kou J, Huang F, Liu B, et al. Quercetin, luteolin and epigallocatechin gallate alleviate TXNIP and NLRP3-mediated inflammation and apoptosis with regulation of AMPK in endothelial cells. European journal of pharmacology. 2014;745:59-68.
528. Liu Y, Wei W, Hong C, Wang Y, Sun X, Ma J, et al. Calreticulin induced endothelial ICAM-1 up-regulation associated with tristetraprolin expression alteration through PI3K/Akt/eNOS/p38 MAPK signaling pathway in rheumatoid arthritis. Molecular immunology. 2019;107:10-20.
529. Glushakova O, Kosugi T, Roncal C, Mu W, Heinig M, Cirillo P, et al. Fructose induces the inflammatory molecule ICAM-1 in endothelial cells. Journal of the American Society of Nephrology. 2008;19(9):1712-20.
530. Venugopal SK, Devaraj S, Yuhanna I, Shaul P, Jialal I. Demonstration that C-reactive protein decreases eNOS expression and bioactivity in human aortic endothelial cells. Circulation. 2002;106(12):1439-41.
531. Jialal I, Devaraj S, Venugopal SK. C-reactive protein: risk marker or mediator in atherothrombosis? Hypertension. 2004;44(1):6-11.
532. Chen Y, Wang J, Yao Y, Yuan W, Kong M, Lin Y, et al. CRP regulates the expression and activity of tissue factor as well as tissue factor pathway inhibitor via NF-κB and ERK 1/2 MAPK pathway. FEBS letters. 2009;583(17):2811-8.
533. Mackman N. Regulation of the tissue factor gene. The faseb journal. 1995;9(10):883-9.
534. Grogan M, Dispenzieri A. Natural history and therapy of AL cardiac amyloidosis. Heart Failure Reviews. 2015;20(2):155-62.
535. Mathur P, Thanendrarajan S, Paydak H, Vallurupalli S, Jambhekar K, Bhatti S, et al. Cardiovascular complications of multiple myeloma in the elderly. Expert review of cardiovascular therapy. 2017;15(12):933-43.
536. Plummer C, Driessen C, Szabo Z, Mateos M-V. Management of cardiovascular risk in patients with multiple myeloma. Blood cancer journal. 2019;9(3):1-12.
537. Engelhardt M, Dold SM, Ihorst G, Zober A, Möller M, Reinhardt H, et al. Geriatric assessment in multiple myeloma patients: validation of the International Myeloma Working

Group (IMWG) score and comparison with other common comorbidity scores. Haematologica. 2016;101(9):1110.
538. Kistler KD, Kalman J, Sahni G, Murphy B, Werther W, Rajangam K, et al. Incidence and risk of cardiac events in patients with previously treated multiple myeloma versus matched patients without multiple myeloma: an observational, retrospective, cohort study. Clinical Lymphoma Myeloma and Leukemia. 2017;17(2):89-96. e3.
539. Dimopoulos MA, Laubach JP, Echeveste Gutierrez MA, Grzasko N, Hofmeister CC, San-Miguel JF, et al. Ixazomib maintenance therapy in newly diagnosed multiple myeloma: an integrated analysis of four phase I/II studies. European journal of haematology. 2019;102(6):494-503.
540. Ye S, Zhou X, Lin J, Chen P. Asymmetric dimethylarginine induced apoptosis and dysfunction of endothelial progenitor cells: role of endoplasmic reticulum stress pathway. BioMed research international. 2017;2017.
541. Huang Q, Yang Z, Zhou J-P, Luo Y. HMGB1 induces endothelial progenitor cells apoptosis via RAGE-dependent PERK/eIF2α pathway. Molecular and cellular biochemistry. 2017;431(1-2):67-74.
542. Hu X-s, Du C-q, Yang L, Yao X-y, Hu S-j. Proteasome inhibitor MG132 suppresses number and function of endothelial progenitor cells: involvement of nitric oxide synthase inhibition. International journal of molecular medicine. 2010;25(3):385-92.
543. Pagan J, Seto T, Pagano M, Cittadini A. Role of the ubiquitin proteasome system in the heart. Circulation research. 2013;112(7):1046-58.
544. Bringhen S, Mina R, Cafro AM, Liberati AM, Spada S, Belotti A, et al. Once-weekly carfilzomib, pomalidomide, and low-dose dexamethasone for relapsed/refractory myeloma: a phase I/II study. Leukemia. 2018;32(8):1803-7.
545. Brioli A, Mügge L-O, Hochhaus A, Von Lilienfeld-Toal M. Safety issues and management of toxicities associated with new treatments for multiple myeloma. Expert review of hematology. 2017;10(3):193-205.
546. Mikhael J. Management of carfilzomib-associated cardiac adverse events. Clinical Lymphoma Myeloma and Leukemia. 2016;16(5):241-5.
547. Goy A, Younes A, McLaughlin P, Pro B, Romaguera JE, Hagemeister F, et al. Phase II study of proteasome inhibitor bortezomib in relapsed or refractory B-cell non-Hodgkin's lymphoma. Journal of Clinical Oncology. 2005;23(4):667-75.
548. Diwadkar S, Patel AA, Fradley MG. Bortezomib-induced complete heart block and myocardial scar: the potential role of cardiac biomarkers in monitoring cardiotoxicity. Case reports in cardiology. 2016;2016.
549. Hacihanefioglu A, Tarkun P, Gonullu E. Acute severe cardiac failure in a myeloma patient due to proteasome inhibitor bortezomib. International journal of hematology. 2008;88(2):219-22.
550. Patriquin CJ, Thomas MR, Dutt T, McGuckin S, Blombery PA, Cranfield T, et al. Bortezomib in the treatment of refractory thrombotic thrombocytopenic purpura. British journal of haematology. 2016;173(5):779-85.
551. Subklewe M, Sebelin-Wulf K, Beier C, Lietz A, Mathas S, Dörken B, et al. Dendritic cell maturation stage determines susceptibility to the proteasome inhibitor bortezomib. Human immunology. 2007;68(3):147-55.
552. Ji X, Zhang L, Peng J, Hou M. T cell immune abnormalities in immune thrombocytopenia. Journal of hematology & oncology. 2014;7(1):1-6.
553. Brignole C, Marimpietri D, Pastorino F, Nico B, Di Paolo D, Cioni M, et al. Effect of bortezomib on human neuroblastoma cell growth, apoptosis, and angiogenesis. Journal of the National Cancer Institute. 2006;98(16):1142-57.
554. Papageorgiou A, Kamat A, Benedict WF, Dinney C, McConkey DJ. Combination therapy with IFN-α plus bortezomib induces apoptosis and inhibits angiogenesis in human bladder cancer cells. Molecular cancer therapeutics. 2006;5(12):3032-41.
555. Selimovic D, Porzig BB, El-Khattouti A, Badura HE, Ahmad M, Ghanjati F, et al. Bortezomib/proteasome inhibitor triggers both apoptosis and autophagy-dependent pathways in melanoma cells. Cellular signalling. 2013;25(1):308-18.

556. Tan P, Chan C, Xue S, Dong R, Ananthesayanan B, Manunta M, et al. Phenotypic and functional differences between human saphenous vein (HSVEC) and umbilical vein (HUVEC) endothelial cells. Atherosclerosis. 2004;173(2):171-83.
557. Bischel LL, Sung KE, Jiménez-Torres JA, Mader B, Keely PJ, Beebe DJ. The importance of being a lumen. The FASEB Journal. 2014;28(11):4583-90.
558. Dardik A, Chen L, Frattini J, Asada H, Aziz F, Kudo FA, et al. Differential effects of orbital and laminar shear stress on endothelial cells. Journal of vascular surgery. 2005;41(5):869-80.
559. Lin K, Hsu P-P, Chen BP, Yuan S, Usami S, Shyy JY-J, et al. Molecular mechanism of endothelial growth arrest by laminar shear stress. Proceedings of the National Academy of Sciences. 2000;97(17):9385-9.
560. Ishibazawa A, Nagaoka T, Takahashi T, Yamamoto K, Kamiya A, Ando J, et al. Effects of shear stress on the gene expressions of endothelial nitric oxide synthase, endothelin-1, and thrombomodulin in human retinal microvascular endothelial cells. Investigative ophthalmology & visual science. 2011;52(11):8496-504.
561. Mitsiades CS, Hideshima T, Chauhan D, McMillin DW, Klippel S, Laubach JP, et al., editors. Emerging treatments for multiple myeloma: beyond immunomodulatory drugs and bortezomib. Seminars in hematology; 2009: Elsevier.
562. Zou Y, Ma X, Yu H, Hu C, Fan L, Ran X. Carfilzomib/pomalidomide single-agent or in combination with other agents for the management of relapsed/refractory multiple myeloma: a meta-analysis of 37 trials. Oncotarget. 2017;8(24):39805.
563. Mushtaq A, Kapoor V, Latif A, Iftikhar A, Zahid U, McBride A, et al. Efficacy and toxicity profile of carfilzomib based regimens for treatment of multiple myeloma: A systematic review. Critical reviews in oncology/hematology. 2018;125:1-11.
564. Ludwig H, Miguel J, Dimopoulos M, Palumbo A, Sanz RG, Powles R, et al. International Myeloma Working Group recommendations for global myeloma care. Leukemia. 2014;28(5):981-92.
565. Han B, Yao W, Oh Y-T, Tong J-S, Li S, Deng J, et al. The novel proteasome inhibitor carfilzomib activates and enhances extrinsic apoptosis involving stabilization of death receptor 5. Oncotarget. 2015;6(19):17532.

Publications arising from this work

Anti-Thrombotic Effects of the Proteasome Inhibitor Carfilzomib on the Endothelium.
Ahmed Hijazi, Celia Gonzalez-Maroto, Maria Elena Rodriguez Gutierrez, Theresa Page and Thomas McKinnon
Submitted to the 2021 Annual Society of Haematology Meeting (ASH), Georgia USA

Anti-Thrombotic Effects of the Proteasome Inhibitor Carfilzomib on the Endothelium.
Ahmed Hijazi, Celia Gonzalez-Maroto, Maria Elena Rodriguez Gutierrez, Theresa Page and Thomas McKinnon
Accepted for presentation at the British Society for Haemostasis and Thrombosis (BSHT) meeting. Aberdeen, UK, 26th – 28th January 2022

Carfilzomib exerts a thromboprotective effect on HUVECS.
Ahmed Hijazi, Celia Gonzalez-Maroto, Maria Elena Rodriguez Gutierrez, Theresa Page and Thomas McKinnon
Manuscript in preperation.